PNNL-13033

# Recharge Data Package for the Immobilized Low-Activity Waste 2001 Performance Assessment

December 1999

Prepared for the U.S. Department of Energy
under Contract DE-AC06-76RLO 1830

**DISCLAIMER**



PACIFIC NORTHWEST NATIONAL LABORATORY
*operated by*
BATTELLE
*for the*
UNITED STATES DEPARTMENT OF ENERGY
*under Contract DE-AC06-76RLO 1830*

**Printed in the United States of America**

**Available to DOE and DOE contractors from the Office of Scientific and Technical Information, P.O. Box 62, Oak Ridge, TN 37831;**
**prices available from (615) 576-8401.**

**Available to the public from the National Technical Information Service, U.S. Department of Commerce, 5285 Port Royal Rd., Springfield, VA 22161**

PNNL-13033

# Recharge Data Package for the Immobilized Low-Activity Waste 2001 Performance Assessment

M.J. Fayer
E.M. Murphy
J.L. Downs
F.O. Khan
C.W. Lindenmeier
B.N. Bjornstad

December 1999

Prepared for
the U.S. Department of Energy
under Contract DE-AC06-76RLO 1830

Pacific Northwest National Laboratory
Richland, Washington 99352

# Summary

Lockheed Martin Hanford Company (LMHC) is designing and assessing the performance of disposal facilities to receive radioactive wastes that are currently stored in single- and double-shell tanks at the Hanford Site. The preferred method of disposing of the portion that is classified as immobilized low-activity waste (ILAW) is to vitrify the waste and place the product in near-surface, shallow-land burial facilities. The LMHC project to assess the performance of these disposal facilities is known as the Hanford ILAW Performance Assessment (PA) Activity, hereafter called the ILAW PA project. The goal of this project is to provide a reasonable expectation that the disposal of the waste is protective of the general public, groundwater resources, air resources, surface-water resources, and inadvertent intruders. Achieving this goal will require predictions of contaminant migration from the facility. To make such predictions will require estimates of the fluxes of water moving through the sediments within the vadose zone around and beneath the disposal facility. These fluxes, loosely called recharge rates, are the primary mechanism for transporting contaminants to the groundwater.

Pacific Northwest National Laboratory (PNNL) assists LMHC in their performance assessment activities. One of the PNNL tasks is to provide estimates of recharge rates for current conditions and long-term scenarios involving the shallow-land disposal of ILAW. Specifically, recharge estimates are needed for a fully functional surface cover, the cover sideslope, and the immediately surrounding terrain. In addition, recharge estimates are needed for degraded cover conditions. The temporal scope of the analysis is 10,000 years, but could be longer if some contaminant peaks occur after 10,000 years.

The elements of this report compose the Recharge Data Package, which provides estimates of recharge rates for the scenarios being considered in the 2001 PA. Table S.1 identifies the surface features and time periods evaluated. The most important feature, the surface cover, is expected to be the modified RCRA Subtitle C design. This design uses a 1-m-thick silt loam layer above sand and gravel filter layers to create a capillary break. A 0.15-m-thick asphalt layer underlies the filter layers to function as a backup barrier and to promote lateral drainage. Cover sideslopes are expected to be constructed with 1V:10H slopes using sandy gravel. The recharge estimates for each scenario were derived from lysimeter and tracer data collected by the ILAW PA and other projects and from modeling analyses.

For the best estimate case, we proposed using a recharge rate of 0.1 mm/yr for the surface cover with a shrub-steppe plant community. This rate is lower than the cover design goal of 0.5 mm/yr because it is closer to the actual drainage rate measured with lysimeters and inferred with modeling. The simulation results showed that erosion of 20% of the silt loam layer did not impair this performance nor did the deposition of 20 cm of dune sand. For the sandy gravel sideslope, we proposed using a recharge rate of 50 mm/yr. This rate is lower than the 75 mm/yr used in the ILAW 1998 PA. For the soil type known as Rupert sand with a shrub-steppe plant community, we proposed using a recharge rate of 0.9 mm/yr. This rate is lower than the 3 mm/yr used in the ILAW 1998 PA. For the soil type known as Burbank loamy sand with a shrub-steppe plant community, we proposed using a recharge rate of 4.2 mm/yr. This soil type was not considered in the ILAW 1998 PA. For the Hanford formation sediments during construction, we proposed using a recharge rate of 55.4 mm/yr. Recharge in Hanford formation sediments during construction was not considered in the ILAW 1998 PA.

**Table S.1**. Recharge Estimates for the Best Estimate Case (and Reasonable Bounding Cases) During Each Period of Interest to the ILAW 2001 PA.

| Surface Feature | Estimated Recharge Rates for the Best Estimate Case (and Reasonable Bounding Cases) (mm/yr) | | | |
|---|---|---|---|---|
| | Time Period of Recharge Evaluation | | | |
| | Pre-Hanford | During Disposal Operations | During Surface Cover Design Life | After Surface Cover Design Life |
| Modified RCRA Subtitle C Cover | NA | NA | 0.1 (0.01, 4.0) | 0.1 (0.01, 4.0) |
| Cover Sideslope | NA | NA | 50 (4.2, 86.4) | 50 (4.2, 86.4) |
| Rupert Sand | 0.9 (0.16, 4.0) | 0.9 (0.16, 4.0) | 0.9 (0.16, 4.0) | 0.9 (0.16, 4.0) |
| Burbank Loamy Sand | 4.2 (2.8, 5.5) | 4.2 (2.8, 5.5) | 4.2 (2.8, 5.5) | 4.2 (2.8, 5.5) |
| Hanford Formation Sediments | NA | 55.4 (50, 86.4) | NA | NA |
| NA = Not applicable. | | | | |

A limited number of sensitivity tests were conducted using numerical simulation. The results showed that the surface cover limited recharge to less than 0.1 mm/yr regardless of the plant type, the presence of plants, or any of the climate change conditions. In contrast, recharge in the Rupert sand showed a significant sensitivity to vegetation type and climate change conditions, but less sensitivity to small variations in hydraulic properties.

Several alternative conceptual models were considered to indicate the effects of conceptual model uncertainty. Under the climate change condition most likely to promote recharge (i.e., increased precipitation and decreased temperature), recharge through the cover remained <0.1 mm/yr in contrast to recharge in Rupert sand, which increased from 2.2 to 27 mm/yr. Replacement of the shrub cover with cheatgrass had no impact on recharge through the surface cover but it increased recharge in Rupert sand from 2.2 to 33.2 mm/yr. Irrigation on the surface cover caused recharge to increase from 0.1 to 26.4 mm/yr as the irrigation efficiency was reduced from 100% to 75%.

Using the available recharge estimates, we identified a set of reasonable bounding rates. The design feature with the largest projected range in performance was the sideslope (4.2 to 87.5 mm/yr). Given that sideslopes could represent a significant fraction of the surface cover footprint, we believe that efforts to improve sideslope performance are warranted.

Planning for FY 2000 includes activities to

- extend the length of record from the lysimeter facility
- estimate recharge rates using tracer data from the borehole samples to be collected in the year 2000

- add needed capability to the simulation model to address multiple plant species, seasonal effects, and snowmelt

- collect vegetation data to fill existing data gaps, including plant water status during the late fall to early spring period, differences in rooting patterns beneath shrubs and in the inter-shrub spaces, and maximum depth of rooting

- initiate a field measurement activity to get site-specific estimates of water status and fluxes within and well below the plant root zone.

Issues remaining to be addressed include the precision of lysimeter leak tests to support the use of lower recharge estimates, possible facility deposition of chloride that could impact tracer analyses, and the importance of temperature and water vapor flow when recharge rate estimates are lower than 1 mm/yr. In addition, the impacts of unstable and preferential flow and flaws in the cover need to be evaluated.

# Acknowledgments

The authors express their gratitude for the helpful comments provided by the reviewers, Dr. John Nimmo of the U.S. Geological Survey in Menlo Park, California; Dr. Bridget Scanlon of the Bureau of Economic Geology at the University of Texas at Austin; and Dr. Glendon Gee at Pacific Northwest National Laboratory. The authors thank the project manager, Dr. Charles Kincaid (PNNL), and the client representative, Dr. Fred Mann (FDNW), for providing guidance and support throughout this multiyear effort. A note of appreciation goes to Jan Tarantino, our tireless and patient editor, and the text processing team: Jean Cheyney, Kay Hass, Trina Russell, and Rose Urbina.

# Contents


Summary ..... iii

Acknowledgments ..... vii

1.0 Introduction ..... 1.1

2.0 Background ..... 2.1

2.1 Source and Destination of ILAW ..... 2.1

2.2 Definition of Recharge ..... 2.1

2.3 Prior Estimates of Recharge at Hanford ..... 2.2

2.4 1998 PA ..... 2.2

2.5 ILAW PA Project Activities ..... 2.3

3.0 Affected Environment ..... 3.1

3.1 Climate and Meteorology ..... 3.1

3.2 Geology and Soils ..... 3.3

3.2.1 Geology ..... 3.4

3.2.2 Soils ..... 3.5

3.3 Hydrology ..... 3.7

3.4 Ecology ..... 3.8

4.0 Disposal Facility Designs ..... 4.1

4.1 Subsurface Disposal Facilities ..... 4.1

4.2 Surface Cover ..... 4.3

4.3 Closure Conditions Around the Surface Cover ..... 4.5

5.0 Analysis Cases and Tests ..... 5.1

5.1 Best Estimate Case ..... 5.1
5.2 Reasonable Bounding Cases ..... 5.2
5.2.1 Lower Bounding Case ..... 5.2
5.2.2 Upper Bounding Cases ..... 5.2
5.3 Sensitivity Tests ..... 5.2
5.4 Uncertainty Tests ..... 5.2
6.0 Recharge Estimation Methods ..... 6.1
6.1 Lysimetry ..... 6.1
6.2 Tracers ..... 6.2
6.3 Modeling ..... 6.4
6.4 Additional Considerations ..... 6.4
7.0 Results ..... 7.1
7.1 Analyses for the Best Estimate and Reasonable Bounding Cases ..... 7.1
7.1.1 Modified RCRA Subtitle C Cover ..... 7.1
7.1.2 Sideslope ..... 7.1
7.1.3 Rupert Sand ..... 7.2
7.1.4 Burbank Loamy Sand ..... 7.3
7.1.5 Hanford Formation Sand ..... 7.4
7.2 Sensitivity Tests ..... 7.4
7.2.1 Vegetation ..... 7.4
7.2.2 Soil Properties ..... 7.4
7.2.3 Climate ..... 7.5
7.3 Uncertainty Tests ..... 7.5

7.3.1 Vegetation Change ..... 7.5

7.3.2 Climate Change ..... 7.6

7.3.3 Irrigation ..... 7.6

7.4 Assignment of Recharge Rates to Scenarios ..... 7.6

7.4.1 Best Estimate Case ..... 7.6

7.4.2 Reasonable Bounding Cases ..... 7.6

7.5 Plans for FY 2000 ..... 7.8

7.6 Remaining Issues ..... 7.9

8.0 Conclusions ..... 8.1

9.0 References ..... 9.1

Appendix A – Field Lysimeter Test Facility Data to Support the 2001 ILAW PA ..... A.1

Appendix B – Recharge Estimates Using Environmental Tracers at the Immobilized Low-Activity Waste Disposal Site ..... B.1

Appendix C – Simulation Estimates of Recharge Rates for the Two ILAW Disposal Sites ..... C.1

Appendix D – Eolian Activity at the ILAW Disposal Site, Central Hanford Site ..... D.1

Appendix E – Evaluation of Anthropogenic Chloride Deposition at the ILAW Disposal Site ..... E.1

Appendix F – Vegetation Data Summary for Supporting Recharge Estimates – FY 1998 and FY 1999 ..... F.1

Appendix G – Quality Assurance and Safety ..... G.1

# Figures


1.1 Map of the Hanford Site and Its Location Within Washington ..... 1.2

1.2 Locations of the ILAW Disposal Site and the Existing Disposal Site Vaults Within the Southeast Corner of 200 East Area at Hanford ..... 1.3

3.1 Soil Types at the Disposal Sites ..... 3.6

3.2 Topography at the Disposal Sites ..... 3.7

3.3 Vegetation Types at the Disposal Sites ..... 3.9

4.1 Grout Disposal Facility—Grout Disposal Vault, Cutaway View ..... 4.1

4.2 Grout Disposal Facility—Closed Vault Pair ..... 4.2

7.1 Aerial View of the New ILAW Disposal Site ..... 7.3


# Tables


S.1 Recharge Estimates for the Best Estimate Case During Each Period of Interest to the ILAW 2001 PA ..... iv

3.1 Monthly Precipitation Variations Between 1946 and 1998 at the HMS ..... 3.2

3.2 Monthly Air Temperature Variations Between 1946 and 1998 at the HMS ..... 3.3

4.1 Summary of Design Criteria for the Modified RCRA Subtitle C Barrier ..... 4.3

4.2 Summary of Modified RCRA Subtitle C Barrier Layers ..... 4.4

5.1 Surface Features To Be Evaluated During Each Period of Interest to the 2001 PA ..... 5.1

7.1 Recharge Estimates for the Best Estimate Case for Disposal Facility Features During Each Period of Interest to the ILAW 2001 PA ..... 7.7

7.2 Recharge Estimates for the Reasonable Bounding Cases During Each Period of Interest to the ILAW 2001 PA ..... 7.7

# 1.0 Introduction

Lockheed Martin Hanford Company (LMHC) is designing and assessing the performance of disposal facilities to receive radioactive wastes that are currently stored in single- and double-shell tanks at the Hanford Site. The preferred method of disposing of the portion that is classified as immobilized low-activity waste (ILAW) is to vitrify the waste and place the product in near-surface, shallow-land burial facilities.

The LMHC project to assess the performance of these disposal facilities is known as the Hanford ILAW Performance Assessment (PA) Activity, hereafter called the ILAW PA project. The goal of this project is to provide a reasonable expectation that the disposal of the waste was protective of the general public, groundwater resources, air resources, surface-water resources, and inadvertent intruders. Achieving this goal will require predictions of contaminant migration from the facility. To make such predictions will require estimates of the fluxes of water moving through the sediments within the vadose zone around and beneath the disposal facility. These fluxes, loosely called recharge rates, are the primary mechanism for transporting contaminants to the groundwater.

Pacific Northwest National Laboratory (PNNL) assists LMHC in their performance assessment activities. One of the PNNL tasks is to provide estimates of recharge rates for current conditions and long-term scenarios involving the shallow-land disposal of ILAW (LMHC 1999).

The ILAW 1998 PA examined the long-term environmental and human health effects associated with the planned disposal of the vitrified low-level fraction of the waste presently contained in the Hanford high-level waste tanks (Mann et al. 1998). In support of that PA, Rockhold et al. (1995) provided estimates of recharge rates using historical data. Since then, the ILAW project has made significant investments in site-specific data collection. In addition to the ILAW activities, other projects have collected data that are relevant to the ILAW disposal. In preparation for a revision of the ILAW PA, called the 2001 PA, a number of data packages are being prepared (LMHC 1999). These packages will bring together recently collected site-specific ILAW data as well as relevant data collected by other projects.

Figure 1.1 shows the boundaries and major facilities of the Hanford Site (PNNL 1999). Figure 1.2 shows the locations of the two disposal sites that are being considered (Mann 1999): the ILAW Disposal Site (located southwest of the PUREX Plant) and the Existing Disposal Site (located east of the PUREX plant and formerly known as the Grout Vaults). For each disposal site, recharge rate estimates are needed for a fully functional surface cover, the cover sideslope, and the immediately surrounding terrain. In addition, recharge estimates are needed for degraded cover conditions. Mann (1999) indicated that the temporal scope of the ILAW 2001 PA is 10,000 years, but could be longer if some contaminant peaks occur after 10,000 years.

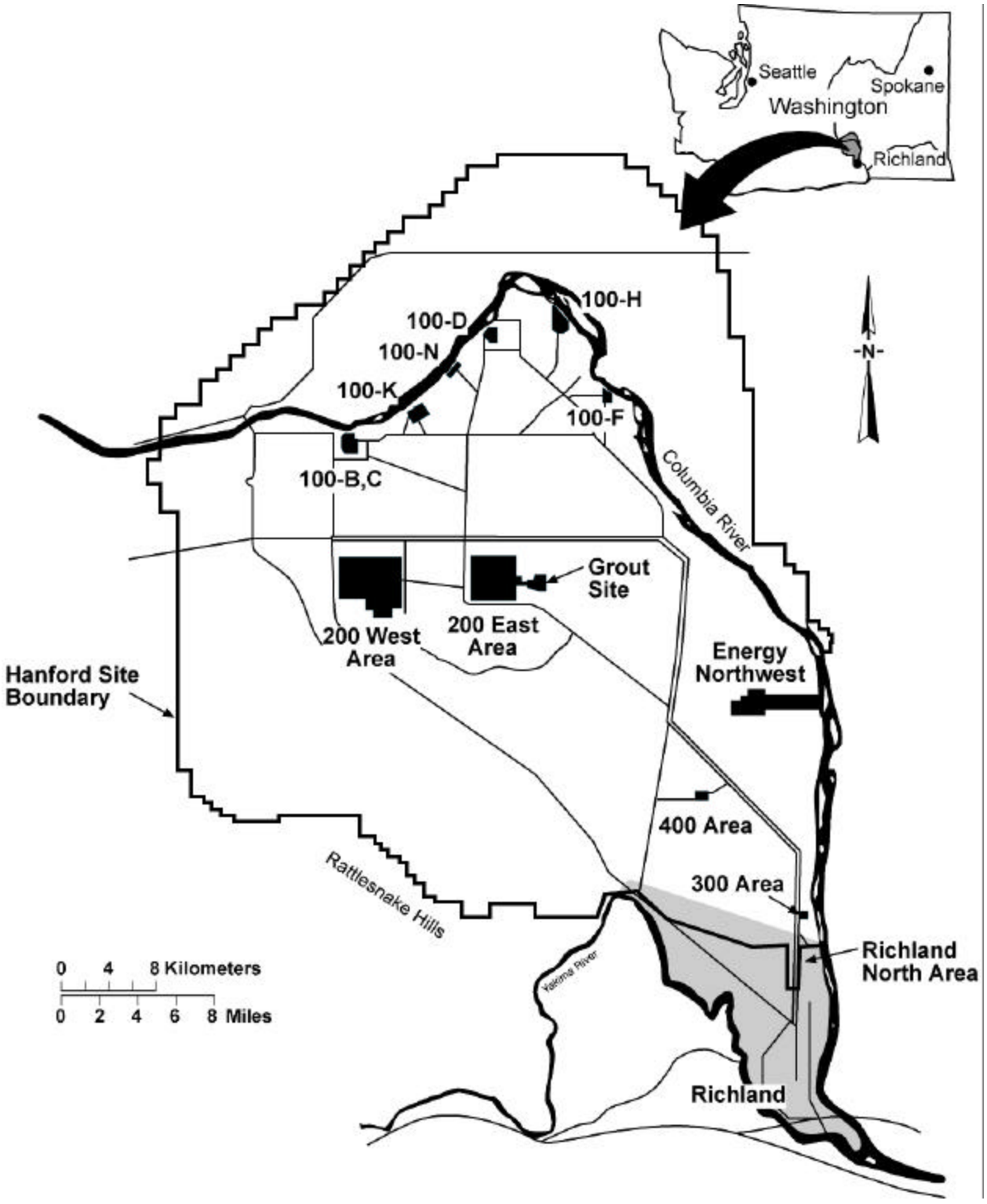


**Figure 1.1**. Map of the Hanford Site and Its Location Within Washington

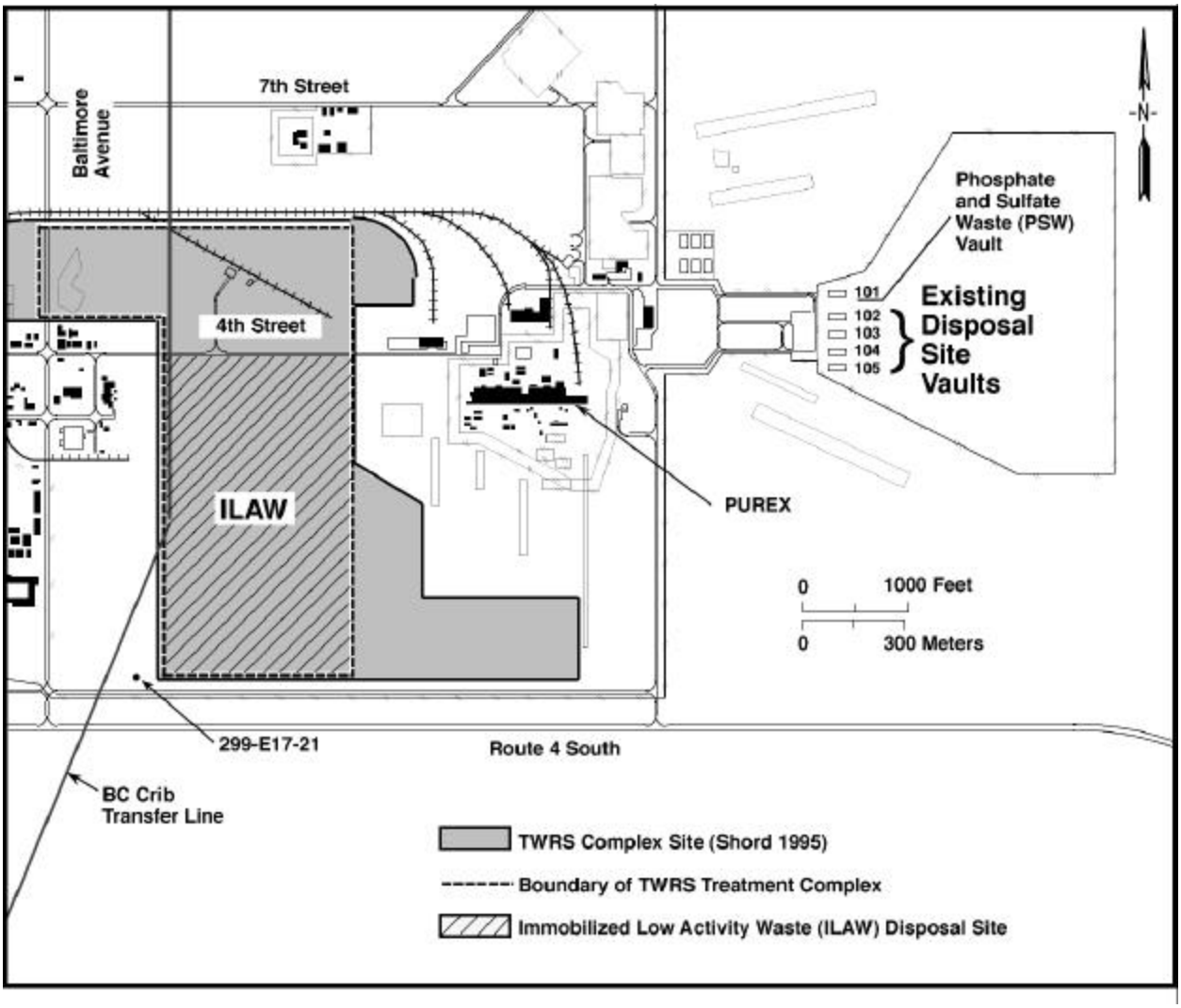


**Figure 1.2**. Locations of the ILAW Disposal Site and the Existing Disposal Site Vaults Within the Southeast Corner of the 200 East Area at Hanford. The ILAW Disposal Site is part of the Tank Waste Remediation Systems (TWRS) Treatment Complex, which lies within the larger TWRS Complex Site.

The elements of this report make up the Recharge Data Package. The objective of this data package is to provide recharge estimates for the scenarios being considered in the 2001 PA. Multiple estimation techniques were used to satisfy the objective, including lysimetry, tracer studies, and modeling studies. The report identifies how the data were used to generate recharge rate estimates for the best estimate case and reasonable bounding cases, as well as indicate the uncertainties in these estimates.

# 2.0 Background

The Hanford Site was established in 1944 as a U.S. Government nuclear materials production facility. During its history, Site missions included nuclear reactor operation, storage and reprocessing of spent nuclear fuel, and management of radioactive and hazardous wastes. Today, activities on the Site involve environmental restoration, energy-related research, and technology development. Fifty-five years of operations have resulted in the accumulation of significant quantities of radioactive and hazardous wastes as well as their intentional and unintentional release to the environment.

## 2.1 Source and Destination of ILAW

The legacy of the earlier Hanford missions consists of more than 209,000 $m^3$ of radioactive and mixed waste stored in 177 buried single- and double-shell tanks in the Hanford Site 200 Areas (Mann et al. 1998). This waste will be retrieved and separated into two fractions: high-level waste to be sent to a federal geologic repository and low-activity waste to be immobilized (i.e., ILAW) and placed in a near-surface disposal system on site. Immobilization will be accomplished through the vitrification process, which will turn the waste slurry into a glass product. Some of the more important radionuclides include $^{79}Se$, $^{90}Sr$, $^{99}Tc$, $^{129}I$, $^{126}Sn$, and $^{137}Cs$, as well as isotopes and progeny of uranium, plutonium, neptunium, and americium (Mann et al. 1998).

Although plans are not final, some form of glass product will be produced and placed in metal containers. These containers will be stacked within belowground disposal vaults. The spaces between containers will be filled with something like sand and the top of the vault sealed with a controlled density fill. A protective surface cover will be constructed over the vaults prior to closure.

## 2.2 Definition of Recharge

The precise definition of recharge is that flux of water reaching ("recharging") the water table. We have no effective way of measuring recharge at the water table, so we resort to shallow unsaturated measurements and analyses. With these, we estimate the deep drainage flux, i.e., that flux leaving the evapotranspiration zone and ostensibly traveling to the water table. Given sufficient time, the deep drainage flux will eventually manifest itself as the recharge flux. However, when deep drainage fluxes change, the change may not be manifested at the water table for hundreds to thousands of years. The length of time will depend on the vadose zone thickness and hydraulic properties and the initial and final deep drainage rates. Sediment stratification can lengthen that time further.

For the 2001 PA, scenarios involving changes in recharge rates should address the time delay between deep drainage rate changes and changes in the flux reaching the water table.

## 2.3 Prior Estimates of Recharge at Hanford

In the early years of the Hanford Site, the perception was that recharge occurred only along the upper elevations of Rattlesnake Mountain and the valleys to the north, and it did not occur across the remainder of the Site. The Hanford Defense Waste Environmental Impact Statement assumed that natural recharge was essentially zero in and around the storage and disposal areas (DOE 1987). A panel of nationally recognized scientists was convened in 1985 to discuss the recharge issue. The reviewers disputed the notion of zero recharge. Data collected before and after the 1985 review showed clearly that recharge can and does occur under favorable conditions. Gee et al. (1992) presented evidence that recharge rates can vary from nearly zero in silt loam soils covered by sagebrush to more than 100 mm/yr in gravel-covered soils without vegetation.

Rockhold et al. (1995) presented a review of past work related to recharge. Appendix B of their report describes the numerous studies conducted since 1969 using field measurements of soil water, matric potential, and temperature; tracer measurements; lysimeter measurements; and numerical modeling. All of these studies showed the potential for recharge to occur if conditions are right (i.e., coarse-textured rather than fine-textured soil, sparse plant community, and shallow-rooted rather than deep-rooted plants).

## 2.4 1998 PA

Mann et al. (1998) is commonly referred to as the 1998 PA. It was the initial effort to demonstrate the feasibility of safely disposing of ILAW at the Hanford Site. Because the ILAW PA project was only just beginning, the analyses were conducted using reasonable estimates of the parameters without having site-specific information. The intention was to initiate a program to collect data relevant to the actual disposal sites and glass product (see next section).

In lieu of site-specific data, Rockhold et al. (1995) assembled their best estimate of recharge rates to use in the 1998 PA (called the preliminary PA in 1995). Their recommendations were

> "The existing recharge data were used to provide recharge estimates that can be used in preliminary performance assessment calculations. Estimates are provided for the barrier, the barrier edge, the surrounding natural ecosystem, and the entire Hanford Site. We recommend assuming a recharge rate of 0.5 mm/yr through the Hanford protective barrier. This assumption is supported by an 8-year record of lysimeter data (Table 3.1) and is consistent with engineering design specifications over the 1000-year design life of the barrier (Wing 1994). At the barrier edge, a higher recharge rate of 75 mm/yr should be assumed. This assumption is based on four years of data for a lysimeter with a graveled surface (Table 3.1) that is similar to the riprap sideslope of the protective barrier. This estimate does not include possible overland flow or lateral drainage from the barrier. Beyond the barrier, the recharge rate of the natural ecosystem can be represented with one of two rates. If the plant community is assumed to be sagebrush, an estimate of 5.0 mm/yr should be used. This is a conservative value chosen to be slightly greater than all the rates reported by Prych (1995) using tracer measurements. If the plant community is assumed to be cheatgrass, an estimate of 25.4 mm/yr should be used. This value is based on an 8-year record of water content observations at the Grass

Site in the 300 Area (Fayer and Walters 1995). For the entire Hanford Site, we recommend using the recharge distribution map reported by Fayer and Walters (1995)."

## 2.5 ILAW PA Project Activities

Shortly after publication of Rockhold et al. (1995), a panel of nationally recognized scientists was convened to review the ILAW project needs for recharge information. The panel concluded that enough information existed to proceed with the 1998 PA, but that site-specific data would be needed to provide technically defensible estimates.[(a)] They supported efforts to use lysimetry, tracers, and modeling. The panel noted that the results might not change the recharge estimates significantly but would strengthen the technical credibility of the final recharge estimates used in the performance assessment. The panel also cautioned that uncertainty in conceptual models and supporting data should not be ignored.

Since 1995, the ILAW PA project has conducted several studies to improve the estimates of natural recharge. These studies included direct measurements of recharge using lysimetry (Appendix A), tracer evaluations of recharge (Appendix B), and numerical simulations of recharge (Appendix C). In addition to these basic studies, the ILAW PA project also supported auxiliary studies. Appendix D analyzes the origin of sand dunes at Hanford and summarizes the results of trenching a dune along the southern edge of the new ILAW Disposal Site. Appendix E describes the results of surface sediment sampling to determine the possibility of deposition of facility emissions (and their possible impact on tracer analyses). Appendix F summarizes the results of vegetation studies designed to characterize the current plant community at the disposal sites and provide better parameters for numerical simulations of recharge. Appendix G briefly summarizes the Quality Assurance Plan.

(a) Honeyman, JO. 1995. Letter to L Erickson transmitting the results of the 1995 workshop entitled "Summary of peer review comments resulting from the second Hanford groundwater recharge workshop." May 22-23, 1995, Richland, Washington.

# 3.0 Affected Environment

An adequate evaluation of the impacts of ILAW disposal requires an understanding of the environment within which the ILAW will be disposed. In this section, we have summarized information on the climate and meteorology, geology and soils, hydrology, and ecology. Portions of this summary were extracted from existing reports, including Neitzel et al. (1998), Hoitink et al. (1999), and Reidel and Horton and Horton and Reynolds (1998). For brevity, references in the original text were not included here.

The Hanford Site lies within the semiarid Pasco Basin of the Columbia Plateau in southeastern Washington State (Figure 1.1). The Hanford Site occupies an area of about 1450 $km^2$ (~560 $mi^2$); only about 6% of the land area has been disturbed and is actively used for the storage of nuclear materials, waste storage, and waste disposal. The Columbia River flows through the northern part of the Hanford Site and forms part of the Site's eastern boundary. The Yakima River runs near the southern boundary of the Hanford Site and joins the Columbia River at the city of Richland, which bounds the Hanford Site on the southeast. Rattlesnake Mountain, Yakima Ridge, and Umtanum Ridge form the southwestern and western boundaries. The Saddle Mountains form the northern boundary of the Hanford Site. Two small east-west ridges, Gable Butte and Gable Mountain, rise above the plateau of the central part of the Hanford Site. Adjoining lands to the west, north, and east are principally range and agricultural land. The cities of Kennewick, Pasco, and Richland (Tri-Cities) constitute the nearest population centers and are located southeast of the Hanford Site.

## 3.1 Climate and Meteorology

The Cascade Mountains, 100 km to the west, greatly influence the climate of the Hanford area by means of their "rain shadow" effect. This mountain range also serves as a source of cold air drainage, which has a considerable effect on the wind regime on the Hanford Site. Climatological data have been collected at the Hanford Meteorological Station (HMS) since 1945 (Hoitink et al. 1999). The HMS is located between the 200 East and 200 West Areas at an elevation of 223 m. The data are representative of the general climatic conditions for the region and describe the specific climate of the 200 Area Plateau. The two ILAW disposal sites are close to the HMS and at nearly the same elevation.

**Precipitation**. Between 1946 and 1998, annual precipitation at the HMS averaged 174 mm (6.89 in.) and varied between 76 and 313 mm. Table 3.1 shows how monthly averages have varied in that time. The wettest season on record was the winter of 1996-1997 with 141 mm (5.4 in.) of precipitation; the driest season was the summer of 1973 when only 1 mm (0.03 in.) of precipitation was measured. Most precipitation occurs during the winter, with more than half of the annual amount occurring from November through February. Days with more than 13 mm (0.5 in.) precipitation occur on average less than one time each year. Rainfall intensities of 13 mm/h (0.5 in./h) persisting for 1 hour are expected once every 10 years. Rainfall intensities of 25 mm/h (1 in./h) for 1 hour are expected only once every 500 years.

**Table 3.1**. Monthly Precipitation Variations Between 1946 and 1998 at the HMS

| Month | Monthly Precipitation (mm) | | |
|---|---|---|---|
| | Maximum | Mean | Minimum |
| January | 62.7 | 23.6 | 2.0 |
| February | 53.3 | 16.0 | 0.0 |
| March | 47.2 | 13.0 | 0.5 |
| April | 39.1 | 11.4 | 0.0 |
| May | 51.6 | 13.5 | 0.0 |
| June | 74.2 | 13.5 | 0.0 |
| July | 44.7 | 5.6 | 0.0 |
| August | 34.5 | 6.1 | 0.0 |
| September | 34.0 | 8.1 | 0.0 |
| October | 69.1 | 14.0 | 0.0 |
| November | 67.8 | 23.1 | 0.0 |
| December | 93.7 | 25.7 | 2.8 |
| Annual | | 173.5 | |

Monthly average snowfall ranges from 8 mm (0.32 in.) in March to 137 mm (5 in.) in December. The record monthly snowfall of 600 mm (23.4 in.) occurred in January 1950. The seasonal record snowfall of 1420 mm (56 in.) occurred during the winter of 1992–1993. Snowfall accounts for about 38% of all precipitation from December through February.

**Air Temperature**. Daily maximum temperatures vary from normal maxima of 2°C (35°F) in late December and early January to 35°C (95°F) in late July. There are, on the average, 52 days during the summer months with maximum temperatures ≥32°C (90°F) and 12 days with maxima ≥38°C (100°F). From mid-November through early March, minimum temperatures average ≤0°C (32°F), with the minima in late December and early January averaging -6°C (21°F). During the winter, there are, on average, 3 days with minimum temperatures ≤-18°C (~0°F); however, only about one winter in two experiences such temperatures. The record maximum temperature is 45°C (113°F), and the record minimum temperature is -31°C (-23°F). Table 3.2 shows the range of monthly temperatures since 1946. The highest winter monthly average temperature at the HMS was 6.9°C (44°F) in February 1958, while the record lowest average temperature was -11.1°C (12°F) during January 1950. The record maximum summer monthly average temperature was 27.9°C (82°F) in July 1985, while the record lowest average temperature was 17.2°C (63°F) in June 1953.

**Humidity**. Since 1950, the average annual relative humidity at the HMS has been 54%; annual values ranged from 49 to 59%. December had the highest monthly average humidity (80%), with values that ranged from 69 to 91%. July had the lowest monthly average humidity (33%), with values that ranged from 22 to 46%.

**Table 3.2**. Monthly Air Temperature Variations Between 1946 and 1998 at the HMS

| Month | Monthly Air Temperature (°C) | | |
|---|---|---|---|
| | Maximum | Mean | Minimum |
| January | 5.8 | -0.8 | -11.1 |
| February | 6.9 | 3.1 | -3.6 |
| March | 10.8 | 7.3 | 4.1 |
| April | 14.6 | 11.6 | 8.6 |
| May | 13.3 | 16.6 | 13.3 |
| June | 24.9 | 20.7 | 17.2 |
| July | 27.9 | 24.7 | 21.4 |
| August | 27.5 | 23.9 | 21.0 |
| September | 22.4 | 19.0 | 14.9 |
| October | 15.3 | 11.7 | 8.8 |
| November | 8.1 | 4.5 | -4.0 |
| December | 3.6 | 0.2 | -6.1 |
| Annual | | 11.9 | |

**Solar Radiation**. Since 1953, the average annual daily solar radiation at the HMS has been 172 $W/m^2$ (355 ly). Daily values were lowest in December, ranging from 4.4 to 95 $W/m^2$ and having an average value of 85 $W/m^2$. Average daily values were highest in July (305 $W/m^2$), but the highest daily value occurred in May (406 $W/m^2$).

**Wind**. Prevailing wind directions on the 200 Area Plateau are from the northwest in all months of the year. Secondary maxima occur for southwesterly winds. Summaries of wind direction indicate that winds from the northwest quadrant occur most often during the winter and summer. During the spring and fall, the frequency of southwesterly winds increases with a corresponding decrease in northwest flow. Winds blowing from other directions (e.g., northeast) display minimal variation from month to month. Monthly average wind speeds are lowest during the winter months, averaging 10 to 11 km/h (6 to 7 mi/h), and highest during the summer, averaging 13 to 15 km/h (8 to 9 mi/h). Wind speeds that are well above average are usually associated with southwesterly winds. However, the summertime drainage winds are generally northwesterly and frequently reach 50 km/h (30 mi/h). These winds are most prevalent over the northern portion of the Hanford Site.

## 3.2 Geology and Soils

Reidel and Horton and Horton (1999) provides a detailed description of the geology of the Hanford Site and the two ILAW disposal sites. A brief geology description is presented here to assist those readers who may not have access to Reidel and Horton and Horton (1999).

The Hanford Site lies within the Columbia Plateau, which is formed from a thick sequence of basalt flows. These flows have been folded and faulted over the past 17 million years, creating broad structural and topographic basins separated by asymmetric anticlinal ridges. Sediments up to 518 m (1700 ft) thick have accumulated in some of these basins. The basalt flows are exposed along the anticlinal ridges,

where they have been uplifted as much as 1097 m (3600 ft) above the surrounding area. Filling the synclinal basins in the basalt flows are sediments of the late Miocene, Pliocene, and Pleistocene age. The Hanford Site lies within one of the larger basins, the Pasco Basin. The Pasco Basin is bounded on the north by the Saddle Mountains and on the south by Rattlesnake Mountain and the Rattlesnake Hills. Yakima Ridge and Umtanum Ridge trend into the basin and subdivide it into a series of smaller anticlinal ridges and synclinal basins. The largest syncline, the Cold Creek syncline, lies between Umtanum Ridge and Yakima Ridge and is the principal structure containing the DOE waste management areas.

### 3.2.1 Geology

The two ILAW disposal sites are situated on the Cold Creek bar, a geomorphic remnant of the cataclysmic floods of the Pleistocene epoch. As the floods raced across the lowlands of the Pasco Basin and Hanford Site, the flood waters lost energy and began leaving behind deposits of gravels. The disposal sites are about 3 km (2 mi) north of the axis of the Cold Creek syncline, which controls the structural grain of the basalt bedrock and Ringold Formation. The basalt surface and Ringold Formation trend roughly southeast-northwest parallel to the major geologic structures of the site. As a result, the Ringold Formation and the underlying basalt dip gently to the south off the Umtanum Ridge anticline into the Cold Creek syncline. Geologic mapping at the Hanford Site has not identified any faults in the vicinity of the ILAW disposal sites. The closest faults are along the Umtanum Ridge-Gable Mountain structure north of the site and the May Junction fault east of the site.

The stratigraphy of the ILAW disposal sites consists of the basalt flows overlain by the Ringold Formation, the Hanford formation, and Holocene eolian deposits. All recharge-related measurements and estimates occur within the Hanford formation and eolian deposits; they are described below.

**Hanford Formation**. The Hanford formation is an informal name that represents all the deposits of the cataclysmic floods of the Pleistocene (1.6 million to 13,000 years ago). Glacial Lake Missoula formed in the Clark Fork River valley in Montana behind continental glaciers that spread south as far as the present Columbia Plateau. The lake may have given way as many as 40 times in the late Pleistocene, allowing the impounded water to spread across eastern Washington and form the Channeled Scablands. These flood waters collected in the Pasco Basin and formed Lake Lewis, which slowly drained through the small water gap in the Horse Heaven Hills called Wallula Gap.

Three principal types of deposits were left behind by the Missoula Floods: 1) high-energy deposits consisting of gravel; 2) coarse to fine sand deposits representing an energy transition environment; and 3) low-energy, slackwater deposits consisting of rhythmically bedded silt and sand of the Touchet Beds. Gravel-dominated strata consist of coarse-grained sand and granule-to-boulder gravels that display massive bedding, plane to low-angle bedding, and large-scale cross-bedding in outcrop. Sometimes the gravel strata lack a matrix material; such gravel strata have an open-framework appearance. The sand-dominated facies consists of fine- to coarse-grained sand and granules that display plane lamination and bedding and, less commonly, plane and trough cross-bedding in outcrop. Small pebbles and pebbly interbeds (<20 cm [8 in.] thick) may be encountered. The silt content of these sands varies, although where its content is low, an open-framework texture may occur. The silt-dominated facies consists of

fine- to coarse-grained sand grading up to silt to form normally graded rhythmites 0.07 to 1.0 m thick. Plane lamination and ripple cross-lamination is common in outcrop.

The Hanford formation is about 90 m (300 ft) thick at the ILAW disposal sites and consists predominantly of sands and gravelly sands. The sandy sequence is interpreted to lie between a slightly gravelly sand and a lower sandy gravel to gravelly sand. The Hanford formation thickens both to the north and south of the site. The lower gravel to gravelly sand is about 35 m (115 ft) thick and probably thins to the east on an irregular Ringold surface. The water table is in this lower gravel sequence. The Hanford formation sandy sequence is about 60 m (200 ft) thick and is the dominant facies in the ILAW disposal areas. The upper 6 m (20 ft) is composed of an irregularly distributed gravelly sand sequence. At other locations at Hanford, vertically oriented sediment features known as clastic dikes cut across the typically horizontal sediment layers (Fecht et al. 1999). These dikes could act as preferential pathways for water and contaminant transport. Clastic dikes have not yet been observed at the ILAW, probably because most of the area remains untouched by construction activities.

**Holocene Deposits**. Holocene deposits consisting of silt, sand, and gravel form a thin (<5 m [16 ft]) veneer across much of the Hanford Site as well as the ILAW disposal sites. The southern 200 m (656 ft) of the new ILAW Disposal Site is covered with a stabilized sand dune that is as much as 8 m (26 ft) high. Appendix D describes the nature of the dune and its relationship to the active dune field that lies to the south and southeast. Mature sagebrush is present on the ILAW sand dune, indicating that the dune has been stable since the 1940s at least. Clastic dike features are not visible on the soil surface.

### 3.2.2 Soils

The Holocene deposits and exposed Hanford formation sediments have experienced soil development and evolved into identifiable soil types. Hajek (1966) produced a soil map of the Hanford Site. Figure 3.1 shows that only two soil types cover the ILAW disposal sites: Rupert sand and Burbank loamy sand. These soils were described by Hajek (1966) as follows:

> **Rupert Sand**. "This mapping unit represents one of the most extensive soils on the Hanford Project. The surface is a brown to grayish brown (10YR5/2) coarse sand, which grades to a dark grayish brown (10YR4/2) sand at about 36 in. Rupert soils developed under grass, sagebrush, and hopsage in coarse sandy alluvial deposits, which were mantled by wind-blown sand. Relief characteristically consists of hummocky terraces and dune-like ridges. This soil may be correlated as Quincy sand, which was not separated here. Active sand dunes are present. Some dune areas are separated; however, many small dunes, blow-outs, and associated small areas of Ephrata and Burbank soils are included."
>
> **Burbank Loamy Sand**. "This is a dark-colored [surface is very dark grayish brown (10YR3/2); subsoil is dark grayish brown (10YR4/2)], coarse-textured soil which is underlain by gravel. The surface soil is usually about 16 in. thick but can be 30 in. thick. The gravel content of the subsoil may range from 20 to 80 volume percent. Areas of Ephrata and Rupert are included."

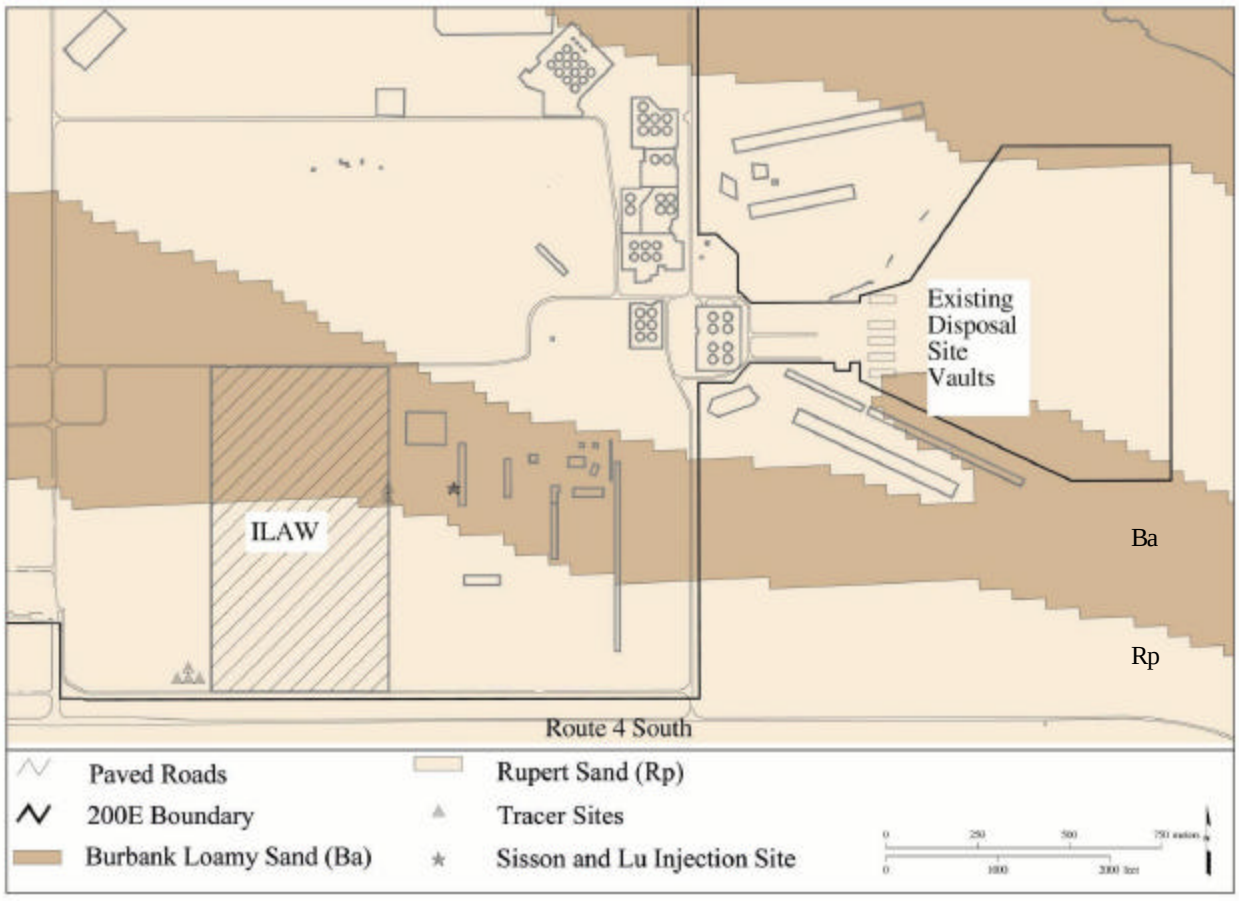


**Figure 3.1**. Soil Types at the Disposal Sites

Figure 3.2 shows that the topography of the two sites is similar. At the new ILAW Disposal Site, the topography is relatively flat with elevations that range between 219 and 222 m. The dune along the southern edge rises above the surrounding terrain by as much as 9 m, with a peak elevation of about 229 m. The eastern most portion of the dune has been excavated for other construction purposes. The remaining portion of the dune is not expected to exist once construction is completed.

Elevations at the Existing Disposal Site range between 204 to 206 m, about 15 m below the ILAW Disposal Site. Figure 3.2 shows the excavation for the existing disposal facility and the spoils pile directly to the east. About 300 m to the north, the topography drops off to the northeast with a slope reaching as high as 7%. The relative flatness of both disposal locations means that the final topography will be determined by the surface cover and grading of the surrounding soils.

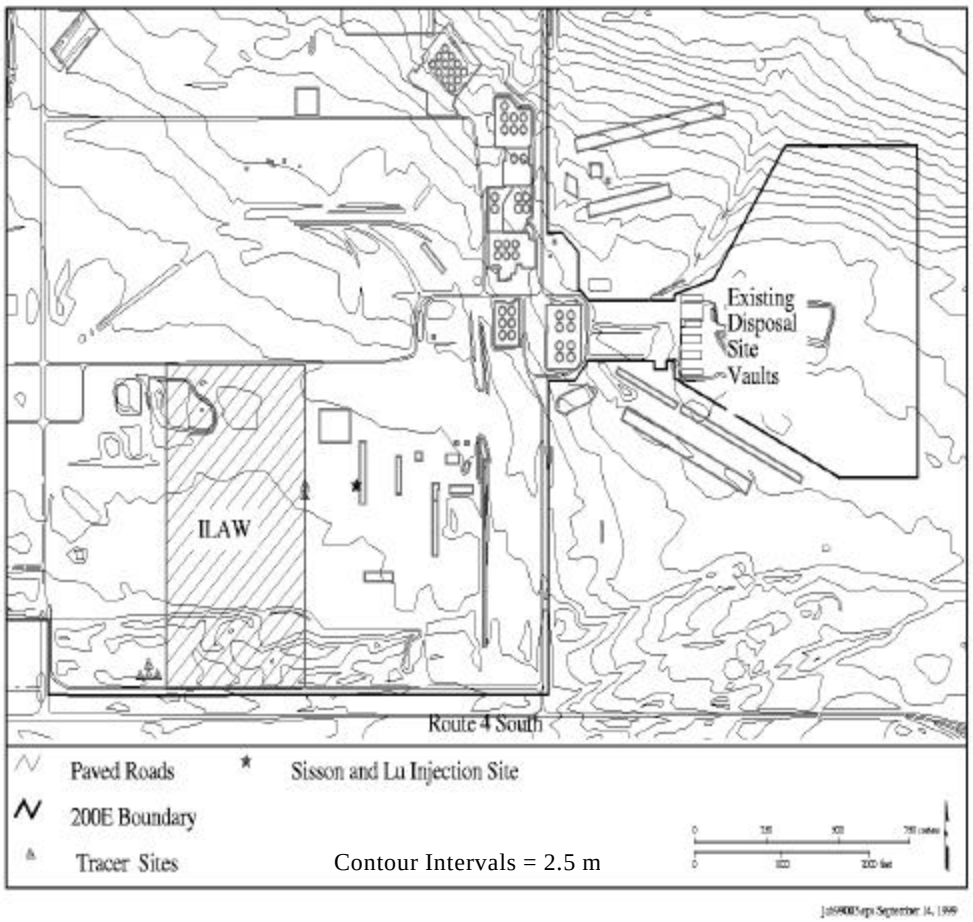


**Figure 3.2**. Topography at the Disposal Sites

## 3.3 Hydrology

The primary surface-water features associated with the Hanford Site are the Columbia and Yakima rivers. The Columbia River is the second largest river in the contiguous United States in terms of total flow and is the dominant surface-water body on the Hanford Site. Annual flows near Priest Rapids Dam just upstream of Hanford averaged nearly 3360 $m^3/s$ (120,000 $ft^3/s$) during the 68 years prior to 1985. The Yakima River, which follows a small length of the southern boundary of the Hanford Site, has an average annual flow of only about 104 $m^3/s$ (3712 $ft^3/s$) based on nearly 60 years of records. Cold Creek and its tributary, Dry Creek, are ephemeral streams within the Yakima River drainage system. Both streams drain areas along the western part of the Hanford Site. Surface flow, which may occur during spring runoff or after heavier-than-normal precipitation, infiltrates and disappears into the surface sediments. The ILAW disposal sites are located well above and away from these surface-water features and are unaffected by them in any direct manner.

Natural recharge rates across the Hanford Site range from near 0 to more than 100 mm/yr (4 in./yr), depending on surface conditions (Gee et al. 1992). Low recharge rates occur in fine-textured sediments

where deep-rooted plants occur. The larger values are interpreted to occur in areas having a coarse gravelly surface and no vegetative cover (e.g., disturbed areas such as around the tank farms).

The hydrogeology of the Pasco Basin is characterized by several confined aquifers within the basalt flows and one unconfined aquifer above the basalt flows. The aquifer above the basalt is a regionally unconfined and locally semi-confined aquifer and is contained largely within the sediments of the Ringold Formation and Hanford formation.

The water table beneath the ILAW disposal sites is within the Hanford formation. Normally, groundwater flows from west to east. However, artificial recharge from wastewater disposal activities has perturbed the flow directions. Currently, the water table is flat beneath the ILAW disposal sites, so a groundwater flow direction cannot be deduced. As wastewater discharges decrease and eventually cease, we expect the general west-to-east flow to resume.

The unsaturated zone beneath the land surface at the two ILAW disposal sites is approximately 96 m (315 ft) thick. This vadose zone lies entirely within the Hanford formation and eolian sediments. The water table in the northeast corner of the new ILAW Disposal Site was at an elevation of approximately 120 m (400 ft) in 1998. The water table surface was within the lower gravel sequence of the Hanford formation; the contact between the Hanford and Ringold formations is 6 m (20 ft) below the water table.

## 3.4 Ecology

The Hanford Site is characterized as a shrub-steppe ecosystem that is adapted to the region's mid-latitude semiarid climate. Such ecosystems are typically dominated by a shrub overstory with a grass understory. In the early 1800s, dominant plants in the area were big sagebrush (*Artemisia tridentata*) and an understory consisting of perennial Sandberg's bluegrass (*Poa sandbergii*) and bluebunch wheatgrass (*Pseudoregneria spicata*). Other species included threetip sagebrush, bitterbrush, gray rabbitbrush, spiny hopsage, bluebunch wheatgrass, needle-and-thread grass, Indian ricegrass, and prairie Junegrass.

With the advent of settlement, livestock grazing and agricultural production contributed to colonization by non-native vegetation species that currently dominate portions of the landscape. Although agriculture and livestock production were the primary subsistence activities at the turn of the century, these activities ceased when the Site was designated in 1943. Range fires that historically burned through the area during the dry summers eliminate fire-intolerant species (e.g., big sagebrush) and allow more opportunistic and fire resistant species to establish. Of the 590 species of vascular plants recorded for the Hanford Site, approximately 20% are non-native. The dominant non-native species, cheatgrass, is an aggressive colonizer and has become well established across the site. Over the past decade, several knapweed species have also become persistent invasive species in areas not dominated by shrubs.

The plant community at the two ILAW disposal sites is shrub-steppe dominated by big sagebrush, Sandberg's bluegrass, and cheatgrass. Figure 3.3 shows that most of the new ILAW Disposal Site has this cover but that the Existing Disposal Site has a significant fraction of area where disturbance occurred

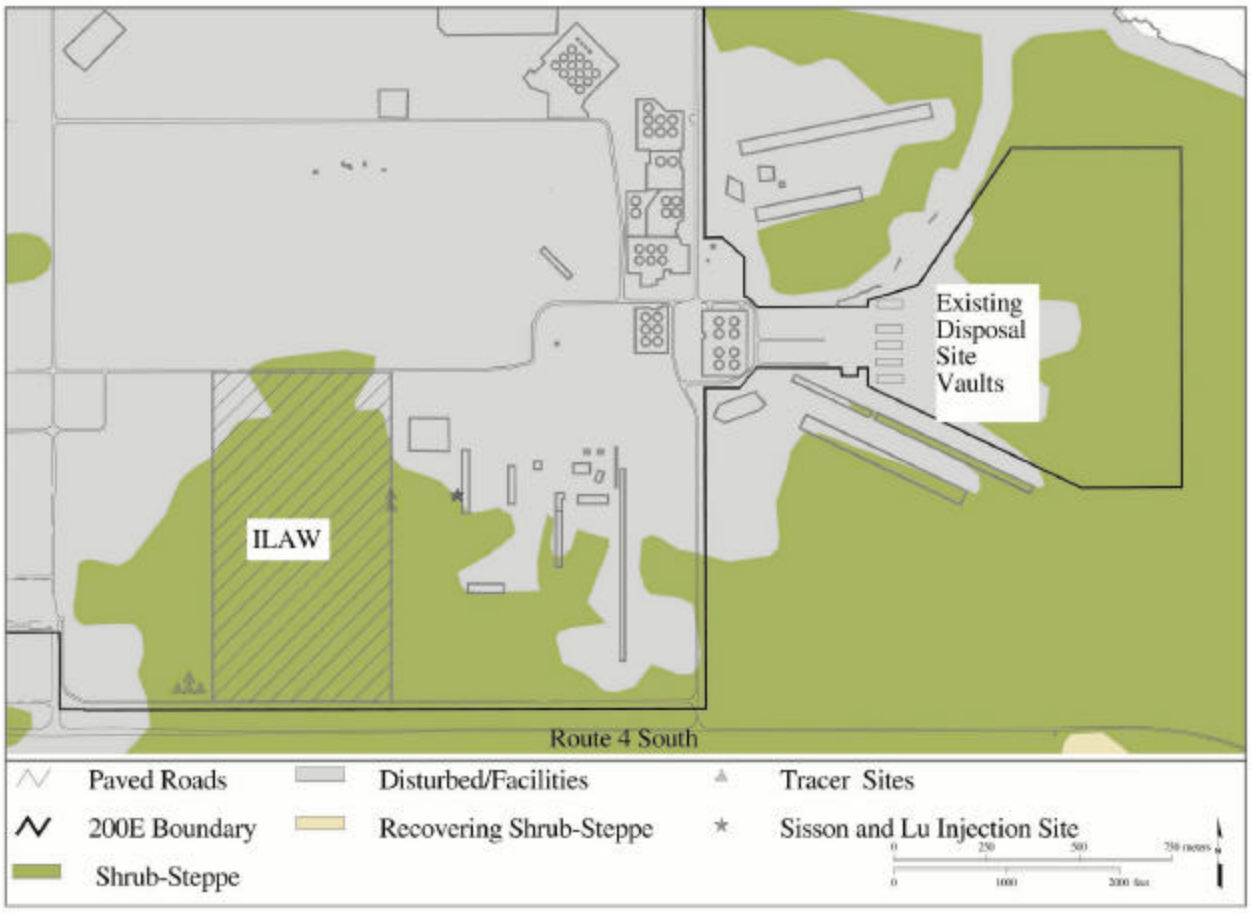


**Figure 3.3**. Vegetation Types at the Disposal Sites

during construction of the vaults. Appendix F describes some of the data collected recently to characterize the plant community at these two sites.

Approximately 300 species of terrestrial vertebrates have been observed on the Hanford Site, including approximately 40 species of mammals, 246 species of birds, 4 species of amphibians, and 9 species of reptiles. Terrestrial wildlife include Rocky Mountain elk, mule deer, coyote, bobcat, badger, deer mice, harvest mice, grasshopper mice, ground squirrels, voles, and black-tailed jackrabbits. The most abundant mammal on the Site is the Great Basin pocket mouse. Bird species commonly found in the shrub-steppe habitats at Hanford include the western meadowlark, horned lark, long-billed curlew, vesper sparrow, sage sparrow, sage thrasher, loggerhead shrike, and burrowing owls.

Butterflies, grasshoppers, and darkling beetles are among the more conspicuous of the approximately 1500 species of insects that have been identified from specimens collected on the Hanford Site. The actual number of insect species occurring on the Hanford Site may reach as high as 15,000. Insects are more readily observed during the warmer months of the year.

The side-blotched lizard is the most abundant reptile species that occurs on the Hanford Site. Short-horned and sagebrush lizards are reported, but occur infrequently. The most common snake species includes gopher snake, yellow-bellied racer, and Pacific rattlesnake. The Great Basin Spadefoot Toad, Woodhouse's Toad, Pacific tree frog, and bullfrogs are the only amphibians found on the Site.

Wildlife species observed at the two ILAW disposal sites include mule deer, black-tailed jackrabbits, cottontail rabbits, coyotes, side-blotched lizards, gopher snakes, sage sparrows, shrikes, meadowlarks, and horned larks.

# 4.0 Disposal Facility Designs

The ILAW will be disposed in vaults and trenches at two locations within the 200 East Area at Hanford. Once completed, both burial facilities will receive a final surface cover and the surrounding land will be re-vegetated.

## 4.1 Subsurface Disposal Facilities

The two disposal facilities for ILAW are the Existing Disposal Site (formerly the Grout Site) and the proposed new ILAW Disposal Site (Figure 1.2).

**Existing Disposal Facility**. The existing disposal facility consists of five subsurface concrete vaults that were built and completed by 1995. Kincaid et al. (1995) described the site and facility extensively. One of the vaults was completed prior to the others and received a grouted waste called phosphate-sulfate waste. The remaining four vaults were built in pairs but never used. Figure 4.1 shows the engineered nature of these vaults. Figure 4.2 shows how the vaults were arranged in pairs. Spacing between each vault is roughly 10 m. The total areal extent of the four empty vaults is about 40 by 90 m. The vaults are currently covered with gravel as indicated just below the RCRA cover in Figure 4.2, but the protective barrier and RCRA cover shown in Figure 4.2 were never placed.

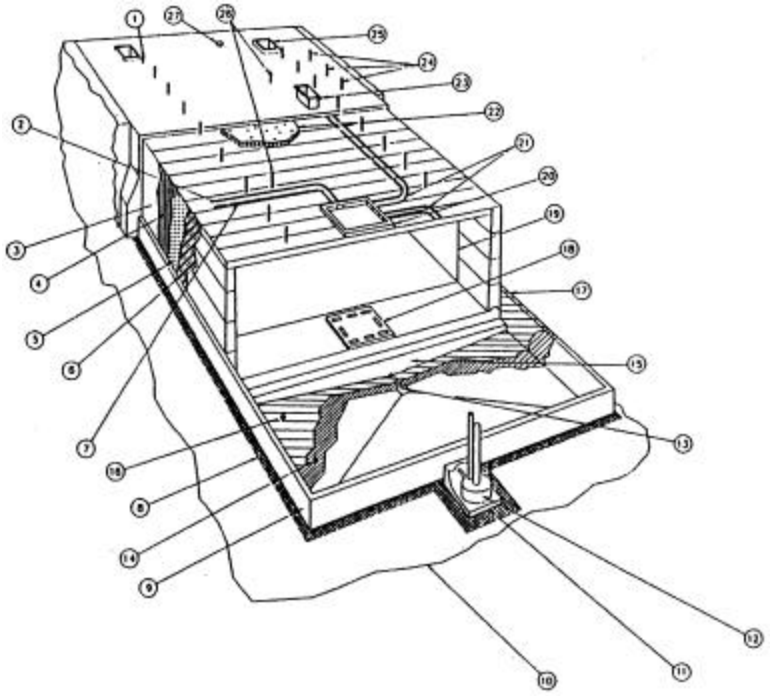

| ITEM | DESCRIPTION |
|---|---|
| 1 | GROUP CAP INJECTION PORTS |
| 2 | GROUT FEED LINE |
| 3 | 1/2" THERMAL BOARD (2 LAYERS) |
| 4 | GEOTEXTILE |
| 5 | (HDPE) PLASTIC CURTAIN |
| 6 | DRAINAGE NET (2 LAYERS) IS |
| 7 | EXCESS LIQUID TRANSPORT LINE |
| 8 | DIFFUSION BREAK |
| 9 | CONCRETE BASIN |
| 10 | STRUCTURAL BACKFILL OR NATIVE SOIL |
| 11 | CONCRETE SUMP ENCASEMENT |
| 12 | LEACHATE COLLECTION SUMP & RISERS |
| 13 | LEACHATE REMOVAL PIPE |
| 14 | HDPE LINER |
| 15 | DRAINAGE GRAVEL |
| 16 | GEOTEXTILE |
| 17 | GEOTEXTILE OVER GRAVEL & UNDER VAULT |
| 18 | 60 mil HDPE PLASTIC SPLASH PAD SECURED WITH EIGHT 70 lb SANDBAGS |
| 19 | ASPHALT COATING |
| 20 | VAULT PIT |
| 21 | EXCESS LIQUID TRANSFER LINES FROM PUMP PITS |
| 22 | CONCRETE CAP |
| 23 | CCTV CAMERA ASSEMBLY |
| 24 | GROUT CORE SAMPLE ACCESS |
| 25 | EXCESS LIQUID PUMP PITS |
| 26 | LEVEL ELEMENTS |
| 27 | VENTILATION INLET |

NOTES:
1. HDPE-HIGH DENSITY POLYETHYLENE
2. CCTV-CLOSED CIRCUIT T.V.

**Figure 4.1**. Grout Disposal Facility—Grout Disposal Vault, Cutaway View (after Mann et al. 1998)

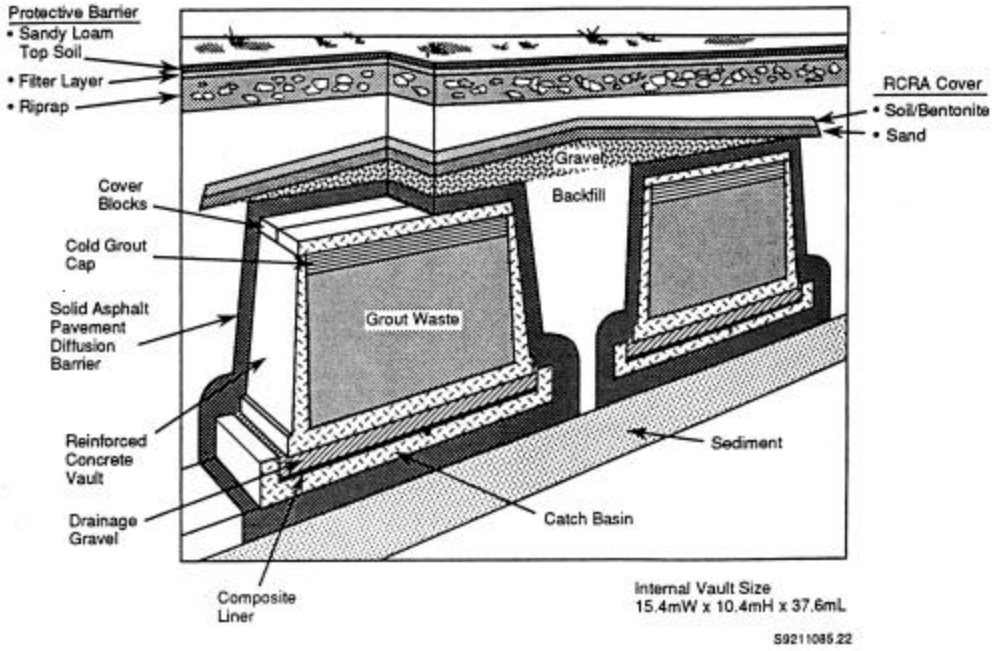


**Figure 4.2**. Grout Disposal Facility—Closed Vault Pair (after Mann et al. 1998). The RCRA cover and protective barrier were never constructed.

Placement of the ILAW in the existing disposal facility will involve excavation and modifications to the vaults. We expect that the vaults will be returned to their original condition after being filled. A final surface cover (Section 4.2) will then be emplaced. After the final cover is placed, we expect the vertical distance from the soil surface to the top of the ILAW to be no less than 5 m.

**New ILAW Disposal Facility**. Several designs have been proposed for the new ILAW disposal facility (Burbank and Klem 1997; Mann et al. 1998; PHMC 1998; Burbank and Hohl 1999; Puigh 1999) but a final decision has not yet been made. Fortunately, all of the designs have enough similar details to proceed with the analyses. The current plan is to build concrete vaults below grade. Nominal dimensions of the vaults will be 23 m wide, 208 m long (oriented north-south), and 9.1 m high. The long dimension of the vaults will be segmented to allow incremental filling followed by sealing with a controlled density fill. Each vault will have a leachate detection and collection system. Once all segments of a vault are completely filled, a surface cover (Section 4.2) will be placed within 180 days. Vault spacing is expected to be 50 m. After the final cover is placed, we expect the vertical distance from the soil surface to the top of the ILAW to be no less than 5 m.

## 4.2 Surface Cover

Burbank and Klem (1997) considered three cover designs in their cost calculations, but recent project discussions indicated the current preferred design is the modified RCRA subtitle C design proposed by DOE/RL (1996). The following description is taken loosely from that report (entitled "Focused Feasibility Study of Engineered Barriers for Waste Management Units in the 200 Areas").

The modified RCRA subtitle C cover is the baseline cover design for sites containing dangerous waste and several categories of low-level and mixed waste. This cover was designed to provide long-term containment and hydrologic protection for a performance period of 500 years. The performance period was based on radionuclide concentration and activity limits for Category 3 low-level waste. Table 4.1 lists the design criteria. The Modified RCRA Subtitle C Barrier is composed of eight layers of durable material with a combined minimum thickness of 1.7 m (5.5 ft). Table 4.2 provides the layer thicknesses and descriptions. This design incorporates *Resource Conservation and Recovery Act of 1976* "minimum technology guidance," with modifications for extended performance. One major change is the elimination of the clay layer, which may desiccate and crack over time in an arid environment. The geomembrane component also has been eliminated because of its uncertain long-term durability. The design incorporates provisions for biointrusion and human intrusion control. However, the provisions are modest relative to the corresponding features in the Hanford Barrier design, reflecting the reduced toxicity of the subject waste and the reduced design-life criterion.

**Table 4.1**. Summary of Design Criteria for the Modified RCRA Subtitle C Barrier

| | |
|---|---|
| 1. | Minimize moisture infiltration through the cover. |
| 2. | Design a multilayer cover of materials that are resistant to natural degradation processes. |
| 3. | Design a durable cover that needs minimal maintenance during its design life. |
| 4. | Design a cover with a functional life of 500 years. |
| 5. | Prevent plants from accessing and mobilizing contamination (i.e., prevent root penetration into the waste zone). |
| 6. | Prevent burrowing animals from accessing and mobilizing contamination. |
| 7. | Ensure that the top of the waste is at least 5 m (16.4 ft) below final grade or include appropriate design provisions to limit inadvertent human intrusion. |
| 8. | Facilitate drainage and minimize surface erosion by wind and water. |
| 9. | Design the low-permeability layer of the cover to have a permeability less than or equal to any natural subsoils present. |
| 10. | Design the cover to prevent the migration and accumulation of topsoil material within the lateral drainage layer (i.e., clogging of the lateral drainage layer). |
| 11. | For frost protection, the lateral drainage layer and the low-permeability asphalt layer must be located at least 0.75 m (30 in.) below final grade. |

**Table 4.2**. Summary of Modified RCRA Subtitle C Barrier Layers

| Layer No. | Thickness cm (in.) | Layer Description | Specifications | Function |
|---|---|---|---|---|
| 1 | 50 (20) | Silt loam topsoil with pea gravel admix | McGee Ranch silt loam containing 15 wt% pea gravel, 2.36 to 9.5 mm in diameter, conforming to ASTM D448 No. 8 aggregate; to be placed at a bulk density of approximately 1.46 g/cc. | The topsoil material was identified for optimal water retention properties and should provide a good rooting medium for cover vegetation. The pea gravel is designed to minimize wind erosion of the silt loam without significantly affecting its moisture retention capabilities. |
| 2 | 50 (20) | Compacted topsoil | McGee Ranch silt loam without pea gravel, compacted to 90% of optimum dry density as determined by standard Proctor test; in-place bulk density will be approximately 1.76 g/cc. | Same as Layer 1. Layer 2 provides a supplemental soil moisture storage capacity. Compaction of this layer is intended to retard the rate of infiltration of soil moisture. The extended residence time of moisture in Layer 2 will increase the amount of moisture removed by evapotranspiration. |
| 3 | 15 (6) | Sand filter | Clean, screened sand meeting the following particle sizes: $D_{15}$ = 0.15 to 0.50 mm, $D_{50}$ = 0.375 to 1.2 mm, and $D_{85}$ = 0.70 to 2.5 mm. | This layer is part of a two-layer graded filter designed to prevent the migration of topsoil particles into Layer 5. |
| 4 | 15 (6) | Gravel filter | Clean, screened aggregate meeting the following particle sizes: $D_{15}$ = 1.5 to 2.0 mm, $D_{50}$ =15 to 20 mm, and $D_{85}$ <37.5 mm. | Same as Layer 3. |
| 5 | 15 (6) | Lateral drainage aggregate | Naturally occurring aggregate, minus 32-mm (1 1/4-in.) material, conforming to the grading identified in WDOT M41-10, 9-03.9(3) for base course, with $D_{10}$ >1 mm and k >1 cm/s. | The lateral drainage layer will intercept and divert moisture along a 2% slope to the margin of the cover for collection and/or discharge. |
| 6 | 15 (6) | Asphaltic concrete with spray-applied asphalt coating | Asphaltic concrete, consisting of asphalt conforming to WDOT M41-10, 9-02.1(4) - Grade AR-4000W, and aggregate with particle size gradation conforming to ASTM C 136. Asphalt will make up 7.5 wt% of total mixture. A spray-applied, styrene-butadiene asphalt material will be sprayed onto the asphaltic concrete surface in two layers, each 100 mils thick minimum. | This layer will function as a hydrologic barrier and as a biointrusion barrier. |
| 7 | 10 (4) | Asphalt base course | Crushed aggregate, minus 16-mm (5/8-in.) diameter material, conforming to WDOT M41-10, 9-03.9(3) for top course surfacing material. | The function of the material in this layer is to provide a stable base for placing and supporting the asphalt layer. |
| 8 | Variable | Grading fill | Clean, bank run sand and gravel conforming to WDOT M41-10, 9-03.18. | This layer will provide a smooth, level subgrade for construction of the overlying layers. |

The designs proposed by DOE/RL (1996) do not provide guidance for sideslopes. We expect that the final cover will be elevated relative to its surroundings, thus requiring sideslopes. Although the ILAW project has not yet chosen a sideslope design, the result of sideslope testing at Hanford can be used to indicate possible sideslope performance.

## 4.3 Closure Conditions Around the Surface Cover

Burbank and Klem (1997) indicated that the disturbed lands around the cover would be re-contoured and re-vegetated with native plant species. We expect that typical Hanford procedures for surface grading and re-vegetation will be pursued. We assume that some effort will be made to promote any surface water drainage away from the cover. We also assume that the topsoil used will be similar to the existing topsoil to promote re-vegetation. An alternative conceptual model is that the Hanford formation sands from the excavation will be used for the topsoil.

# 5.0 Analysis Cases and Tests

The mandate for the recharge task was to identify the scenarios that must be evaluated for the 2001 PA and provide estimates of appropriate recharge rates. These scenarios must be framed within the categories of the best estimate case and reasonable bounding cases. In addition, sensitivity tests must be conducted and alternative conceptual models evaluated to demonstrate our understanding of the system. Section 6.0 describes the methods used to estimate recharge. Section 7.0 describes the estimates and their assignment to the best estimate case and the bounding cases.

## 5.1 Best Estimate Case

The best estimate case represents the situation where all disposal facility features function as expected assuming a shrub-steppe plant community, current climate, no irrigated farming, and no significant subsidence impacts on the cover. Based on the facility design, there are five surface features that need separate evaluations:

- Modified RCRA Subtitle C Cover
- Cover sideslope
- Rupert sand
- Burbank loamy sand
- Hanford formation sediments.

These features will be evaluated for conditions that existed prior to Hanford, during disposal facility operations, during the design life of the surface cover, and following the design life of the surface cover. Table 5.1 shows which features are evaluated for each time period of interest to the 2001 PA. After the cover design life of 500 years, the performance of a possibly degraded surface cover will be evaluated (see the upper bounding cases in next section).

**Table 5.1**. Surface Features To Be Evaluated During Each Period of Interest to the 2001 PA

| Surface Feature | Time Period of Recharge Evaluation | | | |
|---|---|---|---|---|
| | **Pre-Hanford** | **During Disposal Operations** | **During Surface Cover Design Life** | **After Surface Cover Design Life** |
| Modified RCRA Subtitle C Cover | | | **Ō** | **Ō** |
| Cover Sideslope | | | **Ō** | **Ō** |
| Rupert Sand | **Ō** | **Ō** | **Ō** | **Ō** |
| Burbank Loamy Sand | **Ō** | **Ō** | **Ō** | **Ō** |
| Hanford Formation Sediments | | **Ō** | | |

## 5.2 Reasonable Bounding Cases

To specify that a bounding case is "reasonable" presumes some knowledge of its probability of occurrence. Some cases, such as complete replacement of shrub-steppe by cheatgrass, are theoretically possible but not probable (or reasonable). We consider these cases as alternative conceptual models and discuss them in Section 5.4. Some cases, such as renewed glacial activity, were considered too speculative for consideration.

For the reasonable bounding cases, we assumed a shrub-steppe plant community, current climate, and no irrigated farming. We identified a single lower reasonable bounding case that represents the situation in which recharge rates are at their lowest possible values. We identified two upper reasonable bounding cases in which recharge rates are at their highest possible values. These bounding cases represent possible variations in how the system might work and give an indication of the level of uncertainty in the recharge estimates.

### 5.2.1 Lower Bounding Case

We interpret this case to be a fully functional surface cover and a dense shrub-steppe community on the cover and the surrounding soils.

### 5.2.2 Upper Bounding Cases

We interpret these cases to be situations in which recharge is potentially higher than the best estimate case because of degradation of the cover or variations in soil and plant effects.

**Erosion of the Surface Cover**. Wind and water erode 0.2 m of silt loam from the surface of the cover.

**Dune Sand Deposition on the Surface Cover**. Wind deposits a 0.2-m layer of dune sand.

## 5.3 Sensitivity Tests

Recharge sensitivities can be determined through the controlled manipulation of selected parameters and processes. For this report, we elected to vary vegetation (type, presence, and density), soil hydraulic properties, and climate.

## 5.4 Uncertainty Tests

In our conceptual model of recharge, we assumed a shrub-steppe plant community, current climate conditions, and no irrigated farming. Three alternative conceptual models were prepared and tested to demonstrate the impact of these assumptions on recharge estimates.

**Vegetation Change**. Through fire, disturbance, disease, or successful competition with the native species, the shallow-rooted alien species cheatgrass becomes the dominant plant. Cheatgrass is so successful that it precludes the deeper-rooted plants from re-establishing.

**Climate Change**. Precipitation rates increase and temperatures decrease to the maximum levels inferred from a pollen record that covers the last 100,000 years.

**Irrigation**. If, for whatever reason, farming is allowed on or near the disposal sites, irrigation will be a necessity.

A fourth assumption that we made, no significant subsidence, is currently being evaluated (LMHC 1999). Once the likelihood and degree of subsidence is established, we will evaluate the impacts on our recharge estimates.

# 6.0 Recharge Estimation Methods

Recharge rates at the Hanford Site can range from near zero to more than 100 mm/yr (Gee et al. 1992). To effectively cover this range, three complementary methods are used to estimate recharge rates: lysimetry, the tracer technique, and computer simulations. For a discussion of these and other methods, see the January-February 1994 issue of the *Soil Science Society of American Journal.* This issue contains a series of papers that were presented at a symposium titled "Recharge in Arid and Semiarid Regions." Rockhold et al. (1995) described how these methods were used at Hanford. Some of that description is included here along with additional considerations relevant to the presence of the subsurface ILAW disposal facility.

## 6.1 Lysimetry

The goal of lysimetry is to provide both performance data and model testing data for specific combinations of soil, vegetation, and precipitation. A lysimeter is a system that can be used to collect water that has flowed through and below the reach of the evaporation process and plant roots to become deep drainage and eventually recharge. The only method available for directly measuring recharge is lysimetry. One of the strengths of lysimetry is that it can provide a control volume in which a number of water balance components can be measured directly. This control volume provides the data needed to calibrate numerical models that can then be used to forecast recharge.

The Hanford Site has used lysimeters for multiple purposes (Gee and Jones 1985; Freeman and Gee 1989; Wittreich and Wilson 1991; Gee et al. 1993; Ward et al. 1997). The lysimeters used to provide data for this report include containers that isolate the soil from its surroundings and field-scale pads that collect drainage but do not isolate the soil.

The primary source of lysimeter data is the Field Lysimeter Test Facility (FLTF). Appendix A describes this facility and provides an overview of the data available. The facility was constructed in FY 1987 to test the performance of capillary barrier cover designs (Gee et al. 1989). The FLTF contains 18 large lysimeters (surface area > 2 $m^2$; depth from 1.5 to 3.0 m) and six smaller lysimeters (surface area is 0.07 $m^2$; depth 3.0 m). Treatments include variations of material types and thicknesses, the presence of vegetation, and the use of irrigation to mimic the increased precipitation of a possible future climate. Data from this facility include drainage, water content, matric potential, temperature, and vegetation observations.

Another source of lysimeter data for this report is the Hanford Prototype Barrier, a full-scale barrier constructed above an actual waste site (Ward et al. 1997). The Prototype Barrier design differs slightly from most of the tests in the FLTF in that the surface silt loam layer is 2 m thick (rather than 1.5 m) and the upper meter contains gravel for erosion control (only two FLTF lysimeters contain gravel in the silt loam layer, and only in the upper 0.3 m). More importantly, the Prototype Barrier differs from the FLTF tests in that it is a full-scale test that includes sideslope effects.

The Prototype Barrier is instrumented to measure variables such as water content, matric potential, temperature, and drainage. One of the unique and valuable features of the Prototype Barrier is the presence of asphalt collection pads for drainage collection. These pads are part of the asphalt layer that underlies the entire Prototype Barrier. Individual collection pads were constructed using asphalt curbing to separate the different collection zones. Four 322-$m^2$ collection zones underlie the main portion of the Barrier. Two similar zones lie beneath each of the two different sideslope designs (one is sandy gravel, the other is basalt riprap). In addition, a collection lysimeter was constructed beneath the northeast portion of the barrier, under the asphalt layer that lies beneath the basalt sideslope treatment. This lysimeter provides a measure of the effectiveness of the asphalt layer in preventing drainage.

Although they provide the only direct measure of recharge, lysimeters have disadvantages. Lysimeters are usually fixed in space, which limits their ability to quantify the effects of spatial variability. The soils filling the lysimeter may not represent the natural stratification or layering that may be present. The length of record is much shorter than time periods of interest. The lysimeter walls and base alter the natural gradients of temperature, air flow, and vapor flow that could be of importance when trying to measure recharge rates less than 1 mm/yr. Lysimeter walls restrict lateral root growth and promote downward growth. When they involve irrigation, the lysimeter tests are subject to the "oasis effect," in which heat from the un-irrigated surroundings increases the evapotranspiration rate above what it would have been if the entire area had been irrigated. Finally, one of the issues with using lysimeters is verifying that no leaks of drainage water have occurred.

## 6.2 Tracers

The goal of the tracer method is to estimate historical recharge using measurements of tracer distributions in the soil and sediments of the vadose zone. The advantage of this method is that multiple tracers are available that enable estimates of recharge rates for durations of tens to thousands of years. The vertical distribution of tracers represents the integration of many recharge events and can be used to estimate the mean recharge rate for the time scale of interest for a performance assessment.

The two tracers used for this report are chloride (Cl) and chlorine-36 ($^{36}$Cl). Chloride originates from sea water, is deposited naturally, and can provide recharge estimates spanning hundreds to thousands of years. Chlorine-36 originates from two sources: cosmic irradiation of atmospheric chloride and nuclear weapons testing. The natural process of cosmic irradiation produces very minute quantities of $^{36}$Cl. In contrast, nuclear weapons testing in the 1950s and early 1960s injected considerable quantities of $^{36}$Cl into the atmosphere. The $^{36}$Cl originated from sea level testing, which caused the thermal neutron irradiation of chloride in sea water (Phillips 1994). The quantities of $^{36}$Cl created by the testing were far higher than natural production rates and thus became a marker in the environment. The $^{36}$Cl data can be used to estimate the average recharge rate over the last 40 years. Appendix B describes the tracer data collected for the ILAW PA project.

Both chloride and $^{36}$Cl are conservative, nonvolatile, and almost completely retained in the soil when water evaporates or is transpired by plants (Phillips 1994). Some chloride is taken up by plants (e.g., Rickard and Vaughan 1988; Sheppard et al. 1998). Over hundreds to thousands of years, we expect plant cycling has a minimal impact on the evolution of the chloride distribution in the profile beneath plant

nets. In contrast, bomb-pulse $^{36}Cl$ has been around only ~40 years, so caution must be exercised when interpreting such data. In soils with high pH and high adsorption of other anions, anion exclusion can result in faster movement of chloride. Previous studies have shown a direct correlation between clay content and anion exclusion (Warrick et al. 1971). Most of the sandy soils on the Hanford Site have relatively low percentages of clay, so the effects of anion exclusion in these soils should be relatively minor.

Appendix B describes the calculation of chloride deposition at the ILAW Disposal Site. The value, 38.4 mg/m$^2$/yr, is consistent with earlier estimates that ranged from 32.7 to 49.4 mg/m$^2$/yr (Murphy et al. 1996; Prych 1998). At a site to the west of the 200 West Area, Murphy et al. (1996) estimated the deposition rate to be 40.0 ± 7.3 mg/m$^2$/yr. Although year-to-year variability in chloride deposition rates likely exists, we expect the long-term average is adequately represented.

Phillips (1994) suggested that systematic uncertainties in estimated chloride deposition rates can be as great as 20% if the chloride mass balance technique is extended to estimate recharge rates prior to the Holocene epoch (approximately 10,000 years ago). Because the Hanford Site was flooded by glacial melt water about 13,000 years ago, we are not extending our interpretation beyond that time. Therefore, we expect that the uncertainty in chloride deposition rates at the Hanford Site is less than 20%.

There is some uncertainty about the local influence that Hanford Site operations may have had on the time-dependent concentrations of both chloride and $^{36}Cl$ deposited at Hanford. The issue of locally generated chloride is under review (see Appendix E). Murphy et al. (1991) examined the issue relative to $^{36}Cl$ and concluded there was no nearby source that would confuse the $^{36}Cl$ signal in the sediment.

The primary source of tracer data for this report is the analyses of samples collected from boreholes that were drilled by the ILAW PA project in 1995 and 1998. The analyses are described in Appendix B. In addition, a few measurements of tracer profiles have been performed by other projects at the Hanford Site (Murphy et al. 1996; Prych 1998). These data were also used for this report. Descriptions of the measurement procedures can be found in Appendix B, Murphy et al. (1991), Murphy et al. (1996), and Prych (1998). The analysis methods are briefly described below.

**Chloride**. Recharge is estimated from the chloride concentration within a soil profile as follows:

$$J_R = \left( \frac{Cl_o}{Cl_{sw}} \right) P \tag{6.1}$$

where $J_R$ is the liquid water flux at the depth of measurement, $Cl_o$ is the chloride concentration of the precipitation, $Cl_{sw}$ is the chloride concentration in the soil water, and $P$ is the annual precipitation rate. Because chloride can be deposited by dry fallout, the value of $Cl_o$ is adjusted to represent the total annual wet and dry chloride deposition rate divided by the annual precipitation rate. The value of $Cl_{sw}$ can be determined by plotting cumulative chloride content with depth against cumulative water content at the same depths. The slopes of straight-line segments correspond to $Cl_{sw}$ for the depth interval (Phillips

1994). Changes in the slopes of different line segments, corresponding to the different depth intervals, can represent the temporal variability of recharge rates and/or deposition rates.

**Chlorine-36**. An upper limit of the average recharge can be estimated from $^{36}Cl/Cl$ ratios by integrating the water content profile above the depth of the peak ratio or the centroid of the $^{36}Cl/Cl$ profile. A rough estimate can also be obtained by dividing the depth of the peak or centroid by the time since the bomb tests. A disadvantage of this method is that $^{36}Cl$ could still be within the root zone and thus yield too high an estimate of recharge (Tyler and Walker 1994). The likelihood of this problem happening increases for those sites at Hanford where recharge rates are lower than 10 mm/yr. Plant uptake and release can complicate the interpretation of the $^{36}Cl$ signal.

## 6.3 Modeling

The goals of modeling are to provide short-term estimates of recharge rates when there are little to no data and to leverage the existing short-term data into estimates of long-term recharge rates. Simulations of recharge at Hanford have been successful at highlighting the important factors that affect recharge and predicting recharge rates for specific cases. Modeling is the primary tool for forecasting recharge rates for future climate and land use scenarios. The simulations also allow the results of the lysimetry and tracer methods to be merged on a consistent basis.

The UNSAT-H computer code was used to estimate recharge rates for this report (Fayer and Jones 1990). UNSAT-H can simulate nonisothermal water flow processes in both liquid and vapor phases and hysteresis in the soil hydraulic properties. This model has been tested using data from several of the lysimeter experiments at Hanford and elsewhere (Fayer et al. 1992; Fayer and Gee 1992; Khire et al. 1997). Fayer and Gee (1997) tested UNSAT-H and a simpler model and concluded that UNSAT-H provided far better estimates of drainage through a surface cover. Scanlon (1992) used a similar unsaturated flow model to estimate recharge rates in the Chihuahuan Desert of Texas. Appendix C describes the modeling activity undertaken to estimate recharge rates for this report.

One of the disadvantages of numerical modeling is that it requires numerous parameters to represent climate, soils, and vegetation characteristics. In many instances, these parameters are unknown or only marginally known. Another disadvantage is the use of conceptual simplifications to make the modeling tractable. For example, Appendix F suggests that the current plant model may need to be revised. Numerical modeling with a code such as UNSAT-H is the most flexible method for estimating recharge rates, but its data-intensive needs and conceptual simplification could lead to recharge estimates that have the most uncertainty.

## 6.4 Additional Considerations

Several features of the ILAW disposal could affect the analysis of recharge rates, including physical effects, water consumption, temperature, and preferential flow. Physically, the vaults/disposal volume will be located 3 m below the base of the surface cover. At this depth, we do not anticipate any direct physical effect on recharge rates. The very low permeability of the vaults could affect the flow of air through the vadose zone, but we assume that any air exchange with the deep vadose zone is too small to

affect recharge rates significantly. The vaults could also affect the overall temperature gradient within the vadose zone, but we assume the effect to be too small to affect recharge rates significantly.

Silicate glasses such as the ILAW undergo corrosion when in water. The rate of corrosion depends on factors such as glass composition and the availability of water, which is consumed in the corrosion process. The maximum consumption rate was calculated to be 0.34 g of water per gram of glass (BP McGrail, personal communication). This level of water consumption will set up a matric potential gradient that causes water to move toward the ILAW. We recognized that this consumption might increase water flow through the cover. However, we assumed that, because the water was consumed in the corrosion process, the overall effect of this increased downward water movement was not significant to the analysis of recharge.

Radionuclides within the ILAW will undergo radioactive decay and thus generate heat. McGrail and Bacon (1998) reasoned that the long half-life and small concentration of radionuclides in ILAW would minimize any temperature increase over ambient conditions. Using the latest inventory of $^{90}Sr$ and $^{137}Cs$ in the ILAW, McGrail and Bacon (1998) estimated the maximum temperature increase would be 0.25°C between the vault center and the immediately surrounding soil. They concluded that this small temperature rise was within the expected seasonal temperature fluctuations at the site (about 2°C) and therefore not a significant factor affecting the performance of the disposal facility. We assumed that this small temperature perturbation would not affect recharge rates significantly.

Preferential flow paths such as clastic dikes could affect recharge under the right conditions. However, the vadose zone in and around the disposal facility will be excavated, thus eliminating any dikes that may be present near the soil surface. Therefore, we assumed that dikes would not be a factor in recharge. Preferential flow could also occur as a result of focused overland flow, such as at the toe of the cover sideslope. We intend to address this recharge mechanism in the next revision of the data package, once the surface cover and facility designs are more definite. Finally, preferential flow can occur at a very local scale as a result of flow instabilities that lead to "fingering." Hendricks and Yao (1996) found that, for a sand dune in New Mexico, instabilities occurred during a precipitation event only when the total precipitation exceeded 4 cm. At Hanford, total precipitation in a 24-h period has exceeded 4 cm only twice between 1947 and 1997 (by less than 1 cm in both cases). Therefore, we assumed that flow instabilities would not be a dominant phenomenon affecting recharge at Hanford.

# 7.0 Results

The recharge estimation process uses data from multiple and sometimes conflicting sources. The estimation process was an effort to maximize the value of the information in hand without forgetting the limitations of that information. In this section, we analyze the data and recharge estimates for the best estimate and bounding cases, demonstrate some recharge sensitivities, estimate recharge for three alternative conceptual models, and assign recharge rates to the best estimate and bounding cases. Following that, we outline the activities planned for FY 2000 and end with a summation of the known remaining issues.

## 7.1 Analyses for the Best Estimate and Reasonable Bounding Cases

For each of the surface features identified in Section 5.0, we have assessed the data available for estimating recharge rates. Where data are conflicting, we present alternate recharge estimates.

### 7.1.1 Modified RCRA Subtitle C Cover

The surface cover over the ILAW vaults will determine the flux of water directly down to and around the vaults. The FLTF data collected under ambient precipitation conditions showed that drainage rates through the cover were less than 0.001 mm/yr (Appendix A). For the drainage caissons, this rate represents about 3 mL/yr. When rates are seemingly this low, we should exercise caution because other factors could be affecting the results and ought to be considered (e.g., temperature gradients, leaks, and water storage within the basalt). Simulations of the cover indicated rates would be less than 0.1 mm/yr, but no attempt was made to see if the rate might be lower. In the previous PA (Mann et al. 1998), a recharge rate of 0.5 mm/yr was assigned to the cover. This value represented the design objective of the Hanford Prototype Barrier (Wing 1994). The data and simulations reported here support the use of a lower recharge estimate for the cover. Although there are indications of lower rates, we propose using a rate of 0.1 mm/yr for an intact surface cover with or without vegetation.

### 7.1.2 Sideslope

The surface cover may be elevated above the surrounding terrain. If so, the cover will need sideslopes to maintain its stability as well as to blend into the terrain. No specific sideslope designs have yet been chosen. However, the ongoing testing of sideslopes at the Hanford Prototype Barrier provided some useful performance data. Two sideslopes are being tested: basalt riprap and sandy gravel. The high cost of basalt riprap makes the use of sandy gravel attractive. Ward et al. (1997) reported that drainage though the sandy gravel sideslope was 31.4% of the precipitation in a 3-year period. Assuming that fraction remained constant for the long-term average precipitation rate of 160 mm/yr, the long-term drainage rate would be 50 mm/yr. Assuming a 1:10 (V:H) sandy gravel sideslope with vegetation (the same as the Prototype), we estimate a recharge rate of 50 mm/yr under ambient precipitation.

The asphalt layer terminates under the sideslope. The water draining through the sideslope will be collected and routed laterally and infiltrate just beyond the edge of the asphalt. Ward et al. (1997) detected this infiltration zone at the Hanford Prototype Barrier. In addition to the sideslope drainage water, the asphalt layer will also convey any water that drains through the cover's surface layer. This additional water should be inconsequential relative to the quantity of sideslope drainage water.

### 7.1.3 Rupert Sand

Rupert sand covers most of the two disposal sites. We assume that, following closure, the disturbed area surrounding the covers will be reconstituted to mimic Rupert sand. The chloride tracer data in Appendix B suggest a range of recharge rates depending on location and depth. The chloride data above the 5- to 10-m depth represent more recent recharge rates. The analysis of these data shows a recharge rate ranging from 0.013 to 0.065 mm/yr, with an overall average of 0.03 mm/yr. In contrast, the chloride data below 10 m represent recharge rates thousands of years ago (based on the accumulated chloride above 10 m). These data indicate a recharge rate range from 0.16 to 1.8 mm/yr, with an average rate of 0.9 mm/yr. If we ignore the time difference and simply average the multiple estimates, we get an average recharge rate of 0.4 mm/yr.

We have some concern about chloride contamination from nearby facilities. The presence of facility-generated chloride within the soil profile would cause, if unrecognized, an underestimate of the recharge rate using the traditional chloride method. Figure 7.1 shows a photograph looking southeast over the new ILAW Disposal Site. In the foreground are the 200 East Area coal-fired power plant and the water purification plant. Both facilities are suspected to be emitters of chloride. The coal plant, in particular, is a likely source because it began operations in late 1944 and did not use emission controls until 1980, when a baghouse (to filter out particulates) was installed. The new ILAW Disposal Site is directly downwind given that the prevailing wind direction is from the northwest. To determine whether coal plant emissions had deposited chloride at the tracer sampling sites, we collected soil samples from ten locations and analyzed them for multiple constituents, including known constituents of coal. Appendix E describes the testing and results, which were inconclusive but suggestive of deposition. Additional testing is being performed to clear up the uncertainty. If chloride from local facilities was deposited at the ILAW sites, we should still be able to use the deeper chloride data that reflect pre-Hanford conditions.

Appendix B shows that bomb-pulse $^{36}Cl$ still resides entirely within the root zone (the upper 2 m of soil). While still in the root zone, $^{36}Cl$ cannot be used to estimate recharge. However, we can establish a rough upper limit. Assuming an average root zone water content of 0.1 $cm^3/cm^3$, the recharge rate would have to be much less than 5 mm/yr to explain the absence of $^{36}Cl$ below 2 m.

We have two other estimates of recharge in Rupert sand. One of those estimates was derived from the simulations in Appendix C that suggested a recharge rate of 2.2 mm/yr. The other estimate came from Murphy et al. (1996), who measured chloride concentrations in Rupert sand located near the Wye barricade. This site is about 13 km to the southeast of the ILAW disposal sites. At that distance, the site should be unaffected by any emissions from the coal plant or other facilities. The shrub density in that general area is far less than at the ILAW Disposal Site. Using the chloride tracer method, Murphy et al. (1996) estimated a recharge rate of 4 mm/yr. This value is much higher than the estimates for the ILAW

**Figure 7.1**. Aerial View of the New ILAW Disposal Site. The viewing direction is southeast. The 200 East Coal Power Plant and Water Purification Plant are in the foreground. The Existing Disposal Site, which is not shown, is 1.4 km directly east of the coal plant.

Disposal Site despite both sites being classified as shrub-steppe on Rupert sand. The distinctly different recharge estimates likely reflect differences in soil hydraulic properties and vegetation between the two sites.

There is enough variability in the data to exercise caution with this estimate. We propose using the average ILAW-specific estimate of 0.9 mm/yr for Rupert sand based on the deeper chloride data until the concern about facility emissions is resolved.

### 7.1.4 Burbank Loamy Sand

Prych (1998) estimated recharge for Burbank loamy sand using samples from two boreholes drilled less than 1 km north of the ILAW disposal sites. Using the chloride data above the 10-m depth, Prych estimated rates of 0.02 and 0.04 mm/yr. Using the chloride data below the 10-m depth, Prych estimated the recharge rates to be 2.8 and 5.5 mm/yr, which yields an average rate of 4.2 mm/yr. The borehole site is further from the coal plant than the ILAW sites, but it is directly downwind of the peak wind direction (from the southwest). The simulation results in Appendix C showed a recharge rate of 5.5 mm/yr in this soil.

Because of our concern about the shallower chloride data, we would rather use the mean of the deeper chloride estimates reported by Prych (1998). Therefore, we propose using a recharge rate of 4.2 mm/yr for Burbank loamy sand.

### 7.1.5 Hanford Formation Sand

During vault construction and filling, Hanford formation sand will be exposed and vegetation will likely not exist. Fayer and Walters (1995) reported that an unvegetated 7.6-m deep lysimeter containing Hanford sand drained 443 mm from July 1985 to June 1993 for an average rate of 55.4 mm/yr. For the conditions envisioned during facility construction, we propose using a recharge rate of 55.4 mm/yr.

During construction, we expect water will be used for dust control and compaction. The most likely period for water application will be late spring to early fall when the soil is typically driest. Under these conditions, we expect that the added water will not drain deep enough to impact recharge rates.

## 7.2 Sensitivity Tests

Some of the modeling results in Appendix C indicate the sensitivity of certain parameters and processes. These include vegetation presence, type, and abundance; soil properties; and climate.

### 7.2.1 Vegetation

The simulation results showed that the recharge rate through the surface cover was not sensitive to the type of plant or even to the presence of plants, at least to the model precision level of 0.1 mm/yr that was achieved. In contrast, recharge under the Rupert sand increased from 2.2 mm/yr under shrub-steppe to 33.2 mm/yr under cheatgrass to 44.3 mm/yr when plants were absent. Without plants, recharge under the Burbank loamy sand increased by a factor of 10 (from 5.2 to 52.5 mm/yr).

The robustness of the vegetation on Rupert sand was also tested by varying the leaf area index to encompass the range of values measured at the ILAW Disposal Site in 1998 (Appendix F). Increasing the shrub leaf area index by 60% reduced the predicted recharge from 2.2 to 1.6 mm/yr. Decreasing the shrub leaf area index by 60% increased the predicted recharge from 2.2 to 5.6 mm/yr. In both cases, the variation in recharge was within a factor of 2 to 3 of the base estimate of 2.2 mm/yr.

### 7.2.2 Soil Properties

The simulation results showed a minor sensitivity to soil properties. Two alternate hydraulic property descriptions for Rupert sand were used in separate simulations. These properties were obtained from a field infiltration test conducted at the new ILAW Disposal Site. The resulting predicted recharge rates were 2.7 and 3.3 mm/yr, compared to the base case estimate of 2.2 mm/yr.

### 7.2.3 Climate

The simulation results showed that the surface cover would be unaffected by any envisioned change in climate. In contrast, the simulation results showed that recharge in the soils would be significantly affected. Using Rupert sand, the nine combinations of three temperature regimes and three precipitation regimes yielded estimated recharge rates that ranged from less than 0.1 to 27 mm/yr. When precipitation was 50% of modern levels, recharge was less than 0.1 mm/yr regardless of the temperature scenario. For modern precipitation levels, estimated recharge ranged from 0.6 to 7.5 mm/yr for the high to low temperature regimes, respectively. For the high precipitation regime (128% of modern levels), the recharge rates increased, ranging from 5.2 to 27 mm/yr.

## 7.3 Uncertainty Tests

One method to gauge the uncertainty in recharge estimates is to analyze alternative conceptual models. The model results in Appendix C were used to address a change in the vegetation, a change in the climate, and irrigation.

One of the two cover degradation scenarios was that 20% of the silt loam layer was eroded. The simulation results in Appendix C showed that the eroded cover with shrub-steppe vegetation performed as well as the intact cover, i.e., it limited drainage to less than 0.1 mm/yr. The second degradation scenario involved the deposition of 20 cm of dune sand on the cover. The simulation results showed that the cover with dune sand and shrub-steppe vegetation also performed as well the intact cover. The simulation results also showed that the replacement of shrubs with cheatgrass for this particular situation resulted in drainage of 18.4 mm/yr, and the removal of all plants caused drainage to increase to 32.7 mm/yr. We expect that deep-rooted plants like sagebrush will always be present, therefore we propose using a rate of 0.1 mm/yr for the degraded cover scenario.

### 7.3.1 Vegetation Change

The simulation results in Appendix C showed that a surface cover without vegetation limited recharge to less than 0.1 mm/yr. This level of performance is as good as a cover with shrub-steppe vegetation. Without conducting a simulation with cheatgrass, we assumed that a cover with cheatgrass would limit recharge to less than 0.1 mm/yr. The same simulation results were obtained for an eroded cover without plants, showing how robust the silt loam cover is at reducing recharge, even in the absence of plants.

The results in Appendix C indicate that a shift from shrub-steppe to cheatgrass on the Rupert sand will raise the recharge rate from 2.2 to 33.2 mm/yr. This higher estimate of recharge is not unreasonable. Fayer and Walters (1995) used water content measurements to estimate recharge rates for a cheatgrass community growing on Rupert sand in the 300 Area. For an 8-year period, they estimated the average recharge rate was 25.4 mm/yr.

### 7.3.2 Climate Change

The prediction of climate change is a current research topic. Because we cannot foresee the future, we have used the past to see what has happened and possibly could happen again. Appendix C describes the analysis. Under climate change conditions most likely to promote recharge (i.e., higher precipitation and lower temperature), the surface cover continued to limit drainage to less than 0.1 mm/yr as did the eroded surface cover. With 20 cm of dune sand on the cover, this climate scenario resulted in a recharge rate of 16.9 mm/yr. Recharge in the Rupert sand jumped from 2.2 to 27 mm/yr and in the Burbank loamy sand from 5.2 to 36.8 mm/yr. In all cases, a shrub-steppe community was present.

### 7.3.3 Irrigation

All of the land use options currently being considered for Hanford exclude farming on and near the waste disposal sites. Because such institutional controls cannot be guaranteed to survive forever, we evaluated the impacts of irrigated agriculture on recharge. Appendix C describes the numerical simulations that were conducted. For a potato crop grown on the surface cover, recharge was 26.4 and <0.1 mm/yr for irrigation efficiencies of 75 and 100%, respectively. For Rupert sand, the rates were 57 and 30 mm/yr for the same efficiencies. We assumed there would be no farming on Burbank loamy sand because of the high gravel content. An effort was started in FY 1999 to evaluate current and projected irrigation practices around Hanford (LMHC 1999). The results of that effort will be used to improve and refine our recharge estimates for irrigated farming.

## 7.4 Assignment of Recharge Rates to Scenarios

The data and analyses just discussed were used to assign recharge rates to each of the scenarios identified in Section 5.0. The estimated rates were assigned to the best estimate and to the lower and upper bounding cases.

### 7.4.1 Best Estimate Case

Table 7.1 shows the estimated recharge rates for each surface feature during each phase of the disposal evaluation. As discussed in Section 7.1, the cover, cover sideslope, and Hanford formation estimates are based on lysimeter data. The Rupert sand and Burbank loamy sand estimates are based on chloride data.

### 7.4.2 Reasonable Bounding Cases

The lower bounding case represents the situation in which recharge rates are at their lowest possible values. The upper bounding cases represent situations in which recharge rates are at their highest possible values. Table 7.2 summarizes the rate assignments for both cases. We did not include climate change, sand dune migration, or irrigation effects in setting the bounding estimates.

**Table 7.1** Recharge Estimates for the Best Estimate Case for Disposal Facility Features During Each Period of Interest to the ILAW 2001 PA. These estimates reflect current climate conditions. The surface cover, Rupert sand, and Burbank loamy sand have shrub-steppe vegetation.

| Surface Feature | Estimated Recharge Rate (mm/yr) | | | |
|---|---|---|---|---|
| | Time Period of Recharge Evaluation | | | |
| | Pre-Hanford | During Disposal Operations | During Surface Cover Design Life | After Surface Cover Design Life |
| Modified RCRA Subtitle C Cover | NA | NA | 0.1 | 0.1 |
| Cover Sideslope | NA | NA | 50 | 50 |
| Rupert Sand | 0.9 | 0.9 | 0.9 | 0.9 |
| Burbank Loamy Sand | 4.2 | 4.2 | 4.2 | 4.2 |
| Hanford Formation Sediments | NA | 55.4 | NA | NA |
| NA = Not applicable. | | | | |

**Table 7.2**. Recharge Estimates for the Reasonable Bounding Cases During Each Period of Interest to the ILAW 2001 PA

| Surface Feature | Estimated Upper and Lower Reasonable Bounding Recharge Rates (mm/yr) | | | |
|---|---|---|---|---|
| | Time Period of Recharge Evaluation | | | |
| | Pre-Hanford | During Disposal Operations | During Surface Cover Design Life | After Surface Cover Design Life |
| Modified RCRA Subtitle C Cover | NA | NA | 0.01, 4.0 | 0.1, 4.0 |
| Cover Sideslope | NA | NA | 4.2, 86.4 | 4.2, 86.4 |
| Rupert Sand | 0.16, 4.0 | 0.16, 4.0 | 0.16, 4.0 | 0.16, 4.0 |
| Burbank Loamy Sand | 2.8, 5.5 | 2.8, 5.5 | 2.8, 5.5 | 2.8, 5.5 |
| Hanford Formation Sediments | NA | 50, 86.4 | NA | NA |
| NA = Not applicable. | | | | |

The lower bounding case was a fully functional surface cover and a dense shrub-steppe community on the cover and the surrounding soils. We proposed using a recharge rate of 0.01 mm/yr for the cover. Lysimeter evidence suggests the rate is lower, but we are not yet ready to claim credit for that lower rate. We proposed using a rate of 4.2 mm/yr for the cover sideslope. This rate actually comes from our best estimate for Burbank loamy sand. This soil type has a large fraction of gravel (similar to a sandy gravel sideslope) and a shrub-steppe plant community (which sideslope tests to date have not included). We proposed using a recharge rate of 0.16 mm/yr for Rupert sand. This rate is the lowest of the four rates

estimated from site-specific chloride data. We proposed using a recharge rate of 2.8 mm/yr for the Burbank loamy sand. This rate is the lower of two rates estimated from chloride data. We proposed using a recharge rate of 50 mm/yr for the Hanford formation sediments during construction. This rate actually comes from drainage data collected from the sandy gravel sideslope test at the Prototype Barrier. The sideslope test has no shrubs and an extremely sparse cover of annuals.

The upper bounding case was a degraded surface cover and a sparse shrub-steppe community on the cover and the surrounding soils. We proposed using a recharge rate of 4.0 mm/yr for the cover. This rate was the estimate derived from Rupert sand with a sparse shrub cover. Simulation results suggest the rate is lower, but we are not yet ready to claim credit for that lower rate. We proposed using a rate of 86.4 mm/yr for the cover sideslope. This rate actually comes from lysimeter drainage data collected from an unvegetated sandy gravel test in the FLTF. We proposed using a recharge rate of 4.0 mm/yr for Rupert sand. This rate was the estimate derived from chloride data in Rupert sand with a sparse shrub cover. We proposed using a recharge rate of 5.5 mm/yr for the Burbank loamy sand. This rate is the higher of two rates estimated from chloride data. We proposed using a recharge rate of 86.4 mm/yr for the Hanford formation sediments during construction. This rate actually comes from lysimeter drainage data collected from an unvegetated sandy gravel test in the FLTF.

## 7.5 Plans for FY 2000

The ILAW PA project continues to support data collection and analysis activities to improve the estimates of recharge for its scenarios of interest. Current plans call for FY 2000 activities in lysimetry, tracers, modeling, vegetation studies, the initiation of field tests, and continuation of updates to the Recharge Data Package. These plans are described briefly below; details can be found in LMHC (1999).

We will continue to monitor the lysimeters at the FLTF. For some lysimeters, the performance data will eventually span 14 years (by the year 2001), providing a valuable data set for verifying barrier performance and testing model predictions. A subset of the lysimeters is being used to collect performance data for degraded and modified barriers and for recharge in the adjacent land following a change in vegetation, all under both ambient and enhanced precipitation. These tests were initiated in FY 1998 and FY 1999 and will provide performance data through the year 2001.

The chloride and $^{36}Cl$ tracer methods will again be employed to estimate recharge rates. Additional ILAW boreholes will be drilled in a manner similar to the borehole drilled in FY 1998 (see Appendix B). Additional shallow boreholes (~15 m) may be drilled near the new boreholes to provide additional sediment material. The sediments will be analyzed using procedures similar to those used previously and recharge rates will be estimated for each borehole.

The capabilities of the UNSAT-H computer code will be increased to address multiple plant species, plant response to seasonality effects, and snow/snowmelt effects. These additional capabilities will

address comments received during an earlier peer review workshop (Honeyman 1995).[(a)] The modified version of the code will be formally documented and the theory and user manual will be published. The modified code will be tested using data from the lysimeters and the vegetation subtask. An uncertainty analysis will be conducted using UNSAT-H within an existing uncertainty analysis framework.

Based on previous work, additional transects will be sampled for roots in the ILAW Disposal Site. The data will be collected to depths deeper than sampled earlier (i.e., at least 2 m) to confirm the observation of shrub/inter-shrub differences and to provide data to describe the spatial variability of rooting patterns. Based on these and earlier data, a hypothesis will be proposed for describing such rooting behavior. The results will be used to support recharge simulations. We will continue to sample plant water status throughout the year so that the relationship of plant behavior to weather will be clearer and more quantifiable. These measurements will be coordinated with the Field Recharge Study (see below) so that correlations can be made between soil water status and plant water status. Based on these and earlier data, a hypotheses will be proposed for describing transpiration during these times. The results will be used to support recharge simulations.

Acceptance of the ILAW PA will depend, in part, on demonstrating a good understanding of the processes that affect natural recharge rates at the two disposal sites. Although lysimeter, modeling, and tracer studies are being conducted and will be useful, some direct field testing at the sites is necessary. The objectives of the field recharge study are to observe field water behavior during several winters, document the variability of such behavior, provide soil water status information for the vegetation task (i.e., the study of plant water status), and provide a set of field data for model testing. Two locations will be identified at the disposal sites and instrumented to measure water content and matric potential at multiple depths within and below the root zone. The layout will be designed to differentiate between water movement beneath shrubs and water movement in the inter-shrub spaces. These measurements will be coordinated with the Vegetation Task so that correlations can be made between soil water status and plant water status. The data will also be used to support the design of a waste form release field test (LMHC 1999).

Beyond FY 2000, several issues need to be more fully evaluated. These issues include unstable and preferential flow, uniformity and longevity of the cover, and flaws in the cover. These flaws include differential settling and cracking, discontinuities, and points of flow convergence.

## 7.6 Remaining Issues

As with any estimation activity involving multiple data sources, spatial variability, and time frames of thousands of years, there are many issues and concerns that need and deserve attention. Three of the more important issues are lysimeter drainage resolution, possible facility deposition of chloride, and the importance of temperature and water vapor flow when recharge rates are low.

---

(a) Honeyman JO. 1995. Letter to L Erickson transmitting the results of the 1995 workshop entitled "Summary of peer review comments resulting from the second Hanford groundwater recharge workshop." May 22-23, 1995, Richland, Washington.

Lysimeters that have materials in them do not lend themselves well to testing for leaks because the presence of the material can affect the leak test, which is the case for most of the leak tests conducted to date. Recently, some lysimeters were emptied for new tests. The interiors of the lysimeters were in good shape and showed no obvious sign of corrosion near the base where a sealant had been applied. These lysimeters were leak tested, but the tests were short in duration. While we can say the leak rate was less than 0.5 mm/yr, we cannot say with certainty that there was no leakage. Overall, the leak tests show that there were no major leaks, but they have not been precise enough to state unequivocally that the leak rate is zero. The next time a lysimeter is to be emptied for a new test, it should be leak tested much more extensively to verify that leakage is less than 0.01 mm/yr.

The appropriate use of the chloride method to estimate recharge rates in the 200 Areas depends on resolving the issue of possible facility emissions of chloride. Appendix E suggested that sulfate may be a marker of coal plant emissions, although sulfate is somewhat less mobile than chloride (Bohn et al. 1979). Several soil profiles will be analyzed for sulfate in the summer of 1999. If high sulfate and chloride concentrations are not depth-correlated, then we can use the entire chloride profile to estimate deep drainage fluxes along with their dates (see Appendix B). If they are depth-correlated, indicating deposition of coal plant emissions, we will continue to use the deeper chloride data that are located below the sulfate pulse (and presumably pre-Hanford). However, we will not be able to age-date the fluxes using the chloride accumulation technique.

Some of the recharge estimates are in the range of 1 mm/yr and less. At these rates, temperature and vapor flow are more important to accurate estimates of recharge than they are when rates are greater than 10 mm/yr. Past studies have considered these processes using field measurements of temperature and matric potential (e.g., Enfield et al. 1973). However, the methods used to estimate recharge for the ILAW disposal sites did not fully address these processes. Lysimeters, by their nature, de-couple the interior soil from the surrounding soil, thus preventing vapor flow and altering temperature gradients. Because it moves only in liquid water, the chloride tracer cannot indicate the magnitude of the vapor flow contribution to recharge (positive or negative). One way to gather data relevant to low recharge rates is to install instrumentation at the ILAW Disposal Site. In situ measurements of temperature and matric potential gradients at multiple depths would help resolve the magnitude of the low recharge fluxes.

# 8.0 Conclusions

LMHC is conducting a performance assessment for the proposed disposal of ILAW in the 200 East Area of the Hanford Site. The goal of the PA is to provide a reasonable expectation that the disposal is protective of the general public, groundwater resources, air resources, surface water resources, and inadvertent intruders. PNNL assists LMHC in their performance assessment activities. One of the PNNL tasks is to provide estimates of recharge rates for current conditions and long-term scenarios involving the shallow-land disposal of ILAW. Specifically, recharge estimates are needed for a fully functional surface cover, the cover sideslope, and the immediately surrounding terrain. In addition, recharge estimates are needed for degraded cover conditions. The temporal scope of the analysis is 10,000 years, but could be longer if some contaminant peaks occur after 10,000 years.

The elements of this report compose the Recharge Data Package, which provides estimates of recharge rates for the scenarios being considered in the 2001 PA. The estimates were derived from lysimeter and tracer data collected by the ILAW PA and other projects and from modeling analyses.

For the best estimate case, we proposed using a recharge rate of 0.1 mm/yr for the surface cover with a shrub-steppe plant community. This rate is lower than the cover design goal of 0.5 mm/yr because it reflects the actual performance measured with lysimeters and inferred with modeling. The simulation results showed that erosion of 20% of the silt loam layer did not impair this performance nor did the deposition of 20 cm of dune sand. For the sandy gravel sideslope, we proposed using a recharge rate of 50 mm/yr. This rate is lower than the 75 mm/yr used in the 1998 ILAW PA. For the soil type known as Rupert sand and a shrub-steppe plant community, we proposed using a recharge rate of 0.9 mm/yr. This rate is lower than the 3 mm/yr used in the 1998 ILAW PA. For the soil type known as Burbank loamy sand and a shrub steppe-plant community, we proposed using a recharge rate of 4.2 mm/yr. This soil type was not considered in the 1998 ILAW PA. For the Hanford formation sediments during construction, we proposed using a recharge rate of 55.4 mm/yr. Recharge in Hanford formation sediments during construction was not considered in the 1998 ILAW PA.

A limited number of sensitivity tests were conducted. The results showed that the surface cover limited recharge to less than 0.1 mm/yr regardless of the plant type, the presence of plants, or any of the climate change conditions. In contrast, recharge in the Rupert sand showed a significant sensitivity to vegetation type and climate change conditions, but less sensitivity to small variations in hydraulic properties.

Several alternative conceptual models were considered to indicate the effects of conceptual model uncertainty. Replacement of the shrub cover with cheatgrass had no impact on recharge through the surface cover, but it increased recharge in Rupert sand from 2.2 to 33.2 mm/yr. Under the climate change condition most likely to promote recharge (i.e., increased precipitation and decreased temperature), recharge through the cover remained <0.1 mm/yr in contrast to this recharge in Rupert sand, which increased from 2.2 to 27 mm/yr.

Irrigation on the surface cover caused recharge to increase from 0.1 to 26.4 mm/yr as the irrigation efficiency was reduced from 100 to 75%.

Using the available recharge estimates, we identified a set of reasonable bounding rates. The design feature with the largest projected range in performance was the sideslope (4.2 to 87.5 mm/yr). Given that sideslopes could represent a significant fraction of the surface cover footprint, we believe that efforts to improve sideslope performance are warranted.

Issues remaining to be addressed include the precision of lysimeter leak tests to support the use of lower recharge estimates, possible facility deposition of chloride that could impact tracer analyses, and the importance of temperature and water vapor flow when recharge rate estimates are lower than 1 mm/yr. In addition, the impacts of unstable and preferential flow and flaws in the cover need to be evaluated.

# 9.0 References


Allison GB, GW Gee, and SW Tyler. 1994. "Vadose-zone techniques for estimating groundwater recharge in arid and semiarid regions." *Soil Sci. Soc. Am. J.* 58:6-14.

Bentley HW, FM Phillips, and SN Davis. 1986. "Chlorine-36 in the terrestrial environment." pp. 427-480. In *Handbook of Environmental Isotope Geochemistry, Vol. 2B.* P. Fritz and J Ch Fontes (eds). The Terrestrial Environment, Elsevier, Amsterdam.

Bohn HL, BL McNeal, and GA O'Conner. 1979. *Soil Chemistry*. John Wiley & Sons, New York.

Burbank DA and TM Hohl. 1999. *Reanalysis of alternatives for immobilized low-activity waste disposal.* HNF-4003, Lockheed Martin Hanford Co., Richland, Washington.

Burbank DA and MJ Klem. 1997. *Analysis of alternatives for immobilized low-activity waste disposal.* HNF-SD-TWR-AGA-004 Rev 0. SGN Eurisys Services Corporation, Richland, Washington.

DOE. 1987. *Final environmental impact statement: Disposal of Hanford defense high-level transuranic and tank wastes*. DOE/EIS-0113, U.S. Department of Energy, Washington, D.C.

DOE-RL. 1996. *Focused feasibility study of engineered barriers for waste management units in the 200 Areas*. DOE/RL-93-33, Rev. 0, U.S. Department of Energy, Richland, Washington.

Enfield CG, JJC Hsieh, and AW Warrick. 1973. "Evaluation of water flux above a deep water table using thermocouple psychrometers." *Soil Sci. Soc. Amer. Proc*. 37:968-970.

Fayer MJ and TL Jones. 1990. *UNSAT-H version 2.0: Unsaturated soil water and heat flow model.* PNL-6779, Pacific Northwest Laboratory, Richland, Washington.

Fayer MJ, ML Rockhold, and MD Campbell. 1992. "Hydrologic modeling of protective barriers: Comparison of field data and simulation results." *Soil Sci. Soc. Am. J.* 56:690-700.

Fayer MJ and GW Gee. 1992. "Predicted drainage at a semiarid site: Sensitivity to hydraulic property description and vapor flow." In *Proceedings of the International Workshop on Indirect Methods for Estimating the Hydraulic Properties of Unsaturated Soils*. M Th van Genuchten, FJ Leij, and LJ Lund, eds., Riverside, California, October 11-13, 1989, University of California, Riverside.

Fayer MJ and TB Walters. 1995. *Estimated recharge rates at the Hanford Site*. PNL-10285, Pacific Northwest Laboratory, Richland, Washington.

Fayer MJ and GW Gee. 1997. "Hydrologic model tests for landfill covers using field data." In *Landfill capping in the semi-arid west: Problems, perspectives, and solutions*," TD Reynolds and RC Morris, eds., May 21-22, 1997. Jackson, Wyoming. ESRF-019, Env. Sci. Res. Foundation, Idaho Falls, Idaho.

Fecht KR, KA Lindsey, BN Bjornstad, DG Horton, GV Last and SP Reidel. 1999. *An atlas of clastic injection dikes of the Pasco Basin and vicinity*. BHI-01103 Rev. 0, Bechtel Hanford, Inc., Richland, Washington.

Freeman HD and GW Gee. 1989. *Hanford protective barriers program asphalt barrier studies-FY 1988*. PNL-6874, Pacific Northwest Laboratory, Richland, Washington.

Gee GW and TL Jones. 1985. *Lysimeters at the Hanford Site: Present use and future needs*. PNL-5578, Pacific Northwest Laboratory, Richland, Washington.

Gee GW, RR Kirkham, GL Downs and MD Campbell. 1989. *The Field Lysimeter Test Facility (FLTF) at the Hanford Site: Installation and initial tests*. PNL-6810, Pacific Northwest Laboratory, Richland, Washington.

Gee GW, MJ Fayer, ML Rockhold, and MD Campbell. 1992. "Variations in recharge at the Hanford Site." *Northwest Science* 66:237-250.

Gee GW and D Hillel. 1988. "Groundwater recharge in arid regions: review and critique of estimation methods." *Hydrologic Processes* 2:255-266.

Gee GW, DG Felmy, JC Ritter, MD Campbell, JL Downs, MJ Fayer, RR Kirkham, and SO Link. 1993. *Field Lysimeter Test Facility Status Report IV: FY 1993*. PNL-8911, Pacific Northwest Laboratory, Richland, Washington.

Hajek BF. 1966. *Soil survey Hanford project in Benton County, Washington*. BNWL-243, Pacific Northwest Laboratory, Richland, Washington.

Hendrickx JMH and T Yao. 1996. "Prediction of wetting front stability in dry field soils using soil and precipitation data." *Geoderma* 70:265-280.

Hoitink DJ, KW Burk, and JV Ramsdell. 1999. *Hanford Site climatological data summary 1998 with historical data*. PNNL-12087, Pacific Northwest National Laboratory, Richland, Washington.

Khire MV, CH Benson, and PJ Bosscher. 1997. "Water balance modeling of earthen final covers." *J. Geotech. Geoenviron. Engr.* 123(8): 744-754.

Kincaid CT, JW Shade, GA Whyatt, MG Piepho, K Rhoads, JA Voogd, JH Westsik, Jr, MD Freshley, KA Blanchard, and BG Lauzon. 1995. *Volume 1: Performance assessment of grouted double-shell tank waste disposal at Hanford*. WHC-SD-WM-EE-004, Rev. 1, Vol. 1, Westinghouse Hanford Company, Richland, Washington.

LMHC. 1999. *Statements of Work for FY 2000 to 2005 for the Hanford Low-Activity Tank Waste Performance Assessment Program.* HNF-SD-WM-PAP-062, Rev. 4, Lockheed Martin Hanford Company, Richland, Washington.

Mann FM. 1999. *Scenarios for the Hanford Immobilized Low-Activity Waste (ILAW) performance assessment.* HNF-EP-0828, Rev. 2, Fluor Daniel Northwest, Richland, Washington.

Mann FM, RJ Puigh, II, PD Rittmann, NW Kline, JA Voogd, Y Chen, CR Eiholzer, CT Kincaid, BP McGrail, AH Lu, GF Williamson, NR Brown, and PE LaMont. 1998. *Hanford Immobilized Low-Activity Tank Waste Performance Assessment.* DOE/RL-97-69, U.S. Department of Energy, Richland, Washington.

McGrail BP and DH Bacon. 1998. *Selection of a computer code for Hanford low-level waste engineered-system performance assessment.* PNNL-10830, Rev. 1, Pacific Northwest National Laboratory, Richland, Washington.

Murphy EM, TR Ginn, and JL Phillips. 1996. "Geochemical estimates of paleorecharge in the Pasco Basin: Evaluation of the chloride mass-balance technique." *Water Resources Research* 32(9):2853-2868.

Murphy EM, JE Szecsody, and SJ Phillips. 1991. *A study plan for determining recharge rates at the Hanford Site using environmental tracers.* PNL-7626, Pacific Northwest Laboratory, Richland, Washington.

Neitzel DA (ed.). 1998. *Hanford Site National Environmental Policy Act (NEPA) Characterization.* PNNL-6415, Rev. 10, Pacific Northwest National Laboratory, Richland, Washington.

Nimmo JR, DA Stonestrom, and KC Akstin. 1994. "The feasibility of recharge rate determinations using the steady-state centrifuge method." *Soil Sci. Soc. Am. J.* 58(1):49-56.

Pacific Northwest National Laboratory. 1999. *Hanford Site groundwater monitoring for fiscal year 1998.* MJ Hartman, ed., PNNL 12086, Pacific Northwest National Laboratory, Richland, Washington.

Philip JR and DA De Vries. 1957. "Moisture movement in porous materials under temperature gradients." *Trans. Am. Geophys. Union* 38:222-232.

Phillips FM. 1994. "Environmental tracers for water movement in desert soils of the American southwest." *Soil Sci. Soc. Am. J.* 58:15-24.

Phillips FM, JL Mattick, TA Duval, D Elmore, and PW Kubik. 1988. "Chlorine-36 and tritium from nuclear-weapons fallout as tracers for long-term liquid and vapor movement in desert soils." *Water Resour. Res.* 24:1877-1891.

Project Hanford Management Contractor (PHMC). 1998. *Conceptual Design Report, Immobilized Low-Activity Waste Disposal Facility, Project W-520*. HNF-3013, Rev. 0 Draft, Project Hanford Management Contractor, Richland, Washington.

Prych EA. 1998. "Using chloride and chlorine-36 as soil-water tracers to estimate deep percolation at selected locations on the U.S. Department of Energy Hanford Site, Washington." Water-Supply Paper 2481. U.S. Geological Survey, Tacoma, Washington.

Puigh RJ. 1999. "Disposal facility data for the Hanford immobilized low-activity waste." HNF-4950, Rev. 0, Fluor Daniel Northwest, Richland, Washington.

Reidel SP and DG Horton. 1999. *Geologic Data Package for Immobilized Low-Activity Waste 2001 Performance Assessment.* PNNL-12257, Pacific Northwest National Laboratory, Richland, Washington.

Reidel SP, KD Reynolds, and DG Horton. 1998. *Immobilized low-activity waste site borehole 299-E17-21*. PNNL-11957, Pacific Northwest National Laboratory, Richland, Washington.

Reidel SP and KD Reynolds. 1998. *Characterization plan for the immobilized low-activity waste borehole*. PNNL-11802, Pacific Northwest National Laboratory, Richland, Washington.

Rickard WH and BE Vaughn. 1988. "Chapter 6: Plant communities: Characteristics and responses." in *Shrub-Steppe, Balance and Change in a Semi-Arid Terrestrial Ecosystem*, eds. WH Rickard, LE Rogers, BE Vaughn, and SF Liebetrau. 272 pps. Elsevier, New York.

Rockhold ML, MJ Fayer, GW Gee, and CT Kincaid. 1995. *Estimation of natural groundwater recharge for the performance assessment of a low-level waste disposal facility at the Hanford Site*. PNL-10508, Pacific Northwest Laboratory, Richland, Washington.

Scanlon BR. 1992. "Evaluation of liquid and water vapor flow in desert soils based on chlorine-36 and tritium tracers and nonisothermal flow simulations." *Water Resour. Res*. 28:285-298.

Shand AL. 1995. *Tank waste remediation system complex site evaluation report*. WHC-50-WM-SE-021, Westinghouse Hanford Company, Richland, Washington.

Sheppard SC, WG Evenden, and CR Macdonald. 1998. "Variation among chlorine concentration ratios for native and agronomic plants." *J. Environ. Rad.* 43:65-76.

Tyler SW and GR Walker. 1994. "Root zone effects on tracer migration in arid zones." *Soil Sci. Soc. Am. J.* 58:25-31.

Ward AL, GW Gee, and SO Link. 1997. *Hanford Prototype-Barrier Status Report: FY 1997*. PNNL-11789, Pacific Northwest National Laboratory, Richland, Washington.

Wing NR. 1994. *Permanent isolation surface barrier development plan*. WHC-EP-0673, Westinghouse Hanford Company, Richland, Washington.

Wittreich CD and CR Wilson. 1991. "Use of lysimeters to monitor a sanitary landfill." *In Proceedings of the Conference on Lysimeters for Evapotranspiration and Environmental Measurements, Honolulu, Hawaii, July 23-25, 1991*, Irrigation Division, American Society Civil Engineers, pp. 397-405.

# Appendix A

# Field Lysimeter Test Facility Data to Support the ILAW 2001 PA

M. J. Fayer, R. E. Clayton, D. Felmy, and J. C. Ritter

# Appendix A

# Field Lysimeter Test Facility Data to Support the ILAW 2001 PA

## A.1 Introduction

Lockheed Martin Hanford Company (LMHC) is designing and assessing the performance of disposal facilities to receive radioactive wastes that are currently stored in single- and double-shell tanks at the Hanford Site. The preferred method of disposing of the portion that is classified as immobilized low-activity waste (ILAW) is to vitrify the waste and place the product in near-surface, shallow-land burial facilities. The LMHC project to assess the performance of these disposal facilities is known as the Hanford ILAW Performance Assessment (PA) Activity, hereafter called the ILAW PA. Acceptance of ILAW disposal at Hanford depends on demonstrating that public health and the environment are adequately protected. Achieving this goal will require predictions of contaminant migration from the facility. To make such predictions will require estimates of the fluxes of water moving through the sediments within the vadose zone beneath and around the disposal facility. These fluxes, loosely called recharge rates, are the primary mechanism for transporting contaminants to the groundwater.

Mann (1999) indicates that two disposal sites will be considered: the ILAW Disposal Site (located southwest of the PUREX Plant) and the site of the former Grout Vaults. For each, recharge rate estimates are needed for a fully functional surface cover, its sideslope, and the immediately surrounding terrain. In addition, recharge estimates are needed for degraded conditions and for the case of irrigated farming directly on the cover. Mann (1999) indicates that the temporal scope of the 2001 ILAW PA is 10,000 years, but could be longer as some contaminant peaks occur after 10,000 years.

Pacific Northwest National Laboratory (PNNL) assists LMHC in their performance assessment activities. One of the PNNL tasks is to provide defensible estimates of recharge rates for current conditions and long-term scenarios involving the shallow-land disposal of ILAW (LMHC 1999). A major goal of the recharge task is to collect sufficient data for the conditions and scenarios deemed to be important for evaluating the performance of the disposal facilities. These rate estimates will be provided using lysimetry, tracer studies, and modeling studies.

The recharge task uses the lysimeters at the Field Lysimeter Test Facility (FLTF) in the 200 West Area to collect recharge-related data. The two goals of the lysimeter work are to accurately quantify the recharge flux for scenarios pertinent to the ILAW project and provide a set of long-term monitoring data with which to test the recharge model (e.g., Fayer et al. 1992). This model will be used to extend the observations and estimate recharge rates for potential future scenarios. This appendix summarizes the lysimeter data that have been collected from the FLTF through March 31, 1999.

## A.2 Background

The Protective Barrier Program constructed the FLTF in FY 1987 to test the performance of capillary barrier cover designs (Gee et al. 1989; Wing 1994). Figure A.1 shows the location of the FLTF within the 200 Areas. Figure A.2 shows the layout of the FLTF.

The facility contains a total of 24 lysimeters of three types: 14 drainage, 4 weighing, and 6 small-tube lysimeters. The drainage lysimeters are vertical cylinders that are 3 m deep and 2 m in diameter (surface area of 3.08 $m^2$). The drainage lysimeters compose the walls of the FLTF.

The weighing lysimeters are boxes with length and width dimensions of 1.5 m and a depth of 1.7 m. The boxes rest on platform scales to enable hourly weight measurements of water gain and loss. The weighing lysimeters are at the south end of the FLTF (Figure A.2).

The small-tube lysimeters are vertical cylinders that are 3 m deep and 0.3 m in diameter (surface area of 0.07 $m^2$). Unlike the others, the small-tube lysimeters are clear Plexiglas to facilitate root and soil observations. These lysimeters are arrayed along the inner walls of the FLTF but are not shown in Figure A.2.

Treatments involve variations of material types and thickness, presence of vegetation, and the use of irrigation to mimic the possible increased precipitation of future climate. Data from this facility include drainage, water content, matric potential, temperature, and vegetation observations. Discussions of the early data from this facility can be found in Gee et al. (1989), Campbell et al. (1990), Campbell and Gee (1990), and Gee et al. (1993a).

Because a surface barrier is part of the current conceptual model of the ILAW Disposal Site, the data collected at the FLTF are being used to support recharge estimation for the performance assessment. In 1994, the emphasis of the Protective Barrier Program switched from monitoring the FLTF to constructing and monitoring a prototype barrier in the 200 East Area (Gee et al. 1993b). The change in program emphasis created an opportunity for the ILAW PA disposal project to conduct testing in the facility for soil-vegetation-climate treatments of importance to the ILAW PA project.

Fayer and Felmy (1996)[(a)] described the testing and measurement techniques supported by the ILAW PA project from June 1995 to September 1996. The ILAW-supported activities were at a reduced level relative to the measurement activity conducted under the Protective Barrier Program. Since 1996, the irrigation and monitoring activities have continued on the same limited basis and results have been described briefly in monthly reports. In FY 1998, seven lysimeters were modified to address three important PA scenarios: sand deposition on the barrier, erosion of barrier material, and complete coverage of the barrier by a sand dune. In FY 1999, two additional lysimeters were modified to collect performance data on the modified Resource Conservation and Recovery Act (RCRA) Subtitle C surface

(a) Fayer MJ and D Felmy. 1996. "Integrated Recharge Assessment: Summary of FY 1996 Activities at the FLTF." Letter Report to Fred Mann, September 27, 1996.

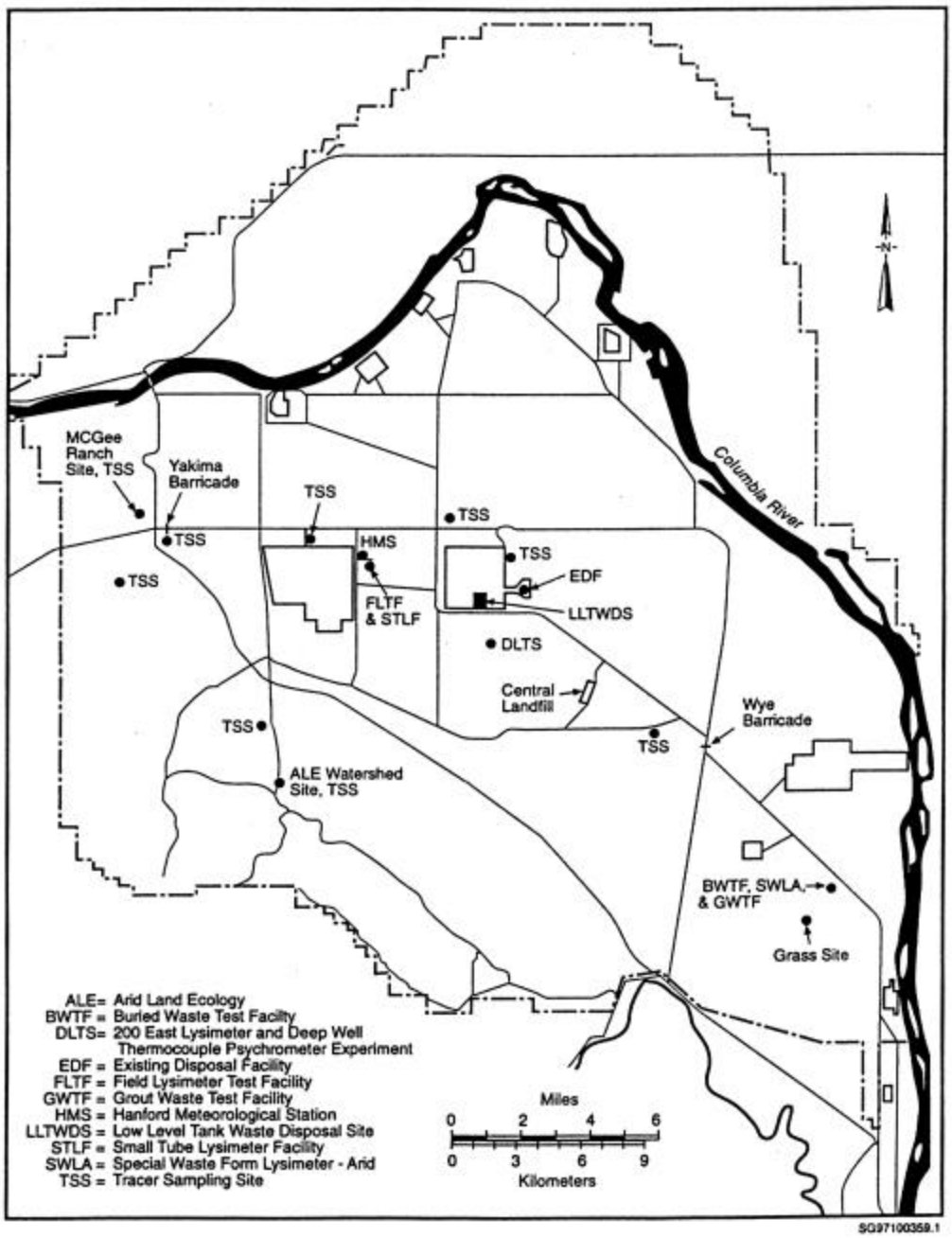


**Figure A.1**. Location of the FLTF

cover design (DOE/RL 1996). The ILAW project is considering this design as a cost-effective substitute to the Hanford Protective Barrier (Myers and Duranceau 1994).

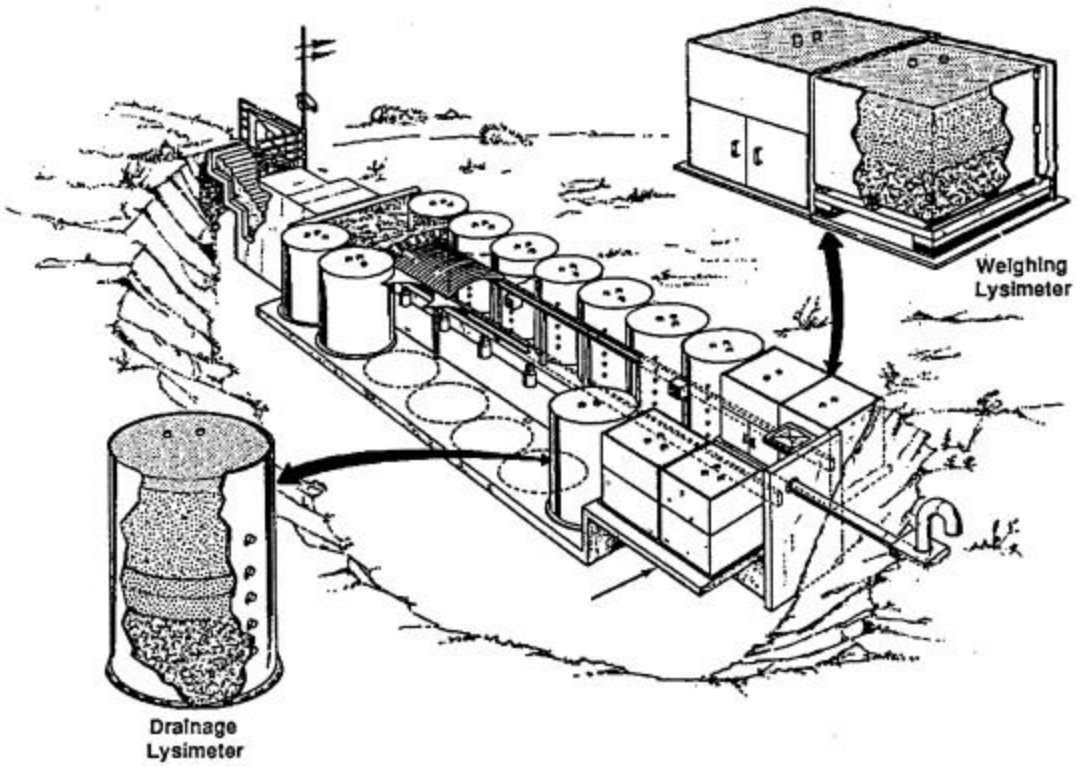


**Figure A.2**. Artist's Rendering of the FLTF

## A.3 Methods

When the FLTF was constructed in 1987, three tests (and seven treatments) were being conducted. When testing was completed for some of the lysimeters, those lysimeters were converted to new tests and treatments. As of March 31, 1999, the number of tests had expanded to 11 and the number of treatments had expanded to 24, reflecting various combinations of soil type and layering, vegetation, and precipitation. The 11 tests and associated data collection activities and frequencies are described below.

### A.3.1 Test Descriptions

Gee et al. (1989), Campbell et al. (1990), Campbell and Gee (1990), and Gee et al. (1993a) provided descriptions of the first five tests. More detail is provided below for the tests initiated in FY 1998 and 1999. Table A.1 summarizes all of the tests and treatments.

**Hanford Barrier**. The objective of this test was to collect data on the performance of a Hanford Barrier. The general configuration consisted of 1.5 m of silt loam that rested on a sequence of materials grading

**Table A.1**. Summary of Treatments and Applicable Dates at the FLTF as of March 31, 1999 ("a" indicates irrigation was accelerated till drainage commenced; "g" indicates sagebrush planted but died, leaving only grasses; treatment 7 lysimeters received special precipitation and evaporation conditions after March 14, 1988; dates in bold italics indicate current configurations).

| Test Description | Treatment ID No. | Precipitation | | | Vegetation | | | Lysimeter ID | Monitoring Period | |
|---|---|---|---|---|---|---|---|---|---|---|
| | | 1x | 2 to 3x | 3x | NV | SRV | DRV | | Start | End |
| Hanford Barrier | 1 | X | | | | | X | D4 | 4 Nov 1987 | 22 Apr 1994 |
| | | X | | | | | X | D7 | 4 Nov 1987 | 22 Apr 1994 |
| | | X | | | | | X | W1 | 4 Nov 1987 | ***31 Mar 1999*** |
| | | X | | | | | X[g] | C3 | 9 Nov 1988 | ***31 Mar 1999*** |
| | 2 | X | | | X | | | D1 | 4 Nov 1987 | ***31 Mar 1999*** |
| | | X | | | X | | | D8 | 4 Nov 1987 | 27 Feb 1998 |
| | | X | | | X | | | W2 | 4 Nov 1987 | 26 Nov 1997 |
| | 3 | | X | | | | X | D13 | 4 Nov 1987 | 27 Feb 1998 |
| | | | X | | | | X | D14 | 4 Nov 1987 | 22 Apr 1994 |
| | | | X | | | | X | W3 | 4 Nov 1987 | ***31 Mar 1999*** |
| | | | X | | | | X | C6 | 9 Nov 1988 | ***31 Mar 1999*** |
| | 4 | | X | | X | | | D10 | 4 Nov 1987 | ***31 Mar 1999*** |
| | | | X | | X | | | D12 | 4 Nov 1987 | 26 Nov 1997 |
| | | | X | | X | | | W4 | 4 Nov 1987 | 26 Nov 1997 |
| | 7 | | X[a] | | X | | | D9 | 4 Nov 1987 | 22 Apr 1994 |
| | | | X[a] | | X | | | D11 | 4 Nov 1987 | 22 Apr 1994 |
| Hanford Barrier w/Gravel Admix | 5 | X | | | | | X | D2 | 4 Nov 1987 | 22 Apr 1994 |
| | | X | | | | | X[g] | D5 | 4 Nov 1987 | 26 Nov 1997 |
| Eroded Hanford Barrier | 6 | X | | | | | X | D3 | 4 Nov 1987 | ***31 Mar 1999*** |
| | | X | | | | | X | D6 | 4 Nov 1987 | 27 Feb 1998 |
| | 18 | | | X | | | X | D13 | 27 May 1998 | ***31 Mar 1999*** |
| Gravel Mulch | 8 | X | | | X | | | C1 | 17 Nov 1989 | ***31 Mar 1999*** |
| | 10 | | X | | X | | | C4 | 17 Nov 1989 | ***31 Mar 1999*** |
| Pitrun Sand | 9 | X | | | | | X[g] | C2 | 17 Nov 1989 | ***31 Mar 1999*** |
| | 11 | | X | | | | X | C5 | 17 Nov 1989 | ***31 Mar 1999*** |
| Basalt Sideslope | 12 | X | | | X | | | D2 | Nov 1994 | ***31 Mar 1999*** |
| | 13 | | | X | X | | | D9 | Nov 1994 | Nov 1998 |
| Sandy Gravel Sideslope | 14 | X | | | X | | | D4 | Nov 1994 | ***31 Mar 1999*** |
| | 15 | | | X | X | | | D11 | Nov 1994 | ***31 Mar 1999*** |
| Hanford Prototype Barrier | 16 | X | | | | | X | D7 | Nov 1994 | Nov 1998 |
| | 17 | | | X | | | X | D14 | Nov 1994 | ***31 Mar 1999*** |
| Hanford Barrier Erosion/Dune Sand Deposition | 19 | X | | | | X | | D5 | 15 Nov 1997 | ***31 Mar 1999*** |
| | | X | | | | X | | W2 | 15 Nov 1997 | ***31 Mar 1999*** |
| | 20 | | | X | | X | | D12 | 15 Nov 1997 | ***31 Mar 1999*** |
| | | | | X | | X | | W4 | 15 Nov 1997 | ***31 Mar 1999*** |
| Sand Dune Migration | 21 | X | | | | X | | D6 | 22 Jul 1998 | ***31 Mar 1999*** |
| | 22 | | | X | | X | | D8 | 22 Jul 1998 | ***31 Mar 1999*** |
| Modified RCRA Subtitle C Cover | 23 | X | | | | | X | D7 | 23 Feb 1999 | ***31 Mar 1999*** |
| | 24 | | | X | | | X | D9 | 23 Feb 1999 | ***31 Mar 1999*** |
| Vegetation Symbols are: NV = no vegetation, SRV = shallow rooted vegetation, and DRV = deep rooted vegetation | | | | | | | | | | |

from sand to gravel filter layers and finally resting on basalt riprap. This test included shrub-steppe vegetation and no vegetation comparisons (treatment numbers 1 through 4, and 7 in Gee et al. 1993a).

**Hanford Barrier with Gravel Admix**. The objective of this test was to collect data on the impact of a gravel admix on the performance of a Hanford Barrier. The basic configuration was a Hanford Barrier, with the exception that the top 0.2 m of silt loam was amended with pea gravel. The gravel content was 15% by weight. This test included shrub-steppe vegetation but addressed only ambient precipitation (treatment number 5 in Gee et al. 1993a).

**Eroded Hanford Barrier**. The objective of this test was to collect data on the performance of an eroded Hanford Barrier. The basic configuration was a Hanford Barrier, with the exception that the silt loam layer thickness was reduced from 1.5 to 1.0 m. This test included shrub-steppe vegetation (treatment number 6 in Gee et al. 1993a and 18 in this appendix).

**Gravel Mulch**. The objective of this test was to collect drainage data on the performance of a gravel mulch layer above Hanford formation sand. The basic configuration was 0.15 m of coarse gravel above 1.35 m of screened pitrun sand (to remove the gravel), on top of unscreened pitrun sand (described below). This test did not include vegetation (treatment numbers 8 and 10 in Gee et al. 1993a). Although not its primary purpose, this test may be useful for characterizing deep drainage rates at the high-level waste tank farms at Hanford.

**Pitrun Sand**. The objective of this test was to collect drainage data on the performance of a coarse gravelly sand taken from a nearby borrow pit (hence "pitrun" sand). The basic configuration was 1.5 m of screened pitrun sand (to remove the gravel), on top of unscreened pitrun sand. This test included shrub-steppe vegetation (treatment numbers 9 and 11 in Gee et al. 1993a).

**Basalt Sideslope**. The objective of this test was to collect drainage data on the performance of basalt riprap that could be used to construct sideslopes for surface covers. The basic configuration was 1.5 m of unscreened basalt riprap. This material is being tested for sideslope use on a larger scale at the Hanford Prototype Barrier in the 200-BP-1 Operable Unit (Ward et al. 1997). Beneath the basalt layer was a 0.15-m thick asphaltic concrete layer that was underlain by gravel and more basalt riprap. Resting on top of the asphaltic concrete was about 2 to 3 cm of silt loam, within which was embedded a 2.54-cm outside diameter fiberglass wick. The wick was splayed out within the silt loam to maximize contact, but exited through the drain outlet as one piece. This test did not include vegetation (treatment numbers 12 and 13 in Gee et al. 1993a).

**Sandy Gravel Sideslope**. The objective of this test was to collect drainage data on the performance of unprocessed local sandy gravel that could be used to construct sideslopes for surface covers. The basic configuration was 1.5 m of sandy gravel resting on an asphaltic concrete layer in a manner similar to the basalt sideslope test. The sandy gravel material was tested for sideslope use on a larger scale at the Hanford Prototype Barrier in the 200-BP-1 Operable Unit (Ward et al. 1997). This test did not include vegetation (treatment numbers 14 and 15 in Gee et al. 1993a). Although not its primary purpose, this test may be useful for characterizing deep drainage rates at the high-level waste tank farms at Hanford.

**Hanford Prototype Barrier**. The objective of this test was to collect data on the performance of the Hanford Prototype Barrier design. The basic configuration was 1.0 m of silt loam amended with pea gravel (15% by weight) above 1.0 m of silt loam, which gave a combined thickness of 2.0 m. Beneath the silt layer were sand and gravel filter layers, then the asphaltic concrete layer described in the basalt sideslope test description. A full-scale cover of the same design was built in the 200-BP-1 Operable Unit (Ward et al. 1997). The test at the FLTF included shrub-steppe vegetation (treatment numbers 16 and 17 in Gee et al. 1993a).

**Hanford Barrier Erosion/Dune Sand Deposition**. The objective of this test was to collect data on the performance of the Hanford Barrier after experiencing some erosion of the silt loam layer and subsequent deposition of dune sand. The top 20-cm of silt loam was removed from four lysimeters containing a Hanford Barrier. The excavated silt loam was replaced with dune sand to study the effect of sand deposition. The dune sand was obtained from the dune that is aligned along the southern edge of the ILAW Disposal Site (Reidel et al. 1998). All instruments remained as before. This test included shallow-rooted vegetation, primarily cheatgrass (treatment numbers were 19 and 20).

**Sand Dune Migration**. The objective of this test was to collect data on the performance of a sand dune that might migrate onto the surface cover. Two lysimeters were completely filled with dune sand. These lysimeters will provide data on the impact of a dune forming on a barrier, as well as provide data on the behavior of dunes that might form around a barrier and elsewhere at the Hanford Site. The dune sand was obtained from the dune that is aligned along the southern edge of the ILAW Disposal Site (Reidel et al. 1998). Tensiometers were installed to measure matric potential at three depths: 100, 150, and 210 cm. An aluminum access tube was inserted vertically for neutron probe measurements of water content. Time-domain-reflectometry probes were installed horizontally to measure water content at nine depths (5, 30, 60, 90, 120, 150, 180, 210, and 240 cm). A tenth time-domain-reflectometry probe was installed vertically from 5 to 35 cm. An array of thermocouples was installed to measure temperature variations. This test included shallow-rooted vegetation, primarily cheatgrass (treatment numbers were 21 and 22).

**Modified RCRA Subtitle C Cover**. The objective of this test was to collect data on the performance of a modified RCRA Subtitle C barrier that was proposed by DOE/RL (1996). This barrier design meets the requirements for a RCRA Subtitle C barrier but uses a thinner silt loam soil than the Hanford Prototype Barrier (1.0 rather than 2.0 m). In addition, the silt layer has two modifications. The first is that the upper 0.5 m of silt loam is amended with pea gravel at the rate of 15% by weight. The second feature is that the lower 0.5 m of silt is compacted. The rationale for the compacted layer was to create a low-conductivity layer to impede downward drainage (DOE/RL 1996). We expect the compacted layer will initially hinder root growth and make it difficult to establish and maintain shrubs. However, we expect roots will eventually penetrate the compacted layer, reduce its density, and thus no other treatment in the FLTF has a layer that has been compacted. Table A.2 describes the materials and the depth intervals within the lysimeters.

The configuration in the lysimeters differs from the modified RCRA Subtitle C design in three ways. First, we discovered that one sand filter layer was not enough to prevent sand movement into the gravel filter. We added a coarser sand layer (No. 8 sand) between the 20/30 sand and the gravel filter. This

**Table A.2**. Material Configuration for the Test of the Modified RCRA Subtitle C Cover

| Material | Depth Intervals (m) | |
|---|---|---|
| | D7 | D9 |
| Warden Silt Loam with 15% gravel | 0-0.5 | 0-0.5 |
| Warden Silt Loam (compacted to 1.6 g/cm$^3$) | 0.5-1.0 | 0.5-1.0 |
| #2030 Granusil #4075 Silica | 1.0-1.10 | 1.0-1.10 |
| #8 Mesh Granusil #2095 Silica | 1.10-1.15 | 1.10-1.15 |
| 1.9 cm (0.75 in.) Chips (gravel filter) | 1.15-1.3 | 1.15-1.3 |
| 3.18 cm (1.25 in.) Chips (lateral drainage) | 1.3.-1.7 | 1.3.-1.5 |

arrangement is the same filter sequence used in the other lysimeters. The overall sand layer thickness remained unchanged at 0.15 m.

The second change involved the lateral drainage layer. The specified material (3.18 cm minus) met the particle size requirements, but the conductivity was much less than 1 cm/s. We replaced this material with 3.18-cm chips, which had conductivity in excess of 1 cm/s.

The final change involved the density of the lower silt loam layer. We had an extremely difficult time trying to compact it to the specified density of 1.76 g/cm$^3$. We tried a tamping bar, a gas-powered plate compactor, a gas-powered upright compactor, and a hydraulic hole compactor. The tamping bar and plate compactor were unable to give us densities above 1.5 g/cm$^3$. The upright compactor was better (about 1.6 g/cm$^3$), but was still not near the target of 1.76 g/cm$^3$. We expected the hydraulic compactor to be the most compactive of all. However, Northwest Testing, using a commercial density meter, determined that the effort of the hydraulic system was not exceeding the densities achieved with the upright compactor.

The square design of the hydraulic compactor made it difficult to be effective in a round lysimeter with a neutron probe access tube in the center. Also, its end plate was large (roughly 28 cm$^2$); a smaller end plate may have enabled the hydraulic compactor to be more successful. After trying several methods, we completed compacting the silt loam layer with the gas-powered upright compactor. A single soil core from D9 (43.18-cm long, 2.54-cm diameter) yielded a density of 1.6 g/cm$^3$.

Both lysimeters contain a tensiometer to measure matric potential at the 100-cm depth, a neutron probe access tube to measure water content, and a series of thermocouples to measure soil temperature distributions. This test included shrub-steppe vegetation (treatment numbers were 23 and 24).

### A.3.2 Data Collection Methods and Frequency

The types of data needed to estimate recharge and test models include water contents and storage, matric suction, temperature, drainage, and vegetation characteristics. Some measurements were conducted manually, while others are made automatically using the facility data logger system. Each lysimeter has a unique combination of sensors, sensor placement, and measurement frequency. Most details are provided by Gee et al. (1989); any variations are explained below.

**Weather**. Weather data were collected at the Hanford Meteorological Station (HMS), which is located at the same elevation about 0.5 km west of the FLTF (Hoitink et al. 1999). The HMS is a complete weather station, providing hourly measurements of all variables, including air temperature, dewpoint temperature, solar radiation, wind speed, cloud cover, and precipitation. The station is operated by another project.

**Irrigation**. A subset of lysimeters received irrigation to mimic an increased precipitation regime. Untreated water from the Columbia River was applied in increments ranging from 3 to 35 mm per application. The rate was typically 4 mm/h. During several years, up to 73 mm of water were applied in a single irrigation event to simulate a 1,000-year storm. The total quantity and frequency of application were determined by the target amount, which was either two or three times the monthly average. The water was delivered through six nozzles spaced 0.41 m apart along a 2.4-m boom that was connected to the water source. The boom was 0.5 m above the ground surface and was moved automatically down the length of the facility at the rate of about 0.7 m/min. Four rain gauges were positioned within the irrigation path and monitored during each application. The weight resolution of the weighing lysimeters was better than the rain gauges, so lysimeter W4 was used to check the application rate.

**Water Content**. Water content was measured primarily with a neutron probe. The measurement frequency was bi-weekly in the first 6 years and sporadic thereafter. The measurement depths were every 15 cm, starting at the 15-cm depth. In lysimeters containing silt loam layers, measurements were not made below the silt loam-sand interface. In FY 1999, the two lysimeters containing dune sand were instrumented with time-domain-reflectometry probes that coincided with neutron probe measurement depths. Water contents were not measured in the sideslope treatments or in the clear tube lysimeters.

**Water Storage**. Water storage was measured directly in the weighing lysimeters. In the other lysimeters, water storage was calculated by integrating the water content measurements for the entire profile. Water storage was not measured in the sideslope treatments or the clear tube lysimeters.

**Matric Potential**. Matric potential was measured intermittently with tensiometers and a pressure transducer. In most lysimeters, two depths were monitored: 100 and 150 cm. In the dune sand treatment, an additional tensiometer was placed at the 210-cm depth. Thermocouple psychrometers were placed in several lysimeters and read independently of the regular data logger program. Matric potential was not measured in the sideslope treatments or the clear tube lysimeters.

**Soil Temperature**. Soil temperature was measured with copper-constantan thermocouples placed at various depths and lateral positions within the lysimeters. The temperatures were measured hourly in some cases, but mostly daily, all by the data logger system. Soil temperature was not measured in the sideslope treatments or the clear tube lysimeters.

**Drainage**. Drainage was measured by collecting free water from the outlet located at the base of each lysimeter. The collected water was weighed immediately at the facility. The nominal collection frequency was bi-weekly. Drainage was measured in all lysimeters.

**Vegetation**. Field observations were used to characterize the phenology of species during the spring of 1988, which was the first growing season. In 1989 and 1992, the height, width, and areal coverage of plants were measured. Minirhizotrons were installed in several lysimeters to monitor root growth. The minirhizotrons, which were 5-cm inside diameter glass cylinders, permitted video camera observations of root activity and location. Monthly observations of plant activity were initiated in November 1998. Each lysimeter is surveyed to identify the species present and their areal coverage, and the height of shrubs.

## A.4 Results

The FLTF has been operated for more than 11 years and, in that time, yielded significant quantities of data. Examples are presented below that illustrate the type of data collected since it was constructed in 1987. Following the data examples is a synthesis of observations relative to the potential for drainage in each of the eleven tests described in Section 2. Finally, the results are discussed relative to unresolved issues and future activities.

### A.4.1 Data Examples

#### A.4.1.1 Weather

Figure A.3 shows that monthly average air temperatures for the period of FLTF operation (defined as November 1987 to March 1999) have been consistently higher than the temperatures for the period from 1961 to 1990. The averages for the period of FLTF operation were warmer by amounts ranging from

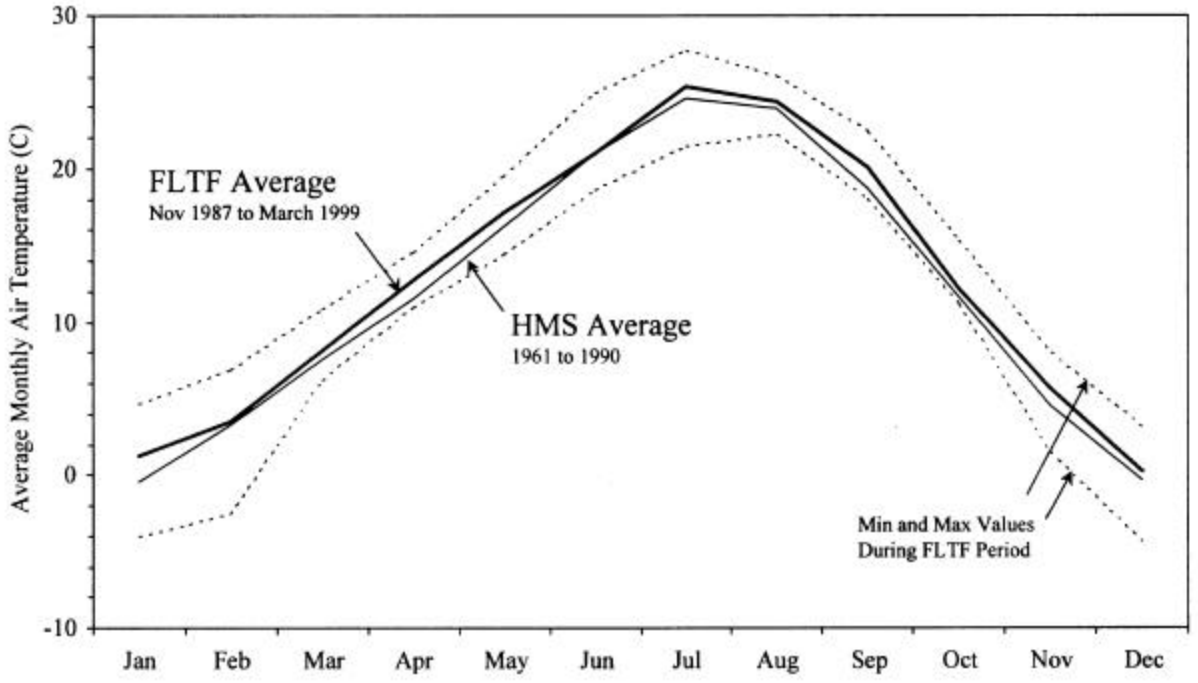


**Figure A.3**. Monthly Air Temperatures Measured at the HMS

0.1 to 1.7°C. Six monthly records for maximum temperature were either set or tied (one monthly minimum record was also set). Overall, average annual air temperature was 0.8°C warmer than the average temperature from 1961 to 1990.

Figure A.4 shows that monthly precipitation amounts were mostly higher than normal amounts. During the FLTF period of operation, monthly amounts ranged from 2.7 mm less than normal to 6.8 mm greater. Four maximum monthly precipitation records were set. The maximum annual precipitation record of 313 mm was set in 1995. This record was nearly broken in the following year when annual precipitation totaled 310 mm. During the FLTF period, two records for maximum monthly snowfall were set: 57.4 cm in December 1996 and 43.2 cm in February 1989. The annual snowfall record of 142.5 cm was set during the winter of 1992-1993. During the FLTF period, the annual average precipitation was 191 mm, which was 30 mm greater than the 1961 through 1990 average of 161 mm.

### A.4.1.2 Irrigation

Figure A.5 shows that the irrigation applications were sufficient to maintain the target rate in most years. Deviations occurred during lysimeter modifications, when it was not possible to run the system because of open lysimeters and construction material.

### A.4.1.3 Water Content

Figure A.6 shows how water content varied annually in the Hanford Barrier for the driest condition (lysimeter D4, with ambient precipitation and vegetation) and the wettest condition (lysimeter D10, with irrigation but without vegetation). Water content in D4 was initially high (between 0.15 and 0.2 $cm^3/cm^3$)

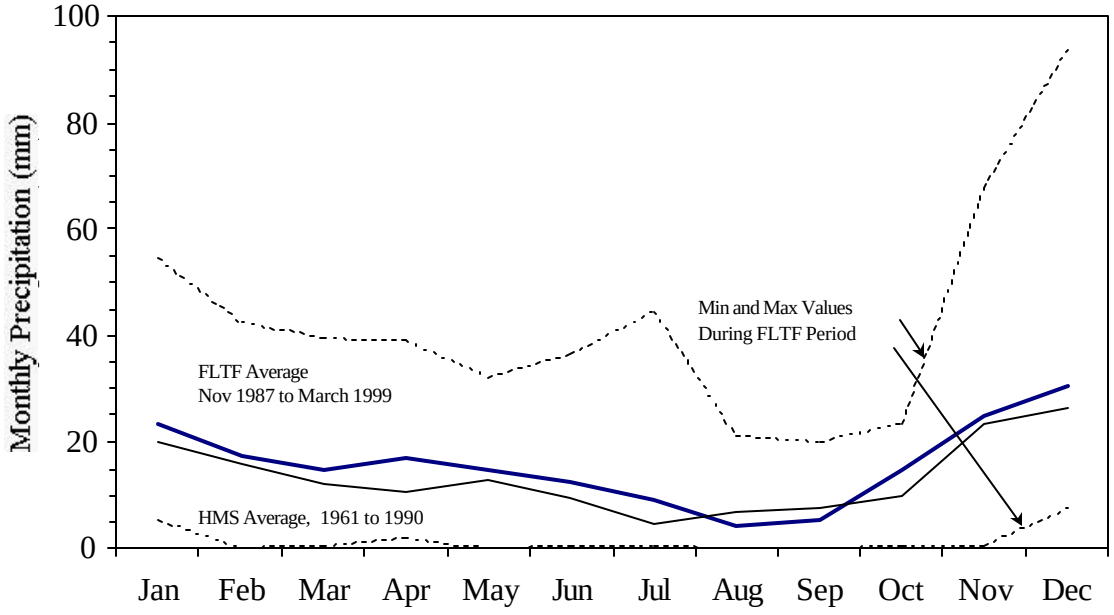


**Figure A.4**. Monthly Precipitation Measured at the HMS

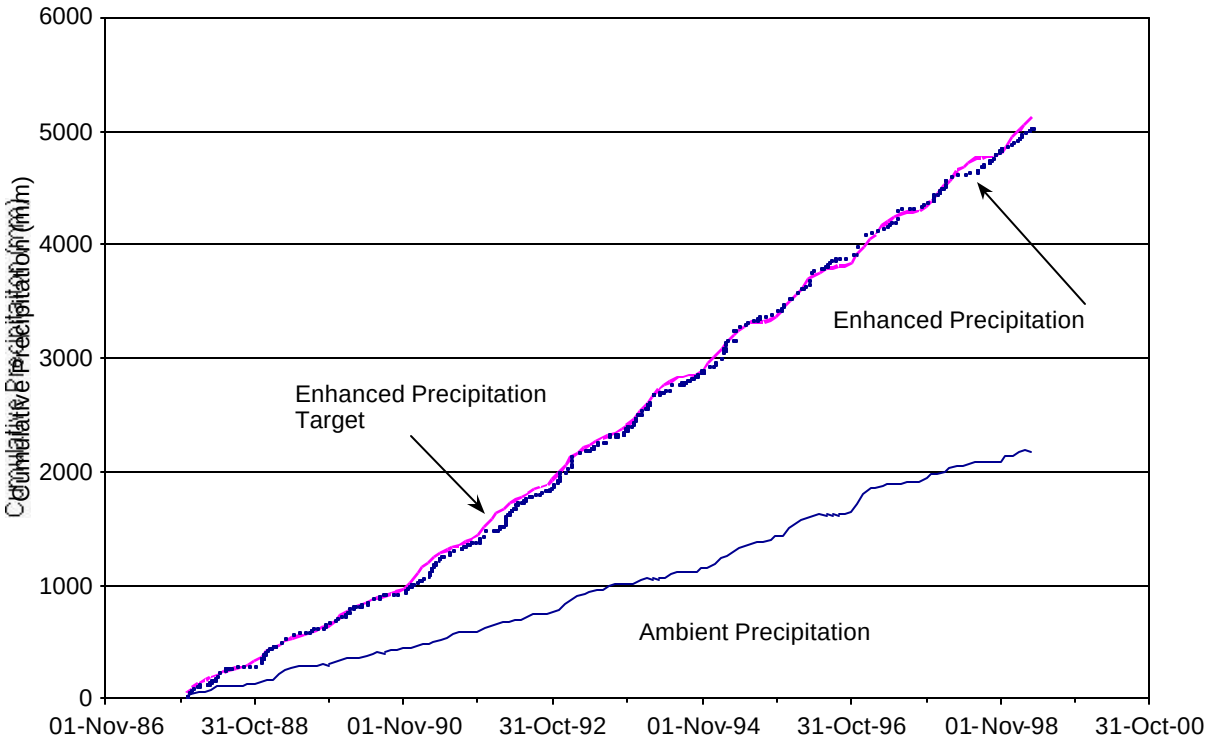


**Figure A.5**. Precipitation Treatments and the Enhanced Precipitation Target

but quickly dropped to 0.05 to 0.07 $cm^3/cm^3$ at all depths in the first summer. This rapid drop in water content at all depths demonstrates the ability of plants to extend roots deep into the profile quickly and extract existing water. In subsequent winters, water content increased in the 30- to 60-cm depth range, but hardly changed at all at deeper depths. The winter increases at 30 cm varied year-to-year, giving some indication of the impact of weather variations. In summers, water content always dropped to the same range, about 0.05 to 0.07 $cm^3/cm^3$ at all depths. This minimum range appears to be the limit to which plants can extract water.

Water content in D10 was much higher than in D4. During the first 3 years, when irrigation raised the water application to 2x normal precipitation, the high water content in winter ranged from 0.22 to 0.33 $cm^3/cm^3$. When irrigation was increased to achieve 3x normal precipitation, the high water content in winter ranged from 0.25 to 0.42 $cm^3/cm^3$. Theoretically, the distribution of water received in each year was the same. However, water content in D10 shows distinct differences from year to year. These differences may be related to several factors, including variations in weather (e.g., warm versus cool spring) changes in vegetation, and responses to irrigation (for some months, ambient precipitation was high and obviated the need for irrigation). Another factor could be the irrigation schedule. Our goal was to apply water each month so that the total amount of water received was consistent with the target (either 2 or 3x the normal monthly precipitation). As mentioned earlier, we were not able to do so consistently.

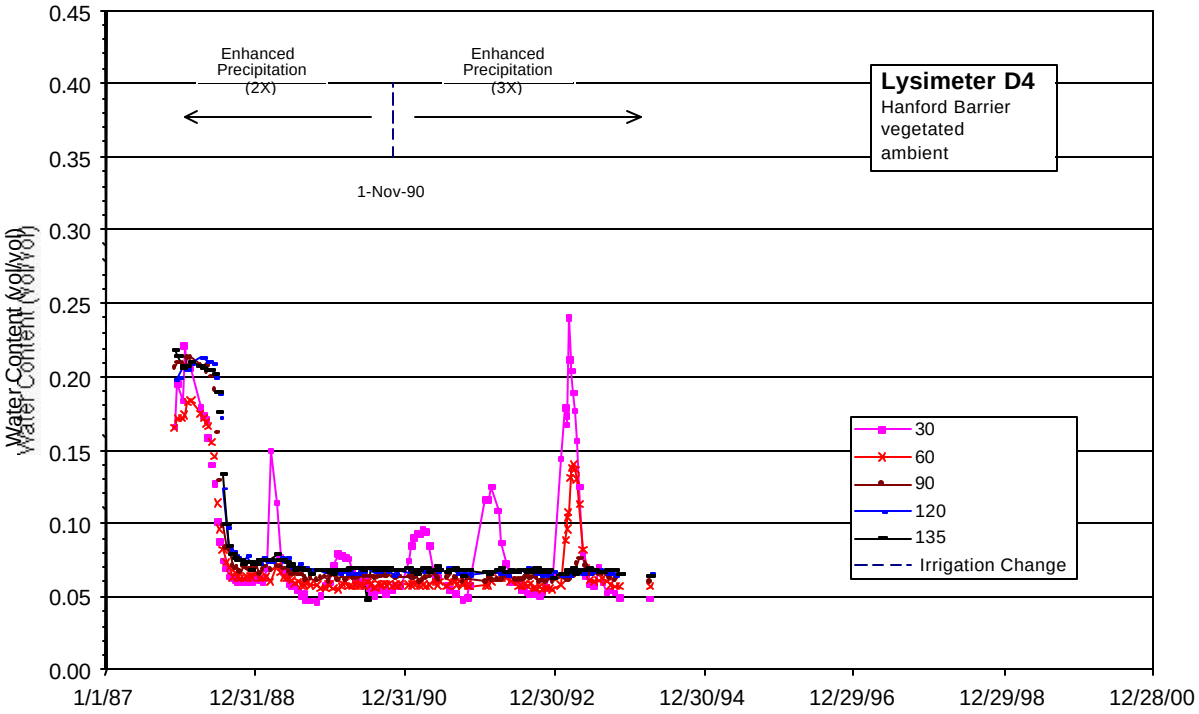


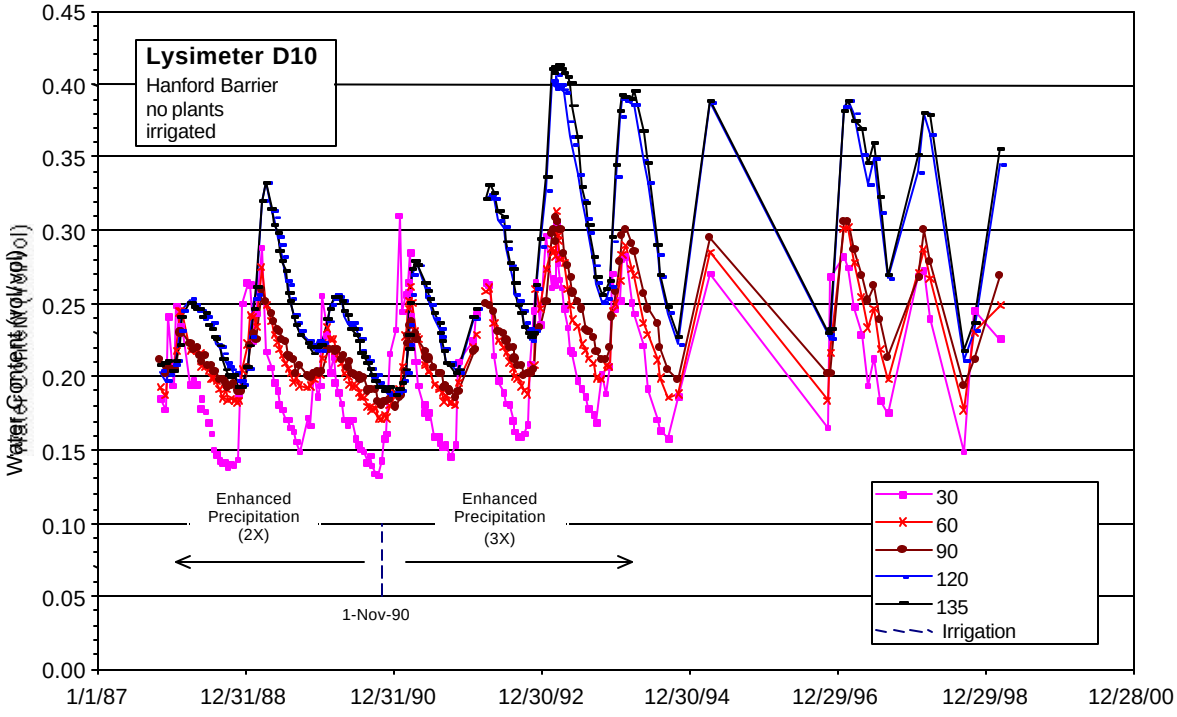


**Figure A.6**. Annual Water Content Variations for Several Depths Within the Hanford Barrier

Water content in D10 during the summer months was as low as 0.14 $cm^3/cm^3$ at the shallower depths. In the first three summers, the water content appeared to persist for a month or two before rising in the fall. This low water content may represent a minimum value that the evaporation process can accomplish under the enhanced precipitation regime. At the deeper depths, water content rarely dropped below 0.2 $cm^3/cm^3$ in the summer.

### A.4.1.4 Water Storage

Figure A.7 shows how water storage varied annually in the Hanford Barrier for the driest condition (lysimeter W1, with ambient precipitation and vegetation) and the wettest condition (lysimeter W4, with irrigation but without vegetation). More than 200 mm of water was removed in the first year, which reduced storage to a minimum of about 100 mm. After the first year, winter water storage was never as high as the initial storage, indicating that W1 started much wetter than could be sustained by ambient conditions. In the summers, storage always returned to a consistent minimum of about 80 mm.

In contrast to W1, much more water was stored in W4. Under 2x precipitation, the peak water storage was 450 mm, and under 3x precipitation, the peak was 590 mm. Despite attempts to replicate the same precipitation regime each year, water storage in W4 showed distinct year-to-year differences, probably for the same reasons outlined above for water content. In summers, water storage never reached a recognizable minimum value, indicating that the lysimeter continued to lose water all summer.

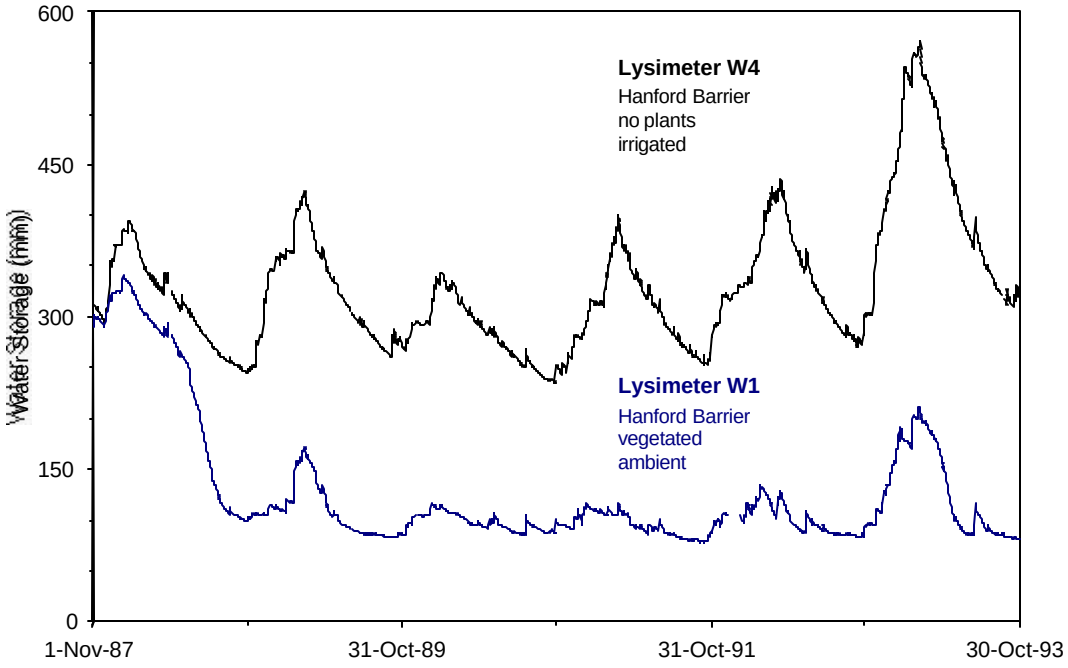


**Figure A.7**. Daily Water Storage for the Hanford Barrier

### A.4.1.5 Matric Potential

Only a few lysimeters had matric potentials high enough to measure with a tensiometer. For these, Figure A.8 shows that potentials at the 150-cm depth were quite consistent from 1995 through 1997. In November 1997, D12 and W4 were modified: 20 cm of silt loam was removed and replaced with 20 cm of dune sand (treatment No. 20). In the following summer, potentials in D10 dropped as in previous years, but potentials in D12 and W4 remained above -100 cm. All three lysimeters were mostly unvegetated, so the contrast in potentials is due primarily to the impact of the surface soil. The dune sand is much less able than the silt loam to store water near, and/or transmit water to, the evaporation surface. These lysimeters were intended to be unvegetated in 1998, but tumbleweeds invaded all three lysimeters and grew to a height of 30 cm in a 1-month period before being removed in May. The results can be seen in Figure A.8 as the rapid drop in matric potentials in the spring of 1998.

Thermocouple psychrometers were placed in several lysimeters, but data from only five of these sensors were reported for a single date, October 22, 1989 (Campbell and Gee 1990). For one of the three psychrometers at the 150-cm depth in W2 and W4, the matric potentials were -0.6 and -0.9 MPa, respectively. For the three psychrometers at the 150-cm depth in W3, the matric potentials were -2.1, -2.5, and -3.1 MPa. These data clearly show the ability of plants in W3 to extract water and reduce the soil water matric potential. Differences among the three potentials in W3 also give an indication of the variability that is possible over a very short distance (< 1.2 m).

In addition to tensiometers and psychrometers, some soil samples were collected and analyzed for matric potential using the filter paper method (Gee et al. 1993a). Samples were collected from six depths

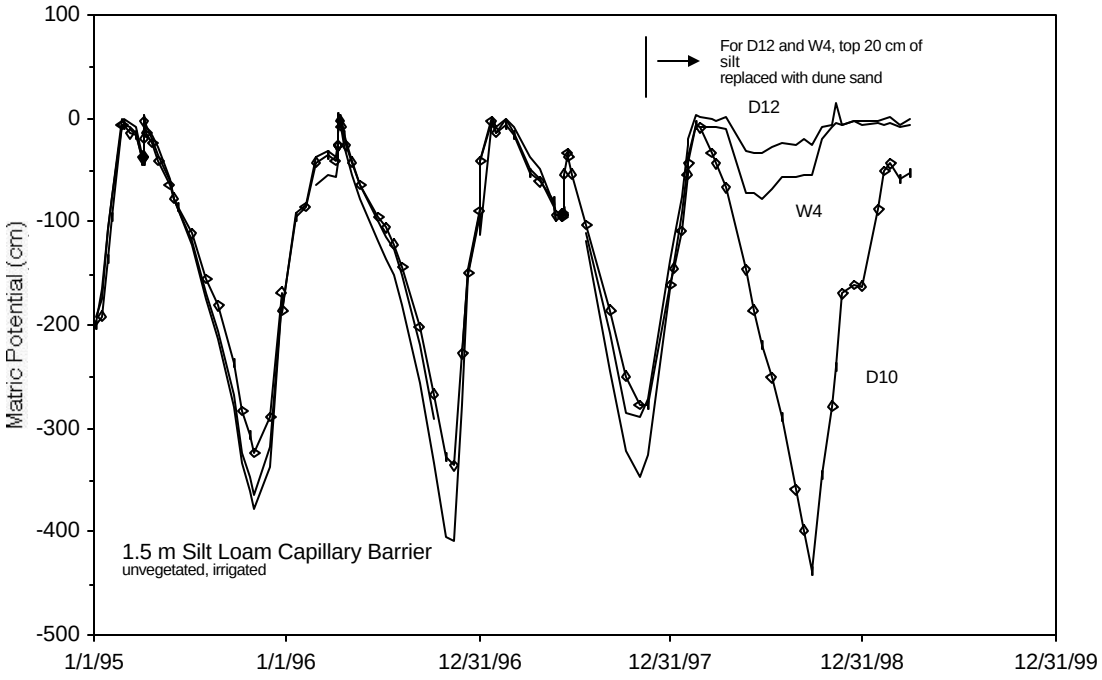


**Figure A.8**. Matric Potentials at the 150-cm Depth in the Irrigated Hanford Barrier with No Plants

(0.5, 1, 5, 10, 15, and 20 cm) in six lysimeters on three dates in October 1991 and two dates in July 1992. The results showed that matric potentials at the soil surface were lower than -100 MPa in all treatments examined; the absolute minimum potential observed was -210 MPa. At the 20-cm depth, the matric potentials in the unvegetated lysimeters were nearly all less than -1.4 MPa, regardless of precipitation treatment. Potentials in the vegetated lysimeters ranged from -1.8 to -48.8 MPa under ambient precipitation and -5.7 to -14.7 MPa under enhanced precipitation.

#### A.4.1.6 Temperature

Hourly soil temperatures were recorded for the thermocouples in the weighing lysimeters and in some of the drainage lysimeters. Figure A.9 shows how temperature varied with depth and time in W2 on September 30, 1993. The response in Figure A.9 is typical of soil temperatures. Near-surface temperatures exhibit the largest temperature range whereas deep temperatures barely change in a day. The progression of the temperature pulse through the soil is delayed and the peak is damped relative to the pulse at the soil surface. The result of the delay and damping is that temperature at the 150-cm depth has a seasonal rather than daily cycle.

#### A.4.1.7 Drainage

Since the fall of 1989, all of the lysimeters containing vegetated Hanford Barrier treatments had no drainage, even under the 3x precipitation treatment. We did not include 1987 and 1988 because of the leak tests (Campbell and Gee 1990), which we could not separate from actual drainage. Through September 1989, two of the vegetated lysimeters drained less than 0.1 kg in 1989, but we suspect this was residual water from leak testing conducted in 1988. In the 10 years since then, no water has drained from vegetated Hanford Barrier lysimeters. The drainage design specification for the Hanford Barrier was to limit drainage to less than 0.5 mm/yr. The FLTF observations are strong evidence that the Hanford Barrier design functions much better than designed.

Between 1989 and 1999, the two drainage caissons (D1 and D8) containing the unvegetated Hanford Barrier test that received ambient precipitation drained an average of 0.05 and 0.2 mm/yr. The drainage always occurred in mid to late summer and was attributed to vapor flow (Campbell and Gee 1990). Figure A.10 shows how the annual drainage amounts for lysimeters D1 and D8 varied. A similar seasonal drainage pattern was observed prior to 1993 in the two drainage caissons containing the unvegetated Hanford Barrier that received enhanced precipitation. Results from these lysimeters are also included in Figure A.10. Two questions arise from these results. First, does the drainage water originate from the basalt riprap and gravel (i.e., residual water from construction and leak testing) or from the silt loam layer above? Second, if seasonal temperature changes are affecting drainage, is the design of the lysimeter facility in any way responsible? Ward et al. (1997) reported “small seasonal discharges” from the Hanford Prototype Barrier test plots. These vegetated test plots were in a full-scale surface cover; thus avoiding any complications such as might be possible in the FLTF. Their data set covered 3 years of monitoring following construction. If they continue to occur during the next several years, the seasonal discharges will provide strong evidence that temperature cycles in the silt loam layer induce water movement into the underlying gravel.

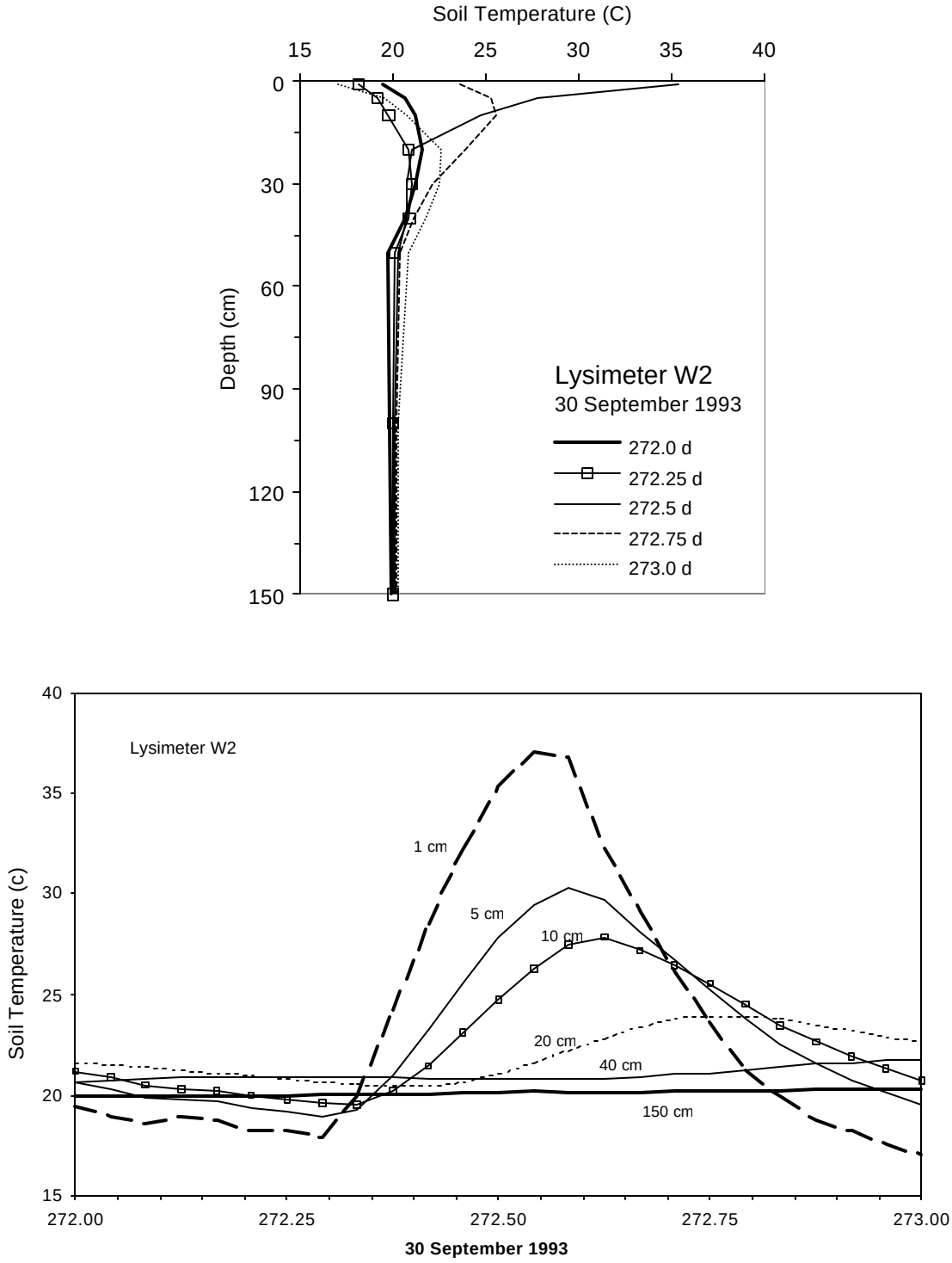


**Figure A.9**. Soil Temperatures

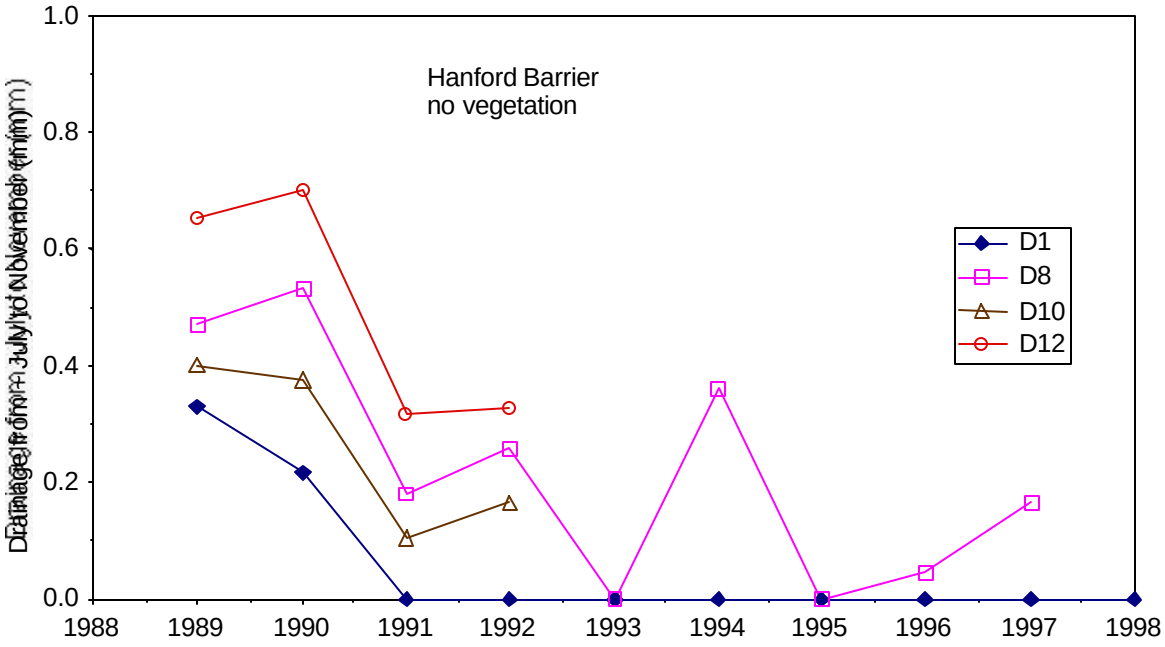


**Figure A.10**. Annual Drainage from the Lysimeters Containing the Unvegetated Hanford Barrier

The four weighing lysimeters, containing the Hanford Barrier test, had zero drainage. In these lysimeters, there is no coarse gravel or basalt layer within which vapor could move downward and condense at greater depths. A complicating factor is that these lysimeters are susceptible to unusual temperature changes. They have an air gap along the sides (to allow free movement up and down on the scale) and their bottoms are somewhat "de-coupled" from the ground temperature because of the scale.

The only condition that led to significant drainage from a Hanford Barrier treatment was 3x precipitation and no vegetation. Figure A.11 shows that, for the first 3 years (under 2x precipitation), the three lysimeters containing an unvegetated Hanford Barrier had no significant drainage. Three years after increasing to 3x precipitation, these lysimeters had significant drainage. The onset of drainage coincided with the melting of a large snowpack in February 1993. In early 1997, a similar event occurred that also resulted in significant drainage from these lysimeters. In the intervening years, and in 1998, individual lysimeters had small amounts of drainage, but there was no consistency in amount. Such differences indicate the drainage variability that could be expected in a real cover.

After D12 and W4 were modified in November 1998, the drainage pattern of the three lysimeters diverged. D10 continued to have very little drainage, while D12 and W4 began to have more drainage than was collected in all of the previous years combined. The increase in drainage resulted from the replacement of 20 cm of silt loam with dune sand on the surface. This result is consistent with the observed increase in matric potential in D12 and W4.

Figure A.12 shows that drainage from the sideslope treatments was consistently significant in every year. The sandy gravel lysimeters drained 536 mm under ambient precipitation (992 mm) and 1424 mm

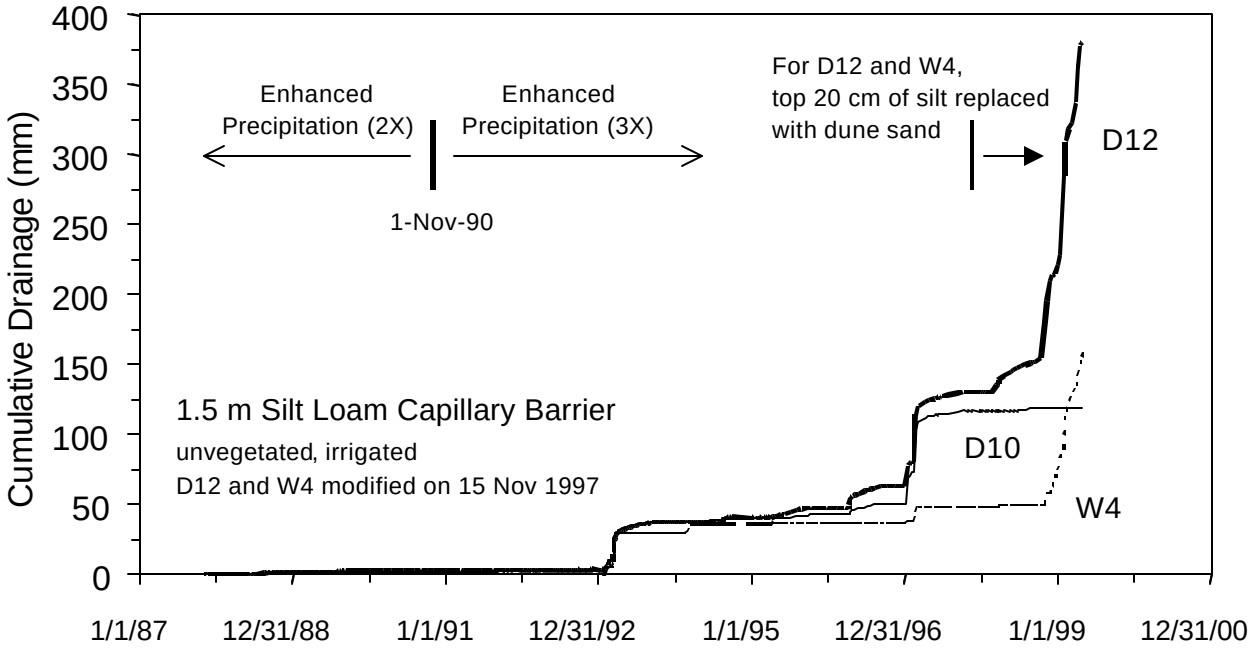


**Figure A.11**. Cumulative Drainage from Irrigated Lysimeters Containing the Unvegetated Hanford Barrier

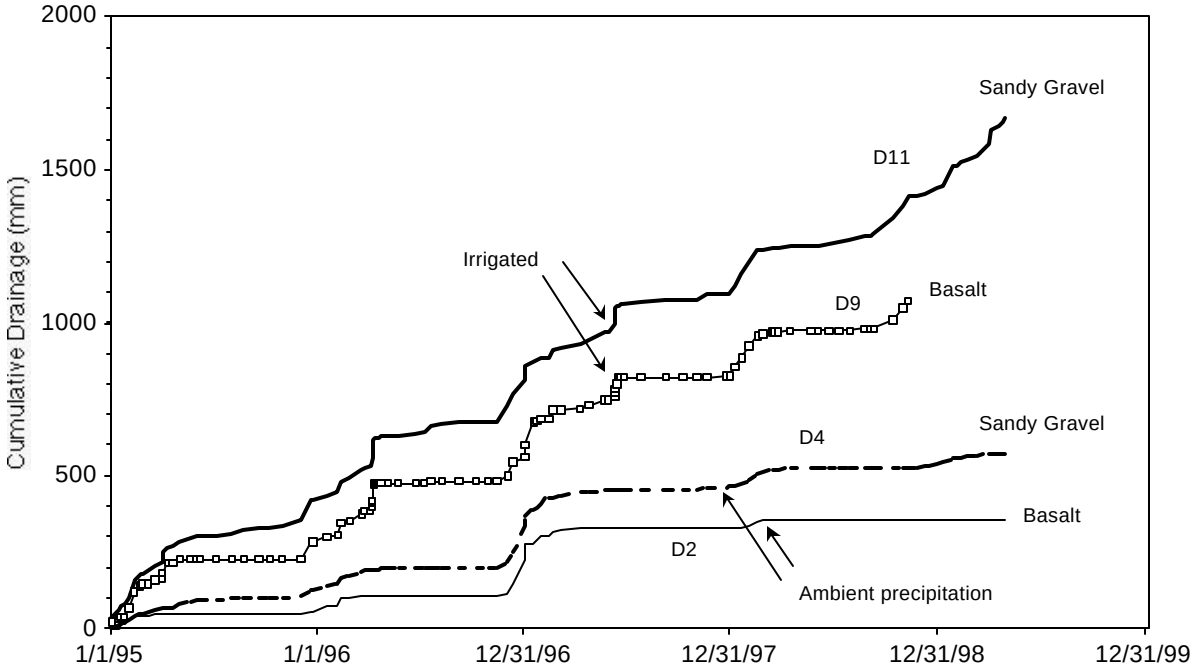


**Figure A.12**. Cumulative Drainage from the Lysimeters Containing Sideslope Tests

under enhanced precipitation (1978 mm) from mid-November 1994 through 1998. For the 4.1-year period, the average drainage rates were 130 and 345 mm/yr, respectively. These rates represent 54% of the amount of water received under ambient conditions and 72% under enhanced precipitation. The level of ambient precipitation received during this time was 48% higher than normal. It may be that, if precipitation rates subside to more-normal levels, the percentage that becomes drainage may fall to something less than 54%. If the percentage remained the same, then the drainage rate associated with the normal precipitation (160 mm/yr) would be 86.4 mm/yr. This rate could also be applied to conditions at the tank farms in the 200 Areas. The precise value for each tank farm would depend on the distribution of sand and gravel on the surface. In addition, this rate does not account for any effects caused by the increased temperature around the tanks.

The higher percentage (of precipitation becoming drainage) for the enhanced precipitation treatment may truly reflect what could happen under wetter regimes. It may also be related to the method of applying irrigation water. With this method, 10 to 20 mm of irrigation water were applied in a single event rather than as more numerous smaller events. Large events may penetrate the profile more deeply, where the water would be less susceptible to evaporation.

Under both precipitation regimes, the basalt sideslope had less drainage and, in some years, had no drainage. These lysimeters drained 357 mm under ambient precipitation and 1051 mm under enhanced precipitation from mid-November 1994 through 1998. For the 4.1-year period, the average drainage rates were 87.1 and 256 mm/yr, respectively. These rates represent 36% of the amount of water received under ambient conditions and 53% under enhanced precipitation. For the long-term average precipitation rate of 160 mm/yr, the basalt drainage data translate to a long-term drainage rate of 57.6 mm/yr.

One theory why drainage rates through basalt riprap are lower than those through sandy gravel is that the voids between the basalt fragments are so large. Significant amounts of air can move in and out of these large voids and thus effectively extend the drying region deeper into the profile than is normal for soil (Ward et al. 1997). Another factor at the FLTF is the design of the test. The lysimeters containing the sideslope treatments have an asphaltic concrete layer at 1.5 m. On top of this layer is about 2 to 3 cm of silt loam within which was embedded a 2.54-cm outside diameter fiberglass wick. The wick was splayed out within the silt loam to maximize contact, but exited through the drain outlet as one piece. We had some difficulty with this arrangement. First, the wick was jammed as it passed through the outlet and we believe this restricted drainage from the lysimeter. By delaying drainage, water was left standing in the caisson and susceptible to evaporation. Second, the silt loam has a fair amount of storage capacity. Water stored in this layer would not have drained through the wick when potentials dropped below -20 cm. This stored water would also be susceptible to evaporation.

Figure A.13 shows that there was significant drainage from four of the clear tube lysimeters, the two with pitrun sand and the two with gravel mulch. The clear tube lysimeters containing the Hanford Barrier configuration (C3 and C6) never had drainage. The pitrun sand lysimeters had drainage in some but not all years. Although the lysimeters are vegetated, the plants were unable to prevent drainage. From February 8, 1990, through February 11, 1998, drainage rates averaged 23.6 and 52.4 mm/yr for the ambient (C2) and enhanced precipitation (C5) treatments, respectively. These drainage rates represented 12 and 11%, respectively, of the total amount of precipitation and irrigation received from 1990 to 1998.

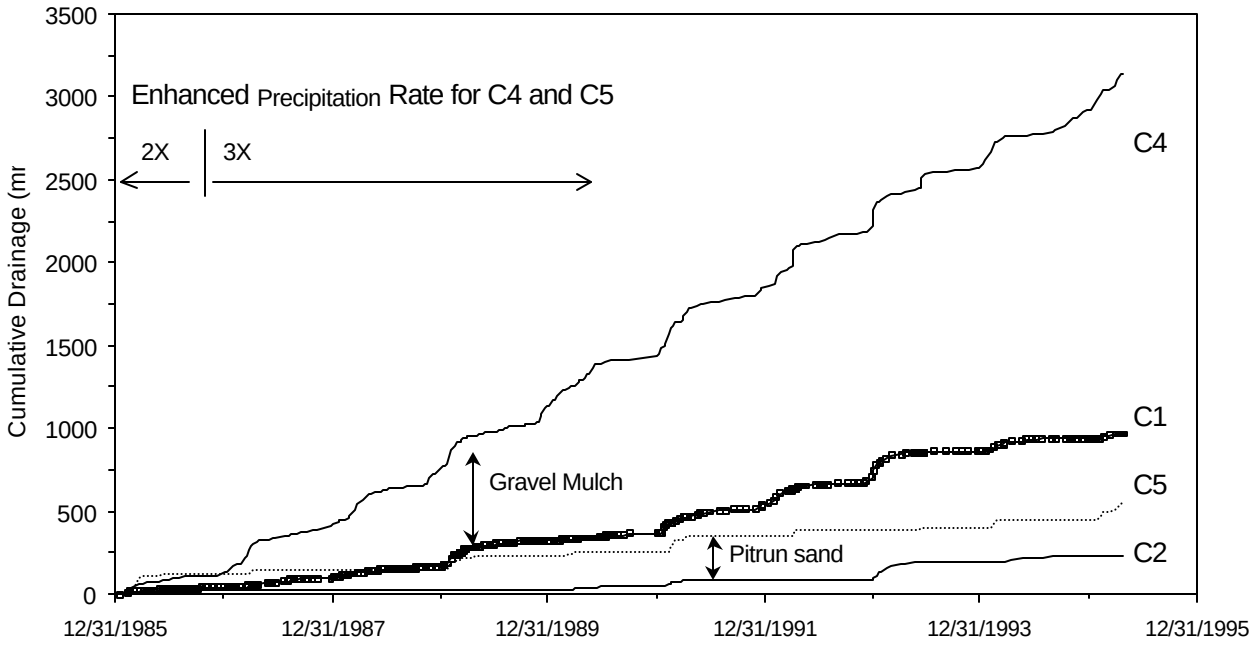


**Figure A.13**. Cumulative Drainage from the Clear Tube Lysimeters

Figure A.13 shows that the gravel mulch lysimeters had much more drainage than the pitrun sand lysimeters. From February 8, 1990, through February 11, 1998, drainage rates averaged 104 and 332 mm/yr for the ambient (C1) and enhanced precipitation (C4) treatments, respectively. These drainage rates represented 52 and 72%, respectively, of the total amount of precipitation and irrigation received from 1990 to 1998. Two factors that explain the higher drainage relative to the pitrun sand test are the lack of vegetation and the suppression of evaporation by the gravel mulch. The suppression occurs because water that infiltrates into the sand beneath the gravel can only evaporate by the slow process of diffusion up through the gravel mulch layer. The other mechanism for water to move upward is for water to flow directly in the liquid phase up through the gravel. Such flow is essentially negligible because of the extremely low hydraulic conductivity of unsaturated gravel.

### A.4.1.8 Vegetation

Vegetation was planted on the lysimeters in November 1987 for the first three tests. Bunchgrasses and sagebrush seedlings were dug at McGee Ranch, which has a shrub-steppe plant community growing on silt loam (Gee et al. 1989). McGee Ranch was the borrow area for the silt loam that was placed in the lysimeters. Species included *Poa sandbergii* (Sandberg's bluegrass), *Oryzopsis hymenoides* (Indian rice grass), and *Artemisia tridentata* (sagebrush). Although *Bromus tectorum* (cheatgrass) was present at McGee Ranch, no attempt was made to transplant it. Gee et al. (1989) assumed that cheatgrass seed was present in the transplant soil masses as well as in the plant community surrounding the FLTF and that cheatgrass would have no difficulty occupying the lysimeter surfaces.

The record of vegetation measurements and observations is sparse. Phenology observations were made in the spring of 1988 only. Phenological stages were delayed about 1 month relative to stages observed in natural settings, possibly because of the wet initial conditions in the lysimeters (Gee et al. 1989).

In May 1989 and the spring of 1992, individual plant height, width, areal coverage, and location within the lysimeters were measured. The main observation was that irrigation caused significant increases (by a factor of 2 to 3) in total plant biomass. Indian rice grass decreased in all lysimeters between 1989 and 1992 but the cause was never determined (Gee et al. 1993a).

Root behavior was observed with the minirhizotrons and reported only once (Campbell et al. 1990). The data, in the form of root counts, suggested higher root density under the enhanced precipitation treatment.

Root observations were also made using the clear tube lysimeters. Sagebrush roots grew downward through the silt loam in lysimeter C6 at an average rate of 2 cm/d, and sometimes at rates as high as 5 cm/d (Campbell and Gee 1990; Campbell et al. 1990). The downward growth rate may have been a function of the constrained rooting volume because the lysimeter diameter was only 0.3 m. When the roots reached the sand filter layer, they penetrated no more than 1 cm presumably because the sand held very little water. In the sandy soil of lysimeters C2 and C5, the downward root growth rate averaged 1.4 and 0.9 cm/d, respectively. All of these lysimeters were moist prior to transplanting. In lysimeter C3, which was not irrigated, roots grew down to the existing wetting front within the silt loam layer and stopped. The sagebrush on this lysimeter died in 1989 and was not replaced. The hypothesis is that the water available in this small lysimeter was insufficient to support the plant.

The sagebrush on C6 died in 1991, despite receiving the enhanced precipitation treatment. Although cheatgrass remained, lysimeter C6 became noticeably wetter in the next two years. By early 1993, the filter layers and basalt riprap were visibly wet. In March 1993, a sagebrush seedling was planted on C6. By late May, a few roots had penetrated the sand filter layer and entered the gravel filter layers. By late July, a few roots appeared to be at the 2-m depth. These observations indicated that gravel layers are not root impediments, or barriers, as long as water is available (Gee et al. 1993a). Between 1993 and 1998, the sagebrush in C6 died and no attempt was made to plant a replacement.

On four dates in late 1998 and early 1999, the FLTF was surveyed to identify the existing plant species and monitor changes in areal coverage. Sagebrush and Sandberg's bluegrass still remained. Indian rice grass was no longer present. A new species was observed on several lysimeters: *Agropyron cristatum* (crested wheatgrass). Cheatgrass was present on most of the vegetated lysimeters. Individuals of eight other species were present. The most notable of this group was *Salsola kali* (tumbleweed), which has a deeply penetrating taproot that allows the plant to extract water stored deep within the profile.

Since 1987, one of the most difficult tasks in operating the FLTF is maintaining the no-vegetation status of those lysimeters that were supposed to be bare. Our experience has been that these lysimeters must be weeded every two weeks in the spring and monthly during the remainder of the year. On several occasions, a one-month hiatus in weeding during the spring resulted in an extensive crop of plants,

usually tumbleweeds but also sagebrush seedlings, cheatgrass, and other species. The implication is that a non-vegetated condition (e.g., due to fire, disturbance, etc.) will probably not persist for silt loam surface barriers for more than a couple of months, and certainly not for more than 1 year.

### A.4.2 Results of the Eleven Tests

We used the FLTF data (primarily the drainage data) to draw conclusions for each of the eleven tests. For the barrier tests, we compared the drainage data to the design standard of 0.5 mm/yr (Wing 1994). For our evaluations, we assumed natural conditions, with no disturbance by humans.

**Hanford Barrier**. For periods ranging from 6.5 to 11 years, there has been no drainage from the lysimeters containing the Hanford Barrier configuration (1.5 m of silt loam above sand and gravel layers) with plants. For Hanford Barrier lysimeters without plants, there has been no significant drainage (i.e., greater than 0.5 mm/yr) under ambient precipitation and under 3 years of 2x normal precipitation. Drainage from these non-vegetated lysimeters eventually occurred, but only after 3 years of 3x normal precipitation. Based on our experience of keeping these lysimeters plant-free, we predict that Hanford Barriers receiving 3x normal precipitation will not remain plant-free for more than a few months at most. Based on all of the data collected to date, we expect that the Hanford Barrier will perform as designed for the conditions envisioned for the ILAW Disposal Site.

**Hanford Barrier with Gravel Admix**. The two lysimeters containing this configuration with plants and receiving the ambient precipitation treatment showed no drainage after 6.5 and 10 years, respectively. The gravel admix did not appear to impair the ability of the Hanford Barrier to prevent drainage. We did not see any recognizable differences in plant community compared to the tests without gravel admix. Although there were no treatments involving enhanced precipitation, we expect that a Hanford Barrier with gravel admix and receiving enhanced precipitation will prevent drainage as designed.

**Eroded Hanford Barrier**. The two lysimeters (containing 1.0 m of silt loam above sand and gravel), with plants, and receiving the ambient precipitation treatment showed no drainage after 10 years. This configuration is similar to the modified RCRA Subtitle C cover. The results suggest that the modified RCRA cover will perform as well. A test of the actual design has been initiated (see below). The single lysimeter receiving the enhanced precipitation treatment was set up and started in May 1998. With a data record less than 1 year long, this test is not complete. However, we expect that it will be just as successful as the ambient treatment in preventing drainage.

**Gravel Mulch**. The two small lysimeters used for this test generated a significant amount of drainage in 8 years: 104 mm/yr (52% of received water) for the ambient treatment and 332 mm/yr (72% of received water) for the enhanced precipitation treatment. These results may be useful for describing an upper limit to deep drainage in tank farms. The gravel mulch used at the FLTF contains very few finer particles (except what the wind deposits). Tank farms, in contrast, have 50% or more sand particles (Figure 3 of Smoot et al. 1989). Of all the tests, the clean gravel mulch without plants resulted in the highest deep drainage rates.

**Pitrun Sand**. The two small lysimeters used for this test generated a measurable amount of drainage, although not consistently in every year. In an 8-year period, drainage rates averaged 23.6 mm/yr (12% of received water) for the ambient precipitation treatment and 52.4 mm/yr (11% of received water) for the enhanced precipitation treatment. These lysimeters are vegetated, mostly with grasses. Several attempts were made to establish sagebrush, but the plants did not survive for more than a few years. Thus, these deep drainage results are probably higher than for a similar sand with a shrub-steppe plant community.

**Basalt Sideslope**. The two lysimeters used for this test generated a significant amount of drainage in 4 years: 87.1 mm/yr (36% of received water) for the ambient treatment and 256 mm/yr (53% of received water) for the enhanced precipitation treatment. As a percentage of total water input, drainage was 36 and 53% for the ambient and enhanced precipitation treatments. These lysimeters had no vegetation, so the drainage rates should be viewed as upper limits. A field-scale test of this sideslope with no vegetation is occurring at the Hanford Prototype. The results after 3 years indicated drainage rates of 22 to 34% of the precipitation (Ward et al. 1997).

**Sandy Gravel Sideslope**. The two lysimeters used for this test generated a significant amount of drainage in 4 years: 130 mm/yr (54% of received water) for the ambient treatment and 345 mm/yr (72% of received water) for the enhanced precipitation treatment. As a percentage of total water input, drainage was 54 and 72% for the ambient and enhanced precipitation treatments. These lysimeters had no vegetation, so the drainage rates should be viewed as upper limits. A field-scale test of this sideslope, with vegetation (albeit limited), is occurring at the Hanford Prototype. The results after 3 years indicated drainage rates of 20 to 30% of the precipitation (Ward et al. 1997). The lysimeter and Hanford Prototype results may be useful for describing deep drainage in tank farms. However, we have no measure of the particle size distribution of the sandy gravel used in the tests.

**Hanford Prototype Barrier**. The two lysimeters used for this test had no drainage in 4.5 years, even under 3x normal precipitation. In addition, matric potentials were always below the tensiometer range, indicating dry soil. We expect that the Hanford Prototype Barrier will perform as designed for the conditions envisioned for the ILAW Disposal Site.

**Hanford Barrier Erosion/Dune Sand Deposition**. The four lysimeters used for this test have been monitored for 1.5 years. The matric potential data indicate that the silt loam is wetting under both precipitation treatments. Drainage has not occurred for the ambient precipitation, but has been significant for the 3x normal precipitation treatment. After 1 to 2 more years, we suspect that drainage may begin from the ambient treatment. Vegetation on the lysimeters is limited to shallow-rooted species, primarily cheatgrass. The combination of dune sand and cheatgrass was intended to mimic a serious but plausible degradation of the cover. In the first year, the cheatgrass cover was not measured because it was sparse to non-existent. By November 6, 1998, one year after the test began, there was no live cheatgrass on D5 and 25% coverage on D12. Because of the limited cheatgrass cover during the first year, the drainage results may more accurately be said to reflect an unvegetated state. Cheatgrass was much more prevalent in spring 1999. It may be that several years are required for vegetation to establish itself in the lysimeters of this test. Till then, we make no predictions except to say that sand deposition on a surface cover has the potential to degrade performance relative to preventing drainage.

**Sand Dune Migration**. The two lysimeters used for this test were started in July 1998, so the length of record is short. By March 31, 1999, no drainage had occurred from the lysimeter receiving ambient precipitation. However, the lysimeter receiving 3x normal precipitation already generated significant drainage. Like the erosion/deposition test above, vegetation is supposed to be shallow-rooted species like cheatgrass. However, plant activity was marginal, so the results are more nearly like an unvegetated test. It may be that several years are required for shallow-rooted vegetation to establish itself. Till then, we make no predictions except to say that a sand dune on a surface cover has the potential to degrade surface cover performance (relative to preventing drainage) and to increase recharge rates in the immediate vicinity of the cover.

**Modified RCRA Subtitle C Cover**. The two lysimeters used for this test were started in February 1999. It will take several years of data to reach conclusions, but we expect that this cover will perform as designed for the conditions envisioned for the ILAW Disposal Site.

## A.5 Conclusions

The data collected at the FLTF have shown how soil type, barrier design, vegetation, and precipitation can impact deep drainage rates. One of the significant results from the FLTF is that the Hanford Barrier described by Wing (1994) worked much more successfully than expected. In concert with vegetation, the barrier reduced drainage to zero (compared to the design goal of 0.5 mm/yr). This performance occurred under ambient and 2x precipitation, with or without plants. Even under 3x precipitation, the vegetated Hanford Barrier prevented drainage. The only condition that resulted in drainage through a Hanford Barrier was when plants were purposefully kept off for three consecutive years under 3x precipitation. All indications are that plants will never be absent for more than a few months and that precipitation will not exceed 128% of modern levels, which is far below the 3x precipitation rate that caused drainage.

A second barrier design, the Hanford Prototype Barrier, also reduced drainage to zero. Data are just starting to be collected for a third design, the Modified RCRA Subtitle C barrier. Two lysimeters with a similar design (i.e., 1 m of silt loam) had zero drainage in 10 years under ambient precipitation conditions. Therefore, we expect the modified RCRA Subtitle C design will work just as well at preventing drainage.

The addition of gravel admix to the surface silt loam layer of the Hanford Barrier did not impact barrier performance, nor did the loss of 0.5 m of silt to erosion. In both cases, there was no drainage. The dune sand test is beginning to show an increase in water storage. Although the length of record is short and there is already measurable drainage under the 3x precipitation treatment. The lysimeters in this test had a sparse cover of shallow-rooted cheatgrass and none of the deep-rooted plants of a shrub-steppe community that might reduce drainage considerably. Without a deep-rooted shrub-steppe plant community, deposition of wind-blown sand on the cover is a concern.

The sideslope tests showed how poorly these materials prevented drainage. The sandy gravel material drained 54% of the ambient precipitation, while the basalt drained 36%. These tests were not vegetated, so the results represent an upper limit to drainage through such sideslopes.

Because the cover systems performed much better than the design goal of 0.5 mm/yr, we propose using a rate of 0.1 mm/yr for the 2001 ILAW PA. The data clearly support this lower rate. We would have proposed a lower rate if we understood the seasonal drainage observations more fully. The possibility of seasonal water vapor movement downward from the surface cover indicates a need to understand the temperature effects.

## A.6 References


Campbell MD, GW Gee, MJ Kanyid, and ML Rockhold. 1990. *Field Lysimeter Test Facility: Second year (FY 1989) test results*. PNL-7209, Pacific Northwest Laboratory. Richland, Washington.

Campbell MD and GW Gee. 1990. *Field Lysimeter Test Facility: Protective barrier test results (FY 1990, the third year)*. PNL-7558, Pacific Northwest Laboratory, Richland, Washington.

DOE (1996). See U.S. Department of Energy.

Fayer MJ, ML Rockhold, and MD Campbell. 1992. "Hydrologic modeling of protective barriers: Comparison of field data and simulation results." *Soil Sci. Soc. Am. J*. 56:690-700.

Gee GW, DG Felmy, JC Ritter, MD Campbell, JL Downs, MJ Fayer, RR Kirkham, and SO Link. 1993a. *Field Lysimeter Test Facility Status Report IV: FY 1993*. PNL-8911, Pacific Northwest Laboratory, Richland, Washington.

Gee GW, LL Cadwell, HD Freeman, MW Ligotke, SO Link, RA Romine, and WH Walters. 1993b. *Testing and monitoring plan for the Permanent Isolation Surface Barrier Prototype*. PNL-8391, Pacific Northwest Laboratory, Richland, Washington.

Gee GW, RR Kirkham, JL Downs, and MD Campbell. 1989. *The Field Lysimeter Test Facility (FLTF) at the Hanford Site: Installation and initial tests*. PNL-6810, Pacific Northwest Laboratory, Richland, Washington.

Hoitink DJ, KW Burk, and JV Ramsdell. 1999. *Hanford Site climatological data summary 1998 with historical data*. PNNL-12087, Pacific Northwest National Laboratory, Richland, Washington.

Lockheed Martin Hanford Company (LMHC). 1999. *Statement of Work for FY 2000 to 2005 for the Hanford Low-Level Tank Waste Performance Assessment Activity*. HNF-SD-WM-PAP-062, Rev. 4, Lockheed Martin Hanford Company, Richland, Washington.

Mann FM. 1999. *Scenarios for the Hanford Immobilized Low-Activity Waste (ILAW) performance assessment.* HNF-EP-0828, Rev. 2, Fluor Daniel Northwest, Richland, Washington.

Myers DR and DA Duranceau. 1994. Prototype Hanford Surface Barrier: Design Basis Document. BHI-00007, Bechtel Hanford Company, Richland, Washington.

Reidel SP, KD Reynolds, and DG Horton. 1998. *Immobilized low-activity waste site borehole 299-E17-21*. PNNL-11957, Pacific Northwest National Laboratory, Richland, Washington.

Smoot JL, JE Szecsody, B Sagar, GW Gee, and CT Kincaid. 1989. *Simulations of infiltration of meteoric water and contaminant plume movement in the vadose zone at single-shell tank 241-T-106 at the Hanford Site*. WHC-EP-0332, Westinghouse Hanford Company, Richland, Washington.

U.S. Department of Energy (DOE). 1996. *Focused feasibility study of engineered barriers for waste management units in the 200 Areas*. DOE/RL-93-33, Rev. 0, U.S. Department of Energy, Richland, Washington.

Ward AL, GW Gee, and SO Link. 1997. *Hanford Prototype-Barrier Status Report: FY 1997*. PNNL-11789, Pacific Northwest National Laboratory, Richland, Washington.

Wing NR. 1994. *Permanent isolation surface barrier development plan*. WHC-EP-0673, Westinghouse Hanford Company, Richland, Washington.

# Appendix B

# Recharge Estimates Using Environmental Tracers at the Immobilized Low-Activity Waste (ILAW) Disposal Site

E. Murphy and J. Phillips

# Appendix B

# Recharge Estimates Using Environmental Tracers at the Immobilized Low-Activity Waste (ILAW) Disposal Site

## B.1 Introduction

This appendix summarizes the analyses of sediments collected from boreholes located in the 200 East Area of the Hanford Site for tracer measurements. This area is a proposed location for the burial of low-level waste encapsulated in glass and is referred to as the Immobilized Low-Activity Waste (ILAW) Site (Figure B.1). In this area, vegetation and, to a lesser degree, heterogeneity in the stratigraphy control the downward movement of water.

Naturally deposited atmospheric tracers were used to determine the rate of water movement through the vadose zone. The natural tracer method based on chloride mass balance (CMB) is one of the simplest, least expensive, and most useful for determining long-term recharge in arid climates (Allison et al. 1994). Recharge is often used interchangeably with deep drainage flux. Technically, recharge is the amount of water over time reaching the water table. Deep drainage flux is the water flux below the evapotranspiration zone, or alternatively, the water flux at a point where the chloride concentration is measured (Phillips 1994). Using the CMB method, recharge is determined by applying a mass balance argument on the

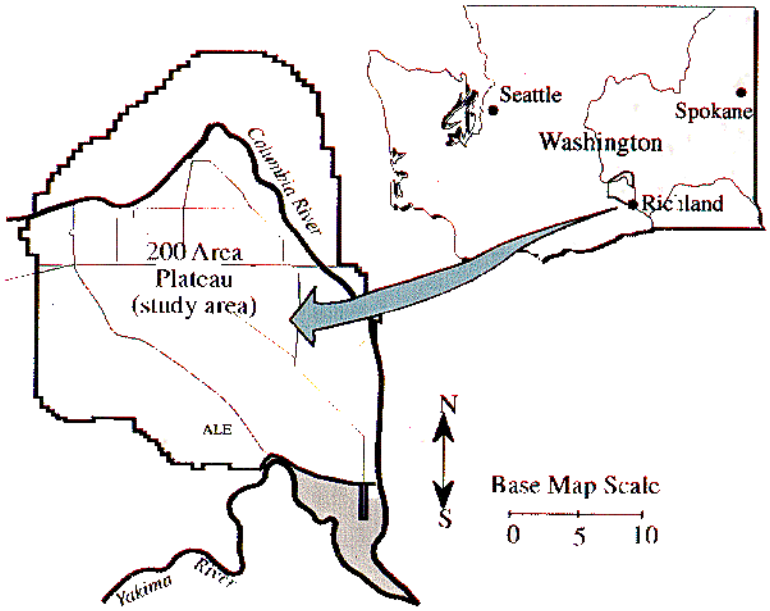


**Figure B.1**. Washington State Map and Location of Study Area at the Hanford Site

chloride ion in which the difference between the chloride concentration in the soil water and the atmospheric input concentration is due to evapotranspirative enrichment.

Environmental tracers give site-specific estimates of deep drainage flux below the evapotranspiration zone. Therefore, this technique is ideal for investigating the effect of spatial variations in vegetation and stratigraphy on recharge. At the proposed ILAW Disposal Site, spatial variations in vegetation and stratigraphy can occur at distances ranging from a meter to tens of meters. Interpretation of chloride profiles at the proposed ILAW Disposal Site suggests that prior to the establishment of a dense sagebrush community, atmospheric tracers such as chloride did not accumulate in the sediment profiles. This indicates rapid water flux through these medium sand sediments. The impact of vegetation and its absence have been demonstrated elsewhere (e.g., Allison 1988). Stratigraphy, in particular the occurrence of silt lenses, impacted the spatial distribution of moisture content across the proposed ILAW Disposal Site. Variations in peak concentrations of chloride in the different boreholes suggest differences in the history of vegetative establishment during the Holocene.

In this appendix we compare information from two exploratory boreholes drilled in 1995, a trench dug in 1995, and four boreholes (B8500 series) drilled in 1998. The objectives of the exploratory drilling in 1995 were to demonstrate the feasibility of collecting continuous cores in these largely sandy sediments and to determine the location of the chloride profiles for recharge estimates. Large volume samples were collected from the trench to develop a profile for the bomb-pulse tracer $^{36}Cl$. An additional objective of the sampling at the B8500 boreholes in 1998 was to provide estimates of natural recharge using tracer methods and to assess the variability in recharge rates across the proposed ILAW Disposal Site.

The application of tracer methods ideally requires the collection and analysis of continuous cores from the surface to below the root zone (approximately to a depth of 15 m at the proposed ILAW Disposal Site). Nearly continuous cores were collected at two previously undisturbed sites in March 1995 using a hollow stem auger with split-tube wire-line sampling. In September 1995, a trench was dug south of the exploratory boreholes to a maximum depth of approximately 5 m. In the spring of 1998, one deep borehole (B8500, also designated 299-E17-21) and two shallow boreholes (B8501 and B8502) were drilled near the proposed ILAW Disposal Site. Unlike previous exploratory drilling in 1995, the drilling for the B8500 series boreholes was not controlled by the researchers who were collecting the data. As a result, many of the standard drilling procedures at the Hanford Site conflicted with or negated the research goals. This impact was most severe on the investigation into recharge mechanisms that are largely controlled by near-surface processes.

Core sediments were not collected above 3 m at B8500, which precludes this borehole being used to estimate recharge with atmospheric tracers. Near-continuous sediment cores were collected from B8501 and B8502. Preliminary results indicate that the near-surface recharge processes at B8501 may have been affected by disturbances associated with the construction of a drilling pad and the standard practice of drilling *through* the gravel pad (as opposed to drilling off the side of the pad in undisturbed sediments). In addition, some of the sediment cores from B8502 were affected at the drill site by storage in ice chests containing standing water. In some cases a wetting front was observed in the core sediment. In other cases, droplets of water were found between the Lexan liner and the duct tape that was used to seal the

ends of the cores. It cannot be determined whether the highly variable moisture profiles at the shallow holes are 1) natural, 2) an artifact of the drilling pad, or 3) lack of end caps and blue ice for sealing and storing the cores. However, in some profiles there is a distinct correlation between increased moisture content and the spatial distribution of silt lenses.

The problems associated with drilling the B8500 boreholes limit the information that can be used from these cores. Except for borehole B8503, which was drilled in undisturbed sediments, the moisture profiles, sediment characterization, and bulk densities should be disregarded in the upper 2 to 3 m of the B8500 boreholes.

## B.2 Site Description

The proposed ILAW Disposal Site is located on the south side of the Cold Creek bar, a depositional bar left in the lee of the Umtanum Ridge during Pleistocene cataclysmic flooding. This bar is dominated by gravel on the north side (closest to the main flood channels) grading to fine sand on the south side.

The proposed ILAW Disposal Site lies along the northern margin of a giant dune field (Appendix D). A long, stabilized dune lying in an east-west direction can be seen along the southern portion of the proposed ILAW Disposal Site in the photograph at the top of Figure B.2. The existence of the dune field appears to be controlled by wind moving from west to east, down the adjacent Dry Creek and Cold Creek valleys and across the expansive Hanford plains toward the Columbia River. Most dunes are stabilized by vegetation and are not actively growing or migrating. The closest point of active dune formation to the proposed ILAW Disposal Site is approximately 3 km south of this area (Gaylord and Stetler 1994). The presence of a dune at the proposed ILAW Disposal Site indicates a history of sand dune development in this area since the last cataclysmic flood (~13,000 years yBP). Appendix D discusses this eolian activity in more detail.

## B.3 Borehole Descriptions

Table B.1 summarizes the six boreholes that have been drilled and used to collect sediment samples for tracer analyses. Two boreholes (designated 299-E24-161 and 299-E24-162) were drilled in 1995 to a depth of approximately 18 m. The stratigraphy consisted of a thin layer of sand, 0.3 to 0.6 m thick, resting on top of the Hanford formation. From 0.6 m to about 4.3 m are gravelly sands, reflecting the strength of the flood currents carrying gravel across the bar. The remainder of the sediments encountered (from 4.3 to 18.0 m) are sands with occasional minor gravel. To minimize surface disturbance, drilling pads were not constructed at these boreholes.

The sand-dominated layers of the Hanford formation were deposited during the late Pleistocene cataclysmic flooding (13,000 to 30,000 years ago). Pedogenic calcium carbonate (Stage 1) forms a partial rind on the underside of some gravel clasts in sediments from 0.3 to 1.2 m deep. No other calcic zones were encountered. Sand grain size is primarily coarse to medium (1 to 0.25 mm in diameter), with more than 70% of the sand consisting of those sizes. This reflects a calmer depositional environment than the north side of the bar, where boulders are up to 0.3 m in diameter. A thin sand layer, formed from reworking of flood deposits, overlies the Hanford formation.

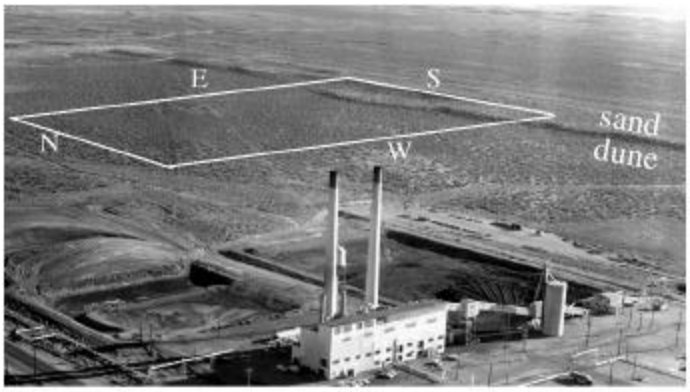


View of ILAW site from north-east. Power plant is in the foreground. The rectangle represents the approximate location of the surface plot below.

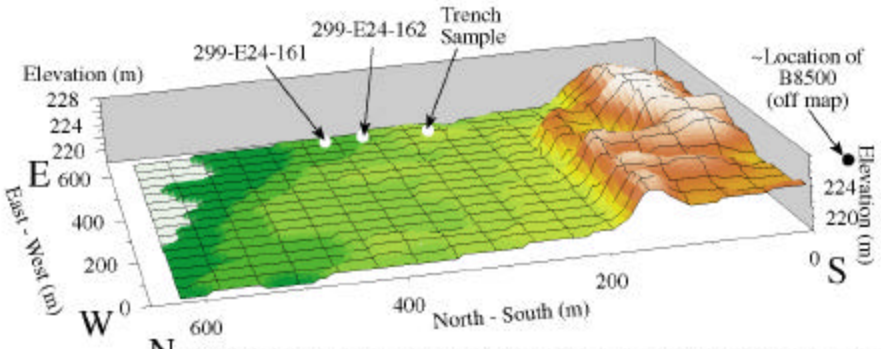


Surface plot of ILAW area. The vertical scale is exaggerated to show relief of the dune at the south end of the site. The locations of exploratory boreholes, trench, and relationship to B8500 borehole are noted.

Hollow-stem auger used in exploratory boreholes.

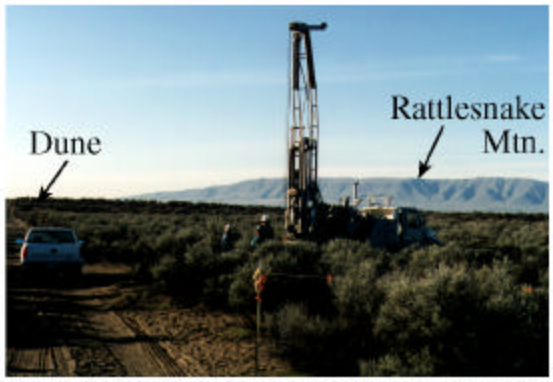


View of the exploratory borehole looking to the south. The dune and Rattlesnake Mtn are visible in the background.

**Figure B.2**. ILAW Site in the 200E Area of the Hanford Site

**Table B.1**. Drilling Locations and Dates for ILAW Tracer Studies

| Borehole ID | Local ID | Northing | Easting | Drilling Start Date |
|---|---|---|---|---|
| 299-E24-161 | NA | N135378 | E574651 | March 1995 |
| 299-E24-162 | NA | N135344 | E574651 | March 1995 |
| 299-E17-21 | B8500 | N134894.21 | E574107.02 | April 6, 1998 |
| NA | B8501 | N134924.68 | E574107.02 | April 24, 1998 |
| NA | B8502 | N134894.21 | E574137.48 | April 27, 1998 |
| NA | B8503 | N134909 | E574127 | ~May 1998 |

The drill pad for the B8500 boreholes was on the western end of the windward side of a dune oriented in an east-west direction. The near surface sediment (apart from the imported sediment fill and drill pad) is primarily the sediment composing the sand dune. Below this dune material the sediments are coarse to medium sands characteristic of the Hanford formation (Reidel and Reynolds 1998).

Many tracer methods rely on accurately measuring the depth below surface of the tracer profiles. To ensure this accuracy, the surface elevations were surveyed using a ground-positioning satellite (GPS) system before the gravel drilling pad was constructed and after the drilling was completed (Table B.2). The natural surface sediments were graded in preparation for the gravel layer as indicated by the large mounds of natural sediments along the northeast edges of the gravel pad. Without GPS readings after grading and prior to application of gravel, it would be difficult to determine the amount of natural sediment that was removed under the existing drilling pad. The sediments under the pad were compacted and visibly wetter than the undisturbed sediments.

**Table B.2**. Pre- and Post-Pad Elevations by Ground-Positioning Satellite

| Well ID | Pre-Pad Elevation ft (m) | Post-Pad Elevation ft (m) | Difference ft (m) |
|---|---|---|---|
| B8500 (2-E17-21) | 734.9 (223.39) | 735.7 (224.24) | +0.8 (+0.85) |
| B8501 | 739.5 (225.40) | 741.1 (224.88) | +1.6 (+1.49) |
| B8502 | 734.9 | 737.8 | +2.9 |

## B.4 Results

The analyses of the borehole samples followed procedures outlined by Murphy et al. (1991) and Murphy et al. (1996). Tables B.3 to B.9 contain the results for every sample analyzed. These results are discussed below.

**Table B.3**. Exploratory Borehole 299-E24-161 Drilled in 1995

| Depth (m) | Moisture Content ($g_{H2O}/g_{dry\ soil}$) | Bulk Density ($g/cm^3$) | Soil Water Chloride ($\mu g_{Cl}/g_{H2O}$) | Soil Water Bromide ($\mu g_{Br}/g_{H2O}$) | Cl/Br | Particle Size Distributions | | | | Sand Sizes | | |
|---|---|---|---|---|---|---|---|---|---|---|---|---|
| | | | | | | Gravel (%) | Sand (%) | Silt (%) | Clay (%) | Coarse (%) | Medium (%) | Fine (%) |
| 0.08 | 0.032 | 1.700 | 106.1 | | | | | | | | | |
| 0.38 | 0.063 | 1.538 | 37.4 | 1.485 | 25 | 0.3 | 82.2 | 14.9 | 2.5 | 8.8 | 13.3 | 60.1 |
| 0.76 | 0.059 | 1.434 | 41.9 | 0.816 | 51 | | | | | | | |
| 1.07 | 0.107 | 1.400 | 31.0 | 2.288 | 14 | | | | | | | |
| 1.37 | 0.085 | 1.450 | 41.9 | 1.768 | 24 | | | | | | | |
| 1.68 | 0.084 | 1.536 | 46.1 | 0.979 | 47 | 10.3 | 64.6 | 23.3 | 1.8 | 12.9 | 11.9 | 39.7 |
| 2.60 | 0.020 | 1.582 | 4129.5 | 15.274 | 270 | | | | | | | |
| 3.15 | 0.014 | 1.524 | 1173.2 | 5.437 | 216 | | | | | | | |
| 3.45 | 0.014 | 1.456 | 1143.8 | 3.068 | 373 | | | | | | | |
| 3.76 | 0.015 | 1.549 | 584.1 | 1.910 | 306 | 6.6 | 90.6 | 2.8 | 0.0 | 59.7 | 23.2 | 7.7 |
| 4.05 | 0.014 | 1.416 | 483.0 | | | | | | | | | |
| 4.36 | 0.016 | 1.494 | 301.4 | 1.586 | 190 | | | | | | | |
| 4.69 | 0.016 | 1.428 | 273.6 | | | | | | | | | |
| 5.03 | 0.016 | 1.490 | 244.3 | | | | | | | | | |
| 5.37 | 0.017 | 1.479 | 213.1 | | | | | | | | | |
| 6.93 | 0.013 | 1.469 | 232.2 | | | 0.7 | 98.3 | 0.0 | 1.0 | 70.5 | 25.1 | 2.7 |
| 7.59 | 0.013 | 1.405 | 251.7 | | | | | | | | | |
| 7.90 | 0.013 | 1.412 | 286.8 | | | | | | | | | |
| 8.23 | 0.015 | 1.584 | 281.0 | | | | | | | | | |
| 8.53 | 0.015 | 1.449 | 254.1 | | | | | | | | | |
| 8.89 | 0.016 | 1.458 | 274.3 | | | | | | | | | |
| 9.19 | 0.017 | 1.458 | 229.7 | | | | | | | | | |
| 9.58 | 0.016 | 1.411 | 273.1 | 1.471 | 186 | | | | | | | |
| 10.08 | 0.016 | 1.417 | 206.4 | | | 4.9 | 92.2 | 1.9 | 1.0 | 66.9 | 20.6 | 4.6 |
| 10.62 | 0.015 | 1.383 | 225.6 | 1.851 | 122 | | | | | | | |
| 11.32 | 0.014 | 1.415 | 250.7 | | | | | | | | | |
| 11.53 | 0.016 | 1.454 | 272.2 | | | | | | | | | |
| 12.07 | 0.016 | 1.484 | 230.2 | | | | | | | | | |
| 12.62 | 0.016 | 1.422 | 234.9 | | | | | | | | | |
| 12.93 | 0.019 | 1.399 | 201.5 | | | | | | | | | |
| 13.51 | 0.015 | 1.410 | 234.5 | | | | | | | | | |
| 13.82 | 0.015 | 1.469 | 240.0 | | | 3.0 | 94.1 | 1.9 | 1.0 | 56.1 | 33.4 | 4.7 |
| 14.20 | 0.014 | 1.603 | 236.8 | | | | | | | | | |
| 14.50 | 0.016 | 1.427 | 213.6 | | | | | | | | | |
| 14.83 | 0.016 | 1.411 | 215.1 | 1.859 | 116 | | | | | | | |
| 15.14 | 0.025 | 1.398 | 208.8 | 1.506 | 139 | | | | | | | |

**Table B.4**. Exploratory Borehole 299-E24-162 Drilled in 1995

| Depth (m) | Moisture Content ($g_{H2O}/g_{dry\ soil}$) | Bulk Density ($g/>cm^3$) | Soil Water Chloride ($\mu g_{Cl}/g_{H2O}$) | Soil Water Bromide ($\mu g_{Br}/g_{H2O}$) | Cl/Br | Depth (m) | Particle Size Distributions | | | | Sand Sizes | | |
|---|---|---|---|---|---|---|---|---|---|---|---|---|---|
| | | | | | | | Gravel (%) | Sand (%) | Silt (%) | Clay (%) | Coarse (%) | Medium (%) | Fine (%) |
| 0.10 | 0.060 | 1.502 | 12.6 | BD | | | | | | | | | |
| 0.53 | 0.057 | 1.534 | 26.6 | 0.659 | 40 | 0.64 | 0.6 | 84.5 | 14.9 | 0.0 | 14.6 | 18.9 | 51.0 |
| 0.95 | 0.094 | 1.572 | 14.7 | 1.342 | 11 | | | | | | | | |
| 1.30 | 0.078 | 1.564 | 17.5 | 1.357 | 13 | | | | | | | | |
| 1.68 | 0.035 | 1.668 | 1382.8 | 7.299 | 189 | | | | | | | | |
| 2.04 | 0.032 | 1.572 | 3688.5 | 15.003 | 246 | | | | | | | | |
| 2.48 | 0.020 | 1.554 | 3350.4 | 14.805 | 226 | 2.52 | 26.0 | 71.8 | 0.7 | 1.5 | 55.4 | 7.3 | 9.1 |
| 3.18 | 0.017 | 1.481 | 716.5 | 3.002 | 239 | | | | | | | | |
| 3.53 | 0.018 | 1.565 | 292.8 | 1.285 | 228 | | | | | | | | |
| 3.97 | 0.018 | 1.529 | 184.7 | 1.356 | 136 | | | | | | | | |
| 4.64 | 0.015 | 1.453 | 93.0 | | | 4.72 | 1.2 | 95.8 | 0.0 | 3.0 | 37.0 | 47.6 | 11.3 |
| 4.99 | 0.016 | 1.465 | 93.0 | 2.293 | 41 | | | | | | | | |
| 5.34 | 0.017 | 1.434 | 78.4 | 1.628 | 48 | | | | | | | | |
| 5.69 | 0.016 | 1.373 | 70.4 | 2.492 | 28 | | | | | | | | |
| 6.04 | 0.018 | 1.365 | 50.8 | 1.354 | 38 | | | | | | | | |
| 6.39 | 0.016 | 1.395 | 74.7 | 1.533 | 49 | | | | | | | | |
| 6.74 | 0.012 | 1.375 | 74.7 | | | 6.74 | 0.4 | 96.6 | 1.0 | 2.0 | 72.8 | 20.0 | 3.8 |
| 7.54 | 0.013 | 1.426 | 69.4 | | | | | | | | | | |
| 7.89 | 0.013 | 1.392 | 77.7 | 1.905 | 41 | | | | | | | | |
| 8.27 | 0.017 | 1.403 | 81.6 | BD | | | | | | | | | |
| 8.62 | 0.016 | 1.453 | 73.2 | BD | | | | | | | | | |
| 9.64 | 0.013 | 1.521 | 71.3 | BD | | | | | | | | | |
| 10.34 | 0.014 | 1.460 | 50.0 | BD | | | | | | | | | |
| 11.07 | 0.015 | 1.398 | 21.8 | BD | | | | | | | | | |
| 12.51 | 0.016 | 1.378 | 51.5 | BD | | | | | | | | | |
| 12.86 | 0.018 | 1.400 | 46.8 | BD | | | | | | | | | |
| 13.24 | 0.016 | 1.440 | 51.4 | BD | | | | | | | | | |
| 13.59 | 0.016 | 1.437 | 53.1 | BD | | | | | | | | | |
| 13.97 | 0.017 | 1.456 | 51.3 | BD | | | | | | | | | |
| 14.32 | 0.020 | 1.442 | 57.8 | BD | | | | | | | | | |
| 14.76 | 0.018 | 1.398 | 56.5 | BD | | 14.84 | 2.2 | 94.9 | 1.0 | 2.0 | 57.1 | 31.9 | 5.8 |
| 15.11 | 0.018 | 1.423 | 53.9 | BD | | | | | | | | | |
| 15.52 | 0.022 | 1.401 | 74.4 | BD | | | | | | | | | |
| 15.87 | 0.021 | 1.394 | 59.4 | BD | | | | | | | | | |
| 16.65 | 0.021 | 1.416 | 50.5 | BD | | | | | | | | | |
| 17.02 | 0.019 | 1.393 | 58.8 | BD | | | | | | | | | |
| 17.37 | 0.011 | 1.431 | 76.1 | BD | | 17.45 | 3.1 | 93.0 | 1.9 | 1.9 | 62.4 | 25.6 | 5.0 |

Note: BD = below detection.

**Table B.5**. Trench Data (1995)

| Depth (m) | Moisture Content ($g_{H2O}/g_{dry\ soil}$) | Bulk Density ($g/>cm^3$) | $^{36}Cl/Cl$ Bkgd-Corrected[(a)] | Error[(b)] |
|---|---|---|---|---|
| 0.30 | 0.0248 | 1.4999 | 8.69E-12 | 9.60E-14 |
| 0.40 | 0.0266 | 1.4812 | 6.14E-12 | 9.10E-14 |
| 0.55 | 0.0258 | 1.4380 | 3.91E-12 | 5.20E-14 |
| 0.85 | 0.0379 | 1.4260 | 8.13E-12 | 1.40E-13 |
| 1.01 | 0.0366 | 1.4965 | 9.48E-12 | 1.50E-13 |
| 1.43 | 0.0465 | 1.8074 | 1.38E-11 | 2.30E-13 |
| 1.62 | 0.0241 | 1.7119 | 5.31E-12 | 1.80E-13 |
| 1.62 | 0.0241 | 1.7119 | 5.41E-12 | 1.30E-13 |
| 1.92 | 0.0368 | 1.6377 | 1.52E-12 | 4.10E-14 |
| 2.01 | 0.0332 | 1.6528 | 1.41E-12 | 2.40E-14 |
| 2.29 | 0.0357 | 1.6652 | 1.10E-12 | 2.70E-14 |
| 2.29 | 0.0357 | 1.6652 | 8.85E-13 | 2.80E-14 |
| 2.41 | 0.0252 | 1.5774 | 9.80E-13 | 2.10E-14 |
| 2.68 | 0.0202 | 1.6721 | 9.26E-13 | 2.30E-14 |
| 2.93 | 0.0156 | 1.5963 | 8.72E-13 | 2.30E-14 |
| 3.26 | 0.0175 | 1.6484 | 8.90E-13 | 2.90E-14 |
| 3.32 | 0.0198 | 1.5939 | 8.31E-13 | 2.10E-14 |
| 3.69 | 0.0194 | 1.6394 | 9.55E-13 | 4.80E-14 |
| 3.75 | 0.0138 | 1.6540 | 8.87E-13 | 2.20E-14 |
| 3.81 | 0.0161 | 1.6300 | 1.16E-12 | 2.90E-14 |
| 4.02 | 0.0150 | 1.5596 | 8.29E-13 | 2.30E-14 |
| 4.51 | 0.0132 | 1.5517 | 8.10E-13 | 2.00E-14 |
| 4.79 | | | 8.85E-13 | 2.80E-14 |

(a) Background-corrected ratios are calculated using the measured ratio for a blank sample.

(b) Uncertainty in the $^{36}Cl/Cl$ is the combined uncertainties in the sample measurement and in the standard measurements used for normalization. The final value reported is the weighted mean of the individual measurements of the sample. Two uncertainties are calculated from this weighted mean: 1) the internal error is the propagated uncertainty in the weighted mean, where the weighting factors are the uncertainties in the individual measurements calculated as stated above; and 2) the external error is the population standard deviation of the individual measurements of the weighted mean. The reported error is the larger of the internal and external error and represents the uncertainty in the final measurement.

**Table B.6**. B8500 (299-E17-21) Drilled in 1998

| Depth (m) | Moisture Content ($g_{H2O}/g_{dry\ soil}$) | Bulk Density ($g/>cm^3$) | Soil Water Chloride ($\mu g_{Cl}/g_{H2O}$) | Soil Water Bromide ($\mu g_{Br}/g_{H2O}$) | Cl/Br | Particle Size Distributions | | | |
|---|---|---|---|---|---|---|---|---|---|
| | | | | | | Gravel (%) | Sand (%) | Silt (%) | Clay (%) |
| 2.71 | 0.0349 | 1.581 | 2331.6 | 13.449 | 173 | 1.0 | 70.3 | 21.3 | 7.4 |
| 2.90 | 0.0334 | 1.555 | 2120.4 | 12.591 | 168 | | | | |
| 2.99 | 0.0254 | 1.661 | 2062.3 | 12.988 | 159 | | | | |
| 3.08 | 0.0353 | 1.545 | 2409.3 | 14.491 | 166 | | | | |
| 3.17 | 0.0270 | 1.501 | 1846.2 | 10.399 | 178 | | | | |
| 3.35 | 0.0278 | 1.489 | 1714.5 | 11.145 | 154 | 14.3 | 76.7 | 4.7 | 4.3 |
| 3.44 | 0.0214 | 1.512 | 1997.0 | 13.101 | 152 | | | | |
| 3.54 | 0.0187 | 1.439 | 1884.8 | 10.721 | 176 | | | | |
| 3.66 | 0.0430 | 1.458 | 1723.0 | 10.920 | 158 | 0.0 | 65.5 | 27.0 | 7.5 |
| 3.75 | 0.0246 | 1.609 | 1414.7 | 8.119 | 174 | | | | |
| 3.84 | 0.0202 | 1.474 | 1032.1 | 6.913 | 149 | | | | |
| 3.93 | 0.0271 | 1.403 | 798.7 | 4.789 | 167 | 0.0 | 89.0 | 6.5 | 4.5 |
| 4.05 | 0.0195 | 1.516 | 619.5 | 3.587 | 173 | | | | |
| 4.15 | 0.0370 | 1.661 | 601.8 | 3.516 | 171 | 0.9 | 61.5 | 30.7 | 6.9 |
| 5.52 | 0.0261 | 1.433 | 137.2 | 1.921 | 71 | 0.0 | 93.0 | 4.0 | 3.0 |
| 5.61 | 0.0285 | 1.400 | 110.2 | 0.702 | 157 | | | | |
| 5.70 | 0.0454 | 1.383 | 108.9 | 0.882 | 124 | | | | |
| 5.82 | 0.0329 | 1.346 | 102.1 | 0.914 | 112 | | | | |
| 5.91 | 0.0275 | 1.474 | 97.6 | 1.821 | 54 | | | | |
| 6.02 | 0.0228 | 1.391 | 92.8 | 1.320 | 70 | | | | |
| 6.13 | 0.0463 | 1.414 | 67.2 | 0.431 | 156 | 2.6 | 69.1 | 20.9 | 7.3 |
| 6.22 | 0.0215 | 1.646 | 70.0 | 0.928 | 76 | | | | |
| 6.31 | 0.0250 | 1.484 | 76.8 | 0.795 | 97 | | | | |
| 8.38 | 0.0119 | 1.493 | 21.1 | BD | | 4.2 | 89.1 | 2.9 | 3.8 |
| 8.53 | 0.0117 | 1.573 | 18.9 | BD | | | | | |
| 8.63 | 0.0119 | 1.558 | 23.4 | BD | | | | | |
| 8.72 | 0.0126 | 1.717 | 31.7 | BD | | | | | |
| 8.81 | 0.0116 | 1.576 | 31.8 | BD | | | | | |
| 8.90 | 0.0142 | 1.572 | 30.4 | BD | | 6.3 | 82.4 | 6.6 | 4.7 |
| 8.99 | 0.0167 | 1.554 | 27.4 | BD | | | | | |
| 9.42 | 0.0111 | 1.486 | 27.8 | BD | | | | | |
| 9.48 | 0.0110 | 1.469 | 29.2 | BD | | | | | |
| 9.57 | 0.0123 | 1.566 | 41.4 | BD | | | | | |
| 9.66 | 0.0123 | 1.622 | 63.4 | BD | | 4.1 | 77.2 | 12.5 | 6.2 |

**Table B.6**. (contd)

| Depth (m) | Moisture Content ($g_{H2O}/g_{dry\ soil}$) | Bulk Density ($g/>cm^3$) | Soil Water Chloride ($\mu g_{Cl}/g_{H2O}$) | Soil Water Bromide ($\mu g_{Br}/g_{H2O}$) | Cl/Br | Particle Size Distributions | | | |
|---|---|---|---|---|---|---|---|---|---|
| | | | | | | Gravel (%) | Sand (%) | Silt (%) | Clay (%) |
| 10.67 | 0.0116 | 1.567 | 40.4 | BD | | 3.2 | 88.1 | 3.9 | 4.8 |
| 10.73 | 0.0122 | 1.584 | 22.2 | 1.646 | 14 | | | | |
| 10.79 | 0.0138 | 1.552 | 38.6 | BD | | | | | |
| 10.88 | 0.0125 | 1.568 | 35.2 | BD | | | | | |
| 10.97 | 0.0155 | 1.574 | 53.0 | BD | | | | | |
| 11.43 | 0.0135 | 1.565 | 30.4 | BD | | | | | |
| 11.52 | 0.0172 | 1.373 | 19.2 | 1.744 | 11 | | | | |
| 11.61 | 0.0156 | 1.440 | 20.5 | BD | | | | | |
| 11.70 | 0.0154 | 1.453 | 25.4 | BD | | | | | |
| 11.80 | 0.0161 | 1.347 | 19.2 | BD | | | | | |
| 11.89 | 0.0154 | 1.529 | 42.4 | BD | | 1.1 | 90.0 | 4.0 | 4.9 |
| 14.30 | 0.0182 | 1.513 | 34.1 | 1.102 | 31 | 0.0 | 81.5 | 11.5 | 7.0 |
| 15.09 | 0.0096 | 1.291 | 87.6 | BD | | 1.5 | 69.0 | 20.7 | 8.9 |
| 15.70 | 0.0117 | 1.578 | 25.6 | BD | | | | | |
| 17.01 | 0.0097 | 1.466 | 37.2 | BD | | | | | |
| 17.92 | 0.0123 | 1.669 | 32.5 | 1.625 | 20 | | | | |
| 18.17 | 0.0118 | 1.570 | 45.0 | BD | | | | | |
| 18.93 | 0.0106 | 1.598 | 44.6 | BD | | | | | |
| 21.31 | 0.0140 | 1.702 | 22.1 | 1.428 | 16 | | | | |
| 22.83 | 0.0128 | 1.483 | 20.3 | BD | | | | | |
| 23.59 | 0.0136 | 1.561 | 28.6 | BD | | | | | |
| 24.17 | 0.0140 | 1.462 | 19.3 | BD | | | | | |
| 24.93 | 0.0148 | 1.596 | 33.3 | 1.358 | 25 | | | | |
| 28.04 | 0.0138 | 1.457 | 21.7 | BD | | | | | |
| 27.28 | 0.0115 | 1.553 | 25.1 | BD | | | | | |
| 30.33 | 0.0123 | 1.471 | 25.1 | BD | | | | | |
| 31.09 | 0.0127 | 1.497 | 31.5 | BD | | | | | |
| 33.16 | 0.0156 | 1.426 | 24.4 | BD | | | | | |
| 33.89 | 0.0182 | 1.452 | 26.4 | BD | | | | | |
| 35.17 | 0.0171 | 1.506 | 18.8 | BD | | | | | |
| 35.94 | 0.0117 | 1.519 | 25.6 | BD | | | | | |
| 36.58 | 0.0158 | 1.482 | 19.6 | BD | | | | | |
| 37.31 | 0.0166 | 1.424 | 25.2 | BD | | | | | |
| 39.23 | 0.0116 | 1.455 | 44.9 | BD | | | | | |

**Table B.6**. (contd)

| Depth (m) | Moisture Content ($g_{H2O}/g_{dry\ soil}$) | Bulk Density ($g/>cm^3$) | Soil Water Chloride ($\mu g_{Cl}/g_{H2O}$) | Soil Water Bromide ($\mu g_{Br}/g_{H2O}$) | Cl/Br | Particle Size Distributions | | | |
|---|---|---|---|---|---|---|---|---|---|
| | | | | | | Gravel (%) | Sand (%) | Silt (%) | Clay (%) |
| 39.99 | 0.0239 | 1.464 | 23.9 | BD | | | | | |
| 43.59 | 0.0227 | 1.487 | 15.0 | BD | | | | | |
| 42.82 | 0.0165 | 1.503 | 33.4 | BD | | | | | |
| 46.76 | 0.0122 | 1.468 | 32.7 | BD | | | | | |
| 45.99 | 0.0234 | 1.507 | 10.7 | BD | | | | | |
| 48.59 | 0.0152 | 1.535 | 42.9 | BD | | | | | |
| 49.35 | 0.0158 | 1.539 | 53.3 | BD | | | | | |
| 54.77 | 0.0205 | 1.459 | 18.6 | BD | | | | | |
| 55.38 | 0.0182 | 1.540 | 19.2 | BD | | | | | |
| 58.13 | 0.0169 | 1.522 | 20.1 | BD | | | | | |
| 60.05 | 0.0155 | 1.511 | 18.1 | BD | | | | | |
| 61.05 | 0.0178 | 1.548 | 17.4 | BD | | | | | |
| 63.09 | 0.0190 | 1.534 | 16.3 | BD | | | | | |
| 64.13 | 0.0173 | 1.547 | 20.2 | BD | | | | | |
| 66.17 | 0.0170 | 1.591 | 14.7 | BD | | | | | |
| 67.24 | 0.0376 | 1.402 | 15.2 | BD | | | | | |
| 69.22 | 0.0226 | 1.508 | 15.5 | BD | | | | | |
| 72.27 | 0.0148 | 1.530 | 30.5 | BD | | | | | |
| 73.30 | 0.0175 | 1.638 | 29.1 | BD | | | | | |
| 82.02 | 0.0191 | 1.729 | 49.3 | BD | | | | | |
| 106.56 | 0.0446 | | 13.5 | BD | | | | | |
| 116.04 | 0.3029 | 1.346 | 4.4 | BD | | | | | |

Note: BD = below detection.

**Table B.7**. B8501 Borehole Drilled in 1998

| Depth (m) | Moisture Content ($g_{H2O}/g_{dry\ soil}$) | Bulk Density ($g/>cm^3$) | Soil Water Chloride ($\mu g_{Cl}/g_{H2O}$) | Soil Water Bromide ($\mu g_{Br}/g_{H2O}$) | Cl/Br | Particle Size Distributions | | | |
|---|---|---|---|---|---|---|---|---|---|
| | | | | | | Gravel (%) | Sand (%) | Silt (%) | Clay (%) |
| 0.06 | 0.06433 | 1.579 | 13.4 | BD | | | | | |
| 0.15 | 0.05966 | 1.529 | 7.4 | BD | | | | | |
| 0.27 | 0.06475 | 1.513 | 6.3 | BD | | 3.17 | 85.69 | 4.84 | 6.29 |
| 0.40 | 0.04861 | 1.528 | 7.4 | BD | | | | | |
| 0.52 | 0.05679 | 1.396 | 3.5 | BD | | | | | |
| 0.64 | 0.06346 | | 3.6 | 0.040 | 91 | | | | |
| 0.82 | 0.01858 | 1.595 | 1030.0 | 5.387 | 191 | | | | |
| 0.98 | 0.01270 | 1.502 | 175.5 | BD | | | | | |
| 1.10 | 0.06043 | 1.572 | 6.9 | BD | | | | | |
| 1.22 | 0.04747 | 1.502 | 4.4 | BD | | | | | |
| 1.34 | 0.03507 | 1.414 | 3.7 | BD | | | | | |
| 1.46 | 0.03896 | 1.317 | 2.3 | BD | | | | | |
| 1.58 | 0.03864 | 1.479 | 4.1 | BD | | | | | |
| 1.77 | 0.04350 | 1.839 | 450.8 | 1.609 | 280 | 62.04 | 25.43 | 9.49 | 3.04 |
| 1.89 | 0.04137 | 1.891 | 441.4 | 1.691 | 261 | | | | |
| 2.32 | 0.03944 | 1.645 | 288.1 | 1.015 | 284 | | | | |
| 2.44 | 0.04958 | 1.666 | 217.0 | 1.008 | 215 | | | | |
| 2.56 | 0.08187 | 1.599 | 9.5 | BD | | | | | |
| 2.68 | 0.10820 | 1.454 | 5.1 | BD | | | | | |
| 2.80 | 0.12394 | 1.456 | 4.8 | BD | | | | | |
| 2.93 | 0.08326 | 1.597 | 0.6 | BD | | | | | |
| 3.05 | 0.04134 | | 12.1 | BD | | | | | |
| 3.17 | 0.02761 | 1.667 | 55.1 | BD | | 47.82 | 43.31 | 4.96 | 3.91 |
| 3.69 | 0.03394 | 1.479 | 2055.1 | 17.079 | 120 | | | | |
| 4.57 | 0.03598 | 1.603 | 1584.5 | 12.503 | 127 | | | | |
| 4.69 | 0.03071 | 1.624 | 1684.2 | 14.005 | 120 | | | | |
| 4.82 | 0.04739 | 1.506 | 2067.1 | 17.077 | 121 | 0.11 | 67.92 | 23.47 | 8.49 |
| 4.97 | 0.02245 | 1.515 | 1082.5 | 9.343 | 116 | | | | |
| 5.09 | 0.02106 | 1.493 | 976.3 | 7.594 | 129 | | | | |
| 5.21 | 0.00654 | 1.524 | 2869.9 | 24.464 | 117 | | | | |
| 5.33 | 0.01923 | 1.421 | 868.5 | 7.276 | 119 | | | | |
| 5.46 | 0.01764 | 1.506 | 879.6 | 8.507 | 103 | | | | |
| 5.58 | 0.04455 | 1.540 | 920.5 | 7.630 | 121 | | | | |
| 5.70 | 0.02864 | 1.659 | 699.8 | 5.936 | 118 | 0.03 | 73.48 | 18.49 | 8 |
| 5.82 | 0.02326 | 1.697 | 777.0 | 7.310 | 106 | | | | |
| 5.94 | 0.02770 | 1.451 | 492.9 | 4.350 | 113 | | | | |
| 6.07 | 0.02095 | 1.546 | 765.5 | 6.204 | 123 | | | | |

**Table B.7**. (contd)

| Depth (m) | Moisture Content ($g_{H2O}/g_{dry\ soil}$) | Bulk Density ($g/cm^3$) | Soil Water Chloride ($\mu g_{Cl}/g_{H2O}$) | Soil Water Bromide ($\mu g_{Br}/g_{H2O}$) | Cl/Br | Particle Size Distributions | | | |
|---|---|---|---|---|---|---|---|---|---|
| | | | | | | Gravel (%) | Sand (%) | Silt (%) | Clay (%) |
| 6.07 | 0.01906 | 1.590 | 693.0 | 6.295 | 110 | 0.94 | 87.67 | 4.46 | 6.93 |
| 6.19 | 0.02337 | 1.598 | 666.8 | 6.852 | 97 | | | | |
| 6.31 | 0.02852 | 1.423 | 641.7 | 5.260 | 122 | 0.17 | 86.85 | 6.99 | 5.99 |
| 6.43 | 0.02079 | 1.527 | 662.5 | 5.773 | 115 | | | | |
| 6.55 | 0.02898 | 1.586 | 668.7 | 6.211 | 108 | | | | |
| 6.77 | 0.02988 | 1.567 | 566.1 | 5.354 | 106 | | | | |
| 6.89 | 0.03073 | 1.513 | 585.7 | 5.209 | 112 | 0.01 | 88.49 | 4 | 7.5 |
| 7.01 | 0.03205 | 1.457 | 564.6 | 4.996 | 113 | | | | |
| 7.13 | 0.03054 | 1.206 | 614.9 | 5.563 | 111 | | | | |
| 7.25 | 0.02242 | 1.497 | 614.0 | 5.351 | 115 | | | | |
| 7.41 | 0.02176 | 1.625 | 706.7 | 6.892 | 103 | | | | |
| 7.53 | 0.02104 | 1.531 | 620.2 | 5.703 | 109 | | | | |
| 7.65 | 0.02361 | 1.503 | 555.4 | 5.507 | 101 | | | | |
| 7.77 | 0.03059 | 1.533 | 574.1 | 4.904 | 117 | | | | |
| 7.89 | 0.03688 | 1.563 | 574.5 | 5.151 | 112 | | | | |
| 8.53 | 0.01434 | 1.460 | 270.6 | BD | | | | | |
| 8.66 | 0.01549 | 1.493 | 250.5 | BD | | | | | |
| 8.78 | 0.01556 | 1.532 | 221.9 | BD | | | | | |
| 8.90 | 0.01581 | 1.495 | 194.2 | BD | | | | | |
| 9.02 | 0.02026 | 1.459 | 137.7 | BD | | | | | |
| 9.14 | 0.03292 | 1.586 | 96.2 | BD | | 1.13 | 83.05 | 9.39 | 6.43 |
| 9.27 | 0.02093 | 1.570 | 246.0 | BD | | | | | |
| 9.39 | 0.01253 | 1.556 | 272.8 | BD | | | | | |
| 9.51 | 0.01214 | 1.518 | 142.5 | BD | | | | | |
| 9.63 | 0.01296 | 1.520 | 120.4 | BD | | | | | |
| 9.81 | 0.01250 | 1.556 | 119.8 | BD | | | | | |
| 9.94 | 0.01252 | 1.504 | 91.9 | BD | | 0.72 | 84.38 | 9.93 | 4.96 |
| 10.06 | 0.01290 | 1.479 | 69.0 | BD | | | | | |
| 10.18 | 0.01279 | 1.488 | 64.9 | BD | | | | | |
| 10.30 | 0.01373 | 1.530 | 55.3 | BD | | | | | |
| 10.42 | 0.01355 | 1.525 | 52.4 | BD | | | | | |
| 10.55 | 0.01520 | 1.523 | 46.7 | BD | | 0.29 | 88.74 | 6.98 | 3.99 |
| 10.67 | 0.01920 | 1.565 | 36.9 | BD | | | | | |
| 10.79 | 0.01315 | 1.564 | 63.1 | BD | | | | | |
| 10.91 | 0.01148 | 1.454 | 53.2 | BD | | | | | |
| 11.00 | 0.01169 | 1.481 | 45.3 | BD | | | | | |
| 11.13 | 0.01370 | 1.453 | 40.1 | BD | | | | | |

**Table B.7**. (contd)

| Depth (m) | Moisture Content ($g_{H2O}/g_{dry\ soil}$) | Bulk Density ($g/>cm^3$) | Soil Water Chloride ($\mu g_{Cl}/g_{H2O}$) | Soil Water Bromide ($\mu g_{Br}/g_{H2O}$) | Cl/Br | Particle Size Distributions | | | |
|---|---|---|---|---|---|---|---|---|---|
| | | | | | | Gravel (%) | Sand (%) | Silt (%) | Clay (%) |
| 11.25 | 0.01563 | 1.474 | 32.0 | BD | | | | | |
| 11.37 | 0.01246 | 1.452 | 41.0 | BD | | | | | |
| 11.49 | 0.01271 | 1.447 | 30.7 | BD | | | | | |
| 11.61 | 0.01574 | 1.471 | 26.0 | BD | | | | | |
| 11.73 | 0.01469 | 1.444 | 30.6 | BD | | | | | |
| 11.86 | 0.01597 | 1.408 | 22.5 | BD | | 0.18 | 87.84 | 7.99 | 3.99 |
| 11.98 | 0.01474 | 1.438 | 25.1 | BD | | | | | |
| 12.10 | 0.01523 | 1.472 | 23.0 | BD | | | | | |
| 12.22 | 0.01371 | 1.477 | 27.0 | BD | | | | | |
| 12.34 | 0.01519 | 1.507 | 22.4 | BD | | | | | |
| 12.47 | 0.01431 | 1.459 | 27.3 | BD | | | | | |
| 12.59 | 0.01397 | 1.532 | 23.6 | BD | | | | | |
| 12.71 | 0.03086 | 1.405 | 11.0 | BD | | | | | |
| 13.81 | 0.01249 | 1.572 | 68.0 | BD | | | | | |
| 14.08 | 0.01607 | 1.473 | 23.0 | BD | | | | | |
| 14.20 | 0.01367 | 1.540 | 16.1 | BD | | | | | |
| 14.33 | 0.01412 | 1.509 | 15.6 | BD | | | | | |
| 14.45 | 0.01367 | 1.480 | 16.8 | BD | | 0.01 | 93.99 | 2 | 4 |
| 14.57 | 0.01459 | 1.526 | 14.4 | BD | | | | | |
| 14.69 | 0.01324 | 1.447 | 14.4 | BD | | | | | |

Note: BD = below detection.

**Table B.8**. B8502 Borehole Drilled in 1998

| Depth (m) | Moisture Content ($g_{H2O}/g_{dry\ soil}$) | Bulk Density ($g/>cm^3$) | Soil Water Chloride ($\mu g_{Cl}/g_{H2O}$) | Soil Water Bromide ($\mu g_{Br}/g_{H2O}$) | Cl/Br | Particle Size Distributions | | | |
|---|---|---|---|---|---|---|---|---|---|
| | | | | | | Gravel (%) | Sand (%) | Silt (%) | Clay (%) |
| 0.00 | 0.0545 | 1.645 | 67.8 | BD | | 25.0 | 55.1 | 14.6 | 5.2 |
| 0.15 | 0.0525 | 1.634 | 60.4 | BD | | | | | |
| 0.27 | 0.0476 | 1.747 | 85.8 | BD | | | | | |
| 0.43 | 0.0567 | 1.454 | 3.0 | BD | | | | | |
| 0.55 | 0.0402 | 1.501 | 2.2 | BD | | 1.0 | 87.2 | 6.9 | 5.0 |
| 0.67 | 0.0670 | 1.497 | 1.3 | BD | | | | | |
| 0.79 | 0.1043 | 1.469 | 1.2 | BD | | 3.5 | 33.8 | 55.0 | 7.7 |
| 0.94 | 0.1302 | 1.467 | 1.0 | BD | | | | | |
| 1.13 | 0.0413 | 1.725 | 100.0 | BD | | | | | |
| 1.25 | 0.0972 | 1.602 | 4.1 | BD | | | | | |
| 1.37 | 0.0752 | 1.677 | 8.6 | BD | | 21.4 | 48.8 | 24.4 | 5.5 |
| 1.49 | 0.0843 | 1.706 | 14.5 | BD | | | | | |
| 1.62 | 0.0698 | 1.732 | 11.9 | BD | | | | | |
| 1.74 | 0.0673 | 1.730 | 12.8 | BD | | | | | |
| 1.86 | 0.0448 | 1.832 | 25.4 | BD | | | | | |
| 2.23 | 0.0425 | 1.640 | 74.1 | BD | | 43.2 | 44.1 | 9.1 | 3.7 |
| 2.35 | 0.0242 | 1.521 | 108.0 | BD | | | | | |
| 2.47 | 0.0587 | 1.540 | 108.5 | 1.363 | 80 | | | | |
| 2.59 | 0.0339 | 1.503 | 133.8 | 1.182 | 113 | | | | |
| 2.71 | 0.0249 | 1.551 | 192.7 | BD | | 13.4 | 80.5 | 1.7 | 4.3 |
| 2.83 | 0.0284 | 1.548 | 111.7 | BD | | | | | |
| 2.96 | 0.0235 | 1.525 | 178.7 | BD | | | | | |
| 3.35 | 0.0333 | 1.506 | 454.2 | 3.905 | 116 | 4.7 | 90.5 | 1.4 | 3.3 |
| 3.47 | 0.0619 | 1.411 | 515.1 | 3.717 | 139 | | | | |
| 3.47 | 0.0297 | 1.515 | 425.8 | 2.690 | 158 | | | | |
| 3.72 | 0.0259 | 1.201 | 983.0 | 6.189 | 159 | | | | |
| 3.84 | 0.0246 | 1.521 | 1180.5 | 8.136 | 145 | | | | |
| 3.96 | 0.0269 | 1.424 | 1125.7 | 7.440 | 151 | | | | |
| 4.08 | 0.0373 | 1.506 | 1228.5 | 8.299 | 148 | | | | |
| 4.27 | 0.0477 | 1.432 | 1227.5 | 7.746 | 158 | | | | |
| 4.39 | 0.0474 | 1.391 | 1125.6 | 6.974 | 161 | 0.0 | 86.0 | 8.0 | 6.0 |
| 4.51 | 0.0357 | 1.610 | 1174.3 | 7.574 | 155 | | | | |
| 4.63 | 0.0262 | 1.582 | 1058.9 | 7.255 | 146 | | | | |
| 4.75 | 0.0235 | 1.460 | 984.8 | 6.378 | 154 | | | | |
| 4.88 | 0.0345 | 1.611 | 1148.0 | 7.238 | 159 | 1.1 | 77.2 | 15.8 | 5.9 |
| 5.00 | 0.0241 | 1.427 | 854.6 | 5.814 | 147 | | | | |
| 5.12 | 0.0242 | 1.475 | 645.3 | 4.126 | 156 | | | | |

**Table B.8**. (contd)

| Depth (m) | Moisture Content ($g_{H2O}/g_{dry\ soil}$) | Bulk Density ($g/>cm^3$) | Soil Water Chloride ($\mu g_{Cl}/g_{H2O}$) | Soil Water Bromide ($\mu g_{Br}/g_{H2O}$) | Cl/Br | Particle Size Distributions | | | |
|---|---|---|---|---|---|---|---|---|---|
| | | | | | | Gravel (%) | Sand (%) | Silt (%) | Clay (%) |
| 5.18 | 0.0212 | 1.677 | 910.0 | 5.896 | 154 | | | | |
| 5.24 | 0.0255 | 1.446 | 361.7 | 2.549 | 142 | | | | |
| 5.30 | 0.0217 | 1.596 | 694.7 | 5.174 | 134 | | | | |
| 5.36 | 0.0432 | 1.478 | 1083.4 | 7.834 | 138 | | | | |
| 5.43 | 0.0224 | 1.679 | 588.2 | 4.020 | 146 | | | | |
| 5.55 | 0.0244 | 1.502 | 419.7 | 3.276 | 128 | 0.3 | 93.2 | 2.5 | 4.0 |
| 5.67 | 0.0284 | 1.589 | 458.0 | 3.521 | 130 | | | | |
| 5.79 | 0.0288 | 1.594 | 391.8 | 2.432 | 161 | | | | |
| 5.91 | 0.0260 | 1.601 | 332.2 | 1.923 | 173 | | | | |
| 6.04 | 0.0301 | 1.395 | 290.6 | 1.663 | 175 | | | | |
| 6.16 | 0.0352 | 1.408 | 255.5 | 1.705 | 150 | | | | |
| 6.28 | 0.0330 | 1.713 | 245.3 | 2.120 | 116 | | | | |
| 6.46 | 0.0563 | 1.427 | 123.0 | 1.065 | 116 | | | | |
| 6.58 | 0.0361 | 1.720 | 223.2 | 1.938 | 115 | 11.9 | 73.1 | 9.3 | 5.7 |
| 6.71 | 0.0170 | 1.601 | 218.6 | BD | | | | | |
| 6.83 | 0.0348 | 1.586 | 81.2 | BD | | | | | |
| 6.95 | 0.0137 | 1.581 | 156.7 | BD | | | | | |
| 7.04 | 0.0281 | 1.551 | 30.3 | BD | | | | | |
| 7.16 | 0.0321 | 1.600 | 31.2 | BD | | 1.8 | 89.9 | 4.4 | 3.9 |
| 7.28 | 0.0275 | 1.541 | 102.0 | BD | | | | | |
| 8.08 | 0.0193 | 1.487 | 30.6 | BD | | | | | |
| 8.14 | 0.0143 | No bulk density | 25.8 | BD | | | | | |
| 8.20 | 0.0159 | 1.587 | 47.2 | BD | | | | | |
| 8.26 | 0.0125 | 1.503 | 28.2 | BD | | | | | |
| 8.26 | 0.0133 | No bulk density | 26.0 | BD | | | | | |
| 8.38 | 0.0138 | 1.507 | 27.3 | BD | | | | | |
| 8.38 | 0.0140 | No bulk density | 29.3 | BD | | | | | |
| 8.50 | 0.0154 | 1.493 | 37.8 | BD | | | | | |
| 8.50 | 0.0134 | No bulk density | 32.0 | BD | | | | | |
| 8.63 | 0.0134 | No bulk density | 39.5 | BD | | | | | |
| 8.75 | 0.0114 | 1.567 | 23.7 | BD | | 1.8 | 90.4 | 3.9 | 3.9 |
| 8.87 | 0.0115 | 1.539 | 26.0 | BD | | | | | |

**Table B.8**. (contd)

| Depth (m) | Moisture Content ($g_{H2O}/g_{dry\ soil}$) | Bulk Density ($g/cm^3$) | Soil Water Chloride ($\mu g_{Cl}/g_{H2O}$) | Soil Water Bromide ($\mu g_{Br}/g_{H2O}$) | Cl/Br | Particle Size Distributions | | | |
|---|---|---|---|---|---|---|---|---|---|
| | | | | | | Gravel (%) | Sand (%) | Silt (%) | Clay (%) |
| 8.99 | 0.0121 | 1.532 | 18.9 | BD | | | | | |
| 9.11 | 0.0174 | 1.622 | 16.1 | BD | | | | | |
| 9.24 | 0.0155 | 1.589 | 18.7 | BD | | | | | |
| 9.39 | 0.0329 | 1.442 | 16.4 | BD | | | | | |
| 9.51 | 0.0140 | 1.558 | 15.0 | BD | | 1.3 | 91.8 | 2.5 | 4.4 |
| 9.63 | 0.0259 | 1.504 | 10.4 | BD | | | | | |
| 9.75 | 0.0187 | 1.465 | 15.5 | BD | | | | | |
| 9.88 | 0.0314 | 1.433 | 8.6 | BD | | | | | |
| 10.24 | 0.0145 | 1.526 | 16.5 | BD | | | | | |
| 10.79 | 0.0189 | 1.581 | 13.8 | BD | | | | | |
| 11.16 | 0.0109 | 1.504 | 25.6 | BD | | | | | |
| 11.31 | 0.0110 | 1.423 | 21.9 | BD | | | | | |
| 11.43 | 0.0111 | 1.510 | 18.1 | BD | | 0.0 | 93.5 | 3.0 | 3.5 |
| 11.55 | 0.0118 | 1.397 | 18.7 | BD | | | | | |
| 11.67 | 0.0111 | 1.462 | 19.9 | BD | | | | | |
| 11.80 | 0.0128 | 1.484 | 20.3 | BD | | | | | |
| 11.92 | 0.0136 | 1.420 | 19.9 | BD | | | | | |
| 12.04 | 0.0139 | 1.437 | 20.1 | BD | | | | | |
| 12.16 | 0.0164 | 1.384 | 19.5 | BD | | | | | |
| 12.28 | 0.0133 | 1.547 | 20.4 | BD | | | | | |
| 12.47 | 0.0159 | 1.566 | 21.4 | BD | | | | | |
| 12.53 | 0.0150 | 1.524 | 21.4 | BD | | | | | |
| 12.62 | 0.0174 | 1.551 | 20.7 | BD | | | | | |
| 12.80 | 0.0154 | 1.537 | 20.8 | BD | | | | | |
| 12.92 | 0.0151 | 1.506 | 17.8 | BD | | | | | |
| 13.05 | 0.0143 | 1.502 | 17.5 | BD | | | | | |
| 13.17 | 0.0161 | 1.509 | 18.0 | BD | | 1.3 | 92.3 | 1.5 | 4.9 |
| 13.29 | 0.0164 | 1.477 | 17.7 | BD | | | | | |

Note: BD = below detection.

**Table B.9**. B8503 Borehole Drilled in 1998

| Depth (m) | Moisture Content ($g_{H2O}/g_{dry\ soil}$) | Bulk Density ($g/>cm^3$) | Soil Water Chloride ($\mu g_{Cl}/g_{H2O}$) | Soil Water Bromide ($\mu g_{Br}/g_{H2O}$) | Cl/Br | Particle Size Distributions | | | |
|---|---|---|---|---|---|---|---|---|---|
| | | | | | | Gravel (%) | Sand (%) | Silt (%) | Clay (%) |
| 0.09 | 0.0284 | 1.280 | 14.7 | BD | | | | | |
| 0.15 | 0.0222 | 1.515 | 16.2 | BD | | | | | |
| 0.21 | 0.0290 | 1.462 | 11.3 | BD | | | | | |
| 0.30 | 0.0284 | 1.502 | 11.9 | BD | | 0.055 | 84.953 | 9.995 | 4.997 |
| 0.37 | 0.0317 | 1.477 | 7.6 | BD | | | | | |
| 0.46 | 0.0320 | 1.450 | 5.9 | BD | | | | | |
| 0.67 | 0.0253 | 1.464 | 11.4 | BD | | | | | |
| 0.76 | 0.0274 | 1.463 | 10.5 | BD | | | | | |
| 0.85 | 0.0323 | 1.483 | 9.6 | BD | | | | | |
| 0.93 | 0.0397 | 1.424 | 3.0 | BD | | | | | |
| 1.01 | 0.0405 | 1.433 | 2.7 | BD | | | | | |
| 1.08 | 0.0460 | 1.379 | 1.7 | BD | | | | | |
| 1.26 | 0.0393 | 1.449 | 18.8 | BD | | | | | |
| 1.34 | 0.0397 | 1.336 | 14.1 | BD | | | | | |
| 1.43 | 0.0379 | 1.404 | 25.6 | BD | | | | | |
| 1.52 | 0.0360 | 1.439 | 33.1 | BD | | 0.019 | 91.483 | 3.499 | 4.999 |
| 1.60 | 0.0351 | 1.406 | 37.6 | BD | | | | | |
| 1.69 | 0.0360 | 1.400 | 40.3 | BD | | | | | |
| 1.83 | 0.0348 | 1.352 | 50.0 | BD | | | | | |
| 1.89 | 0.0290 | 1.436 | 48.3 | BD | | | | | |
| 1.98 | 0.0277 | 1.531 | 55.7 | BD | | | | | |
| 2.06 | 0.0368 | 1.545 | 49.2 | BD | | | | | |
| 2.13 | 0.0398 | 1.545 | 38.5 | BD | | | | | |
| 2.19 | 0.0337 | 1.523 | 38.0 | BD | | | | | |
| 2.29 | 0.0350 | 1.561 | 38.9 | BD | | 0.185 | 85.841 | 9.981 | 3.993 |
| 2.50 | 0.0410 | 1.506 | 31.4 | BD | | | | | |
| 2.58 | 0.0555 | 1.500 | 37.2 | BD | | | | | |
| 2.65 | 0.0745 | 1.464 | 33.1 | BD | | | | | |
| 2.74 | 0.0867 | 1.372 | 39.3 | BD | | 0.494 | 32.837 | 56.718 | 9.951 |
| 2.85 | 0.1010 | 1.369 | 50.5 | BD | | | | | |
| 2.93 | 0.1155 | 1.391 | 69.8 | BD | | | | | |
| 3.11 | 0.0959 | 1.425 | 72.1 | BD | | | | | |
| 3.20 | 0.1347 | 1.503 | 188.3 | 0.817 | 230 | | | | |
| 3.29 | 0.1346 | 1.548 | 227.7 | 1.189 | 192 | | | | |
| 3.41 | 0.0583 | 1.759 | 125.0 | BD | | | | | |
| 3.51 | 0.0240 | 1.687 | 235.3 | BD | | 51.869 | 37.542 | 7.220 | 3.369 |
| 3.69 | 0.0364 | 1.684 | 432.9 | 3.571 | 121 | | | | |
| 3.78 | 0.0422 | 1.441 | 601.5 | 4.262 | 141 | | | | |
| 3.89 | 0.0386 | 1.547 | 490.7 | 3.891 | 126 | | | | |
| 3.96 | 0.0314 | 1.655 | 423.1 | 3.502 | 121 | | | | |
| 4.16 | 0.0336 | 1.707 | 388.6 | 3.276 | 119 | | | | |

**Table B.9**. (contd)

| Depth (m) | Moisture Content ($g_{H2O}/g_{dry\ soil}$) | Bulk Density ($g/cm^3$) | Soil Water Chloride ($\mu g_{Cl}/g_{H2O}$) | Soil Water Bromide ($\mu g_{Br}/g_{H2O}$) | Cl/Br | Particle Size Distributions | | | |
|---|---|---|---|---|---|---|---|---|---|
| | | | | | | Gravel (%) | Sand (%) | Silt (%) | Clay (%) |
| 4.22 | 0.0338 | 1.704 | 400.3 | 3.254 | 123 | 6.004 | 62.507 | 24.439 | 7.050 |
| 4.88 | 0.0240 | 1.604 | 590.3 | 5.404 | 109 | | | | |
| 4.97 | 0.0216 | 1.563 | 685.7 | 5.564 | 123 | | | | |
| 5.06 | 0.0202 | 1.603 | 909.5 | 7.930 | 115 | 0.029 | 86.974 | 9.997 | 2.999 |
| 5.09 | 0.0226 | 1.614 | 990.8 | 7.536 | 131 | | | | |
| 5.14 | 0.0214 | 1.578 | 1152.3 | 9.334 | 123 | | | | |
| 5.18 | 0.0222 | 1.581 | 1127.4 | 8.565 | 132 | | | | |
| 5.24 | 0.0217 | 1.608 | 1152.4 | 9.684 | 119 | | | | |
| 5.67 | 0.0233 | 1.606 | 776.8 | 6.434 | 121 | | | | |
| 5.79 | 0.0227 | 1.589 | 759.0 | 6.178 | 123 | 0.332 | 76.744 | 16.944 | 5.980 |
| 5.91 | 0.0307 | 1.612 | 807.7 | 6.524 | 124 | | | | |
| 6.02 | 0.0285 | 1.711 | 756.2 | 5.971 | 127 | | | | |
| 6.10 | 0.0259 | 1.700 | 704.4 | 6.951 | 101 | 0.126 | 75.904 | 17.977 | 5.992 |
| 6.19 | 0.0291 | 1.447 | 803.2 | 7.211 | 111 | | | | |
| 6.28 | 0.0333 | 1.640 | 786.1 | 6.613 | 119 | | | | |
| 6.37 | 0.0268 | 1.607 | 646.5 | 5.226 | 124 | | | | |
| 6.60 | 0.0319 | 1.634 | 783.1 | 6.592 | 119 | | | | |
| 6.69 | 0.0229 | 1.639 | 663.9 | 5.682 | 117 | | | | |
| 6.77 | 0.0344 | 1.536 | 694.0 | 5.813 | 119 | | | | |
| 6.86 | 0.0289 | 1.581 | 634.4 | 5.534 | 115 | | | | |
| 6.96 | 0.0427 | 1.411 | 814.0 | 7.023 | 116 | 0.126 | 70.411 | 21.972 | 7.491 |
| 7.13 | 0.0235 | 1.595 | 636.5 | 5.965 | 107 | | | | |
| 7.24 | 0.0248 | 1.616 | 639.3 | 6.058 | 106 | | | | |
| 7.32 | 0.0224 | 1.526 | 706.1 | 5.806 | 122 | | | | |
| 7.42 | 0.0287 | 1.468 | 698.3 | 5.923 | 118 | | | | |
| 7.53 | 0.0281 | 1.497 | 685.3 | | | | | | |
| 7.62 | 0.0282 | 1.669 | 684.1 | | | | | | |
| 7.62 | 0.0273 | 1.638 | 683.0 | | | | | | |
| 7.68 | 0.0268 | 1.571 | 681.9 | | | | | | |
| 7.77 | 0.0250 | 1.605 | 680.7 | | | | | | |
| 7.85 | 0.0248 | 1.593 | 679.6 | | | | | | |
| 7.92 | 0.0237 | 1.649 | 678.4 | | | | | | |
| 8.14 | 0.0271 | 1.567 | 677.3 | | | | | | |
| 8.18 | 0.0373 | 1.540 | 676.1 | | | 4.342 | 84.179 | 6.696 | 4.783 |
| 8.23 | 0.0315 | 1.638 | 675.0 | | | | | | |
| 8.31 | 0.0188 | 1.614 | 673.8 | | | 13.252 | 75.471 | 6.940 | 4.337 |
| 8.35 | 0.0176 | 1.657 | 672.7 | | | | | | |
| 8.41 | 0.0154 | 1.668 | 671.5 | | | 6.284 | 79.190 | 7.966 | 6.560 |

Note: BD = below detection.

Sun River Electric and Watts Construction started construction of the drilling pad on February 12 and completed work on February 17, 1998. The site is extremely sandy and a bulldozer was used initially to clear the vegetation and level the area. Gravelly sediments were taken from a borrow pit in the 200 West Area that was used to burn sagebrush. Approximately 15 cm of this material was laid down, and then a large vibratory roller was used to compact the material. This compaction can easily affect the first two feet of sediment. Approximately 7.5 cm of crushed gravel was then laid down and the vibratory roller compaction was repeated. Drilling began on April 6, 1998, at B8500, April 24, 1998, at B8501, and April 27, 1998, at B8502. The gravel drill pad is a very effective structure for reducing evaporation, which increases the movement of water deeper into the profile. Precipitation totaled 22.1 mm between construction and drilling. Our concern is that some of this water may have affected the upper samples.

## B.4.1 Physical Properties

### B.4.1.1 Stratigraphy

Stratigraphic columns were constructed from available geologic information (Figure B.3). In 1995, the columns were reconstructed from geologic notes taken at the drill site. A more thorough analysis was done in 1998 when the split cores were examined in detail in the laboratory.

Distinct layering was evident from the exposed trench wall. This layering was primarily gravels, medium to fine sands, and silts. The structured horizontal layering (seen in the lower portion of the trench photograph in Figure B.3) results from layers of fine and coarse sands and silts, usually on the order of a few centimeters thick. These layers are part of the upper flow regime of the plane-laminated sand facies of the Hanford formation.

### B.4.1.2 Grain Size Analyses

Grain size distributions were determined by sieving according to the Wentworth scale; the amount of silt and clay was determined by sedimentation using a hydrometer (Figure B.4). There is a striking difference between the grain size distributions of the boreholes north of the east-west sand dune compared with the B8500 series boreholes that were located just outside the southern boundary of the proposed ILAW Disposal Site. The exploratory boreholes (299-E24-161 & -162) show less clay and silt and much less layering than the B8500 boreholes. In general, the exploratory boreholes had more uniform grain sizes with depth.

Among the B8500 series of boreholes, borehole B8503, which was drilled in undisturbed sediment, provided the most accurate grain-size distribution in the upper 2 m. The grain-size distributions in the upper 3 m of B8501 and B8502 were likely impacted by the fill sediment and gravel that was used to construct the drill pad.

Although the sediments are predominantly sand, some gravel and silt layering is evident in B8503, similar to what was observed at the exposed face of the trench dug in 1995. At some depths a high gravimetric moisture content correlates well with silt layers as shown in Figure B.5 for borehole B8502. This is in contrast to the labeling on the stratigraphy column of areas of clay-rich silt to silty sand. The

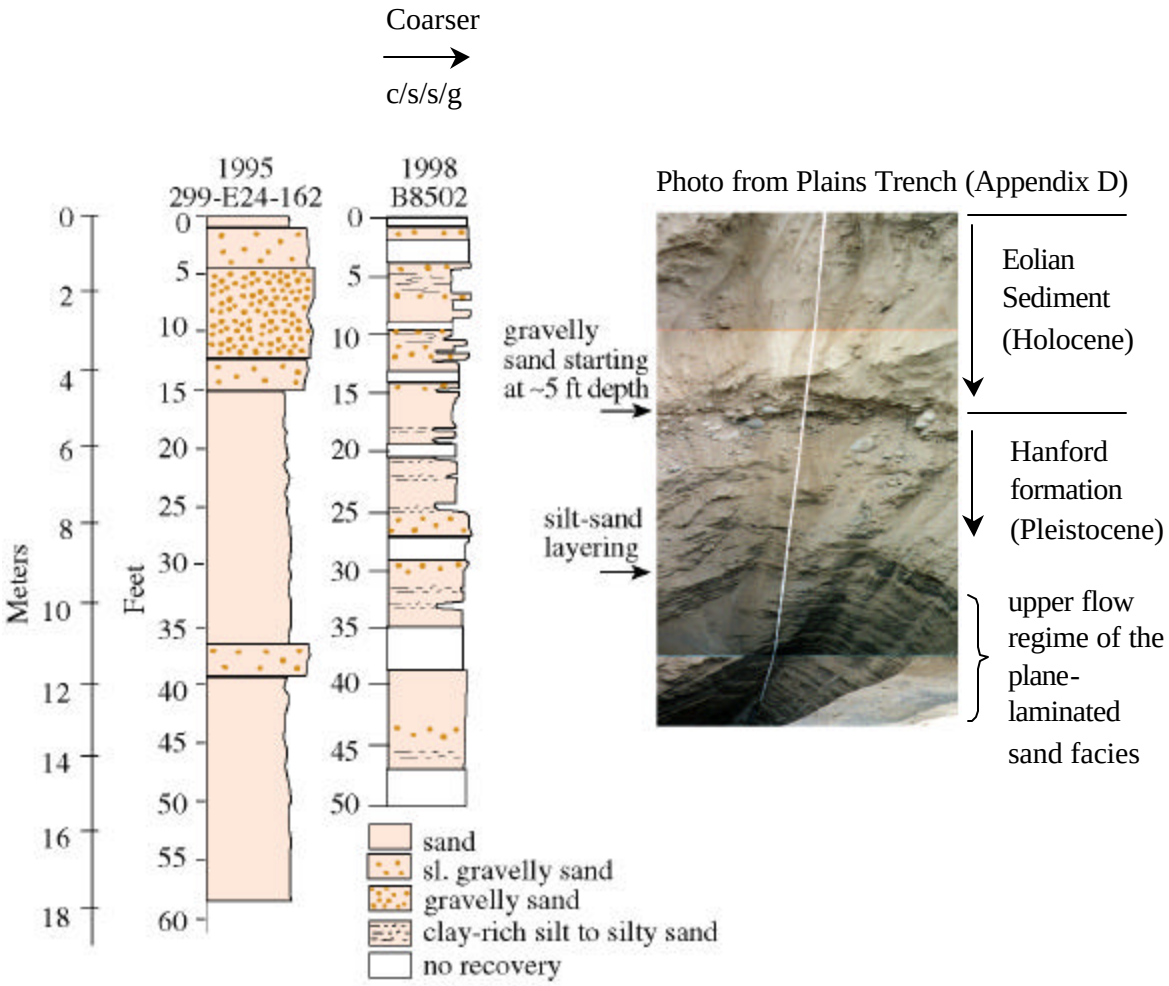


**Figure B.3**. Stratigraphic Columns Constructed from Drill-Site Geologic Logs and a Photograph Taken from the Trench Excavation in 1995

hydrometer methods indicated a fairly uniform low concentration of clay, ranging between ~5 to 10%. Sieve analyses indicated highly variable concentrations of silt in the sediment column. Therefore, the correlation of moisture with specific layers in the profile is likely due to the concentration of silt and not a clay-rich region in the profile.

### B.4.1.3 Gravimetric Moisture Content

Gravimetric moisture contents varied between ~0.01 to 0.13 g/g with the higher values generally in the top 3 m of sediment. The moisture contents of sediments collected from two exploratory boreholes drilled in March 1995 are shown in Figure B.6a along with moisture contents from the B8500 series boreholes (April 1998, Figure B.6b). The 1995 exploratory boreholes (161 and 162) were 35 m apart and were drilled during the same week. The B8500 series boreholes were all within ~22 m and were drilled

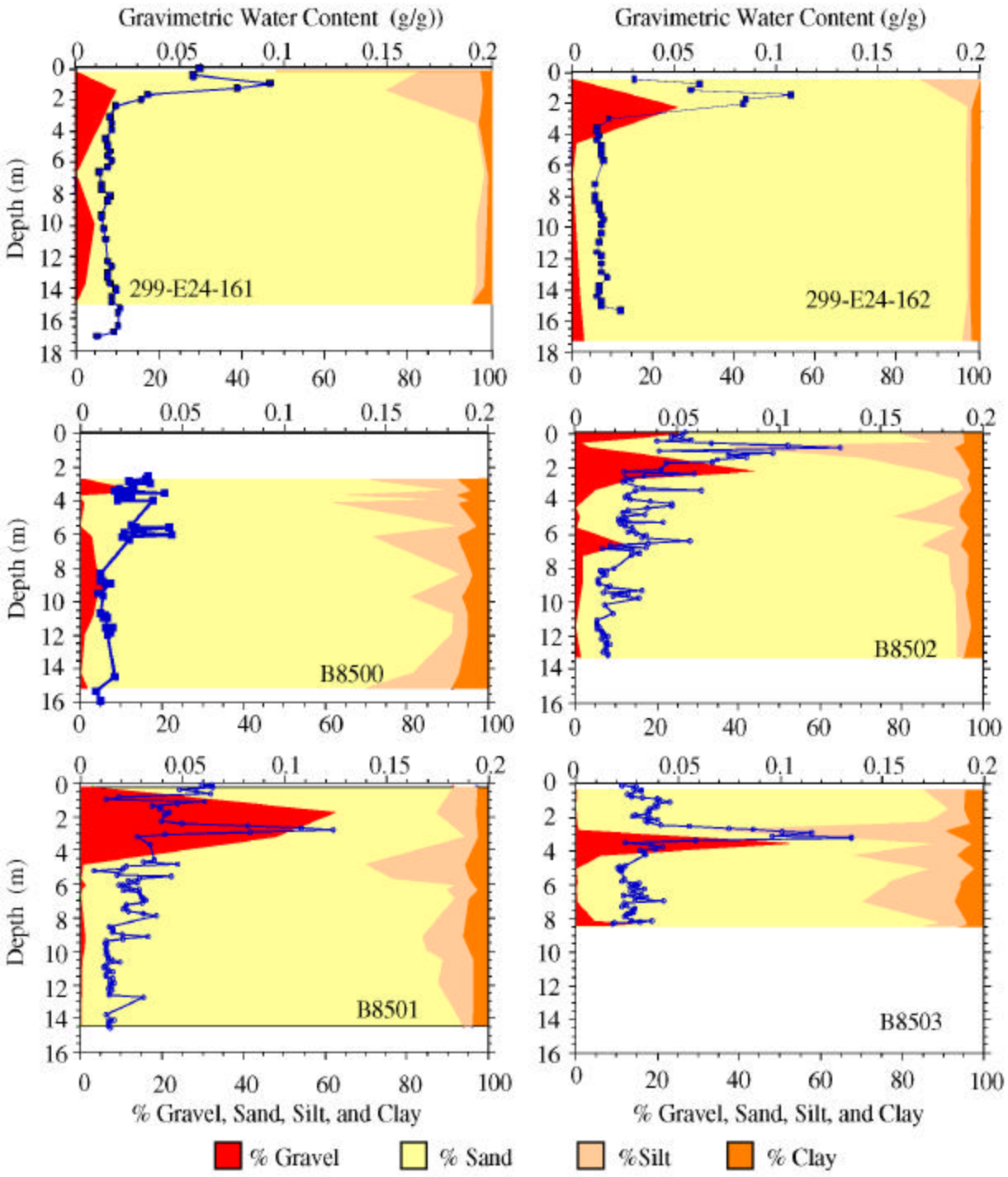


**Figure B.4**. Gravel, Sand, Silt, and Clay Percentages in the B8500 Series Boreholes. The data points show the corresponding gravimetric water content with depth. The lower x-axis of each graph is the percentage for the grain size distribution, while the upper x-axis of each graph is the gravimetric water contents (g/g).

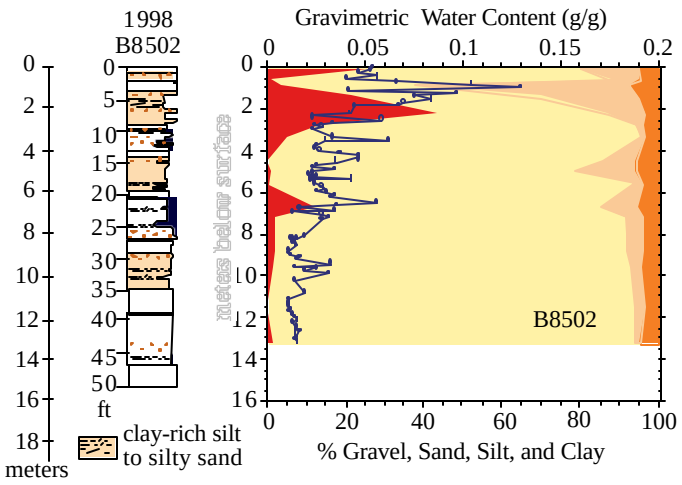


**Figure B.5**. Comparison of Stratigraphy with Particle Size Distribution for Borehole B8502

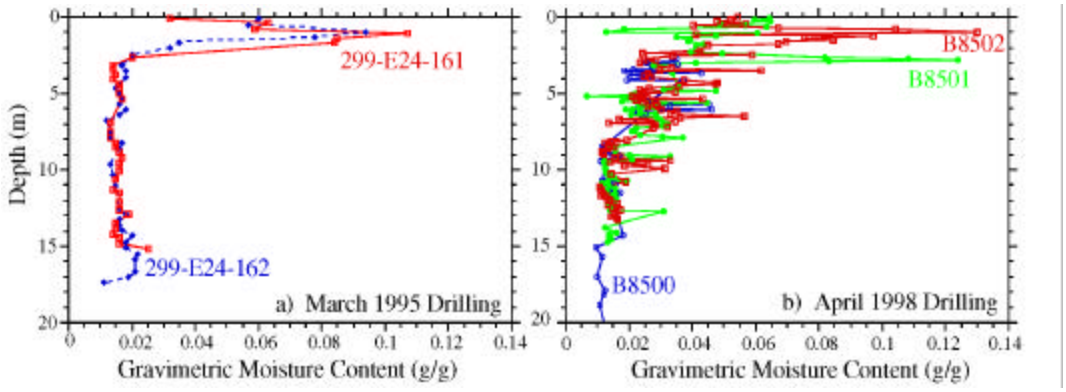


**Figure B.6**. Gravimetric Moisture Content Profiles from 1995 Exploratory Drilling (a) and Profiles from B8500, B8501, and B8502 (b)

The 1995 exploratory holes showed greater consistency in moisture content, which may be due to greater uniformity in the stratigraphy and surface vegetation compared to the B8500 site or handling problems associated with the B8500 sampling. When there was an obvious wetting front in the core sample (due to improper handling), the sediment was not sampled. The resulting moisture profile for the B8500 boreholes show greater variability than the wells drilled in 1995; however, the moisture contents were within the range typically found for Hanford sediments. Although we cannot assess the impact of the drilling pad construction and fill material on the moisture profiles, we can suggest that the more pronounced silt layering in the B8500 boreholes has a direct impact on the moisture variability with spikes in the moisture content generally associated with silt layers (see Figure B.4).

The other primary difference between the exploratory borehole site and the B8500 site is the surface vegetation. The exploratory boreholes were located on the lee side of the sand dune in a dense stand of mature sagebrush. In contrast, the B8500 boreholes are located on the windward side of the sand dune. The vegetation here was much smaller and sparse. The dense, mature vegetative cover at the exploratory

boreholes may promote the greater uniformity seen in the moisture contents. In these profiles, the predominant moisture was confined to the root zone. Below the root zone, the sediments were extremely dry, ranging from 0.01 to 0.02 g/g gravimetric water content. The B8500 moisture profiles showed greater variability and somewhat higher moisture contents at depths below the root zone.

#### B.4.1.4 Dry Bulk Density

Dry bulk density measurements were performed on all samples that were used for tracer analysis. The chloride mass balance approach uses this measurement to estimate recharge. Similar to the moisture content, the dry bulk densities were more variable in the B8500 series boreholes when compared to the 1995 exploratory holes (Figure B.7). A correlation was not evident when moisture content was plotted against dry bulk density.

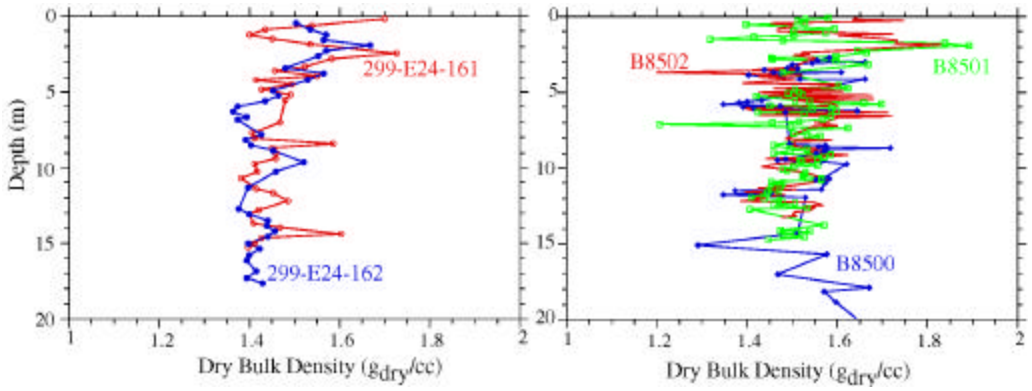


**Figure B.7**. Dry Bulk Density Comparison Between 1995 Exploratory Boreholes (a) and B8500 Series Boreholes (b)

### B.4.2 Tracer Results and Discussion

Unsaturated flow processes have been investigated using indirect physical measurements (e.g., water balance and Darcy flux measurements), direct physical measurements (e.g., lysimetry), and environmental tracers (e.g., Cl, $^{3}H$, and $^{36}Cl$). Allison and others (Allison 1988; Allison et al. 1994) concluded that the indirect physical measurements were the least successful in arid regions and the tracer methods were the most successful. However, Phillips (1995) cautioned that "unless considered in the context of a thorough evaluation of the physical hydrogeology, tracer results are of generally limited value. Conversely, isotopic and environmental tracers can usually provide very useful constraints on interpretations of subsurface flow regimens."

The application of environmental tracers generally yields a site-specific, long-term recharge estimate (where recharge is defined as the net deep drainage flux when measured below the root zone). This section details the results of the environmental tracers, $^{36}Cl$, chloride, and Cl/Br ratios.

### B.4.2.1 Bomb-Pulse $^{36}Cl$

$^{36}Cl$ (half life approximately 301,000 years) was produced indirectly during atmospheric nuclear weapons testing by thermal neutron irradiation of chloride in sea water. Thus, only the explosions carried out by the United States in the South Pacific between late 1952 and mid-1958 activated chloride in sea-water and produced the worldwide $^{36}Cl$ signal (Bentley et al. 1986). The peak in the $^{36}Cl$ fallout occurred in 1955 (Phillips et al. 1988). Water fluxes are estimated for bomb-pulse $^{36}Cl$ from the depth of the center of mass of the $^{36}Cl$ profile. The amount of water in the profile above the center of mass is equal to the water flux over the time period since the $^{36}Cl$ was deposited on the soil surface.

Archived samples were processed for $^{36}Cl$. These samples had been collected in 1995 at the ILAW Disposal Site (previously known as the Low Level Glass Site) in the 200 East Area. Large quantity samples were collected from a trench with a backhoe. Depth measurements were made before each sample was collected. The samples were sealed in plastic buckets and processed for leachable chloride in late 1997 to early 1998. The samples were analyzed for $^{36}Cl/Cl$ by tandem accelerator mass spectrometry (TAMS) at Lawrence Livermore National Laboratory. Blind sample splits were included to determine TAMS measurement variability. The results with measurement error bars are plotted against sample depth in Figure B.8. The samples and sample-splits were processed in two different runs approximately a month apart. The sample splits showed little variability considering the TAMS runs were a month apart.

A sharp $^{36}Cl/Cl$ peak occurs in the trench profile (see Figure B.8) with a center of mass at approximately 1.5 m. The peak is still well within the root zone at this site. When the bomb-pulse $^{36}Cl/Cl$ is located in the root zone, one can infer that the water flux at this site is extremely low (Scanlon et al. 1997). Much of the water in the root zone is eventually removed by evapotranspiration; therefore, estimates of water fluxes by tracers in the root zone will overestimate the amount of net deep drainage flux below the root zone by several orders of magnitude (Tyler and Walker 1994). These types of estimates would also be affected by seasonal moisture variations in the root zone. Recharge is defined as the net deep drainage flux *below* the root zone (e.g., that water that has escaped evapotranspiration processes and can therefore contribute to recharge of the unconfined aquifer).

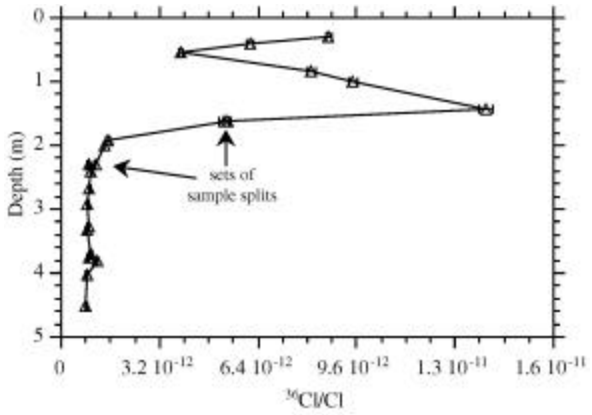


**Figure B.8**. Bomb-Pulse $^{36}C1$ Profile from Samples Collected in the Plains Trench at the ILAW Disposal Site

The shape of the $^{36}Cl/Cl$ pulse in Figure B.8 is significant because it suggests that the center of tracer mass is moving by piston flow through the root zone. Piston-type flow is an underlying assumption in most unsaturated flow models and in methods used to estimate recharge by atmospheric tracers. Deviations from piston flow can occur when there is preferential flow through root channels and macropores created by natural soil activities. Although there is no evidence to indicate that this piston-type flow can persist below the root zone, absence of a strong preferential flow component in the root zone suggests that this mechanism may dominate in these sandy sediments. The ratio $^{36}Cl/Cl$ may not indicate preferential flow if chloride concentrations are high because small variations in $^{36}Cl$ can be overwhelmed by the high chloride. We did not measure the chloride concentrations of these samples, but nearby boreholes indicated the chloride concentrations could be as high as 4000 mg/L.

### B.4.2.2 Chloride Mass Balance

The natural tracer method based on CMB is one of the simplest, least expensive, and most useful for determining recharge in arid climates (Allison et al. 1994). In this mass balance approach, water entering the soil column contains meteoric chloride that is treated as an inert tracer. As water percolates downward through the root zone, evapotranspiration removes water, thus enriching the chloride concentration with depth through the root zone. This increase in chloride concentration quantitatively reflects the corresponding reduction in water flux from the infiltration flux to the deep drainage flux beneath the evapotranspiration zone. The CMB method is especially applicable to arid and semiarid regions where evapotranspirative enrichment of the pore water produces a distinct chloride profile in the unsaturated zone.

Application of the CMB method typically involves the following simplifying assumptions regarding transport: 1) flow is vertically downward of piston type at constant water content and 2) the precipitation and the accumulation rate of atmospheric chloride are steady over the relevant period. An additional assumption of steady state water flux throughout the column is often invoked, but as shown by Ginn and Murphy (1997) this assumption is not required in application of CMB. Recharge or net deep drainage flux is determined by the relationship

$$J_R = \left( \frac{Cl_o}{Cl_{sw}} \right) P \qquad \text{(B.1)}$$

where $J_R$ = net downward deep drainage flux (mm/yr)
$Cl_o$ = average atmospheric chloride concentration in local precipitation and dry fallout (mg/L or equivalent units of $g/m^3$)
$Cl_{sw}$ = average chloride concentration in the soil water (mg/L)
$P$ = average annual precipitation (mm/yr).

$Cl_o$ can be expressed as the total chloride mass deposited at ground surface $q_{Cl}$ ($q_{Cl}$ - units of mg $m^{-2}yr^{-1}$) divided by the precipitation (160 mm/yr at Hanford). Values for $q_{Cl}$ can be measured,

calculated, or obtained from the literature. For the ILAW site, $q_{Cl}$ was determined using the approach outlined by Phillips et al. (1988) and Scanlon et al. (1990):

$$q_{Cl} = \frac{{}^{36}Cl_o \left(atoms\, m^{-2} s^{-1}\right)\left(31.56\ x10^6\, s/yr\right)\left(35.5\, x10^3\, mg/mol\right)}{\left({}^{36}Cl/Cl\right)_m \left(6.023 x\, 10^{23}\, atoms/mol\right)} \qquad \text{(B.2)}$$

where ${}^{36}Cl_o$ = calculated natural fallout of 18.8 atoms $m^{-2}s^{-1}$ for 46°N geographic latitude (Andrews and Fontes 1992)

$({}^{36}Cl/Cl)_m$ = ${}^{36}Cl/Cl$ ratio in the soil water excluding the anthropogenic ${}^{36}Cl$ peak.

Over the Holocene the geographic latitude represents a long-term average of the frequent fluctuations in the geomagnetic latitude (Merrill and McElhinny 1983). Below the bomb pulse, the average ${}^{36}Cl/Cl$ ratio between depths 2.4 and 4.8 m was 911 x $10^{-15}$. The values ranged from 810 x $10^{-15}$ to 1160 $10^{-15}$ and had a median value of 887 x $10^{-15}$. Ratios at other sites at Hanford fall within this range (Murphy et al. 1996; Prych 1998). Using the average ratio of 911 x $10^{-15}$ in Eq. B.2, we calculated a $q_{Cl}$ value of 38.4 mg/$m^2$/yr. This value is consistent with previously reported values for the 200 area plateau, which range from 32.7 to 49.4 mg/$m^2$/yr (Murphy et al. 1996).

Figure B.9 shows the chloride profiles (concentration of chloride in the pore waters) for the two exploratory boreholes in 1995 and the four B8500 boreholes drilled in 1998. The exploratory boreholes both show a peak in chloride starting at approximately 1.5-m depth and ending at approximately 4-m depth (center of mass is approximately 2.5 to 3 m). As can be seen in Figure B.9b, only the bottom portion of the chloride pulse was recovered from borehole B8500. The drilling contractor was not prepared to collect continuous core and did not attempt to collect core above approximately 3 m. The depth of the bottom of the B8500 profile was consistent with the location of the chloride profiles in 1995. By 5 to 6 m the chloride concentration in the porewater has returned to background levels.

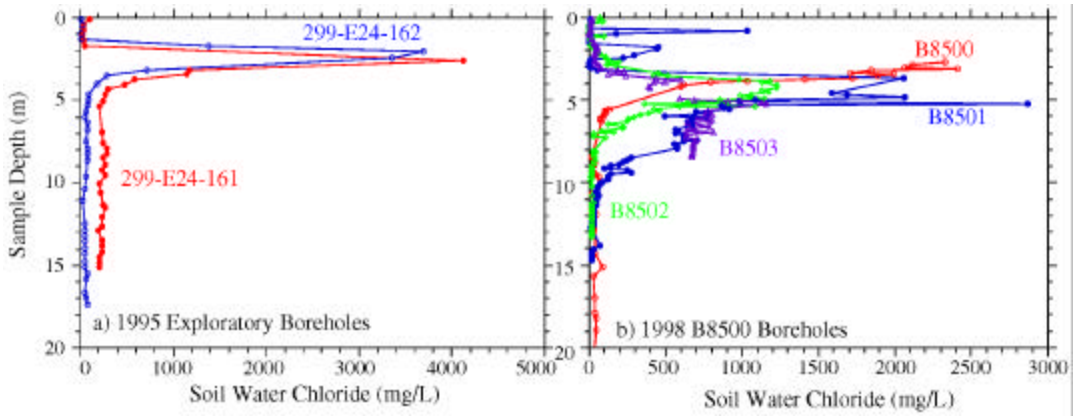


**Figure B.9**. Comparison of Chloride Profiles from B8500, B8501, and Exploratory Boreholes Drilled in 1995

The chloride profile for B8501 is more complete, but much more irregular than what we typically find at undisturbed sites (Figure B.9b). The chloride peaks near the surface (0 to 3 m) are most likely artifacts of the fill dirt/gravels that were deposited at this location and therefore should be disregarded. For example, B8503 is located directly adjacent to B8501, a meter off of the drill pad where the surface was undisturbed. There are no significant peaks in the chloride in the top 3 m of the B8503 profile. The secondary peak of chloride in the B8501 borehole between a depth of 6 to 9 m suggests a past period of lower recharge rates, possibly due to changes in the surface vegetation. It is possible that the B8503 profile may have mimicked the chloride profile in B8501; however a critical portion of the B8503 core, where the peak chloride concentration would likely occur, was not recovered between 4 and 5 m. The chloride profile from the B8502 borehole is deeper than the peaks detailed in the 1995 exploratory boreholes and has a broader peak, suggesting higher recharge rates at this location.

The CMB method for estimating recharge relies on an accurate accounting of the mass of this tracer. If chloride mass is removed by grading or added by applying gravel/fill to the surface, then the mass balance approach will be compromised. So little of the chloride pulse is defined in B8500, that we are unable to determine the peak concentration and cannot estimate recharge using the chloride mass balance method for this particular borehole. In addition, incomplete recovery of the B8503 chloride profile precludes using this profile for estimating recharge rates.

The net downward deep drainage flux can be estimated with the conventional CMB method (Equation B.1). A value for $Cl_{sw}$ is determined by plotting cumulative chloride content with depth against cumulative water content at the same depth (Figure B.10). The slopes of the straight-line segments represent a period over which the precipitation and atmospheric chloride deposition conditions were approximately constant. The recharge rates ranged from 0.013 to 0.016 mm/yr at the 1995 exploratory boreholes (Figure B.10a). Somewhat higher rates were found at the B8500 site, ranging from 0.03 to 0.065 mm/yr; however, these estimated rates are still quite low. The recharge rates are consistent with the differences in surface vegetation at the two locations. Two recharge rates are calculated for B8501, one corresponding to the initial chloride peak and the other corresponding to the secondary bulge in chloride below the initial peak (Figure B.10b).

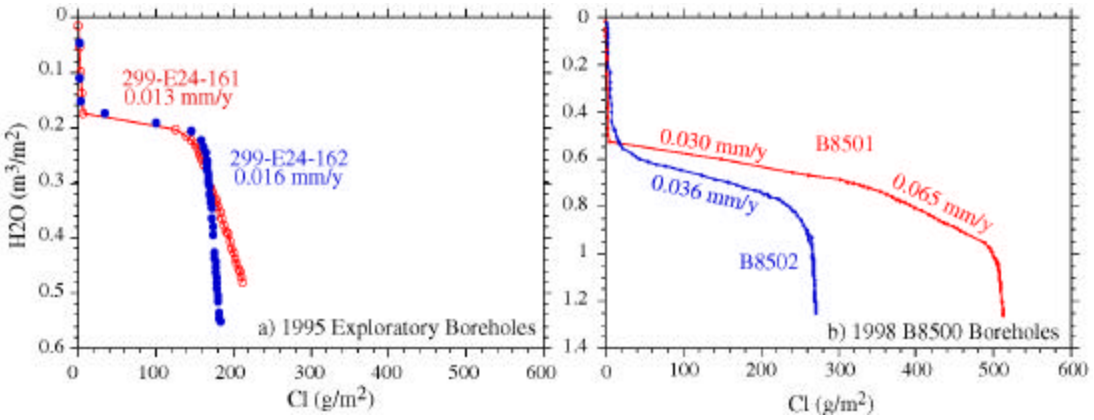


**Figure B.10**. Cumulative Water Versus Cumulative Chloride in the Sediment Profiles

The cumulative masses of chloride are different for the boreholes shown in Figure B.10. In particular, borehole B8501 had more total chloride than the other boreholes. If we assume that the large peak starting at approximately 3 m was not contaminated by fill material, then there are two possible processes that could lead to the differences in total chloride mass: 1) spatial and temporal differences in the extraction rate of water over time, and 2) variable input of chloride at the soil surface.

The variable total masses of the chloride in the different boreholes is most likely caused by spatial and temporal variations in the extraction rate of water over time. The extraction rate is a function of the type and density of the vegetation at a particular location and also is affected by the seasonal timing of precipitation. The two borehole locations were both subjected to repeated flooding during the late Pleistocene, which would have erased the pre-Holocene chloride signal (Murphy et al. 1996). The post-flood depositional history at the two ILAW drilling locations, however, is quite different as evidenced by their stratigraphy. The B8500 boreholes were located on the tail of a long dune lying in an east-west direction, while the 1995 exploratory boreholes were located approximately 300 m north of the dune. At the exploratory boreholes the eolian sands represent the top 0.5 m of the profile followed by the flood deposits of the Hanford formation. Using the accumulation of chloride mass at the exploratory boreholes as a measure of the time of evapotranspirative enrichment, vegetation capable of extracting pore water such that chloride is accumulated was likely established around 5,000 yBP at this site. This timing is consistent with the end of a period of maximum aridity that occurred between 8,000 and 5,500 yBP (Chatters and Hoover 1992; Gaylord et al. 1991) and transition to higher precipitation rates that would have been conducive to the establishment of vegetation.

The stratigraphy at the B8500 location is much more complex. The occurrence of a paleosol at 3 m in B8501 and 1.5 m in B8502 (Reidel et al. 1998) may reflect a time period early in the Holocene (approximately 8,000 to 10,000 yBP) when a grass-steppe vegetation dominated (Chatters and Hoover 1992; Mehringer 1985). This paleosol was also encountered at a backhoe trench that was attempted on the north (leeward) side of the dune in 1995 (the Dune Trench in Appendix D). The entire sequence exposed to approximately 4 m in this trench consisted of eolian sand. The flood deposits of the Hanford formation were not encountered before the trench collapsed at 4 m. However, a dark yellowish brown silty fine sand was found just below 3 m in the trench. Several peat-like clasts consisting of dense, partially decomposed mats of root hairs were located at this depth indicating past establishment of vegetation at this location. The dune lying in an east-west direction at the southern end of the proposed ILAW Disposal Site overlies this paleosol and may have been deposited during a period of maximum aridity, between 8,000 and 5,500 yBP. Therefore, it is possible that the lower chloride bulge in B8501 contains chloride accumulated in the early Holocene (10,000 to 8,000 yBP), followed by an arid period of dune formation (8,000 to 5,500 yBP), followed by establishment of vegetation again in the late Holocene (approximately 5,000 yBP to present). The more recent period is represented by the sharp chloride peak at 4 to 5 m.

In addition to a variable history in extraction rate, spatially variable atmospheric deposition of chloride could lead to differences in the total mass of chloride in the sediment profiles. It is highly unlikely that the atmospheric deposition of chloride would be spatially variable over such a small area (22 m horizontal separation between B8501 and B8502). Non-meteoric sources of chloride, such as

chloride leaching from basalt grains or anthropogenic sources of chloride, may lead to spatially varying masses of chloride in the sediment profile and will be discussed in more detail in the next section.

### B.4.2.3 Cl/Br Ratios

Ratios of ions are often used as tracers in hydrologic studies to determine the origin or evolution of waters or to quantitatively evaluate the mixing of different sources of water. If the two ions used have similar properties, then their ratio should remain relatively constant. In a recent article, Davis et al. (1998) reviewed information on the chemistry, characteristics, and concentrations of chlorine and bromine in nature. We have adopted the terminology of Davis et al. (1998) and have expressed Cl/Br as a ratio of the mass of each element.

Ratios of Cl/Br were analyzed to evaluate non-meteoric sources of chloride (Figure B.11). At the proposed ILAW Disposal Site, non-meteoric sources might include chloride leaching from basalt sand grains and chloride deposited from anthropogenic sources such as fly ash from a nearby power plant or other processing facilities within the 200 East Area. The ratios of potential sources of chloride were either measured or extracted from published reports. The basalt sands in the Hanford formation originate from the Columbia River basalt, which consists of multiple basalt flows that include the Grande Ronde, Saddle Mountain, and Wanapum flows. Flanagan (1973) measured a Cl/Br ratio of 333 for the Grande Ronde basalt. Ratios of Cl/Br in an additional 14 basalt samples ranged from 184 to 500 (Yoshida et al. 1971). The meteoric ratio of Cl/Br is somewhat more difficult to evaluate because approximately 60% of the chloride deposition occurs in dry fallout, while the remaining 40% is associated with precipitation events. The anion ratios may be quite different for wet and dry deposition. However, to evaluate the meteoric source, we need the combined ratio of wet and dry atmospheric deposition. In an extensive survey, Davis et al. (1998) found that most Cl/Br ratios in precipitation were less than 200. They suggested that Cl/Br ratios in precipitation vary geographically between 130 and 180 near the coast, to

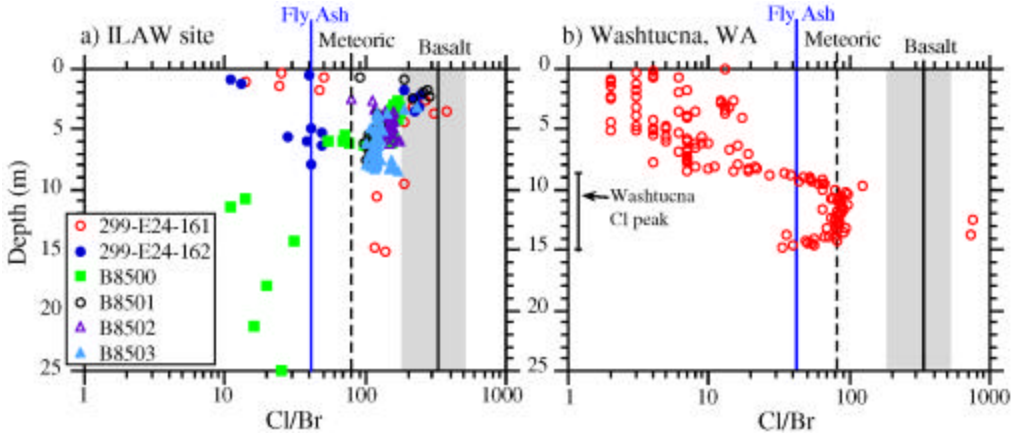


**Figure B.11**. Cl/Br Ratios of Pore Water Extracts from the ILAW Site (a) and the Washtucna Site in the Palouse Region of Eastern Washington State (b). The dashed line represents the meteoric Cl/Br ratio. The solid line represents the Cl/Br ratio of Grand Ronde basalt.

between 75 and 120 several tens to a few hundred kilometers inland, to as low as 50 several hundred kilometers inland. Berg et al. (1980) measured a Cl/Br ratio of 80 in the lower stratosphere at northern latitudes, which represents the total concentration of these anions in air. In the absence of specific measurements of meteoric Cl/Br in the Pasco Basin, shallow porewater ratios should reflect the combined wet/dry fallout ratio of meteoric Cl/Br. As can be seen, however, at the proposed ILAW Disposal Site (Figure B.11a) the Cl/Br ratios in the first few meters of the profile were the most variable, ranging from 10 to over 100. Surface evaporation alone should not affect this ratio.

In all of the boreholes examined to date, the Cl/Br ratio was low in the shallow portion of the bore-hole, increased to a maximum at the depth of the chloride peak, and then declined again below the chloride peak in the lower regions of the profile (Figure B.11). The increase in Cl/Br shifts the ratio closer to the ratio found in basalt. However, the increase in the ratio is not correlated with the basalt composition of the sediments (Murphy et al. 1996) nor is there sufficient chloride in basalt to impact the mass of this peak. The increase in the ratio also is not consistent with fly ash from the power plant located next to the proposed ILAW Disposal Site. Leaching of an 11-cm-deep sample of fly ash yielded a Cl/Br ratio of 41 (Table E.3, Appendix E), somewhat lower than the meteoric signature of 80 reported by Berg et al. (1980). In contrast to the shallow fly ash sample, a deeper sample (61 cm) yielded a Cl/Br ratio of 382. Although based on only two samples, the wide range of Cl/Br ratios in the fly ash may make it difficult to demonstrate a correlation with the ratios observed in the boreholes.

Finally, the ratios from the proposed ILAW Disposal Site are compared to the ratios collected from a borehole in the Palouse region of eastern Washington State (Figure B.11b, Washtucna, Washington). This site is not located near a power plant and is in a region of eolian deposition of fine sand and silt. The precipitation and recharge rates are much higher at the Washtucna site (Ginn and Murphy 1997). The Cl/Br ratios above the chloride peak are much lower than values at the proposed ILAW Disposal Site. It is not known whether these lower Cl/Br ratios reflect the relative distances of the sites from the ocean (approximately 350 kilometers for ILAW versus approximately 450 km for Washtucna) or other atmospheric patterns which might affect the meteoric ratio (Davis et al. 1998). The maximum Cl/Br ratios occurred concurrent with the depth of the chloride peak and then declined below this zone of evapotranspirative enrichment. Plotting the Cl/Br ratio against the chloride concentration in the pore water showed the relationship of an increasing ratio with increasing concentration of chloride (Figure B.12). The chloride and bromide peaks in the ion chromatograph were sufficiently separated that this relationship was not due to analytical interference at high chloride concentrations. We were also unable to find any bias in the ratios with low bromide measurements.

Davis et al. (1998) found a similar relationship of increasing Cl/Br with increasing concentration of chloride in precipitation samples and in groundwater samples. These authors also provide insight into a possible mechanism that leads to higher Cl/Br ratios in the zone of evapotranspirative enrichment of chloride. Chlorine is generally 40 to 8000 times more abundant than bromine. Therefore, a relatively small change in the total mass of bromine will give rise to a large change in the Cl/Br ratio. Additionally, bromide is much more soluble than chloride. McCaffrey et al. (1987) noted that during the evaporation of seawater, the residual brine is enriched in bromide due to bromide's higher solubility. Finally, some researchers have suggested that surface vegetation may concentrate bromine (Gerritse and George 1988; Shotyk 1997).

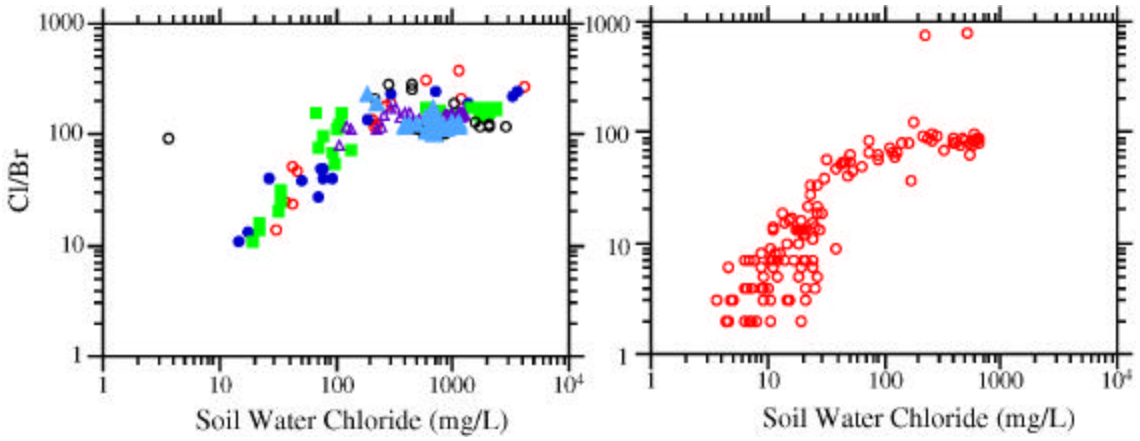


**Figure B.12**. Relationship Between the Soil Water Chloride Concentration and the Cl/Br Ratios at the ILAW Site (a) and the Washtucna Site in Eastern Washington State (b)

Two possible mechanisms could result in greater Cl/Br ratios in the zone of evapotranspirative enrichment: differential solubility and selective plant uptake. The highest soil water chloride concentrations generally range from 1000 to 4000 mg/L at gravimetric moisture contents as low as 0.02 g/g. Theoretically, plants could reduce the water content in the sediment. Under this condition, chloride is more likely than bromide to precipitate out of solution, leaving the soil solution enriched in bromide. As the plants take up soil water, the more soluble bromide will be removed in quantities greater than chloride, because a higher proportion of bromide mass will be in solution. When sediments are processed with distilled water to extract dissolved species, both the precipitated and solution chloride are recovered. Because bromide concentrations are so much lower than chloride to start with, any removal of the more soluble bromide by the plants will produce lower total bromide mass in the evapotranspiration zone. This precipitation mechanism is not likely, however, because the solubility concentration limit of chloride salts is ~220,000 mg/L. In the example above, the plants would have to reduce the water content from 0.02 g/g to the unrealistically low value of 0.0004 g/g for precipitation to occur. The selective plant uptake of bromide relative to chloride remains a viable mechanism.

This process could be tested by 1) extracting the pore water directly from the sediments without adding distilled water, and/or 2) by measuring the ratios of Cl/Br in the plant biomass for direct comparison with the ratios in the zone of evapotranspirative enrichment. Rickard and Vaughan (1988) measured chloride and bromide in two samples of sagebrush leaves, which yielded Cl/Br ratios of 100 and 196. These values bound the limits found in the zone of evapotranspirative enrichment at the proposed ILAW Disposal Site. Ideally, a direct comparison of the Cl/Br ratios in the sediment profile should be made with the plant biomass at the same site.

If the Cl/Br ratios are altered in the zone of evapotranspirative enrichment, then the Cl/Br ratios may be much more useful in tracer studies than just identifying non-meteoric sources of chloride. The Cl/Br ratios may provide an understanding of the recharge mechanisms taking place in the Hanford vadose zone. For example, all of the profiles at the proposed ILAW Disposal Site show the characteristic

increase in the Cl/Br ratio in the zone of evapotranspirative enrichment (Figure B.11a). Most of the profiles show a decline in the Cl/Br ratio below this zone, suggesting that little water is escaping the root zone. In one of the 1995 exploratory boreholes, 299-E24-161, high Cl/Br ratios persist at depth and somewhat higher total chloride mass. On a mass basis, approximately 5% of the chloride may be displaced below the chloride peak. There are two possible mechanisms that may lead to this displacement of chloride from the peak: 1) preferential flow, or 2) displacement of sands during drilling. Although preferential flow cannot be ruled out, we might expect to see some indication of chloride mass displacement in the shape of the chloride peak (e.g., multiple peaks). The chloride peak at this site is extremely sharp. In addition, the $^{36}Cl$ profile, which was evaluated in nearby, similar sediments, also does not indicate preferential flow processes. The depth affected by elevated chloride mass cannot be assessed because the borehole did not extend beyond 15 m and the depth to groundwater at this location is 100 m. The other mechanism that may result in a small amount of the chloride mass displaced below the zone of evaporative enrichment is simply displacement of sands during drilling. The sands are extremely dry below the root zone and can "flow" during the drilling process. This makes sediment recovery difficult and can easily lead to cross-contamination along the vertical borehole.

## B.5 Conclusions

Tracer measurements are effective in providing direct estimates of recharge in the natural environment. This approach can yield a range in recharge rates that often reflect the spatial heterogeneity in stratigraphy, surface land forms, and vegetation, as well as the temporal history at a particular site. Tracer measurements and physical characteristics were evaluated at two different locations at the proposed ILAW Disposal Site. In 1995, two exploratory boreholes were drilled within the ILAW boundaries. In 1998, one deep and three shallow boreholes (B8500 series) were drilled just outside the southern boundary of the proposed ILAW Disposal Site. The fine-scale stratigraphy at the two locations is quite different, which is not unusual for the Hanford formation. At the B8500 location, the shallow stratigraphy (0 to 15 m) shows slightly higher clay contents (5 to 10%) and higher and more variable silt contents. These variations lead to more pronounced horizontal layering at the B8500 site and greater fluctuations in water content and bulk density along the vertical profiles than was evident in the profiles from the exploratory boreholes. The mature and dense sagebrush vegetation at the exploratory boreholes would also contribute to the more uniform (and low) gravimetric moisture profiles at this site.

Although drilling is relatively easy in the predominantly sandy sediments found at the proposed ILAW Disposal Site, core recovery is quite difficult. The depth of the bottom of the root zone was defined operationally as the depth of the zone of evapotranspirative enrichment of chloride. At and below this depth the sediments were extremely dry, loose, and uncompacted, and it was sometimes impossible to keep the sediment within the split tube samplers. The chloride mass balance method was applied to samples from those boreholes that had relatively continuous core recovery within the critical zone of evapotranspirative enrichment of chloride. Recharge rates were estimated for two exploratory boreholes (299-E24-161 and -162) and two shallow boreholes (B8501 and B8502). In all cases the tracer measurements showed relatively low long-term averages of recharge, ranging from 0.013 to 0.036 mm/yr. At one borehole, B8501, a secondary chloride bulge below the initial peak suggests a past period of recharge (possibly in the early Holocene) with an average rate of 0.065 mm/yr.

The variable total masses of the chloride in the different boreholes is most likely caused by spatial and temporal variations in the extraction rate of water over time. The two borehole locations were subjected to repeated glacial-outburst flooding during the late Pleistocene, which would have erased the pre-Holocene chloride signal (Murphy et al. 1996). The stratigraphy at the different locations suggests early Holocene establishment of vegetation at the B8500 location followed by a period of dune formation in the mid-Holocene, and then vegetation establishment again in the late Holocene. The exploratory borehole stratigraphy, north of the sand dune, shows no evidence of establishment of vegetation in the early Holocene. It is likely that no evapotranspirative enrichment of chloride occurred prior to the establishment of vegetation approximately 4,000 to 5,000 yBP. Without vegetation, the movement of water through the vadose zone would be rapid.

A bomb-pulse $^{36}Cl$ peak was measured in samples excavated from a trench with a backhoe. A sharp peak at a depth of 1.5 m showed that this tracer was still in the root zone and, therefore, could not be used to estimate recharge. Scanlon et al. (1997) suggested that the presence of $^{36}Cl$ near the surface indicates little or no water flux below the root zone. The sharp $^{36}Cl$ profile suggests that the water is moving by piston flow through the root zone. If preferential flow is occurring in a particular sediment, we would expect to see evidence of this process in the root zone where old root channels and macropores are common. However, the chloride concentrations are too high to draw firm conclusions.

Ratios of Cl/Br were also used as a tracer in this study to investigate non-meteoric sources of chloride input. These ratios, which were consistently elevated in the zone of evapotranspirative enrichment of chloride, may be due to preferential uptake of bromide into the plant biomass. Although the Cl/Br ratios do not quantify recharge, the ratios have the potential to suggest invalidation of some recharge estimates. At the ILAW Disposal Site, the Cl/Br evidence does not contradict the recharge estimates from other methods.

## B.6 References

Allison GB. 1988. "A review of some of the physical, chemical, and isotopic techniques available for estimating groundwater recharge." In *Estimation of Natural Groundwater Recharge,* ed. I. Simmers, pp. 49-72. D. Reidel Publishing Company.

Allison GB, GW Gee, and SW Tyler. 1994. "Vadose-zone techniques for estimating groundwater recharge in arid and semiarid regions." *Soil Sci. Soc. Am. J.* 58:6-14.

Andrews JN and JC Fontes. 1992. "Importance of in-situ production of chlorine-36, argon-36, and carbon-14 in hydrology and hydrogeochemistry." *International Symposium on the Use of Isotope Techniques in Water Resources Development,* Vienna, Austria.

Bentley HW, FM Phillips, and SN Davis. 1986. "Chlorine-36 in the terrestrial environment." In *Handbook of Environmental Isotope Geochemistry,* Vol. 2 (ed. P Fritz and J C Fontes), pp. 427-480. Elsevier, Science, New York.

Berg WW, PJ Crutzen, FE Grahek, SN Gitlin, and WA Sedlacek. 1980. "First measurements of total chlorine and bromine in the lower stratosphere." *Geophys. Res. Lett.* 7(11):937-940.

Chatters JC and KA Hoover. 1992. "Response of the Columbia River fluvial system to Holocene climatic change." *Quaternary Research* 37:42-59.

Davis SN, DO Whittemore, and J Fabryka-Martin. 1998. "Uses of chloride/bromide ratios in studies of potable water." *Ground Water* 36(2):338-350.

Flanagan FJ. 1973. "1972 values for international geochemical reference samples." *Geochim. Cosmochim. Acta* 37:1189-1200.

Gaylord DR and LD Stetler. 1994. "Aeolian-climatic thresholds and sand dunes at the Hanford Site, south-central Washington." U.S.A. *J. Arid Environ.* 28:95-116.

Gaylord DR., LD Stetler, GD Smith, and RW Mars. 1991. *Summary of 1990 Eolian characterization studies, Hanford Site, Washington.* PNL-8862, Pacific Northwest Laboratory, Richland, Washington.

Gerritse RG and RJ George. 1988. "The role of soil organic matter in the geochemical cycling of chloride and bromide." *Journal of Hydrology* 101(1-4):83-95.

Ginn TR and EM Murphy. 1997. "A transient flux model for convective infiltration: Forward and inverse solutions for chloride mass balance studies." *Water Resources Research* 33(9):2065-2079.

McCaffrey MA, B Lazar, and HD Holland. 1987. "The evaporation path of seawater and the coprecipitation of Br- and K+ with halite." *J. Sedimentary Petrology* 57(5):928-937.

Mehringer PJ Jr. 1985. "Late Quaternary pollen records from the interior Pacific Northwest and northern Great Basin of the United States." In *Pollen Records of Late-Quaternary North American Sediments* (ed. V. A. Bryant and R. G. Holloway), pp. 167-189. American Association of Stratigraphic Palynologists.

Merrill RT and MW McElhinny. 1983. *The earth's magnetic field, its history, origin and planetary perspective*. Academic Press.

Murphy EM, JE Szecsody, and SJ Phillips. 1991. *A study plan for determining recharge rates at the Hanford Site using environmental tracers*. PNL-7626, Pacific Northwest Laboratory, Richland, Washington.

Murphy EM, TR Ginn, and JL Phillips. 1996. "Geochemical estimates of paleorecharge in the Pasco Basin: Evaluation of the chloride mass-balance technique." *Water Resources Research* 32(9):2853-2868.

Phillips FM, J Mattick, T Duval, D Elmore, and P Kubik. 1988. "Chlorine-36 and tritium from nuclear weapons fallout as tracers for long-term liquid and vapor movement in desert soils." *Water Resources Research* 24(11):1877-1891.

Phillips FM. 1994. "Environmental tracers for water movement in desert soils of the American Southwest." *Soil Science Society America Journal* 58:15-24.

Phillips FM. 1995. "The use of isotopes and environmental tracers in subsurface hydrology." U.S. National Report to IUGG, 1991-1994, *Rev. Geophys*. Vol. 33 Suppl., American Geophysical Union.

Prych EA. 1998. "Using chloride and chlorine-36 as soil-water tracers to estimate deep percolation at selected locations on the U.S. Department of Energy Hanford Site, Washington." Water-Supply Paper 2481. U.S. Geological Survey, Tacoma, Washington.

Reidel SP and KD Reynolds. 1998. *Characterization plan for the immobilized low-activity waste borehole*. PNNL-11802, Pacific Northwest National Laboratory, Richland, Washington.

Reidel SP, KD Reynolds, and DG Horton. 1998. *Immobilized low-activity waste site borehole 299-E17-21*. PNNL-11957, Pacific Northwest National Laboratory, Richland, Washington.

Rickard WH and BE Vaughan. 1988. "Chapter 6: Plant communities: Characteristics and responses." In *Shrub-Steppe, Balance and Change in a Semi-Arid Terrestrial Ecosystem,* eds. W. H. Rickard, L. E. Rogers, B. E. Vaughan, and S. F. Liebetrau. 272 pps. Elsevier, New York.

Scanlon BR, PW Kubik, P Sharma, BC Richter, and HE Gove. 1990. "Bomb chlorine 36 analyses in the characterization of unsaturated flow at a proposed radioactive waste disposal facility, Chihuahuan Desert, Texas." *Nuclear Instruments and Methods in Physics Research B52*, 489-492.

Scanlon BR, SW Tyler, and PJ Wierenga. 1997. "Hydrologic issues in arid, unsaturated systems and implications for contaminant transport." *Reviews of Geophysics* 35(4):461-490.

Shotyk W. 1997. "Atmospheric deposition and mass balance of major and trace elements in two oceanic peat bog profiles, northern Scotland and the Shetland Islands." *Chemical Geology* 138(1-2):55-72.

Tyler SW and GR Walker. 1994. "Root zone effects on tracer migration in arid zones." *Soil Science Society America Journal* 58:25-31.

Yoshida M, K Takahashi, N Yonehara, T Ozawa, and I Iwasaki. 1971. "The fluorine, chlorine, bromine, and iodine contents of volcanic rocks in Japan." *Bull. Chem. Soc. Jpn.* 44:1844-1850.

# Appendix C

# Simulation Estimates of Recharge Rates for the Two ILAW Disposal Sites

M. J. Fayer

# Appendix C

# Simulation Estimates of Recharge Rates for the Two ILAW Disposal Sites

## C.1 Introduction

Lockheed Martin Hanford Company (LMHC) is designing and assessing the performance of disposal facilities to receive radioactive wastes that are currently stored in single- and double-shell tanks at the Hanford Site. The preferred method of disposing of the portion that is classified as immobilized low-activity waste (ILAW) is to vitrify the waste and place the product in near-surface, shallow-land burial facilities. The LMHC project to assess the performance of these disposal facilities is known as the Hanford ILAW Performance Assessment (PA) Activity, hereafter called the ILAW PA. Acceptance of ILAW disposal at the Hanford Site depends on demonstrating that public health and the environment are adequately protected. Achieving this goal will require predictions of contaminant migration from the facility. To make such predictions will require estimates of the fluxes of water moving through the sediments within the vadose zone beneath and around the disposal facility. These fluxes, loosely called recharge rates, are the primary mechanism for transporting contaminants to the groundwater.

Mann (1999) indicated that two disposal sites will be considered: the ILAW Disposal Site (located southwest of the PUREX Plant) and the Existing Disposal Site (the former Grout Vaults). For each, recharge rate estimates are needed for a fully functional surface cover, its sideslope, and the immediately surrounding terrain. In addition, recharge estimates are needed for degraded conditions and for the case of irrigated farming directly on the cover. Mann (1999) indicates that the temporal scope of the 2001 ILAW PA is 10,000 years, but could be longer as some contaminant peaks occur after 10,000 years.

Pacific Northwest National Laboratory (PNNL) assists LMHC in their assessment activities. One of the PNNL tasks is to provide defensible estimates of recharge rates for current conditions and long-term scenarios involving the shallow-land disposal of ILAW (LMHC 1999). A major goal of the PNNL task is to collect sufficient data for the conditions and scenarios deemed to be important for evaluating the performance of the disposal facilities. These rate estimates will be provided using lysimetry, tracer studies, and modeling studies.

The recharge task uses a numerical recharge model to estimate the recharge fluxes for scenarios pertinent to the ILAW PA for which data do not currently exist. Because of the long time periods involved, data do not exist for many of the scenarios. Therefore, the model is used to extend the observations and to estimate recharge rates for potential future scenarios. This appendix summarizes the process used to provide LMHC with recharge estimates for scenarios identified for the 2001 ILAW PA.

## C.2 Methods

PNNL used a one-dimensional numerical model to estimate recharge rates for the two proposed ILAW disposal locations—the ILAW Disposal Site and the Existing Disposal Site. Figure C.1 shows where the two sites are located within the 200 East Area. Two soil types (Rupert sand and Burbank loamy sand) occupy both sites (Hajek 1966). Much of the proposed ILAW Disposal Site is covered by a relatively undisturbed shrub-steppe plant community. A shrub-steppe community existed at the Grout Vault Site at one time, but it was removed to construct the four existing vaults and place the spoils pile (located to the east). Most elevations at the proposed ILAW Disposal Site range from 219 to 222 m. The dune along the southern edge rises above the surrounding terrain by as much as 9 m, with a peak elevation of about 229 m. Elevations at the Existing Disposal Site are slightly lower, ranging from 204 to 206 m.

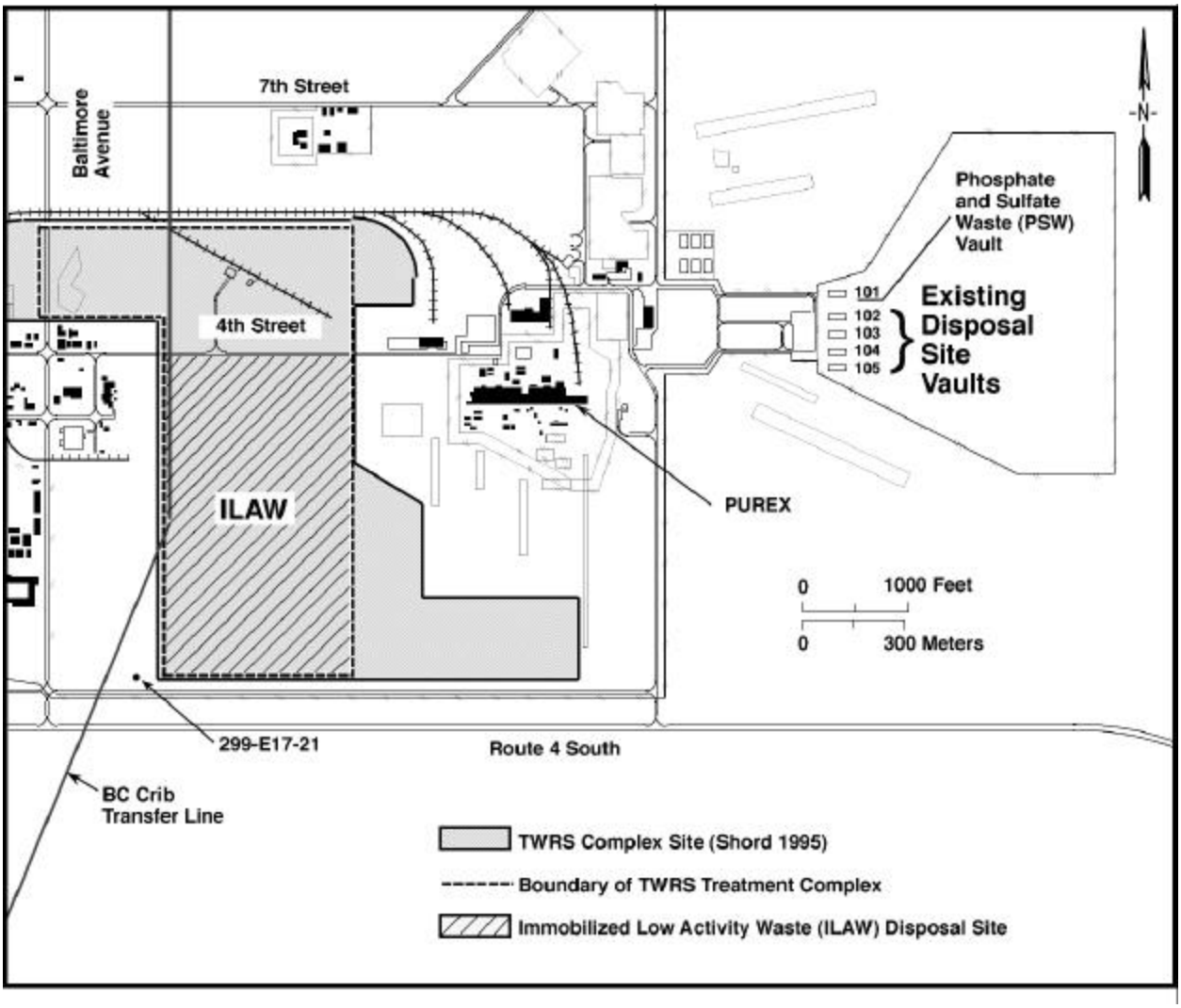


**Figure C.1**. Locations of the ILAW Disposal Site and the Grout Disposal Vaults

Based on this information, three scenarios were identified for simulation: the surface cover, Rupert sand, and Burbank loamy sand. Two additional scenarios were included to address two types of surface cover degradation. The sideslope component of the cover was not evaluated here. The simulation cases and associated model parameters are described in the following sections. The purpose of the surface cover is to store water and promote evapotranspiration rather than promote lateral flow. Thus, the one-dimensional UNSAT-H model is appropriate.

### C.2.1 Simulation Cases

Table C.1 shows the five scenarios that were evaluated to estimate the response of recharge rates to variations in several variables, including climate, vegetation, soil properties, and irrigation. The first three scenarios addressed functional disposal facility features: the proposed surface cover and the two soil types found in the surrounding terrain. The fourth scenario addressed the impacts of dune sand deposition on the surface cover. The fifth scenario addressed the impact of erosion of a portion of the surface cover. All five scenarios were evaluated for current climate conditions and for the future climate possibility most likely to promote recharge (i.e., increased precipitation and decreased temperature, denoted P↑T↓ symbolically).

**Table C.1**. Scenarios and Variables Tested with Simulations Using the Isothermal, Non-Hysteretic Mode of UNSAT-H and a Shrub-Steppe Plant Community (unless noted otherwise)

| Variable | Condition | Scenario | | | | |
|---|---|---|---|---|---|---|
| | | **Modified RCRA Subtitle C Cover** | **Rupert Sand** | **Burbank Loamy Sand** | **Dune Sand on Cover** | **Eroded Surface Cover** |
| Climate | Current | √ | √ | √ | √ | √ |
| | P↓ | | √ | | | |
| | P↑ | | √ | | | |
| | T↓ | | √ | | | |
| | T↑ | | √ | | | |
| | P↓T↑ | | √ | | | |
| | P↑T↓ | √ | √ | √ | √ | √ |
| Vegetation | Cheatgrass | | √ | | | |
| | No plants | √ | √ | √ | √ | √ |
| | No plants, future climate (P↑T↓) | | √ | √ | | |
| Shrub Leaf Area Index | High (0.4 vs. 0.25) | | √ | | | |
| | Low (0.1 vs. 0.25) | | √ | | | |
| Rupert Sand Properties | Higher $K(h)$ vs. Rupert sand | | √ | | | |
| | Lower $K(h)$ vs. Rupert sand | | √ | | | |
| Complete Area1 Plant Coverage | Cheatgrass | | √ | | | |
| | Sagebrush | | √ | | | |
| Irrigation Efficiency | 75% | √ | √ | | | |
| | 100% | √ | √ | | | |

Plant community composition will likely change in response to climate changes. Wing et al. (1995) reported that the plant communities in the Columbia Basin have fluctuated between sagebrush-dominated shrub-steppe and bunchgrass-steppe in the Holocene. Also, there is modern evidence of invasive plant species supplanting native species. Finally, the modern record clearly indicates that fires occur regularly, removing vegetation in the short term and altering the composition of the plant community for years after a fire.

### C.2.2 Model Description

Simulations were conducted using the UNSAT-H computer code (Fayer and Jones 1990). UNSAT-H was accepted for use at Hanford via the Tri-Party Agreement process (DOE 1991). The ILAW project has used this code for several years specifically to calculate recharge rates. In FY 1998, the code was updated to include new features such as hysteresis and the ability to simulate multiple years with one input file.

The UNSAT-H code has been tested with lysimeter data. Fayer et al. (1992) and Martian (1994) compared predicted and measured water storage values for lysimeters at Hanford. Both found that calibration of several parameters improved the match of predicted to measured values as determined by the root-mean-square (RMS) error. For a 1.5-year test of a lysimeter receiving an enhanced precipitation treatment, Fayer et al. (1992) calculated a RMS error of 0.8 cm after calibration (versus 2.2 cm without calibration). Martian (1994) looked at a much longer time period (5.5 versus 1.5 years) and found the RMS error was higher—about 1.8 cm for the calibrated model. The analysis was not done for the uncalibrated model. Martian determined the correlation coefficient for the comparison of measured and simulated soil water storage was 0.94, which is quite good. Fayer and Gee (1997) extended the comparison to 6 years. The data were collected from a non-vegetated weighing lysimeter containing 150 cm of silt loam over sand and gravel. They found that the RMS error for water storage predictions was about 2.3 cm regardless of whether the model was calibrated or whether it included heat flow or hysteresis. Fayer and Gee (1997) extended the comparison to matric potential and drainage. They found that the simulation with hysteresis was far better at predicting matric potentials throughout the 6-year period and it was the only simulation to predict drainage (52% of the measured amount, with timing that matched the observations). Fayer and Gee (1997) concluded

- UNSAT-H can reasonably predict the water balance components of a capillary-break type cover.
- The inclusion of heat flow has only a minor effect on surface evaporation and vapor flow within the soil (the impacts of heat flow on snow accumulation and melt and on soil freezing were not evaluated).
- A calibrated model will not necessarily apply well outside of the calibration period.

Khire et al. (1997) tested UNSAT-H for simulating water movement in surface cover test plots in a semiarid setting in Washington and a humid setting in Georgia. They tested the model using a 3-year record of data that included overland flow, soil water storage, evapotranspiration, and percolation. Time series plots of the data and predictions showed that UNSAT-H generally mimicked the seasonal trends.

The authors noted several conceptual features that were important to the Washington site but were not included in the model: snow cover, snow melt, and freezing soil. These features are scheduled for inclusion starting in FY 2000 (LMHC 1999).

The UNSAT-H code has been used at the Hanford Site to estimate the areal distribution of recharge rates (Fayer et al. 1996). The code has also been used elsewhere to evaluate infiltration through surface covers (Magnuson 1993) and surficial sediments (Martian and Magnuson 1994).

### C.2.3 Model Domain and Discretization

The model domain for the surface cover extended to the base of the gravel filter layer, which was located at a depth of 130 cm. We would have extended it to the base of the gravel drainage layer, but the hydraulic properties of this material were too difficult to simulate using the standard hydraulic functions. Fortunately, our experience has shown that neglecting the additional thickness of gravel has only a minimal impact on the results. Differences in drainage caused by variations in filter gravel thickness were less than 0.1 mm/yr. For the other simulation cases, the model domain was extended to 400 cm. The node spacing in all simulations started at 0.2 cm at the soil surface and gradually increased with depth. At material interfaces, the node spacing was decreased to 2 cm. Changes in node spacing from node to node were limited to less than 50%. Time step sizes were allowed to range from $10^{-10}$ to 1 hour, depending on the mass balance error.

### C.2.4 Soil Hydraulic Properties

Soil hydraulic properties consist of the soil water retention function and the hydraulic conductivity model. For all materials in this report, soil water retention was described with the van Genuchten function and hydraulic conductivity was described with the Mualem conductivity model. Three soil models were considered: modified RCRA Subtitle C Cover, Rupert sand, and Burbank loamy sand. Table C.2 lists the parameters for the materials making up each soil model. We did not address possible changes in soil hydraulic properties in response to soil development.

Martian (1994) simulated the performance of the modified RCRA Subtitle C Cover by accounting for all five materials that reside above the asphalt layer: silt loam/gravel admix, compacted silt loam, filter sand, filter gravel, and drainage gravel. For this report, the sand and gravel parameters were described using the Martian (1994) parameters without modifications. In contrast, some of the silt loam parameters were modified to accord with known relationships and/or measurements. The silt loam admix parameters were derived using the parameters for silt loam reported by Martian (1994) and correcting for a gravel content of 15% by weight using relationships in Bouwer and Rice (1983). The gravel and silt loam particle densities were assumed to be equal (i.e., 2.72 g/cm$^3$). The gravel correction changed $q_s$, $q_r$, and $K_s$. The parameters $a$ and $n$ were not changed from the Martian (1994) values because no known relationship with gravel content exists.

The values of the compacted silt loam parameters $q_s$ and $K_s$ differ from the values reported by Martian (1994). $q_s$ was calculated to be 0.353 cm$^3$/cm$^3$ based on the uncompacted bulk density

**Table C.2**. Parameters Used to Describe Soil Hydraulic Properties in the Simulations. The van Genuchten parameter *m* was set equal 1-1/*n*. The pore interaction term was specified using the standard value of 0.5.

| Soil Type (depth interval, cm) | $q_s$ $cm^3/m^3$ | $q_r$ $cm^3/m^3$ | $a$ 1/cm | $n$ -- | $K_s$ cm/h |
|---|---|---|---|---|---|
| **Modified RCRA Subtitle C Surface Cover** | | | | | |
| Silt Loam Admix (0 to 50) | 0.422 | 0.0042 | 0.0163 | 1.37 | 2.64 |
| Compacted Silt Loam (50 to 100) | 0.353 | 0.111 | 0.0077 | 1.78 | 0.0049 |
| Filter Sand (100 to 115) | 0.445 | 0.01 | 0.0726 | 2.8 | 392 |
| Filter Gravel (115 to 130) | 0.419 | 0.005 | 4.93 | 2.19 | 1260 |
| Drainage Gravel (130 to 145) | 0.4 | 0.005 | 10.0 | 3.0 | 3600 |
| **Rupert Sand** | | | | | |
| BWTF Sand (0 to 400) | 0.433 | 0.0381 | 0.106 | 1.78 | 35.3 |
| Sensitivity Case 1 (0 to 400) | 0.357 | 0.007 | 0.155 | 1.72 | 21.6 |
| Sensitivity Case 2 (0 to 400) | 0.408 | 0.035 | 0.0355 | 2.04 | 21.6 |
| **Burbank Loamy Sand** | | | | | |
| BWTF Sand (0 to 41) | 0.433 | 0.0381 | 0.106 | 1.78 | 35.3 |
| Loamy Sand, 45% gravel (41 to 76) | 0.279 | 0.0160 | 0.0292 | 1.35 | 2.44 |
| Loamy Sand, 85% gravel (76 to 89) | 0.0760 | 0.0040 | 0.0292 | 1.35 | 0.519 |
| Sandy Gravel (89 to 400) | 0.0833 | 0.0084 | 0.0061 | 1.52 | 0.572 |

(1.37 g/cm$^3$), compacted bulk density (1.76 g/cm$^3$), and particle density (2.72 g/cm$^3$). The $K_s$ value was set equal to the value 0.0049 cm/h based on measurements of compacted silt loam reported by Skelly (1994).

The Rupert sand is very deep sand (Hajek 1966; also called Quincy sand by USDA 1971). The hydraulic properties of this sand were represented using parameters describing the sand in the lysimeters at the Buried Waste Test Facility (Fayer and Gee 1992). The values of $q_s$, $q_r$, and $K_s$ were used directly. Because Fayer and Gee (1992) used the Brooks-Corey (BC) function, two parameters had to be converted for use in the van Genuchten (VG) function used for this report. The BC parameter $h_e$ was inverted to yield the VG $a$ parameter and the BC parameter $b$ was transformed into the VG $n$ parameter using the relationship $n = 1+1/b$.

Ward et al. (1998)[(a)] conducted a field infiltration test at the proposed ILAW Disposal Site. They collected water content and matric potential data for five depth increments in the upper 1.5-m of soil for six different infiltration fluxes. Ward et al. then used the data collected in situ to fit parameters for the van Genuchten retention function. The resulting five functions were similar and appeared to bracket the Rupert sand function determined above, supporting the use of a single function to represent Rupert sand.

(a) Ward AL, RL Clayton, and JC Ritter. 1998. "Hanford Low-Activity Tank Waste Performance Assessment Activity: Determination of in situ hydraulic parameters of Hanford Sediments," Letter Report to Fred Mann, Fluor Daniel Northwest, Richland, Washington, August 31, 1998.

The Burbank loamy sand consists of loamy sand from the soil surface to 41 cm, gravelly loamy sand (45% gravel) from 41 to 76 cm, very gravelly loamy sand (85% gravel) from 76 to 89 cm, and sand and gravel below 89 cm (USDA 1971). The hydraulic properties of the surface layer of loamy sand were described using the properties for Rupert sand. The properties of the second and third layers were obtained by scaling the properties of Sample 25 C (a loamy sand from Rockhold et al. 1993) using the gravel percentages of each layer. The properties of the fourth sample (a sandy gravel) were assigned those from the 4.1-m sample from Well 216-B-61-A (p. A-55 of Connelly et al. 1992). This sample was referred to as sandy gravel, and the particle size distribution (p. A-56 of Connelly et al. 1992) shows it to contain 76% gravel. Therefore, the hydraulic properties were scaled to account for the gravel.

The hydraulic properties of the soil profiles described in Table C.2 are shown in Figures C.2 to C.4. In addition to Rupert sand, Figure C.3 shows the retention functions determined for five soil depths with an infiltration test at the proposed ILAW Disposal Site (Ward et al. 1998).[(a)] The retention properties for two of those depth ranges (0.0 to 0.25 m for sensitivity case 1and 0.75 to 1.0 m for sensitivity case 2) were used to show the impact of variations in the Rupert sand properties. The $K_s$ value for these depths was set to 21.6 cm/h, which represent the median of 29 surface measurements distributed across the proposed ILAW Disposal Site (Fayer et al. 1996).[(a)]

### C.2.5 Initial Conditions

All simulations were started using the weather data for 1957. Initial matric potential values were not available for any of the scenarios, so the initial conditions were specified as $-10^3$ cm. This value is wetter than some measured vadose zone potentials (e.g., Prych 1998), so early drainage could reflect this initial water if recharge rates are lower for the given scenario. However, this limitation was overcome by repeating the 41-year sequence until the beginning and ending water storage values were within 0.1 mm of each other. This procedure uncoupled the results from the impact of using arbitrary initial conditions. The implicit assumption is that the 41-year weather record, when repeated, is representative of much longer periods.

### C.2.6 Boundary Conditions

Boundary conditions describe the water inputs and outputs at the top and bottom of the model domain. For this report, these conditions are the weather data that affect the calculation of evapotranspiration, precipitation, and the drainage rate from the bottom of the profile. The weather data were derived from the meteorological data collected at the Hanford Meteorological Station (HMS) for the years 1957 to 1997 (Table C.3 shows typical 30-year variations in some of the annual values). The HMS is located about 6 km west-northwest of the proposed ILAW Disposal Site at an elevation of 223 m (Hoitink et al. 1999). This elevation differs by less than 10 m from the elevations of the two disposal sites so that topographic differences in weather between the HMS and the proposed disposal sites should be negligible.

---

(b) Fayer MJ, JL Downs, BN Bjornstad, and K Mahan. 1996. "Integrated recharge assessment: Summary of FY 1995 Activities," Letter report to Fred Mann, Fluor Daniel Northwest, Richland, Washington, April 1996.

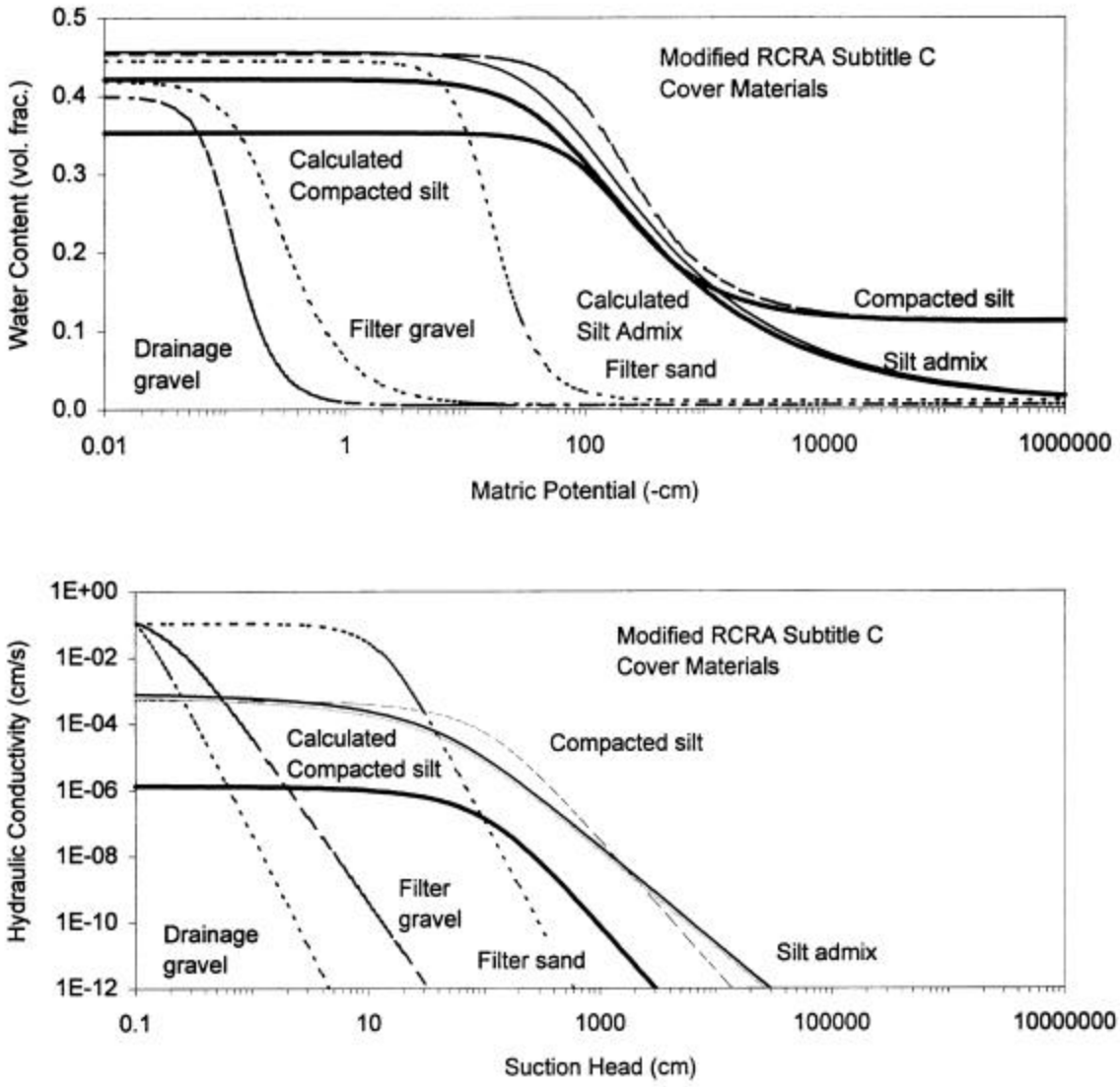


**Figure C.2**. Hydraulic Properties of the Materials Composing the Modified RCRA Subtitle C Cover

The current climate conditions were represented using the daily weather data. Measured hourly precipitation rates were used to describe the water inputs. Snowfall was treated as an equivalent rainfall at the time it occurred. Weather data such as wind speed, cloud cover, relative humidity, solar radiation, and maximum and minimum air temperature were used to calculate potential evaporation using the Penman Method (Doorenbos and Pruitt 1977).

Future climate conditions were represented by scaling the current temperature and precipitation data to match paleoclimate observations derived from pollen data. Whitlock and Bartlein (1997) described a 125,000-year paleoclimate record constructed from the pollen record in cores taken from Carp Lake, near Goldendale, Washington. Carp Lake is located about 175-km southwest of the Hanford Site, at an

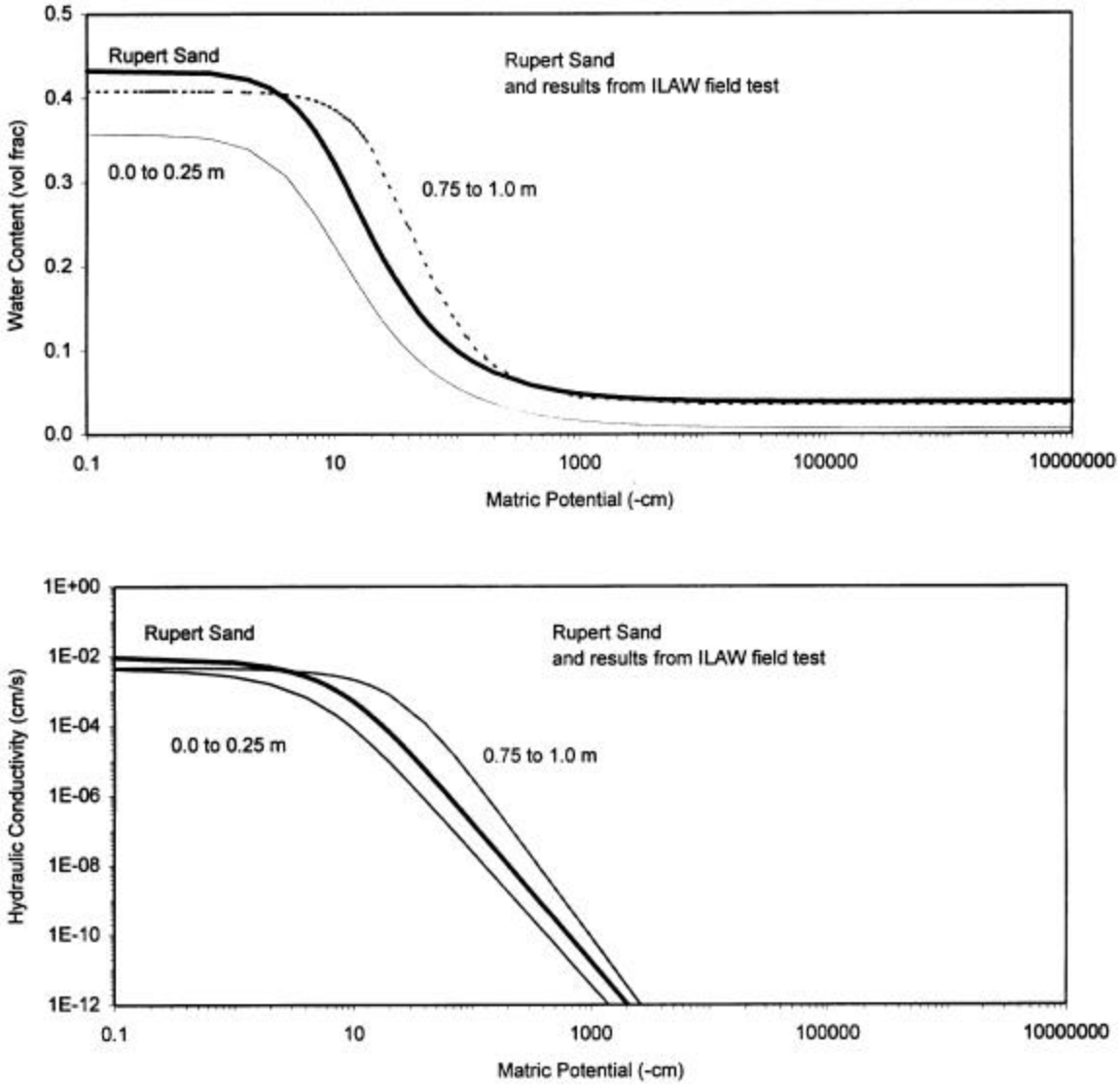


**Figure C.3**. Hydraulic Properties of the Rupert Sand

elevation of 714 m. Similar pollen records at the Hanford Site were eliminated during the glacial flooding 13,000 years ago. Thus, Carp Lake provides a proxy for paleoclimate information. Wing et al. (1995) described the Carp Lake pollen interpretation relative to precipitation and temperature. For the entire Holocene (i.e., the last 10,000 years), the data suggest that annual temperatures and precipitation ranged from 0 to 2.8°C warmer and 0 to 50% drier compared to modern climate. During the glacial period prior to the Holocene, annual temperatures ranged from 0.2°C warmer to 2.5°C cooler and precipitation ranged from 75 to 128% of modern levels. In summary, for the last 100,000 years, annual precipitation ranged from 50 to 128% of modern levels and annual temperatures ranged from -2.5 to 2.8°C (-4.5 to 5°F) of modern levels.

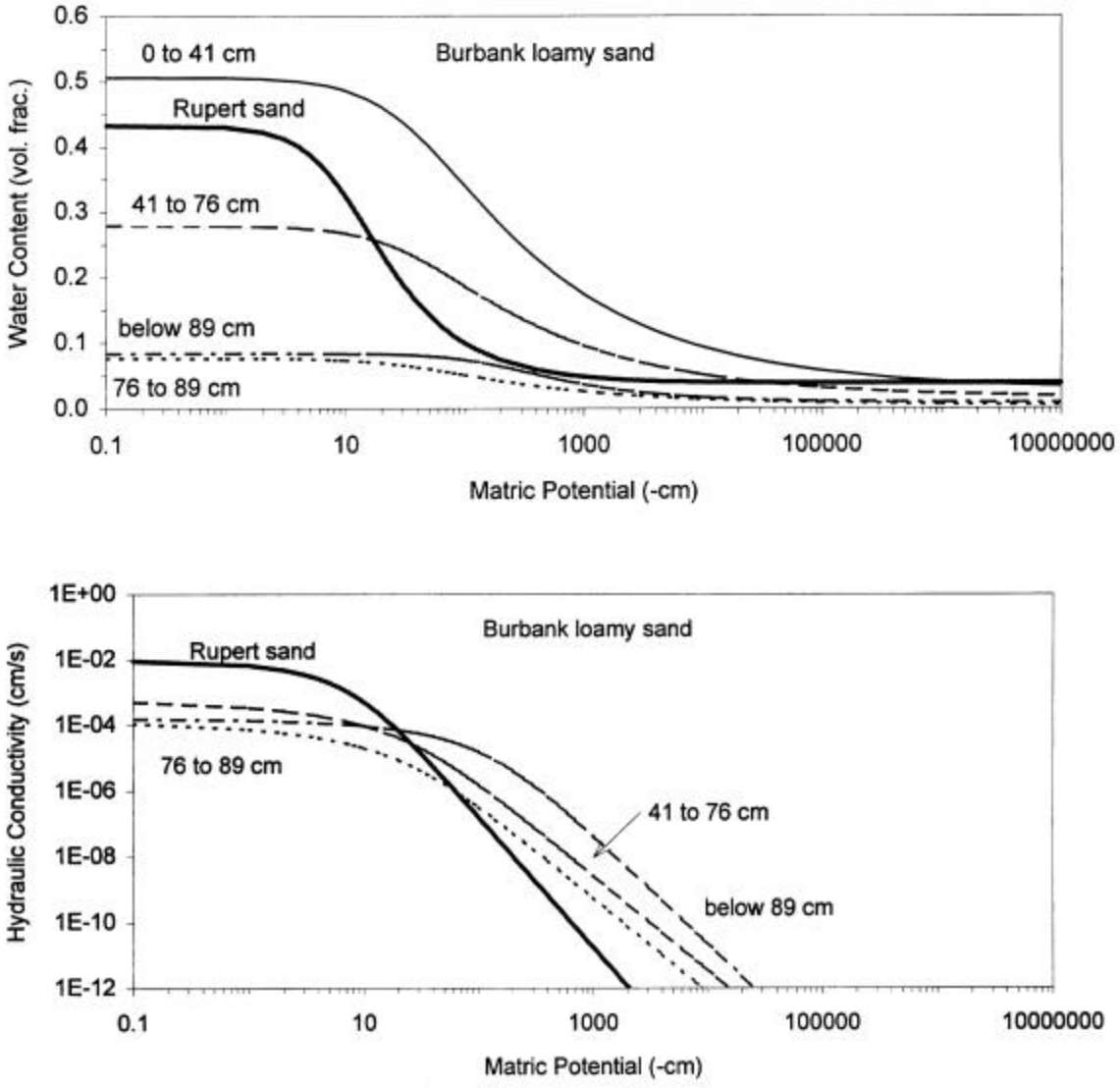


**Figure C.4**. Hydraulic Properties of the Burbank Loamy Sand

**Table C.3**. HMS Weather Statistics for 1961 to 1990 (* indicates a daily value)

| Weather Variable | Period of Record | Annual Values | | |
|---|---|---|---|---|
| | | Average | Minimum | Maximum |
| Precipitation, mm (in.) | 1961-1990 | 163 (6.26) | 75.9 (2.99) | 313 (12.31) |
| Air Temperature, °C (°F) | 1961-1990 | 11.8 (53.3) | 9.8 (49.6) | 13.6 (56.4) |
| Dewpoint Temperature, °C (°F) | 1950-1997 | 1.3 (34.4) | -0.3 (31.5) | 3.2 (37.7) |
| Wind at 15.2 m (50 ft), kph (mph) | 1945-1997 | 12.2 (7.6) | 10.0 (6.20) | 13.5 (8.4) |
| Solar Radiation, $W/m^2$ (ly/d) | 1953-1997 | 172 (355)* | 4.4 (9)* | 406 (838)* |

To represent future climate conditions with weather information, the Hanford weather record for 1957 to 1997 was used as the base data. From that base, future precipitation conditions were constructed by linearly scaling the current data. Future temperature conditions (daily maximum and minimum air temperatures) were constructed by adding or subtracting the projected temperature change. Changes in dewpoint temperature (humidity), solar radiation, wind speed, and cloud cover were not addressed. Seasonal changes implied by the pollen record will be addressed in subsequent work for the 2003 PA. Also not considered here are possible short-term changes caused by increased carbon dioxide. To date, the suggested carbon dioxide-induced changes fall within the range of climate changes inferred from the pollen record and so were not considered any further.

For the irrigation simulations, we modified the precipitation input files to include irrigation events. If a precipitation event coincided with an irrigation event, the two were added to yield a single water application event. Irrigation was applied between the hours of 0600 and 1200 once every 8 days. James et al. (1989) estimated the total crop irrigation requirement of about 81 cm for potatoes grown on silt loam in Richland, assuming 100% irrigation efficiency. This requirement was met using an hourly irrigation rate of 0.75 cm/h. If the efficiency dropped to 75%, James et al. (1989) estimated the irrigation requirement would increase to 108 cm for the season. This requirement was met using an hourly irrigation rate of 1.0 cm/h.

The bottom boundary was represented with a unit-gradient condition. This condition is generally acceptable when the boundary is well below the deepest plant roots, which were at 2 m in this report, and the drainage rate exceeds 1 mm/yr. For lower drainage rates, temperature cycling can have a significant effect on overall water movement via the temperature effect on vapor flow. In these cases, heat flow modeling can be used to examine total flux rates (such modeling was not done for this report).

### C.2.7 Plant Information

The plant community is an important component of the disposal facility. The two major functions performed by the plants are the efficient removal of water stored in the near-surface soil (thus minimizing recharge) and protection of the soil surface from wind and water erosion (thus protecting the integrity of the surface cover). By minimizing recharge and protecting the integrity of the surface cover, plants help to ensure the successful long-term protection of the disposal facility.

The majority of simulations performed for this report included a shrub-steppe plant community, which is the dominant community in and around the 200 Areas. As indicated earlier, Holocene pollen records indicated that plant communities in the Columbia Basin have alternated between shrub-steppe and bunchgrass-steppe. Recently, non-native species such as cheatgrass have been shown to compete successfully with native species and, in some cases, can dominate disturbed areas for years. Finally, range fires and industrial and waste management activities can eliminate vegetation for short periods of time. To address some of these alternate conditions, supporting simulations were conducted in which the plant community was either cheatgrass or no plants. A bunchgrass-steppe community was not included in this analysis; we assumed its impact would fall between that of shrub-steppe and cheatgrass. Finally, an irrigation scenario was evaluated using a potato crop.

To simulate plants with UNSAT-H Version 3.0 requires the following information:

- the method of partitioning potential evapotranspiration (PET)
- the active season
- the bare fraction
- the root length density
- the maximum rooting depth during the year
- the effectiveness of plant water withdrawal as a function of matric potential.

UNSAT-H allows only one plant to be simulated at a time. For this report, the shrub-steppe was simulated using shrub parameters and the cheatgrass community was simulated using cheatgrass parameters. In both cases, other species that might be present were not considered (e.g., shrub under-story species). Table C.4 shows the parameters that were chosen based on literature parameters or reasonable estimates of parameters. The plant parameters were held constant for each simulation year. Not addressed by this study were the potential plant community responses to yearly precipitation and temperature variations, fire, diseases, nutrient cycling, grazing, and land use changes.

For shrubs and potatoes, the leaf area index (LAI) method was used to partition potential evapotranspiration into potential evaporation and potential transpiration. Figure C.5 shows the shrub leaf area variation throughout the year. Link et al. (1990a) reported a maximum LAI value of 0.25 for sagebrush for 4 years in a sagebrush-bunchgrass community growing on a silt loam soil on the Fitzner/Eberhardt Arid Lands Ecology (ALE) Reserve. Our preliminary measurements at the proposed ILAW Disposal Site are showing similar LAI values. The maximum potato LAI was 2.5. Although not shown in Figure C.5, the variation throughout the year was similar to that of the shrub. For cheatgrass, the PET-partitioning method used was the cheatgrass model in UNSAT-H. This model was developed by Hinds (1975) using field data from a 2-month cheatgrass experiment.

**Table C.4**. Plant Parameters for UNSAT-H Simulations (see text for descriptions)

| Parameter Description | Parameter Value | | |
|---|---|---|---|
| | **Shrub** | **Cheatgrass** | **Potatoes** |
| PET Partition Function | LAI | Cheatgrass | LAI |
| Active Days of the Year | Mar 1 to Nov 30 | Mar 1 to May 31 | April 9 to Sep 16 |
| Bare Fraction | 0.27 | 0.27 | 0.0 |
| Maximum Rooting Depth (m) | 2.0 | 0.6 | 0.6, Surface cover<br>0.9, Rupert sand |
| Root Density Coefficients | | | |
| $a$ = | 0.217 | 1.17 | 1.17 |
| $b$ = | 0.0267 | 0.131 | 0.131 |
| $c$ = | 0.0109 | 0.0206 | 0.0206 |
| Plant Uptake Potentials (-MPa) | | | |
| $h_n$ = | 0.003 | 0.003 | 0.003 |
| $h_d$ = | 0.1 | 0.1 | 0.04 |
| $h_w$ = | 7.0 | 2.0 | 1.6 |

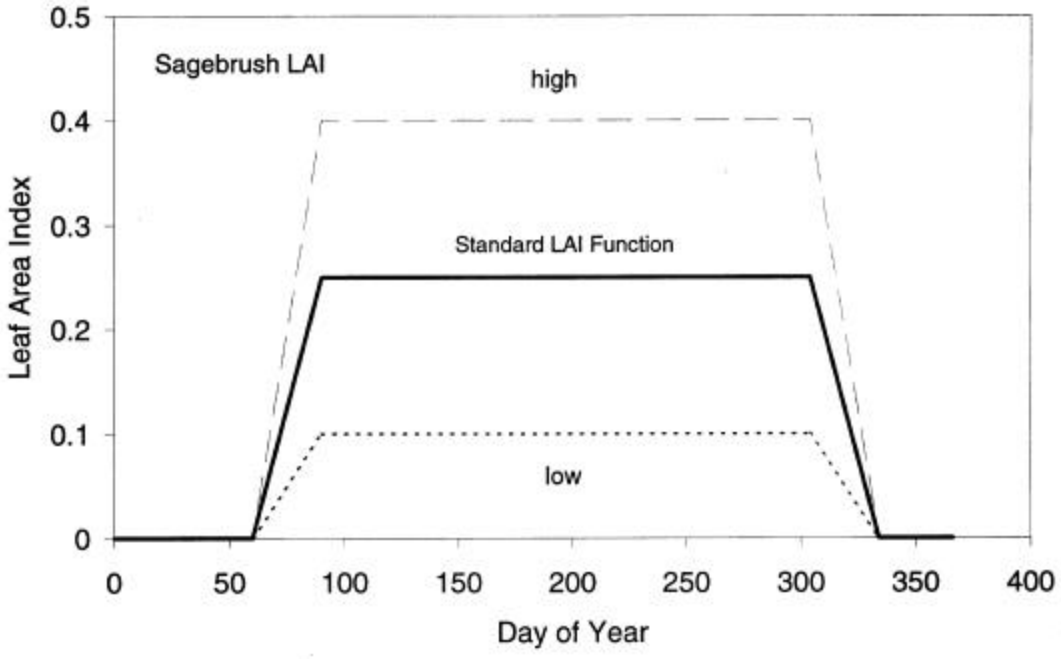


**Figure C.5**. Leaf Area Index for Sagebrush

The start and end dates of plant activity determine when during a growing season to calculate transpiration and root growth. Rickard and Vaughan (1988) reported that many plant species generally become active around March 1 in a normal year on the ALE Reserve. This start date coincides with the onset of air temperatures in excess of 3°C, a temperature suggested by Hanson et al. (1987), as the minimum needed for positive shrub and cool-season grass activity. Both shrubs and cheatgrass were started on March 1. Potatoes were started on April 9. This date was set 30 days prior to the initiation of irrigation, which was determined by air temperature. Irrigation was initiated on May 9, which is the average date when the 30-day running average of air temperature equals or exceeds 12.8°C (55°F) (James et al. 1989).

Because shrubs maintain LAI throughout the year, this minimum temperature was used to determine when shrub activity ceased in the fall. Based on the average temperatures reported by Hoitink et al. (1999), shrubs were allowed to be active until November 30. The end date for cheatgrass is earlier than that for shrubs. An ending date of May 31 was chosen for cheatgrass based on observations of cheatgrass at the Grass Site in 1986 and 1987 (Link et al. 1990b). The end date for irrigated potatoes was 130 days after the start date for irrigation (James et al. 1989).

The bare fraction represents the fraction of the soil surface devoid of vegetation. This value is used to scale the potential transpiration, which was calculated assuming a 100% plant cover. Roots from plants around the bare areas may (and likely do) penetrate some of the bare area. However, the one-dimensional nature of the UNSAT-H model does not allow it to represent multidimensional root behavior. Thus, reducing potential transpiration based on the bare fraction may underestimate transpiration. For the simulations with a shrub-steppe component, the bare fraction was set to 0.69. This value was derived

from preliminary measurements at the proposed ILAW Disposal Site and the Existing Disposal Site (Downs and Kahn 1998).[(a)] A slightly lower value of 0.577 was used for the cheatgrass simulations based on data from Downs and Kahn. Reductions to potential transpiration caused by bare areas are added to potential evaporation. Two additional simulations were conducted in which the bare fraction was set to zero for both the cheatgrass and shrub cases; a bare fraction value of zero represents 100% plant cover. A full canopy was assumed for the potato simulation; thus the bare fraction was set to zero.

Root parameters were obtained directly from the simulations reported by Fayer and Walters (1995). They used root length density data from Mayer et al. (1981) to fit the root density function

$$rld = a \exp(-bz) + c \qquad (C.1)$$

where rld = root length density (cm roots/cm soil)
z = soil depth (cm)
a, b, and c = fitting parameter.

The resulting parameters are shown in Table C.4. Maximum rooting depths were 2.0 m for shrub and 0.6 m for cheatgrass. The roots of shrubs were considered to be at their maximum depth throughout the growing season. Being an annual, cheatgrass roots were assumed to have a uniform growth rate of 1 cm/d for their entire growing season. Potatoes were simulated using the same rooting parameters as cheatgrass.

The plant water uptake parameters in Table C.4 were obtained directly from the simulations reported by Fayer and Walters (1995). There is some support for the wilting point values ($h_w$), which are the lowest matric potentials at which plant water withdrawal becomes zero. Sagebrush was reported to operate in soils with potentials as low as -7.0 MPa (Fernandez and Caldwell 1975; Branson et al. 1976). Cline et al. (1977) showed that cheatgrass could remove water at potentials as low as -1.5 MPa. In their first year of measurements at the proposed ILAW Disposal Site, Downs and Khan (1998 Letter Report to F Mann) have observed the lowest plant potentials in shrubs (values as low as -2.5 MPa). The parameter $h_d$ represents soil water potential below which plant uptake decreases below the potential water uptake rate. The parameter $h_n$ represents the soil water potential above which plant water is zero because of anaerobic conditions. Between $h_n$ and $h_d$ plant water uptake is set to its potential rate. For rangeland simulations, Hanson et al. (1987) suggested that plant water uptake was reduced by half when the soil potential was -0.64 MPa. Using the parameters in Table C.4, the potentials corresponding to halving the uptake rate are -0.84 and -0.45 MPa for shrubs and cheatgrass, respectively. These values are in line with the value suggested by Hanson et al. (1987). Plant water uptake parameters for potatoes were obtained from Feddes et al. (1978).

## C.3 Results

Each 41-year simulation took approximately 2 hours of dedicated time to run on a UNIX workstation. In most cases, repeating the weather sequence just once was enough to establish a condition indicative of

(a) Downs JL and FO Khan. 1998. "Brief status report: FY 1998 vegetation field studies on the LLTWDS Site," Letter report to Fred Mann, Fluor Daniel Hanford, Richland, Washington, September 1998.

the long-term average. In several cases, three to four repetitions of the weather sequence were required for the profile to achieve a condition indicative of the long-term average. In some cases, one sequence was enough to establish that the soil profile was drying and that further repetition of the weather sequence would dry out the profile even more.

Table C.5 shows the average long-term deep drainage rate for all simulations conducted. The average rate was calculated for all 41 years of the last simulation sequence. For those simulations that indicated drying, the rate was assigned a value of < 0.1 mm/yr. The less than symbol was used to indicate the uncertainty of specifying such a small rate, especially given the types of assumptions used (e.g., constant plant communities and isothermal flow).

The results in Table C.5 indicate that the surface cover will perform better than the design goal of 0.5 mm/yr. This performance occurred even in the absence of plants. When the cover was exposed to the future climate state most conducive to drainage, the simulation results still indicated a drainage rate of < 0.1 mm/yr.

**Table C.5**. Simulated Long-Term Drainage Rates Using the Isothermal, Non-Hysteretic Mode of UNSAT-H and a Shrub-Steppe Plant Community (unless noted otherwise)

| Variable | Condition | Simulated Long-Term Drainage Rates (mm/yr) | | | | |
|---|---|---|---|---|---|---|
| | | **Modified RCRA Subtitle C Cover** | **Rupert sand** | **Burbank loamy sand** | **Dune sand on cover** | **Eroded Surface Cover** |
| Climate | Current | < 0.1 | 2.2 | 5.2 | < 0.1 | < 0.1 |
| | P↓ | na[(a)] | < 0.1 | na | na | na |
| | P↑ | na | 13.2 | na | na | na |
| | P↓T↑ | na | < 0.1 | na | na | na |
| | P↓T↓ | na | < 0.1 | na | na | na |
| | T↓ | na | 7.5 | na | na | na |
| | T↑ | na | 0.6 | na | na | na |
| | P↓T↑ | na | 5.2 | na | na | na |
| | P↑T↓ | < 0.1 | 27.0 | 36.8 | 16.9 | < 0.1 |
| Vegetation | Cheatgrass | na | 33.2 | na | 18.4 | na |
| | No plants | < 0.1 | 44.3 | 52.5 | 32.7 | < 0.1 |
| | No plants, future climate (P↑T↓) | na | 88.6 | 98.0 | na | na |
| Shrub Leaf Area Index | High (0.4 vs 0.25) | na | 1.6 | na | na | na |
| | Low (0.1 vs 0.25) | na | 5.6 | 15.2 | 4.1 | na |
| Rupert Sand Properties | Higher $K(h)$ vs Rupert sand | na | 2.7 | na | na | na |
| | Lower $K(h)$ vs Rupert sand | na | 3.3 | na | na | na |
| Complete Areal Plant Coverage | Cheatgrass | na | 26.6 | na | na | na |
| | Shrub | na | <0.1 | na | na | na |
| Irrigation Efficiency | 75% | 26.4 | 58 | na | na | na |
| | 100% | < 0.1 | 30 | na | na | na |
| (a) na = not analyzed | | | | | | |

The results in Table C.5 indicate that the two soils, under shrub-steppe vegetation, have long-term drainage rates of 2.2 and 5.2 mm/yr., respectively. When plants were removed, the drainage rates jumped by a factor of 10 to 20. Under the future climate state most conducive to drainage, the drainage jumped by factors of 7 and 12, respectively.

Two cover degradation cases were evaluated. In the first, dune sand was deposited on the cover to a depth of 20 cm. The results in Table C.5 indicate that the cover still had drainage rates < 0.1 mm/yr under the shrub-steppe vegetation. When shrubs were removed to leave just cheatgrass, simulated drainage increased dramatically to 18.4 mm/yr. Clearly, deeper rooted plants like shrubs are needed to prevent drainage under these conditions. When all plants were removed, the cover drainage rate jumped to 32.7 mm/yr. The simulated increase in drainage is consistent with lysimeter data (e.g., Sackschewsky et al. 1995).

Under the future climate state most conducive to drainage, the drainage went from zero to 16.9 mm/yr. These results indicate that barrier performance in limiting drainage could be significantly degraded by the deposition of wind-borne sand. Efforts are under way to collect data on this case at the Field Lysimeter Test Facility under a separate ILAW task.

The second degradation case was an eroded surface cover, in which 20 cm of the surface silt layer was removed. The results in Table C.5 indicate that cover performance in limiting drainage was not impaired, even for the case without plants.

The simulation results in Table C.5 demonstrate that irrigation and its efficiency can have a large impact on recharge. Reducing the efficiency from 100 to 75% increased recharge on the cover from 0.1 to 26.7 mm/yr. The same reduction of irrigation efficiency for Rupert sand increased recharge from 30 to 58 mm/yr.

The sensitivity of long-term drainage rates was evaluated using the Rupert soil primarily because this soil yielded reportable rates. The rates for the surface cover were too low to be effective for this evaluation. Table C.6 shows that decreasing precipitation led to nearly zero drainage regardless of the temperature conditions. For modern precipitation conditions, drainage was inversely related to temperature. If temperatures rise in the near future in response to rising carbon dioxide levels, we can

**Table C.6**. Comparison of Rupert Sand Drainage Rates for Various Future Climate States (data from Table C.5)

| Air Temperature | Long-Term Deep Drainage Rates (mm/yr) | | |
|---|---|---|---|
| | Precipitation | | |
| | Low (50% of modern) | Modern | High (128% of modern) |
| Low (modern - 2.5°C) | < 0.1 | 7.5 | 27.0 |
| Modern | < 0.1 | 2.2 | 13.2 |
| High (modern + 2.8°C) | < 0.1 | 0.6 | 5.2 |

expect a decrease in drainage rates. If an ice age recurs, the decreasing air temperatures will lead to an increase in deep drainage rates. At the high precipitation level, drainage rates will increase for all temperature conditions. The magnitude of the increase will be more than four times greater for the high temperature versus the low temperature condition.

Table C.7 shows that the median annual drainage rate is much less than the average rate. The large difference is indicative of a non-normal distribution, where many years of drainage are punctuated by just a few years with very high rates. In all cases, the standard deviation was roughly one-half to one-third of the average rate. Figure C.6 shows the annual drainage rate for two of the cases in Table C.7. For the Rupert sand under the current climate, there was only one time in the entire 41-year period when significant drainage occurred.

Additional simulations were conducted to highlight sensitivities to three parameters: hydraulic properties, shrub LAI, and the fraction of bare ground. Two alternative sets of hydraulic properties for Rupert sand were derived from a field infiltration experiment at the ILAW Disposal Site. The alternative properties resulted in drainage rates of 2.7 and 3.3 mm/yr under shrub-steppe vegetation. These rates are not much different than 2.2 mm/yr predicted using the original properties for Rupert sand.

The second set of simulations compared different shrub LAI values selected to encompass the range of values measured at the ILAW Disposal Site in 1998 (Appendix F). For LAI values ranging from 0.1 to 0.25 (the original LAI value) to 0.4, the predicted drainage rates were 5.6, 2.2, and 1.6 mm/yr, respectively, for Rupert sand. These results show that recharge is sensitive to this plant parameter.

The third set of simulations assessed the impact of the fraction of bare ground. For cheatgrass, reducing the bare fraction from 0.577 to 0.0 reduced drainage from 33.2 to 26.6 mm/yr, which is still a high drainage rate. For the shrub-steppe, reducing the bare fraction from 0.69 to 0.0 reduced the drainage rate from 2.2 to < 0.1 mm/yr.

An alternative method for characterizing drainage rates for the heterogeneous shrub-steppe plant community is to weight the predicted drainage rates for the different conditions according to their areal

**Table C.7**. Statistical Summary of Annual Drainage Rates Beneath a Shrub-Steppe Plant Community Under Two Climate States ($n$ = 41)

| Scenario | Simulated Long-Term Drainage Rates (mm/yr) | | | | | | | | | |
|---|---|---|---|---|---|---|---|---|---|---|
| | Current Climate | | | | | Climate Extreme ($P - \bar{T}$) | | | | |
| | Min. | Mean | Median | Max. | SD[(a)] | Min. | Mean | Median | Max. | SD |
| Rupert Sand | 0.2 | 2.2 | 0.5 | 27.1 | 5.4 | 1.6 | 27.0 | 11.5 | 178.5 | 55.2 |
| Burbank Loamy Sand | 0.1 | 5.2 | 0.8 | 96.8 | 15.7 | 2.2 | 36.8 | 194.2 | 359.6 | 43.0 |
| Dune Sand on Cover | < 0.1 | < 0.1 | < 0.1 | < 0.1 | < 0.1 | < 0.1 | 16.9 | 0.1 | 142.4 | 33.1 |
| (a) SD = standard deviation | | | | | | | | | | |

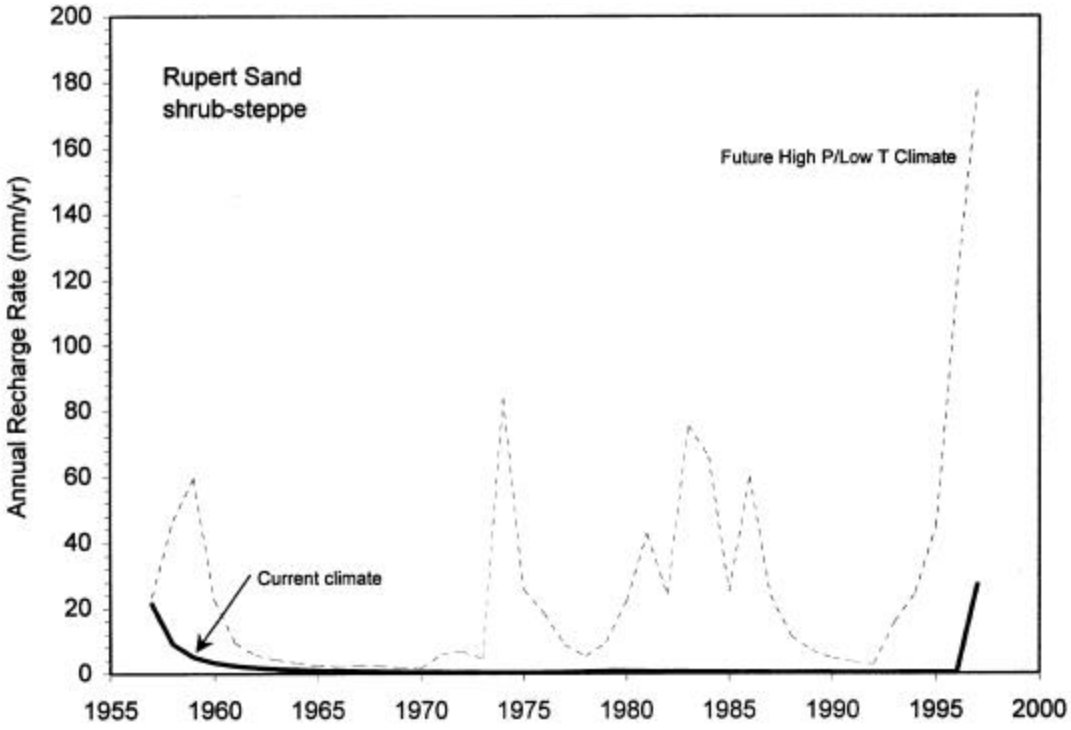


**Figure C.6**. Predicted Annual Recharge Rates for Rupert Sand, Shrub-Steppe Plant Community, and Two Climate States: Current and High Precipitation/Low Temperature

coverage. Based on FY 1998 data from the proposed ILAW Disposal Site, shrub coverage is 31%, grass coverage is 42.3%, and bare ground accounts for 26.7%. Assuming plant coverage is 100% within each zone, the lumped predicted recharge rate is (0.31*0.0 + 0.423*26.6 + 0.267*44.3 = ) 23.1 mm/yr. This value is biased high because the method assumes there are no plant roots penetrating adjacent bare areas, which we know not to be the case. Work is ongoing to document the lateral extent of these roots. It may be possible to adjust the effective area covered by the shrubs to provide a more realistic estimate of recharge for these types of plant communities.

## C.4 Conclusion

A set of simulations was used to estimate recharge rates for scenarios pertinent to the 2001 ILAW PA. The scenarios included the surface cover and two surrounding soil types, as well as two types of surface cover degradation. The simulations were conducted using a 41-year sequence of weather collected at the Hanford Site from 1957 to 1997. This sequence was repeated until the results remained unchanged to uncouple results from assumed initial conditions.

The low LAI value was tested for two other cases on Burbank loamy sand, lowering LAI sand on cover from 0.25 to 0.1 increased recharge from 5.2 to 15.2 mm/yr. On the surface cover with dune sand, lowering LAI increased recharge from <0.1 to 4.1 mm/yr.

The simulation results indicated that the surface cover limits drainage to < 0.1 mm/yr, which is much better than the design goal of 0.5 mm/yr. The cover maintained this performance level when plants were removed, when the climate became wetter and cooler, and when 20 cm of the silt loam layer was eroded. The cover also maintained this performance when windblown sand was deposited, but significant drainage (32.7 mm/yr) occurred when plants were removed. Under a wetter, cooler climate, the cover had 16.9 mm/yr of annual drainage even though shrub-steppe vegetation was present.

Drainage rates in the two surrounding soils were 2.2 to 5.2 mm/yr under shrub-steppe vegetation. Additional simulations highlighted model sensitivities to variations in climate, soil hydraulic properties, plant parameters, and irrigation.

## C.5 References


Bouwer H and RC Rice. 1983. "Effect of stones on hydraulic properties of vadose zones." In *Proceedings of the characterization and monitoring of the vadose (unsaturated) zone*. National Water Well Association, Worthington, Ohio.

Branson FA, RF Miller, and IS McQueen. 1976. "Moisture relationships in twelve northern desert shrub communities near Grand Junction, Colorado." *Ecology* 57:1104-1124.

Cline JF, DW Uresk, and WH Rickard. 1977. "Comparison of soil water used by a sagebrush-bunchgrass and a cheatgrass community." *J. Range Mgmt.* 30:199-201.

Connelly MP, JV Borghese, CD Delaney, BH Ford, JW Lindberg, and SJ Trent. 1992. *Hydrogeologic model for the 200 East groundwater aggregate area*. WHC-SD-EN-TI-019, Rev. 0., Westinghouse Hanford Company, Richland, Washington.

DOE. 1991. *Descriptions of codes and models to be used on risk assessment.* DOE/RL-91-44, U.S. Department of Energy, Richland, Washington.

Doorenbos J and WO Pruitt. 1977. *Guidelines for predicting crop water requirements*. FAO Irrigation Paper No. 24, Food and Agriculture Organization of the United Nations, Rome, Italy, pp. 1-107.

Fayer MJ and GW Gee. 1992. "Predicted drainage at a semiarid site: Sensitivity to hydraulic property description and vapor flow." In *Proceedings of the international workshop on indirect methods for estimating the hydraulic properties of unsaturated soils*, MTh van Genuchten, FJ Leij, and LJ Lund, eds., Riverside, California, October 11-13, 1989, University of California, Riverside.

Fayer MJ and GW Gee. 1997. "Hydrologic model tests for landfill covers using field data." In *Landfill capping in the semi-arid West: Problems, perspectives, and solutions*. TD Reynolds and RC Morris, eds. May 21-22, 1997, Jackson, Wyoming, ESRF-019, Env. Sci. Res. Foundation, Idaho Falls, Idaho.

Fayer MJ, GW Gee, ML Rockhold, MD Freshley, and TB Walters. 1996. "Estimating recharge rates for a groundwater model using a GIS." *J. Environ. Qual.* 25:510-518.

Fayer MJ and TL Jones. 1990. *UNSAT-H version 2.0: Unsaturated soil water and heat flow model.* PNL-6779, Pacific Northwest Laboratory, Richland, Washington.

Fayer MJ, ML Rockhold, and MD Campbell. 1992. "Hydrologic modeling of protective barriers: Comparison of field data and simulation results." *Soil Sci. Soc. Am. J.* 56:690-700.

Fayer MJ and TB Walters. 1995. *Estimated recharge rates at the Hanford Site*. PNL-10285, Pacific Northwest Laboratory, Richland, Washington.

Feddes RA, PS Kowalik, and H Zaradny. 1978. *Simulation of field water use and crop yield.* John Wiley & Sons, New York.

Fernandez OA and MM Caldwell. 1975. "Phenology and dynamics of root growth of three cool semi-desert shrubs under field conditions." *J. Ecol.* 63:703-714.

Hajek BF. 1966. *Soil survey, Hanford project in Benton County Washington*. BNWL-243, Pacific Northwest Laboratory, Richland, Washington.

Hanson JD, JW Skiles, and WJ Parton. 1987. "Plant component." In *SPUR: Simulation of production and utilization of rangelands*," JR Wight and JW Skiles, eds., U.S. Department of Agriculture, Agricultural Research Service, ARS 63, 372 p.

Hinds T. 1975. "Energy and carbon balances in cheatgrass: An essay in autecology." *Ecological Monographs*, 45:367-388.

Hoitink DJ, KW Burk, and JV Ramsdell. 1999. *Hanford Site climatological data summary 1998, with historical data*. PNNL-12087, Pacific Northwest National Laboratory, Richland, Washington.

James LG, JM Erpenbeck, DL Bassett, and JE Middleton. 1989. *Irrigation requirements for Washington – Estimates and methodology*. EB1513, Washington State University, Pullman, Washington.

Khire MV, CH Benson, and PJ Bosscher. 1997. "Water balance modeling of earthen final covers." *J. Geotech. Geoenviron. Engr.* 123(8):744-754.

Link SO, GW Gee, ME Thiede, and PA Beedlow. 1990a. "Response of a shrub-steppe ecosystem to fire: Soil water and vegetational change." *Arid Soil Research and Rehabilitation*, 4:163-172.

Link SO, GW Gee, and JL Downs. 1990b. "The effect of water stress on phenological and ecophysiological characteristics of cheatgrass and Sandberg's Bluegrass." *J. Range Mgmt.* 43:506-513.

LMHC. 1999. *Statements of work for FY 2000 to 2005 for the Hanford Low-Activity Tank Waste Performance Assessment Program.* HNF-SD-WM-PAP-062, Rev. 4, Lockheed Martin Hanford Company, Richland, Washington.

Magnuson SO. 1993. *A simulation study of moisture movement in proposed barriers for the Subsurface Disposal Area, INEL*. EGG-WM-10974, EG&G;Idaho, Idaho Falls, Idaho.

Mann FM. 1999. *Scenarios for the Hanford Immobilized Low-Activity Waste (ILAW) Performance Assessment.* HNF-EP-0828, Rev. 2, Fluor Daniel Northwest, Richland, Washington.

Martian P. 1994. *Calibration of HELP Version 2.0 and performance assessment of three infiltration barrier designs for Hanford Site remediation*. EGG-EES-11455, EG&G Idaho, Inc., Idaho Falls, Idaho.

Martian P and SO Magnuson. 1994. *A simulation study of infiltration into surficial sediments at the Subsurface Disposal Area, Idaho National Engineering Laboratory*." EGG-WM-11250, EG&G Idaho, Inc., Idaho Falls, Idaho.

Mayer DW, PA Beedlow, and LL Cadwell. 1981. *Moisture content analysis of covered uranium mill tailings*. PNL-4132, Pacific Northwest Laboratory, Richland, Washington.

Prych EA. 1998. *Using chloride and chlorine-36 as soil-water tracers to estimate deep-percolation at selected locations on the U.S. Department of Energy Hanford Site, Washington*. Open File Report 94-514, U.S. Geological Survey, Tacoma, Washington.

Rickard WH and BE Vaughan. 1988. "Plant community characteristics and responses." In *Shrub-steppe balance and change in a semi-arid terrestrial ecosystem.* WH Rickard et al., ed., Developments in Agricultural and Managed-Forest Ecology 20, Elsevier Science Publishers, New York.

Rockhold ML, MJ Fayer, and PR Heller. 1993. *Physical and hydraulic properties of sediments and engineered materials associated with grouted double-shell tank waste disposal at Hanford*. PNL-8813, Pacific Northwest Laboratory, Richland, Washington.

Sackschewsky MR, CJ Kemp, SO Link, and WJ Waugh. 1995. "Soil water balance changes in engineered soil surfaces." *J. Environ. Qual.* 24:352-359.

Skelly WA. 1994. *Material properties data and volume estimate of silt loam soil at the NRDWL Reserve, McGee Ranch*. WHC-SD-EN-TI-218, Westinghouse Hanford Company, Richland, Washington.

USDA. 1971. *Soil survey, Benton County Area, Washington*. U.S. Department of Agriculture, Washington, D.C. Issued July 1971.

Whitlock C and PJ Bartlein. 1997. "Vegetation and climate change in Northwest America during the past 125 kyr." *Nature* 388:57-61.

Wing NR, KL Petersen, C Whitlock, and RL Burk. 1995. *Long-term climate change effects task for the Hanford Site Permanent Isolation Barrier Development Program: Final Report*. BHI-00144, Bechtel Hanford Company, Richland, Washington.

# Appendix D

# Eolian Activity at the ILAW Disposal Site, Central Hanford Site

B. N. Bjornstad

# Appendix D

# Eolian Activity at the ILAW Disposal Site, Central Hanford Site

## D.1 Introduction

The U.S. Department of Energy is planning to vitrify the low-activity waste from single- and double-shell tanks. This immobilized low-activity waste (ILAW) will then be disposed in a near-surface burial facility at Hanford. Lockheed Martin Hanford Company is designing and assessing the performance of this disposal facility. An issue of concern is the possibility of sand dunes forming on or around the surface cover and affecting recharge rates. For example, active sand dunes at the Hanford Site lack vegetation, which could lead to an increase in the rate of natural recharge (Gee et al. 1992). An increase in natural recharge would increase water contact with the waste as well as transport through the vadose zone to the groundwater.

In 1995, three trenches were excavated at Hanford to collect samples for tracer analyses of recharge and to look for datable soil horizons to determine the approximate age of surface soil and sand dune formation. This appendix describes sand dune formation and age at the Hanford Site and reports the results of trench studies.

## D.2 Dunes at Hanford

The proposed ILAW Disposal Site is located in the south-central portion of the 200 East Area. Figure D.1 shows that the disposal site lies along the northern margin of a giant dune field that extends from the northeastern flank of Rattlesnake Mountain to the Columbia River (a distance of 27 km) and southward to the boundary of the city of Richland. The existence of the dune field in this area appears to be controlled by wind moving, from west to east, down the adjacent Dry Creek and Cold Creek valleys and across the central Hanford Site toward the Columbia River. Most dunes are stabilized by vegetation and are not actively growing or migrating, except locally within a narrow 3.2 to 4.8-km-wide area that extends westward from the natural wind gap created by Ringold/Koontz Coulee (Gaylord et al. 1991). The northern limit of dune formation lies in the southern portion of the 200 East Area and consists of stabilized dunes that occupy part of the proposed ILAW Disposal Site. Presently, the point of active sand dune formation that is closest to the proposed ILAW Disposal Site is ~3.2-km south of the 200 East Area (Figure D.1).

Although eolian features are generally not present elsewhere in the 200 East Area and the Hanford Site, there is still a significant amount of wind energy available. Apparently, in these areas the material available is too coarse grained making it unsuitable for transport and dune development; or the surface is

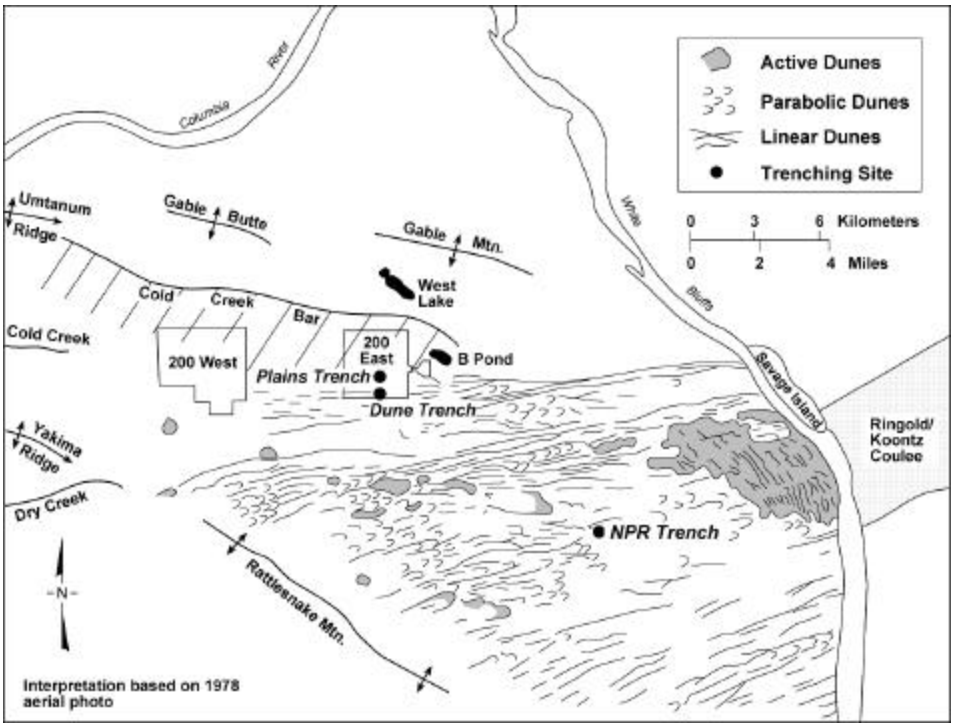


**Figure D.1**. Locations of the Sand Dune Features at the Hanford Site and the Trenching Studies Conducted in 1995

stable, which inhibits dune formation (Kasper and Glantz 1987). Dune formation and migration is complex and the result of the interaction between time, topography, climate, and man-related activities such as fire or construction.

### D.2.1 Dune Types/Wind Directions

Figure D.1 shows that the most predominant eolian bedforms (i.e., the shapes of wind-formed sediment deposits) on the Hanford Site are linear sand ridges aligned in the direction of the strongest winds (southwest to northeast). This is particularly true where dunes are stabilized by vegetation. In some cases, the same ridge can be traced for miles with little or no discontinuity. In other cases, ridges may divide in two or end at a parabolic dune in the downwind direction. Linear sand ridges are reported to form in variable wind regimes (Brookfield 1984). The predominant wind direction at Hanford is from the northwest (Glantz et al. 1990). The strongest winds blow out of the southwest, although less frequently than the northwest. Based on recent meteorological data, winds capable of moving sand-sized particles occur ~40 days/year at the Hanford Site (Gaylord and Stetler 1994).

Where dunes are active or dune blowouts occur, parabolic dunes are the predominant bedform. Parabolic dunes are convex in the downwind direction with arms that point in the upwind direction. From aerial photographs (the basis of Figure D.1), it appears that linear ridges result from the migration of the parabolic dunes. In these situations, the arms become anchored with vegetation while the central part of the dune continues to migrate forward. Linear ridges can also result from the interaction of winds coming

from two directions (i.e., northwest and southwest), but the evidence of linear dunes parallel to the predominant high-wind direction does not support this mechanism. In areas where dunes are extremely active and void of any vegetation, a wide range of bedforms has developed, including transverse, parabolic, and complex barchanoid bedforms. This is the case for the very active dune field that is present immediately west of Ringold/Koontz Coulees (Figure D.1).

### D.2.2 Volcanic Time Markers

At least three distinct volcanic ash layers may be associated with Quaternary age sediments at the Hanford Site. These provide key time markers from which to perform regional stratigraphic correlation. The layers of volcanic ash are recognized by their white color and gritty texture. The oldest Quaternary-age volcanic layer observed at the Hanford Site is the Mount St. Helens "set S" layer. This layer was dated at 13,000 years ago using a technique that relates time to the reference year 1950 (Mullineaux et al. 1978). All subsequent time estimates are relative to this reference year. This layer occurs as a couplet; the upper layer is about 2.5-cm thick while the lower layer is often barely visible and is about 0.16-cm thick. When observed, this ash layer lies near the top of the cataclysmic flood sequence and thus forms a lower stratigraphic marker for identifying eolian and other post-cataclysmic flood deposits at the Hanford Site. The second volcanic layer that may be observed also occurs as a couplet and is related to the two closely spaced eruptions from Glacier Peak around 11,200 years ago (Mehringer et al. 1984). Where found within the Pasco Basin, the combined thickness of the Glacier Peak ash couplet is about 8 cm. The third volcanic layer that may be observed is from an eruption 6,850 years ago of Mount Mazama commonly known as Crater Lake (Bacon 1983). Where preserved, Mount Mazama ash usually has a pink cast and may be 30- to 90-cm thick, especially where it has been eroded and redeposited. The latest Quaternary ash layer, from the May 18, 1980, eruption of Mount St. Helens, is preserved in the extreme northern portion of the Pasco Basin. It is not found in the southern part of the basin, including the proposed ILAW Disposal Site. We can obtain information to determine the time and rate of eolian deposition by observing the relationships between these volcanic layers and adjacent eolian deposits.

### D.2.3 Age of Sand Dunes at Hanford

Sand dunes found at the Hanford Site appear to be late Pleistocene to Holocene in age. The maximum age of the dunes is limited to 13,000 years ago, the age of the last cataclysmic flood from glacial Lake Missoula (Mullineaux et al. 1978). Petrologic and petrographic analyses demonstrate Hanford dune sands were derived primarily from reworking of Pleistocene Missoula flood deposits (Gaylord et al. 1991). While eolian activity occurred prior to this time, wind-related deposits were probably either buried beneath younger flood deposits or eroded away during subsequent flooding. Due to erosion and deposition that occurred during flooding, most of the area below 366-m elevation in the vicinity of the Hanford Site was probably void of vegetation immediately following the floods (Baker et al. 1991). Without the anchoring effects of vegetation, the bare ground would have produced abundant sedimentary material for eolian transport. For this reason, a significant amount of eolian transport may have occurred immediately following the floods, slowly tapering off over time as vegetation took hold. It is likely the sand dunes at the proposed ILAW Disposal Site formed soon after the last flood. Smith (1992) estimated that sand transport was most active prior to 4,400 years ago, at which time they had become mostly stabilized. On the other hand, Gaylord et al. (1991) reported that the dune sands they

examined appear to have developed since volcanic ash from Mount Mazama was deposited 6,850 years ago. Dunes are presently active in the central and eastern portions of the dune field (Figure D.1). It is not certain whether these areas have been continuously active since the late Pleistocene or whether they have been reactivated due to range fire or some other natural event.

## D.3 Trenching Results

Three trenches were excavated at the Hanford Site on September 28-29, 1995. Trenches as deep as 4.6 m were dug with a backhoe. The purpose of the trenches was to collect samples to determine moisture content and to estimate recharge via chlorine-isotope analysis. Another purpose of the trenches was to look for datable horizons in the soil column that could be used to determine the approximate age and rate of deposition. Samples were collected every 0.15 to 0.3 m from the surface to the bottom of the trench. Two trenches, referred to here as the Plains Trench and the Dune Trench were dug within the proposed ILAW Disposal Site. A third trench was dug about 13 km to the southeast, near the Wye Barricade. This site, which is referred to as the New Production Reactor (NPR) Trench (Figure D.1), was chosen to provide a contrast to the proposed ILAW Disposal Site trenches. It also lies within the zone of stabilized sand dunes. Descriptions of the three sites are presented in the following sections.

### D.3.1 Plains Trench

The Plains Trench was dug to a depth of ~4.3 m. The sediments within this trench consisted of essentially two stratigraphic units. The upper unit was composed of 1.2 m of a structureless, loose, light gray, silty sand. This unit, consisting of eolian material, contains reworked windblown sand deposited since the last cataclysmic flood less than 13,000 years ago. The lower unit consisted of a stratified coarse-grained, basaltic sand and gravel from 1.2 m to the bottom of the trench. This unit contains deposits known as the Hanford formation that were laid down during the last cataclysmic flood(s). No buried soil horizons were observed in this trench, suggesting the flood deposits are probably entirely late Wisconsin 13,000 to 18,000 years in age. There were no volcanic layers or other datable horizons observed in this trench. The absence of the thick Mazama ash layer indicates significant wind reworking of sediments as recently as 6,850 years ago.

### D.3.2 Dune Trench

The Dune Trench was excavated just south of the Plains Trench, on the north (leeward) side of a prominent east-west linear sand ridge (Figure D1). The trench was oriented north-south, perpendicular to the axis of the sand ridge (Figures D.2 and D.3). This aspect of the sand ridge was chosen for the trench because it was believed this is where volcanic layers or other marker horizons would most likely be preserved. The maximum depth of the trench was 4.0 m. The entire sequence exposed within the trench appeared to consist of eolian sand; no cataclysmic flood deposits of the Hanford formation were observed. The absence of flood deposits is not surprising because the 6.1- to 9.1-m-high sand ridge is an eolian feature that developed since the last flood. Thus, flood deposits probably lie at depths well below the bottom of the trench.

**Figure D.2**. Looking North from the Dune Trench Overlooking Old-Growth Sagebrush of the Proposed ILAW Disposal Site. The Plains Trench is located about 600 m north along the dirt road. Facilities in the distance are about 900 m north.

**Figure D.3**. Looking East from the Dune Trench Over Old-Growth Sagebrush and Parallel to the Axis of the Dune

Figure D.4 shows several contrasting layers within the eolian sequence. The upper 2.4 m consisted of a relatively uniform, structureless, loose, brown (10YR5/3) silty fine sand. Of this 2.4 m, the uppermost 0.6 m is slightly darker in color (Figure D.5) due to staining and weathering associated with surficial soil processes. From a soil development viewpoint, the upper 0.6 m would probably be classified as a weakly

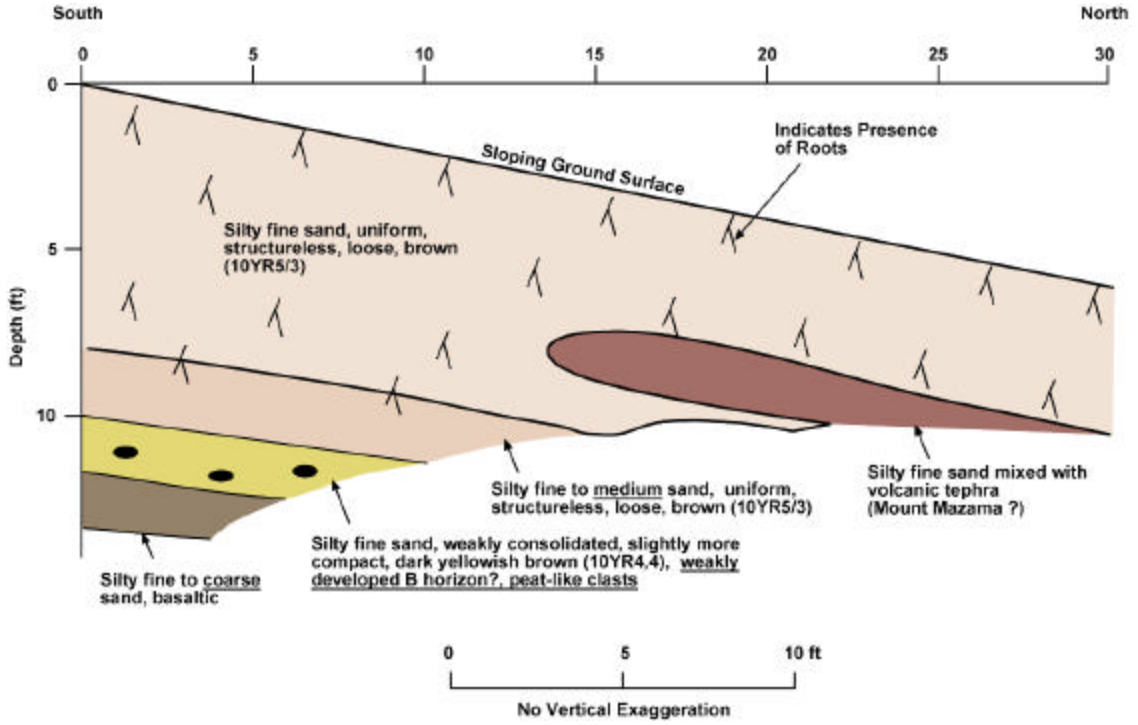


**Figure D.4**. Cross Section View of the Dune Trench Showing the Approximate Location of the Possible Tephra Layer

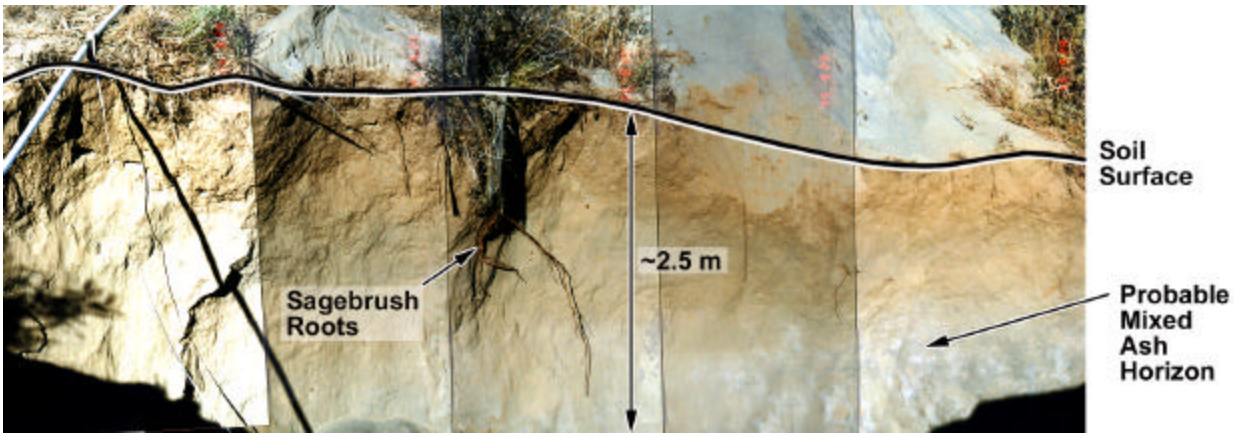


**Figure D.5**. Profile of the Dune Trench Showing the Lighter Colored Horizon Suspected of Containing Reworked Ash from the Mt. Mazama Eruption that Occurred 6,700 Years Ago

developed A or B horizon. Modern roots appeared to penetrate to a depth of about 2.4 m. Between 2.4 and 3.0 m is a slightly coarser layer of silty fine to medium-grained sand (Figure D.4). Underlying this layer was 0.45 m of weakly consolidated, slightly more compact, dark yellowish brown (10YR4/4) silty fine sand. This layer of finer-grained material may represent possibly a weak B paleosol horizon. Several peat-like clasts, consisting of a dense, partially decomposed mat of root hairs were collected for carbon-14 dating from this layer. At the very bottom of the excavated trench was a coarser textured layer of fine to coarse sand. Mineral grains in the coarse sand fraction were composed of about 50% basalt.

After attaining the maximum depth (~4 m) the equipment would allow, the backhoe was relocated downhill to extend the length of the trench to about 9.1 m. Soon after moving the backhoe downhill the trench caved, and it was no longer possible to keep the trench open to more than 2.4 to 3.0 m deep. About 4.6 m from the beginning of the trench and around a depth of ~1.2 to 1.5 m, there was a lighter colored layer 0.3 m or more thick, that appeared to be soil mixed with what appeared to be light-colored volcanic ash (Figure D.4). The ash is probably from Mount Mazama. This implies that the upper 1.2 to 1.5 m must be ≤ 6,850 years old and that at least 3.0 m of eolian sediments were deposited between 6,850 and 13,000 years ago.

### D.3.3 NPR Trench

The NPR Trench was excavated to a depth of 4.4-m (Figure D.6). The stratigraphy was similar to that observed at the Plains Trench, which consisted of a thin layer of eolian sand over flood deposits. Overall, the exposed sedimentary sequence became finer grained nearer the surface. The eolian material at the surface was limited to about 0.15 m of pale brown, structureless, silty fine sand (Figure D.7). Immediately below this was another 0.15 m of silty medium to coarse basaltic sand, which represents the top of the cataclysmic flood deposits (Hanford formation). This layer of sand was moderately cemented with calcium carbonate (i.e., near-surface calcic-soil development) and displayed well-developed cross bedding to the east. This is consistent with the west-to-east paleocurrent direction associated with cataclysmic floods in this area. From the 0.3- to 1.5-m depth was a layer of gravelly medium-to-coarse basaltic sand that displayed low angle cross bedding. From 1.5 m to the bottom of the trench, the sediments consisted of a poorly sorted, gravelly coarse sand to sandy gravel typical of the Hanford formation. There were no volcanic layers or other datable horizons observed in this trench. The absence of the thick Mazama ash layer indicates significant wind reworking of sediments as recently as 6,850 years ago.

## D.4 Conclusion

The existence of eolian sand dunes at the proposed ILAW Disposal Site demonstrates the potential for sand dune development, at least under the conditions of the early-to-middle Holocene period. Lack of a Mount Mazama ash layer in the Plains Trench and NPR Trench suggests significant wind reworking of sediments at these sites as recently as 6,850 years ago. A mixed ash/sediment layer in the Dune Trench suggests that 1.2 to 1.5 m of eolian sand has been deposited there in the last 6,850 years. Deposition rates like this will have to be considered when interpreting hydrologic and tracer data from these sites. Modern

**Figure D.6**. View to the North of the NPR Trench. The vegetation is primarily big sagebrush, Sandberg's bluegrass, and cheatgrass. The nearest shrub in the photograph is about 10 m from the trench.

land use patterns may preclude any major sand dune formation or movement in the near future. However, the potential for some sand deposition still exists and its impact on facility performance needs to be considered.

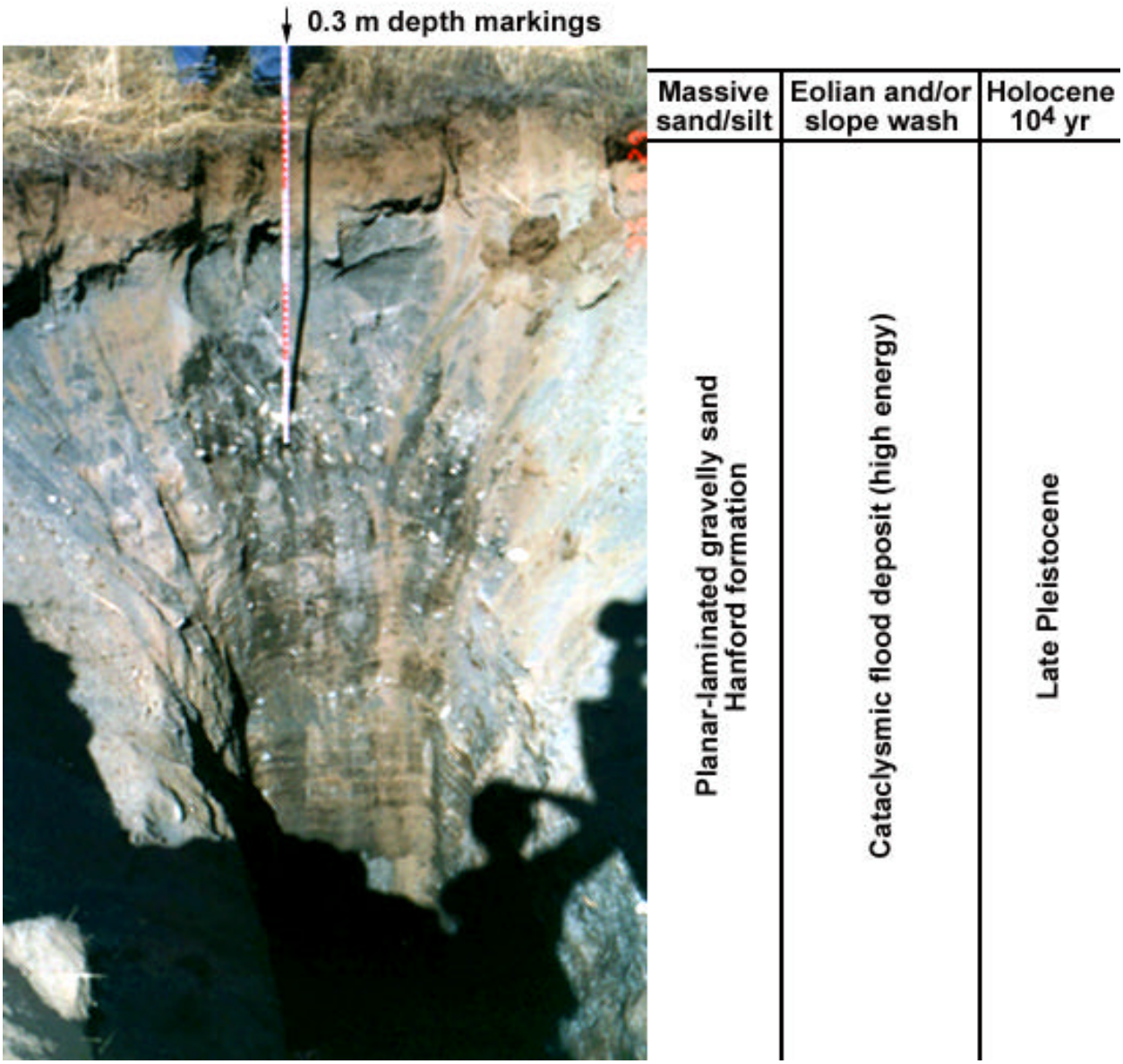


**Figure D.7**. Profile of the NPR Trench Showing the Thin Surface Veneer of Eolian Material on Top of the Coarser Flood Deposits of the Hanford Formation. The base of the trench (at 4.4 m) is in shadow.

## D.5 References


Bacon CR 1983. "Eruptive history of Mount Mazama and Crater Lake Caldera, Cascade Range, U.S.A." In *Arc Volcanism: Journal of Volcanology and Geothermal Research*, S Aramaki and I Kushiro, eds. 18(1-4):57-115.

Baker VR, BN Bjornstad, AJ Busacca, KR Fecht, EP Kiver, UL Moody, JG Rigby, DF Stradling, and AM Tallman. 1991. "Quaternary geology of the Columbia Plateau." In *Quaternary Nonglacial Geology; Conterminous U.S.* RB Morrison, ed., The Geology of North America, v. K-2. Geological Society of America, Boulder, Colorado.

Brookfield ME 1984. "Eolian sands." In *Facies Models*, RG Walker, ed., Reprint Series 1, pp. 91-104. Geosciences Canada, Toronto, Ontario, Canada.

Gaylord DR and LD Stetler. 1994. "Aeolian-climatic thresholds and sand dunes at the Hanford Site, south-central Washington, U.S.A." *Journal of Arid Environments* 28:95-116.

Gaylord DR, LD Stetler, GD Smith, and JC Chatters. 1991. *Holocene and recent eolian activity at the Hanford Site*. Abstract Volume with Meeting Program, p 15. 38th Pacific Northwest Regional Meeting, American Geophysical Union, Richland, Washington.

Gee GW, MJ Fayer, ML Rockhold, and MD Campbell. 1992. "Variations in recharge at the Hanford Site." *Northwest Science* 66:237-250.

Glantz CS, MN Schwartz, KW Burk, RB Kasper, MW Ligotke, and PJ Perrault. 1990. *Climatological summary of wind and temperature data for the Hanford Meteorology Monitoring Network.* PNL-7471, Pacific Northwest Laboratory, Richland, Washington.

Kasper RB and CS Glantz. 1987. *Preliminary estimate of potential sand transport and surface wind patterns at the U.S. Department of Energy's Hanford Site*. WHC-EP-0058, Westinghouse Hanford Company, Richland, Washington.

Mehringer PJ Jr, JC Sheppard, and FF Franklin Jr. 1984. "The age of Glacier Peak tephra in west-central Montana." *Quaternary Research* 21:36-41.

Mullineaux DR, RE Wilcox, WF Ebaugh, R Fryxell, and R Rubin. 1978. "Age of the last major scabland flood of the Columbia Plateau in eastern Washington." *Quaternary Research* 10:171-180.

Smith GD 1992. *Sedimentology, stratigraphy, and geoarchaeology of the Tsulim Site, on the Hanford Site, Washington*. M.S. Thesis, Washington State University, Pullman, Washington.

# Appendix E

# Evaluation of Anthropogenic Chloride Deposition at the ILAW Disposal Site

C. W. Lindenmeier, R. J. Serne, M. J. Fayer, and R. E. Clayton

# Appendix E

# Evaluation of Anthropogenic Chloride Deposition at the ILAW Disposal Site

## E.1 Introduction

As part of the performance assessment under way to evaluate the suitability of the unsaturated zone of the Hanford Site for Immobilized Low-Activity Waste (ILAW), Pacific Northwest National Laboratory (PNNL) conducted a preliminary site investigation to determine if human activities in years past may influence data used for the determination of recharge rates. Because the natural recharge rate is a key parameter needed to perform calculations of the transport of water and contaminants through the vadose zone and into the groundwater, several methods are currently being employed to estimate the long-term recharge rate. One method under consideration is the chloride mass balance (CMB) method described by Murphy et al. (1991, 1996). This method uses chloride as an environmental tracer to estimate natural recharge rates. However, one concern about using this method is the potential for excess chloride deposition in the region of investigation due to anthropogenic activity. Excess chloride that is not accounted for in the calculations would change the mass balance ratios and subsequently bias the calculated recharge rate lower than the actual value.

The proposed ILAW Disposal Site is located in the 200 East Area (Figure E.1) just southeast of the 284-E Power House and Steam Plant (Figure 7.1). The site contains a relatively undisturbed old growth sagebrush area and has two predominant sediment types: Burbank loamy sand, and Rupert sand (Hajek 1966). Because this site is near a formerly active coal-fired power plant, we focused on examining the assumption that this power plant could have been a potential source of chloride deposition. This assumption is supported by the premise that the predominant form of chlorine released during the combustion of coal is an HCl aerosol that would have high affinity for particulates released in the stack of the plant. Additionally, we expected that deposits from stack emissions would correlate with prevailing wind patterns, readily determined from meteorological data. Wind data collected from the 60-m tower in the 200 Area between 1986 and 1998 (Hoitink et al. 1999) suggest that the proposed ILAW Disposal Site is downwind of the power plant.

## E.2 Objective

The objective of this task was to develop and implement a quick and inexpensive chemical screening technique that would be sufficient to indicate whether or not emissions from the 284-E coal-fired power plant may have contributed excess chloride into the sediments at the proposed ILAW Disposal Site. The

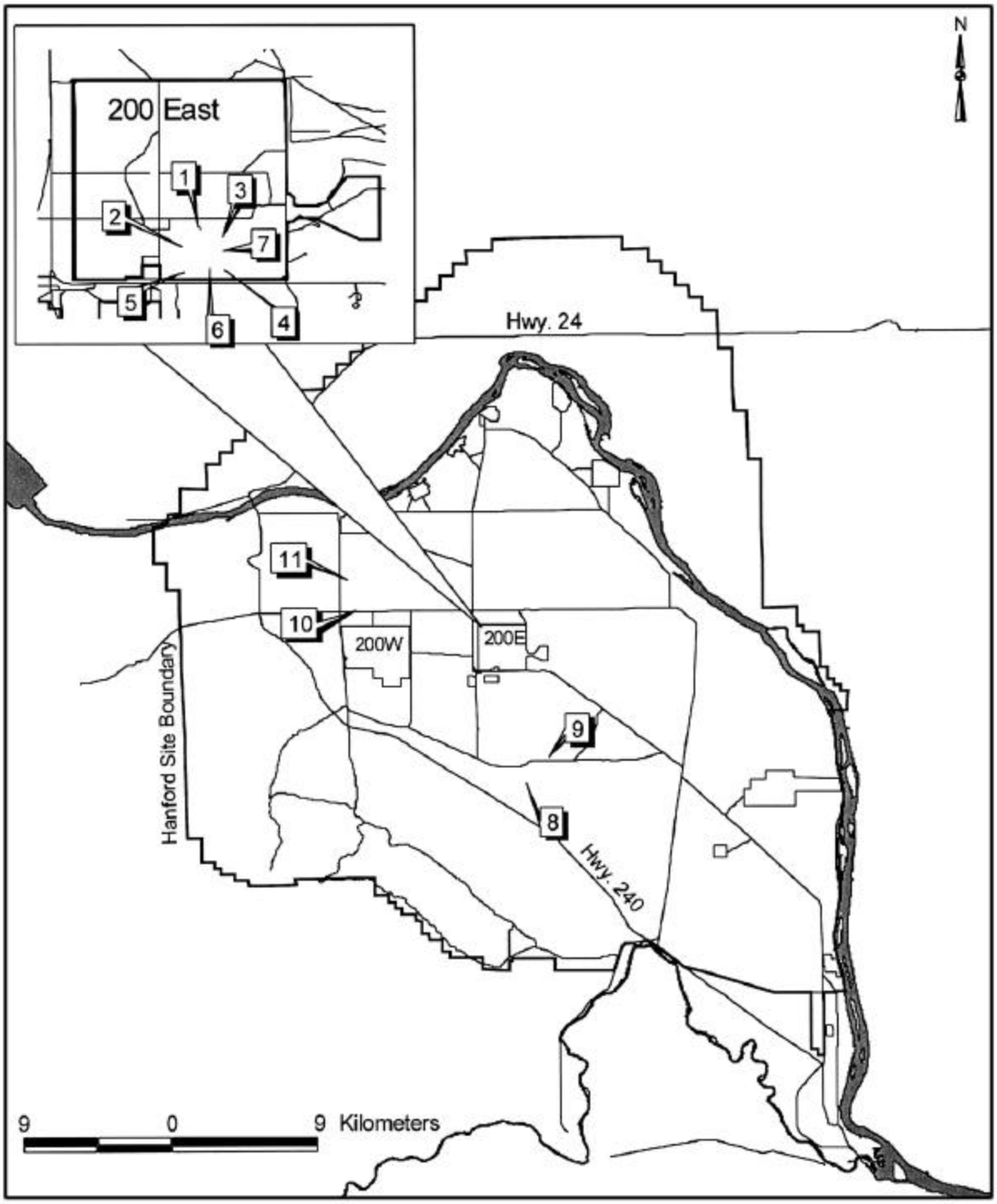


**Figure E.1**. Sampling Location Map

coal power plants at the Hanford Site began operation in 1945 and did not use emission control devices until 1980 (Fayer et al. 1996).[(a)] Coal power plants without emission controls are known to emit large quantities of nitrous oxides, sulfur oxides, and particulates, as well as a suite of trace metals such as arsenic, cadmium, chromium, or manganese. First we sought to determine if a chemical "fingerprint" could be identified from analyses of coal and fly ash materials found near the proposed ILAW Disposal Site. This fingerprint would be used to compare surface and below surface sediment samples removed from the proposed ILAW Disposal Site along with representative background sediment samples collected at various locations on the Hanford Site. X-ray fluorescence analysis of surface sediments was used to determine metal and trace metals. Ion chromatography (IC) analysis was used to determine major anions in water from leached sediments.

## E.3 Methods

As shown in Table E.1, sample cores were collected from

- the top of the coal ash pile (Station 1)
- the remaining coal pile (Station 12)
- locations southwest of the proposed ILAW Disposal Site (Stations 8 and 9)
- locations northwest of the proposed ILAW Disposal Site (Stations 10 and 11)
- locations within the proposed ILAW Disposal Site boundaries (Stations 2, 3, 4, 5, 6, and 7).

Our rationale for sampling at these stations was based on the need to collect screening data that would be fairly representative of the entire site. Thus core samples were collected from the four corners of the proposed ILAW Disposal Site, a sample from a large sand dune laying along a southern, east-west transect, and two internal locations that were selected in part because they were accessible with the sampling truck. Additionally, for Stations 3 and 7, sample cores were removed from two separate locations—one an area clear of sagebrush, and the other under the canopy of living sagebrush. Dual sampling at Stations 3 and 7 was done to determine if different vegetation conditions might create significant variability and thus be a factor to consider when assessing the data. Background sampling stations were selected by a combination of visual examination, using sediment charts (Fayer and Walters 1995) that identified similar sediments associated with the proposed ILAW Disposal Site, and using a minimum distance of 5 km from the proposed ILAW Disposal Site. The 5-km distance was selected by using a calculated deposition rate for chloride as a function of distance as reported by Fayer et al. (1996).[(a)] Based on their simple model, at 3.4 km from the point source, deposition rates for chloride would essentially equal the natural rates. A 5-km point source distance minimum was thought to be both conservative and practical for selecting representative background sediments.

For most of the sampling, 5.08-cm-diameter cores were collected to an average depth of 152 cm using aluminum pipe (Type 6061-T6 with 5.08 cm OD x 0.12 cm wall) and a motorized impact driver (Bosch Rotary Hammer). The coring was accomplished by driving one segment of pipe to a depth of 76.2 cm to

(a) Fayer MJ, JL Downs, BN Bjornstad, and K Mahan. 1996. *Integrated recharge assessment: summary of FY 1995 activities*. Letter report to Fred Mann, Fluor Daniel Northwest, Richland, Washington.

**Table E.1**. ILAW Sampling Locations

| | Station | Description | Sampling Location | Sample No. | Depth Sampled | |
|---|---|---|---|---|---|---|
| | | | | | in. | cm |
| Coal Ash Pile | 1 | Ash pile located east of the 200 East coal power plant | Top of the ash pile | Surface | 24 | 61 |
| ILAW Disposal Site | 2 | NW Corner | Bare spot within dense shrub-steppe | 02-1 | 0-35 | 0-89 |
| | | | | 02-2 | 36-47 | 91-119 |
| | 3 | NE Corner | Bare spot with cheatgrass, within shrub-steppe | 03-1a | 0-34 | 0-86 |
| | | | | 03-2a | 34-52 | 86-132 |
| | | | | 03-3a | 52-56 | 132-142 |
| | | | Next to sagebrush | 03-1b | 0-40 | 0-102 |
| | | | | 03-2b | 40-60 | 102-152 |
| | 4 | SE Corner, on side of sand dune | Cheatgrass with scattered shrubs | 04-1a | 0-39 | 0-100 |
| | | | | 04-2a | 39-66 | 100-168 |
| | 5 | SW Corner, about 50 m northeast of FY 98 ILAW borehole | Cheatgrass with scattered shrubs; hit rock at 1 m | 05-1x | 0-33 | 0-84 |
| | | | Cheatgrass with scattered shrubs, about 1 m from above location | 05-1a | 0-34.5 | 0-88 |
| | | | | 05-2a | 34.5-67 | 88-170 |
| | 6 | SE Corner, on top of sand dune | Cheatgrass with scattered shrubs | 06-1a | 0-37 | 0-102 |
| | | | | 06-2a | 37-70 | 0-94 |
| | 7 | SE Middle | Mostly bare, with scattered shrubs | 07-1a | 0-40 | 0-102 |
| | | | | 07-2a | 40-67 | 102-170 |
| | | | Next to sagebrush | 07-1b | 0-38 | 0-97 |
| | | | | 07-2b | 38-60 | 97-152 |
| Rupert Sand Background | 8 | Near Well A5069, about 9 km west of the Wye barricade | Cheatgrass with no shrubs (a 1984 fire may have removed shrubs) | 08-1a | 0-29 | 0-74 |
| | | | | 08-2a | 29-47 | 74-119 |
| | | | | 08-3a | 42-54 | 107-137 |
| | 9 | Just off Army Loop Road, about 8 km west of the Wye barricade | Cheatgrass with no shrubs (a 1984 fire may have removed shrubs) | 09-1a | 0-35 | 0-89 |
| | | | | 09-2a | 35-52 | 89-132 |
| | | | | 09-3a | 52-61 | 132-155 |

**Table E.1**. (contd)

| | Station | Description | Sampling Location | Sample No. | Depth Sampled | |
|---|---|---|---|---|---|---|
| | | | | | in. | cm |
| Burbank Loamy Sand Background | 10 | Northwest of 200 West Area | Shrub-steppe, surface sample because of rocks | 10-1a | 0-16 | 0-41 |
| | 11 | Northwest of 200 West Area | Rocky soil, very few shrubs, surface sample | 11-1a | 0-10 | 0-25 |
| | | | Rocky soil, very few shrubs, surface sample, about 5 m from above location | 11-1b | 0-10 | 0-25 |
| Coal Pile | 12 | Coal pile south of 200 East coal power plant, between the end of the rail spur and the power plant building | Grab sample | | | |

91.4 cm. A second segment was driven down as far as possible usually resulting in a recovery of approximately 50.8 additional cm. The second core was partially hand dug out of the ground to facilitate removal. In one case at Station 3, a third segment of pipe was used allowing for the recovery of an additional 10.2 cm. After reaching the desired depth, the tubes were extracted by hand or with pipe wrenches. Excess tube length was removed and the cores were labeled and taped for transport to the lab. This method helped minimize material loss from the end of the pipe and reduced core shrinkage due to compaction. Depth measurements were taken from the hole and compared to the actual core material collected in each pipe segment. We noted an average of 5.08 to 10.2 cm shrinkage in both segments inside the pipes compared to the open hole. Following the completion of core removal, a flagged fence post was placed at the location. One exception to our collection protocol occurred when we attempted to collect the background samples for the Burbank sediment. We were successful only in obtaining shorter cores—a 25.4-cm depth in one case and 40.6-cm depth in the other.

Samples were identified using the station number as the first number followed by a dash; a second number representing the core number followed by a lowercase letter identifying the hole at a specific station. Thus a sample such as 3-3a represents Station 3, the third core removed at hole 'a.' Sub-samples sent for analyses followed this notation with the addition of a depth value. The cores were then transported to PNNL's Sigma 5 Building and placed in cold storage for sub-sampling at a later time. Actual sampling locations were recorded using a Trimble Geoexplorer2 Geographical Positioning System (GPS) unit. The GPS locations collected from each station were downloaded to a computer and corrected by differential correction for real-time data. The locations were then mapped on a Hanford Site map (Figure E.1).

The screening method selected to determine total chemical composition and chlorine extraction measurements (x-ray fluorescence analysis and water leach followed by chlorine analysis by ion chromatograph) involved separating the core into 25-g aliquots beginning at the surface and continuing until we reached the 10-cm depth. Each 25-g portion was sealed in a 30-mL glass bottle; a 10-g portion was then removed from each of the first surface samples and the last samples near 10-cm depth. These

10-g portions were stored in other 30-mL glass bottles and delivered to Ron Sanders (KLM Analytical) for x-ray fluorescence analysis.

Preliminary IC and pH analyses were performed using a 2:1 ratio water to sediment extract (Methods of Soil Analysis. Part 2; 62-1.3.2.2) with the remaining 15 g of sediment from the sample taken at the 10-cm depth, and 15 g of sediment taken from the bottom of the last core removed from a given sampling site (ranging from 119 to 178 cm deep). Each 15-g sediment sample intended for IC and pH analyses was then combined with 30-mL of deionized water in a 50-mL Nalgene centrifuge tube and gently agitated for 24 hours, centrifuged at 2500 rpm for 20 minutes, decanted into a syringe, and passed through a 0.2 µm membrane filter into a 30-mL glass bottle. The filtrate was then submitted for IC and pH analyses. In addition, a 10-g sample from the 11- to 12-cm depth was carefully weighed and placed in an oven at 105°C for 24 hours to determine moisture content.

## E.4 Results and Discussion

Table E.2 shows the moisture content and 2:1 extract pH data of all sub-sampled depths for each core. Anion data from IC analysis are shown in Table E.3, and metals data from x-ray fluorescence analysis are shown in Tables E.4, E.5, and E.6.

Our preliminary assessment of the data does not offer a conclusive answer to the question of whether or not chloride data obtained from the proposed ILAW Disposal Site and used in recharge calculations may be compromised by operation of the 284-E power plant. It was our hope that by using trace metal analysis from the coal-ash and coal materials, a clear fingerprint could be identified. This fingerprint could then be readily compared to sediments within the proposed ILAW Disposal Site and sediments used for background comparison. This does not appear to be the case when reviewing the x-ray fluorescence data. The x-ray fluorescence analyses were performed only on near-surface samples because we expected the trace metals to be sorbed near the surface. However, if emission controls began in 1980, then the majority of deposition likely occurred prior to 1980. In the 20 years since then, precipitation could have leached trace metal deeper in the soil. Therefore, x-ray fluorescence analyses of deeper samples are warranted.

The ion chromatograph sulfate data, however, suggest that atmospheric deposition resulting from power plant emissions may have occurred. Specifically, sample 3-3a at the 142-cm depth shows a sulfate concentration of 182 ppm, sample 3-2b at the depth of 120 cm shows a sulfate concentration of 144 ppm, sample 6-2a shows a sulfate concentration of 35 ppm, sample 7-2a at the depth of 170 cm shows a concentration of 11 ppm, and sample 7-2b at the depth of 152 cm shows a concentration of 38.6 ppm. Sulfate concentrations at each of these sites are at least 3 times greater, and in one case, as much as 46 times greater than the highest background sulfate value from a comparable depth. These high sulfate values are at depths far below x-ray fluorescence analyses. If the high sulfate values represent deposition of coal emissions, then trace metals (if present and relatively weakly adsorbing) are likely much deeper than the 10-cm samples analyzed during this task.

In reviewing Environmental Protection Agency (EPA) data associated with sulfur dioxide emissions from coal-fired plants (EPA 1998), it could be assumed that the sulfur dioxide emitted over the life of the

**Table E.2**. Sample Site Depths, Moisture Content, and pH

| Station No. | ILAW-1B Description | Core Samples Label | Depths in. | Depths cm | $H_2O$ % (grav) Sample Bottom | $H_2O$ % (grav) Sample ~10 cm depth | pH Sample Bottom | pH Sample ~10 cm depth |
|---|---|---|---|---|---|---|---|---|
| 1 | Coal Ash Pile | | 24 | 61 | 18 | 8.0 | 5.9 | 7.9 |
| 2 | NW Corner | 02-1<br>02-2 | 0-35<br>36-47 | 0-89<br>91-119 | 3 | 7.0 | 8.7 | 8.3 |
| 3 | NE Corner | 03-1a<br>03-2a<br>03-3a | 0-34<br>34-52<br>52-56 | 0-86<br>86-132<br>132-142 | 3 | 6.2 | 9.0 | 7.9 |
| | NE Corner Sage Brush | 03-1b<br>03-2b | 0-40<br>40-60 | 0-102<br>102-152 | 3 | 5.4 | 9.1 | 7.5 |
| 4 | SE Corner | 04-1a<br>04-2a | 0-39<br>39-66 | 0-99<br>99-168 | 3 | 9.2 | 8.4 | 8.0 |
| 5 | SW Corner (rock) | 05-1x | 0-33 | 0-84 | | | | |
| | SW Corner | 05-1a<br>05-2a | 0-34.5<br>34.5-67 | 0-88<br>88-170 | 3 | 6.3 | 8.8 | 7.5 |
| 6 | SE Corner bluff area | 06-1a<br>06-2a | 0-37<br>37-70 | 0-94<br>94-178 | 3 | 6.4 | 9.0 | 7.8 |
| 7 | SE Middle | 07-1a<br>07-2a | 0-40<br>40-67 | 0-102<br>102-170 | 4 | 5.7 | 9.4 | 8.3 |
| | SE Middle sage brush | 07-1b<br>07-2b | 0-38<br>38-60 | 0-97<br>97-152 | 5 | 5.8 | 8.8 | 7.8 |
| 8 | Rattlesnake Well A5069 | 08-1a<br>08-2a<br>08-3a | 0-29<br>29-47<br>42-54 | 0-74<br>74-119<br>107-137 | 1 | 4.6 | 8.4 | 8.2 |
| 9 | Near Ecology | 09-1a<br>09-2a<br>09-3a | 0-35<br>35-52<br>52-61 | 0-89<br>89-132<br>132-155 | 6 | 8.2 | 8.7 | 7.4 |
| 10 | 200W (mile marker 12) | 10-1a | 0-16 | 0-41 | 9 | 5.5 | 7.9 | 7.6 |
| 11 | 200W (surface) | 11-1a<br>11-1b | 0-10<br>0-10 | 0-25<br>0-25 | 9<br>10 | 8.2<br>8.1 | 8.0<br>7.8 | 8.2<br>8.1 |
| 12 | Coal Grab Sample | | | | | | 7.3 | |

plant may be related to elevated levels of sulfate within the proposed ILAW Disposal Site. It is also possible that chloride deposition would coincide with sulfur dioxide deposition from stack emissions.

**Table E.3**. IC Analysis

Dionex AI450 Chromatographic System Analysis Results
(all results in ppm unless otherwise stated)

| Ion | D.L.* | 1-1a 11-cm | 1-1a 61-cm | 2-1a 11-cm | 2-2a 119-cm | 3-1a 11-cm | 3-3a 142-cm | 3-1b 11-cm | 3-2b 152-cm | 4-1a 11-cm | 4-2a 167-cm |
|---|---|---|---|---|---|---|---|---|---|---|---|
| **Fluoride** | **0.05** | 1.19 | <0.05 | 0.37 | 0.76 | 0.26 | 0.91 | 0.35 | 0.72 | 0.13 | 0.48 |
| **Chloride** | **0.05** | 2.89 | 15.3 | 0.32 | 0.63 | 0.81 | 76.2 | 5.86 | 111 | 0.39 | 0.74 |
| **Nitrite** | **0.04** | 0.05 | <0.04 | <0.04 | <0.04 | 0.09 | <0.04 | 0.38 | <0.04 | 0.06 | <0.04 |
| **Bromide** | **0.04** | 0.07 | <0.04 | <0.04 | <0.04 | <0.04 | 0.28 | <0.04 | 0.44 | <0.04 | <0.04 |
| **Nitrate** | **0.06** | 43.5 | 1390 | 6.41 | 1.03 | 2.95 | 0.66 | 16.24 | 0.44 | 3.06 | 0.82 |
| **Phosphate** | **0.20** | 0.51 | <0.2 | 4.09 | <0.2 | 3.72 | <0.2 | 2.33 | 0.63 | 3.24 | <0.2 |
| **Sulfate** | **0.20** | 391 | 969 | 1.74 | 1.84 | 2.00 | 182 | 7.36 | 144 | 0.85 | 12.3 |
| **Oxalate** | **0.20** | <0.2 | <0.2 | <0.2 | <0.2 | <0.2 | 0.28 | <0.2 | <0.2 | <0.2 | <0.2 |

| Ion | D.L.* | 5-1a 11-cm | 5-2a 170-cm | 6-1a 11-cm | 6-2a 177-cm | 7-1a 11-cm | 7-2a 170-cm | 7-1b 11-cm | 7-2b 152-cm | 8-1a 11-cm | 8-3a 137-cm |
|---|---|---|---|---|---|---|---|---|---|---|---|
| **Fluoride** | **0.05** | 0.13 | 0.32 | 0.14 | 0.56 | 0.21 | 2.32 | 0.09 | 2.58 | 0.13 | 0.26 |
| **Chloride** | **0.05** | 0.21 | 0.27 | 0.30 | 0.79 | 0.27 | 1.16 | 0.23 | 12.08 | 0.37 | 0.26 |
| **Nitrite** | **0.04** | <0.04 | <0.04 | <0.04 | <0.04 | <0.04 | <0.04 | <0.04 | <0.04 | <0.04 | <0.04 |
| **Bromide** | **0.04** | <0.04 | <0.04 | <0.04 | <0.04 | <0.04 | <0.04 | <0.04 | <0.04 | <0.04 | <0.04 |
| **Nitrate** | **0.06** | 1.28 | 0.24 | 2.80 | <0.06 | 0.60 | 0.17 | 1.42 | 1.22 | 1.35 | 0.34 |
| **Phosphate** | **0.20** | 2.89 | <0.2 | 2.24 | <0.2 | 1.09 | 0.92 | 1.80 | <0.2 | 1.22 | <0.2 |
| **Sulfate** | **0.20** | 0.61 | 0.80 | 0.78 | 35.1 | 0.64 | 11.00 | 0.77 | 38.6 | 0.86 | 3.25 |
| **Oxalate** | **0.20** | <0.2 | <0.2 | <0.2 | <0.2 | <0.2 | <0.2 | <0.2 | 0.36 | <0.2 | <0.2 |

| Ion | D.L.* | 9-1a 11-cm | 9-3a 155-cm | 10-1a 11-cm | 10-1a 41-cm | 11-1a 11-cm | 11-1a 25-cm | 11-1b 11-cm | 11-1b 25-cm | 12-1a NA | |
|---|---|---|---|---|---|---|---|---|---|---|---|
| **Fluoride** | **0.05** | 0.19 | 1.24 | 0.12 | 0.19 | 0.18 | 0.22 | 0.38 | 0.21 | 0.38 | |
| **Chloride** | **0.05** | 1.05 | 0.42 | 0.36 | 0.53 | 0.16 | 0.36 | 0.52 | 0.31 | 1.88 | |
| **Nitrite** | **0.04** | 0.14 | <0.04 | <0.04 | <0.04 | <0.04 | <0.04 | <0.04 | <0.04 | <0.04 | |
| **Bromide** | **0.04** | <0.04 | <0.04 | <0.04 | <0.04 | <0.04 | <0.04 | <0.04 | <0.04 | <0.04 | |
| **Nitrate** | **0.06** | 13.3 | 0.40 | 2.15 | 2.31 | 1.95 | 2.61 | 2.86 | 1.57 | 1.86 | |
| **Phosphate** | **0.20** | 3.67 | <0.2 | 1.07 | 0.41 | 4.00 | 1.57 | 3.55 | 1.50 | <0.2 | |
| **Sulfate** | **0.20** | 11.0 | 3.94 | 1.18 | 1.76 | 0.77 | 1.51 | 1.36 | 0.92 | 111 | |
| **Oxalate** | **0.20** | <0.2 | <0.2 | <0.2 | <0.2 | <0.2 | <0.2 | <0.2 | <0.2 | <0.2 | |

NOTE: Sample numbers contain the station number (i.e., "12" in sample number 12-1a)
< = below detection limit

**Table E.4**. X-ray Fluorescence Analysis of Stations 1 through 4

| | | Sample Number | | | | | | | | | |
|---|---|---|---|---|---|---|---|---|---|---|---|
| | | 1-1a | 1-1a | 2-1a | 2-1a | 3-1a | 3-1a | 3-1b | 3-1b | 4-1a | 4-1a |
| Units | Element | 0-1 (cm) | 9-10 (cm) | 0-1 (cm) | 9-10 (cm) | 0-1 (cm) | 9-10 (cm) | 0-1 (cm) | 9-10 (cm) | 0-1 (cm) | 9-10 (cm) |
| % | AL | 8.38 | 11.03 | 7.19 | 7.72 | 7.99 | 7.82 | 6.34 | 7.59 | 7.22 | 7 |
| % | SI | 27.4 | 24.1 | 27.8 | 30.4 | 30.7 | 30.4 | 22.2 | 29.4 | 29.4 | 28.9 |
| % | P | 0.145 | 0.093 | 0.1 | 0.11 | 0.111 | 0.11 | 0.1 | 0.1 | 0.108 | 0.099 |
| % | S | 0.045 | 0.075 | 0.045 | 0.023 | 0.023 | 0.023 | 0.093 | 0.022 | 0.022 | 0.022 |
| % | CL | 0.011 | 0.01 | 0.011 | 0.012 | 0.012 | 0.011 | 0.01 | 0.011 | 0.012 | 0.011 |
| % | K | 1.6 | 0.835 | 1.73 | 1.88 | 1.78 | 1.87 | 1.295 | 1.75 | 1.65 | 1.73 |
| % | CA | 2.59 | 2.06 | 2.7 | 2.82 | 2.85 | 2.95 | 2.62 | 2.72 | 2.49 | 2.48 |
| % | TI | 0.476 | 0.443 | 0.606 | 0.718 | 0.697 | 0.749 | 0.496 | 0.667 | 0.611 | 0.628 |
| PPM | V | 75 | 28 | 167 | 199 | 213 | 205 | 131 | 174 | 119 | 138 |
| PPM | CR | 34.9 | 11.6 | 25.1 | 21 | 21.6 | 25.3 | 24.8 | 21.5 | 27.8 | 32.1 |
| PPM | RB | 57.8 | 35.7 | 59.8 | 61.6 | 56.6 | 57.6 | 44.7 | 57.2 | 56.4 | 55.6 |
| PPM | U | 3.9 | 3.5 | 5.1 | 3.9 | 3.7 | 3.9 | 5 | 3.8 | 4.3 | 3.7 |
| PPM | SR | 777 | 1850 | 381 | 363 | 378 | 367 | 401 | 366 | 373 | 349 |
| PPM | Y | 30.6 | 28 | 27.2 | 29 | 29.2 | 30.3 | 26 | 26.9 | 27.9 | 26.3 |
| PPM | ZR | 200 | 233 | 254 | 223 | 252 | 226 | 205 | 237 | 276 | 229 |
| PPM | NB | 11 | 11.8 | 10.8 | 10.2 | 10.3 | 9.5 | 10.6 | 11.4 | 11.6 | 11.7 |
| PPM | MO | 2.5 | 2.8 | 2.5 | 2.4 | 2.4 | 2.4 | 2.4 | 2.5 | 2.5 | 2.4 |
| PPM | TH | 16.5 | 12.5 | 7.4 | 7.5 | 7.3 | 7.6 | 6.7 | 6.5 | 6.8 | 6.2 |
| PPM | MN | 447 | 207 | 744 | 861 | 822 | 871 | 646 | 819 | 775 | 768 |
| % | FE | 3.28 | 3.25 | 4.21 | 4.72 | 4.61 | 5.01 | 3.45 | 4.69 | 4.31 | 4.38 |
| PPM | NI | 31.4 | 22.4 | 16 | 25.1 | 18.6 | 20.7 | 22 | 21.6 | 24.4 | 26.9 |
| PPM | CU | 38.1 | 53.3 | 34.2 | 19.6 | 26 | 24 | 44.6 | 21.3 | 23.7 | 20.2 |
| PPM | ZN | 59.9 | 43.6 | 81.9 | 73.2 | 75.9 | 73 | 77.8 | 75.8 | 81.9 | 73.9 |
| PPM | GA | 18.8 | 19 | 12.9 | 16.5 | 13.8 | 15.7 | 15.1 | 16.8 | 15.7 | 18 |
| PPM | HG | 3.1 | 3 | 3.3 | 3.5 | 3.4 | 3.5 | 2.9 | 3.3 | 3.2 | 3.2 |
| PPM | SE | 2.99 | 4.2 | 1.4 | 1.53 | 1.5 | 1.5 | 1.3 | 1.4 | 1.4 | 1.4 |
| PPM | PB | 19 | 21.2 | 22.4 | 15.3 | 12.7 | 7.6 | 18.5 | 9 | 14.8 | 11 |
| PPM | AS | 8.5 | 8.2 | 5.4 | 3.9 | 5.8 | 6.5 | 5.2 | 5 | 5.1 | 4.2 |
| PPM | BR | 2.28 | 2.42 | 1.2 | 1.3 | 1.3 | 1.4 | 3.27 | 1.4 | 1.2 | 1.3 |
| PPM | RB | 58.5 | 36.7 | 61.9 | 63.1 | 59.3 | 63.2 | 42.7 | 59.8 | 59.2 | 60.7 |
| PPM | SR | 761 | 1878 | 373 | 369 | 390 | 385 | 394 | 384 | 382 | 370 |
| PPM | RU | 8.5 | 8.6 | 8.5 | 8 | 7.4 | 7.6 | 8.3 | 7.8 | 7.4 | 7.7 |
| PPM | RH | 10 | 10 | 10 | 9.6 | 8.7 | 9 | 9.6 | 9.2 | 8.7 | 8.7 |
| PPM | PD | 13 | 13 | 14 | 12 | 11 | 12 | 12 | 12 | 11 | 11 |
| PPM | AG | 15 | 15.3 | 15 | 14 | 12 | 13 | 14 | 13 | 13 | 13 |
| PPM | CD | 16 | 16 | 19.8 | 15 | 13 | 13 | 15 | 15 | 13 | 13 |
| PPM | IN | 17 | 17 | 16 | 15 | 14 | 15 | 16 | 15 | 14 | 14 |
| PPM | SN | 18 | 18 | 18 | 17 | 16 | 16 | 17 | 17 | 16 | 16 |
| PPM | SB | 21 | 19 | 22 | 21 | 18 | 19 | 20 | 19 | 18 | 18 |
| PPM | TE | 26 | 24 | 23 | 21 | 21 | 22 | 23 | 21 | 21 | 21 |
| PPM | I | 32 | 31 | 32 | 29 | 25 | 28 | 28 | 28 | 24 | 26 |
| PPM | CS | 39 | 44 | 40 | 41 | 32 | 35 | 42 | 39 | 38 | 38 |
| PPM | BA | 956 | 1832 | 745 | 756 | 748 | 670 | 648 | 691 | 712 | 714 |
| PPM | LA | 50 | 52 | 51 | 47 | 45 | 73 | 74 | 49 | 43 | 42 |
| PPM | CE | 68 | 102 | 69 | 97 | 75 | 88 | 65 | 63 | 73 | 93 |

**Table E.5**. X-ray Fluorescence Analysis of Stations 5 through 8

| | | Sample Number | | | | | | | | | |
|---|---|---|---|---|---|---|---|---|---|---|---|
| | | 5-1a | 5-1a | 6-1a | 6-1a | 7-1a | 7-1a | 7-1b | 7-1b | 8-1a | 8-1a |
| Units | Element | 0-1 (cm) | 9-10 (cm) | 0-1 (cm) | 9-10 (cm) | 0-1 (cm) | 9-10 (cm) | 0-1 (cm) | 9-10 (cm) | 0-1 (cm) | 9-10 (cm) |
| % | AL | 7.41 | 7.52 | 7.27 | 7.38 | 7.76 | 7.91 | 7.3 | 7.06 | 7.69 | 7.52 |
| % | SI | 29.8 | 30.6 | 28.8 | 29.4 | 30.8 | 31.3 | 30 | 30.5 | 32.2 | 31.8 |
| % | P | 0.131 | 0.11 | 0.114 | 0.106 | 0.12 | 0.11 | 0.143 | 0.116 | 0.094 | 0.099 |
| % | S | 0.023 | 0.023 | 0.023 | 0.021 | 0.023 | 0.023 | 0.023 | 0.022 | 0.021 | 0.023 |
| % | CL | 0.011 | 0.011 | 0.011 | 0.011 | 0.012 | 0.011 | 0.012 | 0.011 | 0.011 | 0.012 |
| % | K | 1.7 | 1.74 | 1.56 | 1.7 | 1.66 | 1.77 | 1.72 | 1.83 | 1.96 | 2.01 |
| % | CA | 2.81 | 2.95 | 2.83 | 3 | 3.07 | 2.68 | 2.96 | 2.67 | 1.74 | 1.86 |
| % | TI | 0.671 | 0.717 | 0.628 | 0.769 | 0.75 | 0.684 | 0.71 | 0.682 | 0.349 | 0.333 |
| PPM | V | 129 | 164 | 140 | 182 | 200 | 165 | 174 | 167 | 40 | 58 |
| PPM | CR | 30.5 | 19.4 | 24.7 | 28.2 | 18.5 | 33.2 | 24.3 | 17.3 | 29 | 23.2 |
| PPM | RB | 56.3 | 51 | 50.2 | 50.6 | 49.5 | 55.5 | 52.3 | 55.7 | 67.5 | 65.8 |
| PPM | U | 3.7 | 3.7 | 3.6 | 3.9 | 3.6 | 5 | 3.7 | 4 | 4.3 | 4.3 |
| PPM | SR | 364 | 365 | 395 | 372 | 385 | 366 | 378 | 372 | 380 | 396 |
| PPM | Y | 25.4 | 28.9 | 26 | 29.9 | 27.1 | 27.5 | 23.1 | 28.4 | 22.1 | 17.5 |
| PPM | ZR | 184 | 187 | 211 | 228 | 210 | 220 | 166 | 220 | 153 | 119.7 |
| PPM | NB | 11.2 | 11.6 | 10.8 | 11.8 | 9.7 | 9.8 | 11 | 9.4 | 8.5 | 8.3 |
| PPM | MO | 2.3 | 2.3 | 2.4 | 2.6 | 2.3 | 2.4 | 2.3 | 2.4 | 2.4 | 2.1 |
| PPM | TH | 6 | 6.3 | 7.7 | 6.5 | 6.4 | 6.4 | 6.2 | 6.4 | 6.5 | 6.1 |
| PPM | MN | 792 | 875 | 747 | 907 | 873 | 855 | 828 | 828 | 553 | 534 |
| % | FE | 4.61 | 4.91 | 4.38 | 5.33 | 5.12 | 4.86 | 4.91 | 4.7 | 2.91 | 2.81 |
| PPM | NI | 29.2 | 17.8 | 24.4 | 23.3 | 21.7 | 25.8 | 21.4 | 16.3 | 23 | 22 |
| PPM | CU | 19.4 | 17 | 24.9 | 20.1 | 23 | 17.3 | 18.4 | 18.5 | 24.2 | 16.7 |
| PPM | ZN | 77.2 | 70.7 | 77.5 | 80.6 | 79.6 | 69.1 | 75.8 | 68.1 | 56.8 | 52.6 |
| PPM | GA | 17.2 | 16.5 | 15.8 | 15.6 | 15.6 | 16.9 | 17.7 | 15.7 | 15.6 | 16.4 |
| PPM | HG | 3.2 | 3.5 | 3.1 | 3.5 | 3.4 | 3.3 | 3.4 | 3.4 | 3.2 | 3.2 |
| PPM | SE | 1.4 | 1.5 | 1.4 | 1.5 | 1.5 | 1.48 | 1.5 | 1.4 | 1.4 | 1.4 |
| PPM | PB | 11.4 | 10.7 | 11.5 | 13.7 | 11.6 | 10.4 | 10.8 | 11.1 | 13.7 | 10.6 |
| PPM | AS | 3.4 | 3 | 4.8 | 2.3 | 5.3 | 5.4 | 4.1 | 4.3 | 2.6 | 2.8 |
| PPM | BR | 1.3 | 1.2 | 1.3 | 1.4 | 1.3 | 1.3 | 1.3 | 1.3 | 1.3 | 1.2 |
| PPM | RB | 58.9 | 57.4 | 51.7 | 56.6 | 52.8 | 60.5 | 54.5 | 59.9 | 73.5 | 73.4 |
| PPM | SR | 386 | 385 | 413 | 382 | 410 | 378 | 399 | 375 | 397 | 420 |
| PPM | RU | 7.4 | 7.2 | 7.6 | 7.3 | 7.7 | 7.6 | 7.3 | 7.9 | 8.5 | 7.2 |
| PPM | RH | 8.7 | 8.2 | 8.8 | 9.2 | 8.4 | 9 | 9.1 | 9.3 | 9.9 | 8.9 |
| PPM | PD | 11 | 10 | 11 | 12 | 11 | 11 | 12 | 12 | 13 | 11 |
| PPM | AG | 12 | 12 | 14.4 | 14 | 12 | 13 | 13 | 13 | 14 | 13 |
| PPM | CD | 13 | 13 | 14 | 15 | 13 | 13 | 15 | 15 | 16 | 14 |
| PPM | IN | 14 | 13 | 15 | 16 | 14 | 14 | 16 | 16 | 17 | 15 |
| PPM | SN | 16 | 15 | 16 | 17 | 15 | 16 | 17 | 17 | 18 | 16 |
| PPM | SB | 18 | 18 | 18 | 18 | 18 | 19 | 19 | 19 | 20 | 18 |
| PPM | TE | 20 | 20 | 21 | 23 | 20 | 21 | 23 | 22 | 26 | 20 |
| PPM | I | 25 | 24 | 27 | 29 | 23 | 27 | 25 | 28 | 30 | 24 |
| PPM | CS | 33 | 31 | 33 | 35 | 33 | 39 | 36 | 39 | 39 | 38 |
| PPM | BA | 687 | 753 | 706 | 655 | 752 | 667 | 763 | 708 | 861 | 843 |
| PPM | LA | 58 | 42 | 44 | 46 | 43 | 46 | 47 | 47 | 52 | 44 |
| PPM | CE | 52 | 49 | 91 | 62 | 60 | 78 | 112 | 63 | 82 | 94 |

**Table E.6**. X-ray Fluorescence Analysis of Stations 9 through 12

| | | Sample Number | | | | | | | | |
|---|---|---|---|---|---|---|---|---|---|---|
| | | **9-1a** | **9-1a** | **10-1a** | **10-1a** | **11-1a** | **11-1a** | **11-1b** | **11-1b** | **12-1a** |
| **Units** | **Element** | **0-1 (cm)** | **9-10 (cm)** | **0-1 (cm)** | **9-10 (cm)** | **0-1 (cm)** | **9-10 (cm)** | **0-1 (cm)** | **9-10 (cm)** | **NA** |
| % | **AL** | 6.91 | 7.68 | 7.66 | 7.6 | 8.06 | 7.58 | 6.99 | 7.36 | 1.53 |
| % | **SI** | 30.8 | 32.2 | 31.1 | 30.9 | 30.7 | 29.6 | 28 | 28.6 | 2.93 |
| % | **P** | 0.096 | 0.098 | 0.11 | 0.135 | 0.185 | 0.133 | 0.155 | 0.11 | 0.047 |
| % | **S** | 0.022 | 0.022 | 0.024 | 0.023 | 0.024 | 0.023 | 0.022 | 0.023 | 0.407 |
| % | **CL** | 0.011 | 0.011 | 0.012 | 0.012 | 0.012 | 0.012 | 0.011 | 0.012 | 0.023 |
| % | **K** | 1.94 | 1.92 | 1.76 | 1.9 | 1.68 | 1.81 | 1.6 | 1.68 | 0.111 |
| % | **CA** | 1.92 | 2.17 | 2.81 | 2.81 | 3.35 | 3.07 | 3.15 | 3.03 | 0.417 |
| % | **TI** | 0.384 | 0.463 | 0.59 | 0.685 | 0.804 | 0.821 | 0.688 | 0.796 | 0.084 |
| PPM | **V** | 78 | 94 | 131 | 155 | 184 | 220 | 166 | 200 | 9.7 |
| PPM | **CR** | 24.7 | 35.8 | 19.9 | 25.1 | 34.2 | 23.4 | 24.4 | 35.2 | 2.7 |
| PPM | **RB** | 62.8 | 61.5 | 55.6 | 60.7 | 49.8 | 56.3 | 53.7 | 57.5 | 5.77 |
| PPM | **U** | 3.9 | 3.8 | 3.8 | 3.8 | 3.9 | 4 | 4 | 3.9 | 2 |
| PPM | **SR** | 389 | 393 | 378 | 369 | 362 | 362 | 351 | 356 | 200 |
| PPM | **Y** | 20.2 | 21.5 | 24.4 | 25 | 27.6 | 32 | 25.6 | 28.3 | 5.83 |
| PPM | **ZR** | 144 | 174 | 189 | 213 | 215 | 219 | 172 | 220 | 40.6 |
| PPM | **NB** | 8.2 | 9.7 | 9.1 | 10.9 | 11.8 | 9.6 | 10 | 10.5 | 3.16 |
| PPM | **MO** | 2.3 | 2.3 | 2.4 | 2.3 | 2.5 | 2.5 | 2.5 | 2.4 | 1.7 |
| PPM | **TH** | 6.3 | 6.2 | 6.4 | 6.4 | 6.4 | 6.7 | 6.5 | 6 | 4.4 |
| PPM | **MN** | 569 | 669 | 760 | 778 | 971 | 1038 | 976 | 1093 | 66.3 |
| % | **FE** | 3.04 | 3.49 | 4.19 | 4.57 | 5.51 | 5.62 | 5.43 | 5.82 | 0.576 |
| PPM | **NI** | 19.3 | 20.9 | 27.9 | 22.8 | 23 | 24.1 | 26.7 | 27.9 | 4 |
| PPM | **CU** | 18.3 | 16.6 | 20.4 | 16.8 | 22.9 | 20.9 | 29 | 24.3 | 8.13 |
| PPM | **ZN** | 57 | 59.2 | 68.4 | 66.6 | 87.4 | 86.9 | 88.3 | 85.1 | 18.7 |
| PPM | **GA** | 16.8 | 17.8 | 19.5 | 18.7 | 16.6 | 18.2 | 17.5 | 20.1 | 3.68 |
| PPM | **HG** | 3.2 | 3.3 | 3.4 | 3.6 | 3.6 | 3.6 | 3.6 | 3.9 | 1.4 |
| PPM | **SE** | 1.4 | 1.4 | 1.5 | 1.5 | 1.6 | 1.6 | 1.5 | 1.7 | 1.12 |
| PPM | **PB** | 10.5 | 10.3 | 17.5 | 9.9 | 13.7 | 9.6 | 13.7 | 12.8 | 4.4 |
| PPM | **AS** | 5.3 | 6.2 | 2.4 | 5.7 | 2.7 | 5.7 | 4.8 | 4.2 | 2.01 |
| PPM | **BR** | 1.3 | 1.3 | 1.4 | 1.4 | 1.5 | 1.4 | 1.4 | 1.5 | 3.18 |
| PPM | **RB** | 68.6 | 64.2 | 62.2 | 64.8 | 54.6 | 65.1 | 55.7 | 61.1 | 5.3 |
| PPM | **SR** | 402 | 403 | 395 | 389 | 382 | 384 | 364 | 376 | 164.3 |
| PPM | **RU** | 7.6 | 7.6 | 7.8 | 7.4 | 7.1 | 7.5 | 8.1 | 7.2 | 8 |
| PPM | **RH** | 9.4 | 9.3 | 9.3 | 8.7 | 9 | 8.8 | 9.7 | 8.4 | 10 |
| PPM | **PD** | 12 | 12 | 12 | 11 | 12 | 11 | 12 | 11 | 14 |
| PPM | **AG** | 13 | 13 | 14 | 12 | 13 | 13 | 14 | 12 | 16 |
| PPM | **CD** | 15 | 14 | 14 | 14 | 14 | 14 | 16 | 13 | 16 |
| PPM | **IN** | 16 | 16 | 16 | 14 | 16 | 14 | 17 | 14 | 17 |
| PPM | **SN** | 17 | 17 | 17 | 16 | 16 | 16 | 18 | 15 | 26.7 |
| PPM | **SB** | 19 | 18 | 19 | 18 | 19 | 18 | 19 | 18 | 21 |
| PPM | **TE** | 23 | 22 | 24 | 20 | 21 | 22 | 24 | 21 | 24 |
| PPM | **I** | 27 | 27 | 27 | 24 | 25 | 25 | 31 | 25 | 32 |
| PPM | **CS** | 37 | 34 | 35 | 34 | 36 | 35 | 38 | 37 | 42 |
| PPM | **BA** | 805 | 673 | 605 | 710 | 700 | 691 | 686 | 688 | 240 |
| PPM | **LA** | 49 | 47 | 72 | 67 | 47 | 44 | 51 | 44 | 53 |
| PPM | **CE** | 101 | 60 | 69 | 52 | 77 | 85 | 59 | 106 | 60 |

## E.5 Conclusions

To resolve the issue of where coal emissions might be within the profile, we recommend additional analyses of the entire core from at least two stations—one from the proposed ILAW Disposal Site and one from a representative background site. Preferably, these would be Stations 3 and 9. As reported, Station 3 has the highest indication of being potentially affected, and its location is well within the prevailing wind pattern located on the northeast corner of the proposed ILAW Disposal Site. X-ray fluorescence data appear to indicate that Station 9 is reasonably representative of background sediment. Profiling should involve sub-sampling each of the cores at a minimum of 20-cm intervals for 2:1 extract IC analyses, and sediment x-ray fluorescence analysis along the entire length of each core. Additionally it is recommended that, using stable isotope ratio mass spectrometry, an effort should be made to determine if a chemical fingerprint for isotopic sulfur could help determine the source of the sulfate.

## E.6 References


Fayer MJ and TB Walters. 1995. *Estimated recharge rates of the Hanford Site*. PNL-10285, Pacific Northwest Laboratory, Richland, Washington.

Hajek BF. 1966. *Soil survey, Hanford project in Benton County Washington.* BNWL-243, Pacific Northwest Laboratory, Richland, Washington.

Hoitink DJ, KW Burk, and JV Ramsdell. 1999. *Hanford Site climatological data summary 1998 with historical data*. PNNL-12087, Pacific Northwest National Laboratory, Richland, Washington.

Murphy EM, JE Szecsody, and SJ Philips. 1991. *A study for determining recharge rates at the Hanford Site using environmental tracers*. PNL-7626, Pacific Northwest Laboratory, Richland, Washington.

Murphy EM, TR Ginn, and JL Philips. 1996. "Geochemical estimates of paleorecharge in the Pasco Basin: evaluation of the chloride mass balance technique." *Water Resour. Res*., Vol. 32, No. 9, 2853-2867.

U.S. Environmental Protection Agency. 1998. *External combustion sources*. EPA AP-42, ed. 5, Vol. 1, 1.1-1 – 1.1-47, U.S. Environmental Protection Agency, Washington, DC.

# Appendix F

# Vegetation Data Summary for Supporting Recharge Estimates - FY 1998 and FY 1999

J. L. Downs and F. O. Khan

# Appendix F

# Vegetation Data Summary for Supporting Recharge Estimates - FY 1998 and FY 1999

## F.1 Introduction

Pacific Northwest National Laboratory (PNNL) manages the "PNNL Geotechnical Support of Hanford Immobilized Low-Activity Waste (ILAW)" project to assist Lockheed Martin Hanford Company (LMHC) in designing and assessing the performance of a disposal facility for radioactive wastes currently stored in single- and double-shell tanks at the Hanford Site. A major challenge in assessing long-term performance of buried waste disposal facilities involves characterizing and understanding the distribution of mean recharge rates across the heterogeneous landscape at Hanford. Location-specific recharge rates are determined by site-specific climate, soils, and topography (aspect and slope), as well as the disturbance or land use history (fire, erosion, grazing), soil properties, and vegetation properties.

The overall objective of the recharge task is to provide defensible estimates of recharge rates for current conditions and long-term scenarios involving the shallow-land disposal of low-level waste at the Hanford Site (WHC 1995). Rockhold et al. (1995) outlined the conditions and scenarios that could impact the disposal facility and provided estimates of recharge rates from existing lysimeter and tracer data for four conditions. However, for most of the conditions and scenarios identified by Rockhold et al. (1995), very limited data were available with which to estimate recharge rates. Thus, a major goal of the recharge task is to collect sufficient data to enable estimation of recharge rates for the conditions and scenarios deemed to be important for evaluating the performance of the disposal facility.

This letter report outlines the vegetation studies accomplished during FY 1998 and 1999 to support the prediction of recharge rates over the lifetime of the disposal facility. Under Subtasks 2c, 2d, and 2e of the recharge task, PNNL has gathered and compiled vegetation data from the literature and at the proposed ILAW Disposal Site for use in predicting the long-term water balance and recharge. The information gathered addresses data gaps (previously identified in the letter report, Review of Existing Vegetation Data for Performance Assessment Modeling of the ILAW Disposal Site) to the extent possible given current funding levels. PNNL modeling staff have been and will continue to be consulted to prioritize data collection and interpretation. Field data are summarized and presented, along with a discussion of how these data meet future modeling requirements.

### F.1.1 Background and Study Objectives

The plant community existing at a site of interest influences a number of factors that determine recharge rates for that site. Vegetation can influence the surface-water runoff, the infiltration of

precipitation in the soil, the amount of water stored in the soil, and even the amount of precipitation that reaches the soil surface. The greatest effect of vegetation on surface-water budgets is in the transpiration fraction of the total evapotranspiration. Plants growing in arid systems may actually remove all water stored in the soil column, depending on the rooting depth, plant phenology and form, and the soil type; thus, plants can effectively reduce drainage and subsequent recharge (Gee et al. 1992, 1994; Link et al. 1994).

In general, models used to estimate recharge rates for different conditions will require certain vegetative parameters including estimates of plant transpiration and plant water status (leaf water potential) that can be correlated with soil water potentials. Knowledge of rooting depths, root densities, and root distributions are also required for modeling efforts to accurately simulate sequential removal of water from different depths within the soil profile. Depending on surface, vegetation, and soil conditions, recharge rates at Hanford can range 1000-fold: from less than 0.01 cm/yr under a complete cover of shrubs to more than 10 cm/yr under graveled surfaces without vegetation (Murphy et al. 1996; Gee et al. 1992).

Because vegetation is a function of the physical environment, differences in environmental conditions such as soil depth or soil type are readily reflected by differences in the plant community composition and structure across the landscape. The density and canopy cover of mixed shrub and grass communities can vary greatly across relatively short distances. Changes in soil type and/or slope and aspect can create sharp delineations between community types or change the abundance of a particular species. Understanding the patterns of plant distribution—both above- and belowground—is key to understanding plant water use and its impact on recharge rates.

The objectives of the vegetation subtasks are to provide the descriptive information and data that are needed to better understand and predict recharge rates at the proposed ILAW disposal facility on the Hanford Site. These data will aid in understanding how and to what extent plants may control recharge at the Site and be used to develop the appropriate ranges and distributions of plant parameters that can be used in computer modeling efforts to assess recharge. In FY 1998, field data collected under these subtasks included information concerning the existing and potential plant community structure: plant canopy cover, species diversity, shrub density and distribution of size classes, plant root spatial distribution and biomass, total leaf area and biomass, and determination of leaf area index. In FY 1999, our objectives were to collect physiological and life history information over a 7-month period from November 1998 through May 1999.

Our investigation concentrated on defining water relations for three dominant plant species on the site: big sagebrush (*Artemisia tridentata*), cheatgrass (*Bromus tectorum*), and Sandberg's bluegrass (*Poa sandbergii*). The FY 1999 study focused on defining plant water status with respect to soil water status for each of the species of interest during winter and spring months. We conducted the following studies throughout the year:

- documentation of plant phenology
- measurement of leaf (xylem) water potential through winter until late spring
- concurrent measurement of leaf-level conductance as feasible

- concurrent measurement of soil water content
- finalizing measurements of root distribution and biomass of shrubs and grasses.

We also sampled plants for leaf area index (LAI) to compare with the 1998 leaf area and biomass data and to refine the community level estimates for LAI. To the extent feasible, measurements were made to document seasonal changes in LAI.

## F.2 Methods

The field study area is located at the proposed ILAW Disposal Site in the 200 East Area of the Hanford Site (Figure F.1). The current plant community can be classified as either *Artemisia tridentata*/*Bromus tectorum* (Big Sagebrush/Cheatgrass) or *Artemisia tridentata*/*Poa Sandbergii* (Big Sagebrush/Sandberg's bluegrass) depending on the extent to which cheatgrass has replaced bluegrass as the understory grass species. Soils of the ILAW site are predominantly sands and loamy sands (see Section 3.0 of the main report). The topography of the ILAW site to the south and west of the plutonium-uranium extraction (PUREX) facility is relatively flat with the exception of a stabilized dune running in

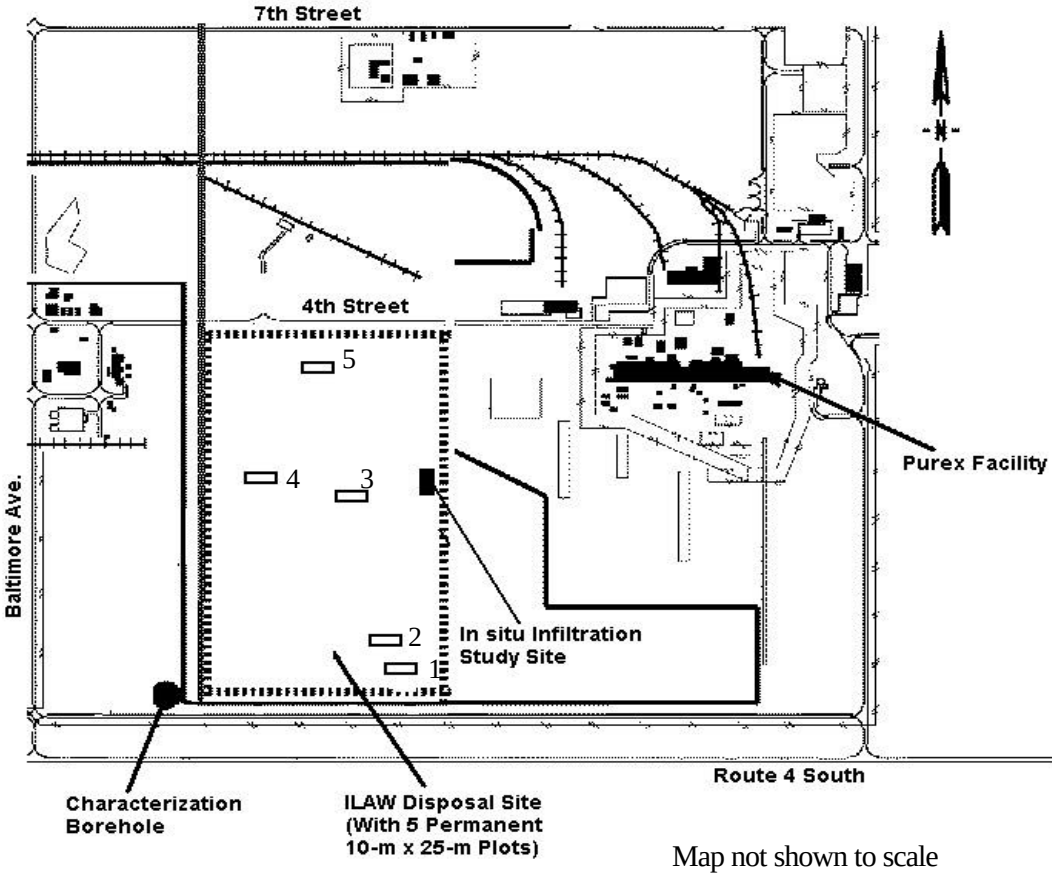


**Figure F.1**. Map of the Immobilized Low Activity Waste Disposal Site in the 200 East Area Displaying the Five Permanent Vegetation Monitoring Plots

an east-west direction along the southernmost edge of the site. The general climate at the Hanford Site is best described as semiarid with hot dry summers and cold, wet winters. During the 1998-1999 measurement period, winter temperatures were warmer than the long-term averages for the site. November was 5.3°F above the normal monthly average (40.2°F), December was 5.4°F above the normal monthly average (31.4°F), January was 1.6°F above the normal monthly average (31.3°F), and February was 3.7°F above the normal monthly average (38.0°F).

Efforts in FY 1998 were focused on characterizing two types of plant communities that might establish on the ILAW disposal facility: the existing sagebrush-steppe type community currently occupying the proposed disposal area, and abandoned fields that represent the unaided establishment of vegetation after construction or possible successional stages following fire. Characterization efforts included measurements of plant canopy cover, shrub density and height, species diversity, leaf area and biomass. In addition, root distributions were sampled to a depth of 1 m on the in situ infiltration test plot.[(a)] Leaf-level conductance, leaf water potential growth and phenology, and concurrent soil water status were measured from November 1998 through May 1999.

### F.2.1 Species Diversity and Canopy Cover of Herbaceous Plants

Five 100-m transects were randomly established in 1998 at the ILAW Disposal Site and three 100-m transects at the Existing Disposal Site to determine plant diversity, abundance, and canopy cover by species for the sagebrush-steppe community. On each 100-m transect, three 10-m x 10-m plots were established along the transect at 25, 50, and 75 m. In each 10-m x 10-m plot, shrub height, widest diameter ($d_1$), and diameter ($d_2$) perpendicular to the first diameter measurement were recorded. Shrub canopy cover was calculated using this plot data. An ellipsoidal area was calculated for each shrub

$$Area = \pi\left(\frac{d_1\, d_2}{4}\right) \tag{F.1}$$

and the total shrub area was summed for each plot and expressed as a percentage of ground area to determine percent canopy cover. These were averaged for each transect and a mean canopy cover was determined for each site (ILAW, n = 5; Grout, n = 3). Understory canopy cover by species was visually estimated in 0.2 x 0.5-m plots using a modification of Daubenmire's (1959) method. These 0.1-m quadrants were systematically placed along the transect to provide 25 to 30 samples of plant cover and compostion along each transect. Species lists were compiled for the area adjacent to each transect. Where feasible, percent bare ground and percent of ground covered by biotic crust was also estimated.

Data were also gathered in a similar fashion from five additional transects established randomly on abandoned fields on fine-textured soils on the Hanford Site (two transects at McGee Ranch, two transects at Lower Snively field, and one transect at Benson Ranch). No shrubs were found on abandoned field

(a) Ward AL, RL Clayton, and JC Ritter. 1998. "Hanford Low-Activity Tank Waste Performance Assessment Activity: Determination of in situ hydraulic parameters of Hanford Sediments," Letter Report to Fred Mann, Fluor Daniel Northwest, Richland, Washington, August 31, 1998.

transects, so no 10-m by 10-m plots were established on those transects. These data are compared with data obtained from the ILAW Disposal and Existing Disposal Sites.

### F.2.2 Leaf Area Index and Shrub Biomass

During February 1998, all sagebrush plants were harvested from a 2-m x 10-m plot on the borehole site, southwest of the PUREX facility, and in April 1998 from the 5-m x 8-m in situ infiltration test plot, including its borders and measured for canopy cover, LAI, and shrub biomass. At the same time, herbaceous groundcover was harvested for leaf area determination from eight 1-$m^2$ plots at the borehole site (February 1998) and from six random 0.1-m x 0.5-m plots at the in situ infiltration test plot (April 1998). All leaves were separated from each plant and a total leaf area for that shrub obtained using a LI-COR 3100 Area Meter. Leaves and stems were dried and weighed for a total biomass of each shrub. For each harvested understory plot, all live herbaceous plant material was separated from litter and a total leaf area obtained using a LI-COR 3100 Area Meter. Equations were developed to relate sagebrush volume to leaf area and sagebrush leaf biomass to leaf area. These relationships are used with shrub density and size measurements to evaluate variability in leaf area across the assessment site.

Nine additional shrubs were harvested in spring 1999 in the ILAW Disposal Site for LAI values and shrub biomass measurements. Shrubs harvested were selected in three categories, three of each; small, medium, and large, and all plants were measured for height and diameter before harvesting. At the same time, herbaceous groundcover was harvested for leaf area determination from six random 0.1-m x 0.5-m plots at the site. These data have not been summarized for this report, but will be included at a later date.

All sagebrush in 14 randomly selected 10-m x 10-m plots across the site were measured in 1998 to obtain average shrub size, shrub density, and canopy cover. Measurements were also obtained from nine additional 10-m x 10-m plots near the Existing Disposal Site for comparison.

Root distribution sampling was conducted before excavation of the in situ permeability plot during July 1998. Approximately 75 core samples of soil 0.05 m x 1 m deep were removed in sections (>450 subsamples) for processing. Root samples were washed of soils and oven dried. Dried roots were weighed to determine root biomass. Samples were grouped for analysis according to distance from the main stem of sagebrush plants in the area.

### F.2.3 Plant Phenology and Growth

Five large (10-m x 25-m) permanent plots were established in November 1998 across the proposed ILAW Disposal Site to monitor phenological changes and growth of the dominant grass species (cheatgrass and Sandberg's bluegrass) during FY 1999 (Figure F.1). Two of the five plots are located in the southeastern corner of the site adjacent to each other. One plot was established on each of two slopes located on the site: a north-facing slope and a south-facing slope. The location of these plots will enable us to monitor plant growth and development under different exposure to sunlight and rainfall determined by aspect. The other three plots were randomly located across the ILAW Disposal Site so that data collected will represent vegetation characteristics sitewide.

Within each of the five large permanent plots, ten subplots (0.5-m x 0.2-m) were established to monitor phenological changes of the two grass species of interest during the growing season. Subplots were equally apportioned either beneath shrubs or in inter-shrub spaces. Five shrubs within each 10-m x 25-m plot were chosen randomly to establish the sub-plots: five sub-plots close to or beneath the shrub canopy (one plot per shrub), and five sub-plots located in inter-shrub space.

From November 1998 through May 1999, growth and development were observed monthly in the winter and bi-weekly in the spring in each subplot, when the grasses were most active. Estimated canopy cover and growth stage for both grass species of interest were recorded at each observation period. Grass height of each species was measured at the same time through March. Growth was also measured for each of the five marked shrubs in each permanent plot. Initial height and diameter measurements were taken in November 1998 when the plots were established and a second set of similar measurements was taken in the spring 1999.

### F.2.4 Leaf Water Potential and Conductance

Seven individuals of both juvenile and mature sagebrush (14 individual plants) were selected randomly on the ILAW site from outside the permanent plots and marked for measurement. Leaf water potential and stomatal conductance measurements were taken on these plants. Seven randomly selected sites in the vicinity of the marked shrubs were established for similar measurements for cheatgrass and Sandberg's bluegrass. Leaf water potential of sagebrush and cheatgrass was determined by a series of replicated measurements during the winter and spring months. These measurements were conducted monthly in the winter months (November, December, January, February, and March) and bi-weekly in the spring months (April and May) during peak growing season. Leaf water potential of Sandberg's bluegrass was measured only during April and May 1999, when the size of the leaves was large enough to allow measurement. Pre-dawn and midday leaf water potential measurements were conducted during the same day using the pressure chamber technique as described by Koide et al. (1989).

Two measurements were conducted on each shrub and grass site during each sample period. Because the entire cheatgrass plant was used for each measurement, the area of sampling was permanently marked and consecutive sampling was conducted as close to the original sample as possible. Because Sandberg's bluegrass is a bunchgrass, the bunch in each selected site was marked and samples were obtained from that bunch for each measurement. In cases where the size of the selected bunch was not adequate, bunches of bluegrass close to the original sample were used for measurements.

Stomatal conductance was measured for sagebrush and the two dominant understory grasses using standard porometry methods (Pearcy et al. 1989). A LI-COR 1600 Steady State Porometer was used for these measurements. Peak (midday) conductances were determined for sagebrush from February 1999 to May 1999, for cheatgrass from March 1999 to May 1999, and for Sandberg's bluegrass in May 1999. Because of its size, we were unable to conduct any conductance measurements on Sandberg's bluegrass until May. These measurements were taken in concert with leaf water potential measurements. Data collected were summarized to evaluate the magnitude and variability of seasonal changes in leaf water potential and conductance.

### F.2.5 Soil Moisture

Soil samples were obtained at the same time as leaf water potential measurements to determine water content of the soil in the area of the plants being measured. Samples were obtained in two locations, under shrub canopies and in inter-shrub space, at depths from surface to a maximum of 1.5 m; 0 to 10 cm, 10 to 20 cm, 40 to 50 cm, 90 to 100 cm, and 140 to 150 cm. Where feasible, two or three sets of samples (near shrub and inter-shrub space) at different locations were obtained for accuracy. Soil water content (weight %) was determined by the gravimetric technique.

## F.3 Results And Discussion

Work done during the 1998 fiscal year resulted in significant progress in characterizing existing plant community characteristics and defining the variability and condition of the shrub community at the ILAW site. Sampling and data analysis in FY 1999 presented here provide important information concerning the water relations of dominant species and phenology and life history information for the winter to spring growth period.

### F.3.1 Plant Community Structure

The density and canopy cover of big sagebrush found on the two disposal sites vary slightly (Table F.1) and are representative of cover values reported for big sagebrush/Sandberg's bluegrass associations (average cover, 24%; range, 8 to 35%; Franklin and Dyrness 1988). It is interesting to note that although shrub canopy cover is nearly equal at the two locales (ILAW = 32% and Existing Disposal Site = 29%), the density of shrubs at the ILAW site is about 1.5 times the sagebrush density found on the Existing Disposal Site area. The overall age of shrubs in the two study areas appears to be similar with large spreading shrubs common at both sites. However, at the ILAW site, very dense patches of sagebrush are scattered across the northern and center portion of the site. Some of these patches are distinguished by multiple stemmed plants with relatively small canopy diameters that represents a slightly unusual growth form for big sagebrush in this vegetation association.

**Table F.1**. Summary of Sagebrush Characteristics Measured Across The ILAW Site and Existing Disposal Site

| Location | Average Density Shrubs/Hectare | Average Height of Shrubs (cm) | Height Range Low - High (cm) | Average Canopy Cover (%) of Shrubs |
|---|---|---|---|---|
| ILAW Disposal Site | 4000 | 101 | 7 - 225 | 32.0 |
| Existing Disposal Site | 2590 | 89 | 10 - 175 | 29.6 |

Table F.2 indicates that total plant cover on the Existing Disposal Site is also lower than that found on the ILAW Disposal Site (64% versus 83%). Native grass cover (principally Sandberg's bluegrass) and native forb cover are higher on the ILAW site than on the Existing Disposal Site. This difference is also reflected in the higher species diversity found on the ILAW site. The percent bare ground and percent biotic crust cover were also estimated on a subset of the transects. Estimates of bare ground were 19.9% at the ILAW site and 34.8% at the Grout Site; biotic crust estimates were 8.3% at the ILAW site and 12.6% at the Existing Disposal Site.

**Table F.2**. Summary of Species Diversity and Canopy Cover Data

| Location | Plant Form | Native Species | Alien Species | Totals | Average Native Species Cover (%) | Average Alien Species Cover (%) | Total Average Cover (%) |
|---|---|---|---|---|---|---|---|
| **ILAW Disposal Site** | Forbs | 12 | 5 | 17 | 7.0 | 1.40 | 8.4 |
| | Grasses | 2 | 1 | 3 | 13.6 | 28.6 | 42.2 |
| **Total Herbaceous** | | 14 | 6 | 20 | 20.6 | 30.0 | 50.6 |
| | Shrubs | 1 | 0 | 1 | 32.0 | 0 | 32 |
| **Total** | | 15 | 6 | 21 | 52.6 | 30.0 | 82.6 |
| **Existing Disposal Site** | Forbs | 8 | 4 | 12 | 2.2 | 0.9 | 3.1 |
| | Grasses | 1 | 1 | 2 | 4.0 | 26.8 | 30.9 |
| **Total Herbaceous** | | 9 | 5 | 14 | 6.3 | 27.7 | 34.0 |
| | Shrubs | 1 | 0 | 1 | 29.6 | 0 | 29.6 |
| **Total** | | 10 | 5 | 15 | 35.9 | 27.7 | 63.6 |
| **Abandoned Fields** | Forbs | 6 | 5 | 11 | 4.1 | 13.2 | 17.2 |
| | Grasses | 1 | 2 | 3 | 1.3 | 63.7 | 65.0 |
| **Total** | | 7 | 7 | 14 | 5.4 | 76.9 | 82.0 |

Communities on abandoned (disturbed) agricultural fields were evaluated as analogs to unaided vegetation development on a constructed cover. Mean canopy cover of all plant functional types on the abandoned fields was about the same as total cover at the ILAW site, but was greater than the total mean canopy cover found on the Existing Disposal Site. However, 77% of the total cover on abandoned fields is composed of alien grasses (64% canopy cover), specifically cheatgrass. Alien grass cover on abandoned fields is more than twice that found on shrub-dominated sites. Fewer native species (which are more likely to be deeper-rooted perennial plants) are found on the abandoned fields than in shrub-dominated communities. No shrubs were encountered along transects placed in abandoned fields. Although shrubs may be present in abandoned fields, canopy cover is less than 1% and considered negligible.

### F.3.2 Phenology and Growth

Cheatgrass is a winter annual, and although most seeds germinate in the fall after sufficient rainfall, a second recruitment of seedlings in early spring months also occurs. Sandberg's bluegrass is a

*'cool-season'* perennial grass that is senescent and dormant during the dry hot summer and becomes green and active after fall rains. Both species maintain green leaves and are assumed to lie quiescent when temperatures become cold over the winter months. Observations of phenology and growth of the two dominant grass species at the ILAW site from November 1998 through May 1999 indicated that both species were active throughout the winter months. Warmer than normal winter temperatures during the measurement period (see study site description) must be taken into consideration when evaluating these data. Nighttime temperatures in December and January fell to the low- to mid-20s F, but daytime temperatures were often in the upper 30s to low 40s (Hanford Meteorological Station data for 1998 and 1999).

Plant growth as evidenced by changes in canopy cover of dominant grasses at the ILAW site was estimated over the 7-month period (November 1998 through June 1999) and is shown in Figures F.2 and F.3. Canopy cover of the grasses more than doubled between October and February, indicating the grasses were not quiescent; growth and development continued throughout the winter, as weather allowed. Direct measurements of plant height for the two species over the winter months also provide evidence of growth and plant activity during the winter (Table F.3). Measurements of big sagebrush on the fire plots indicated increases in shrub canopy between November 1998 and April 1999. On average, canopy increased by about 5 cm and the two diameters ($d_1$ and $d_2$) increased by 7 and 5 cm.

Measurements of plants in different microhabitats showed significant differences in plant growth determined by spatial and structural relationships with the shrub component of the plant community. Plants of both grass species showed greater growth and canopy cover under shrubs than plants in inter-shrub spaces. This increased growth under the shrub canopies may be a result of several factors. The microclimate under shrubs may be more favorable for growth than that found in more open areas. Also, soil nutrient levels may be higher underneath shrub canopies, which can act to create "islands of fertility" within semiarid systems (Allen 1991).

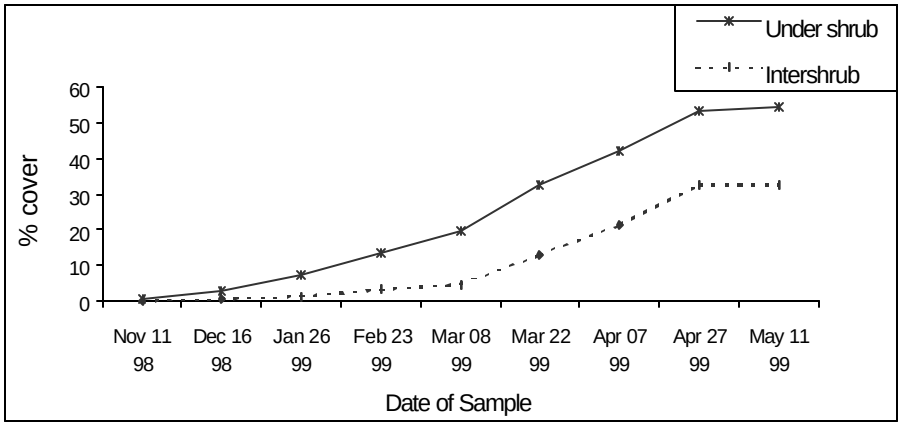


**Figure F.2**. Mean Percent Canopy Cover for Cheatgrass at the ILAW Site Throughout the Measurement Period

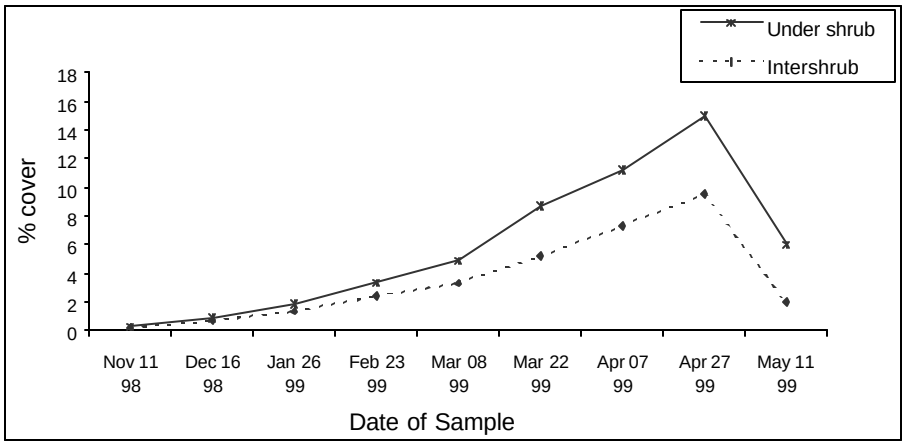


**Figure F.3**. Mean Percent Canopy Cover for Sandberg's Bluegrass at the ILAW Site Throughout the Measurement Period

Cheatgrass developed two to three times greater mean canopy cover than Sandberg's bluegrass at the proposed ILAW site, depending on the microhabitat. In Figure F.3, we can see that the peak canopy cover of Sandberg's bluegrass occurred at the end of April at the ILAW site and that the bluegrass began to senesce by early May. Cheatgrass maintained green canopy for approximately 2 weeks longer than Sandberg's bluegrass, although total canopy cover did not change significantly between April 27 and May 11.

Phenological stages recorded from November through May (shown in Figure F.4) indicate that both species initiate floral structures very early in the spring, about mid-March. These data along with the canopy cover estimates indicate that growth and development of these two cool season grasses occurs very early during the growing season. Observations in this study indicated that cheatgrass initiated floral structures about 1 week earlier than Sandberg's bluegrass. In contrast, previous study of phenology for these species on the Hanford Site (Link et al. 1990) found that Sandberg's bluegrass initiated floral structures approximately three weeks before cheatgrass.

**Table F.3**. Grass Height (cm) Measured at the Proposed ILAW Site During Winter 1998-1999

| Species | October | November | December | January | February | March |
|---|---|---|---|---|---|---|
| Cheatgrass | 2 | 3 | 4.5 | 5 | 6 | 7.5 |
| Sandberg's Bluegrass | 2 | 3.5 | 6 | 8 | 8.5 | 10 |

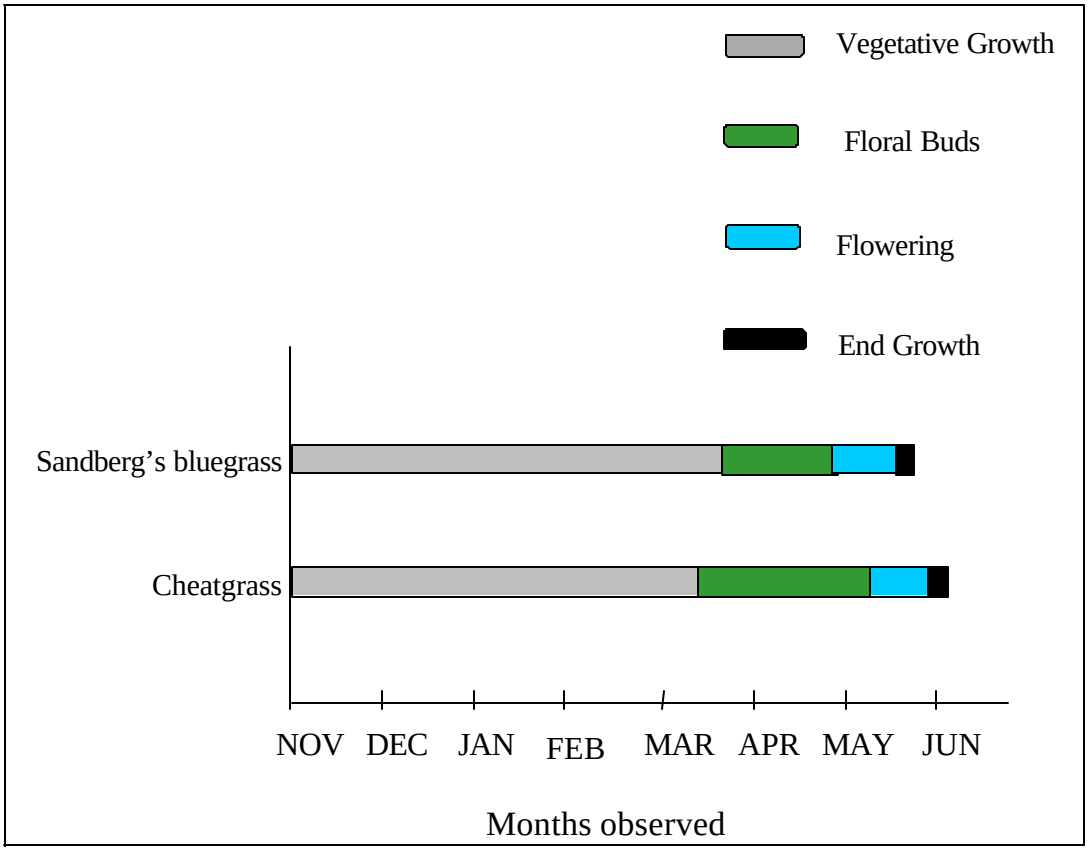


**Figure F.4**. Phenological Stages of Cheatgrass and Sandberg's Bluegrass at the ILAW Site Over the Measurement Period (Nov. 1998 – June 1999)

### F.3.3 Leaf Area and Biomass Measures

Data collected on shrub and understory leaf area in 1998 and 1999 were compiled to provide an estimate of LAI at near peak biomass (Tables F.4a and F.4b). These values were developed using both measured leaf area indices and relationships developed from morphometric measurements of shrubs. Regression relationships were developed to relate leaf biomass to leaf area and to relate calculated shrub volume to leaf area for two different time periods: February and April (Figures F.5 and F.6). The equation describing the relationship between leaf biomass and leaf area shows a reasonable fit to the data

**Table F.4a**. Estimated Leaf Area Index for Shrubs Measured in 1998

| Month | Location | LAI |
|---|---|---|
| February | ILAW Site | 0.102 |
| April | ILAW Site | 0.204 |
| June[(a)] | ILAW Site | 0.282 |
| July[(a)] | Grout Site | 0.140 |
| (a) Values estimated using morphometric and plot data. | | |

**Table F.4b**. Estimated Leaf Area Index for Understory Plants Measured in 1998 and 1999

| Date | Location | LAI |
|---|---|---|
| February 1998 | ILAW Site | 0.118 |
| April 1998 | ILAW Site | 0.904 |
| May 1999 | ILAW Site | 0.395 |

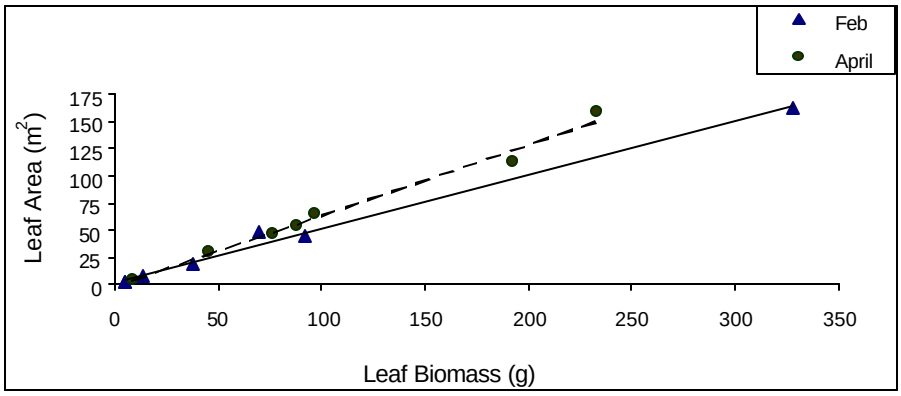


**Figure F.5**. Regression Relationship of Leaf Area to Biomass for Shrubs Measured in February and April 1998

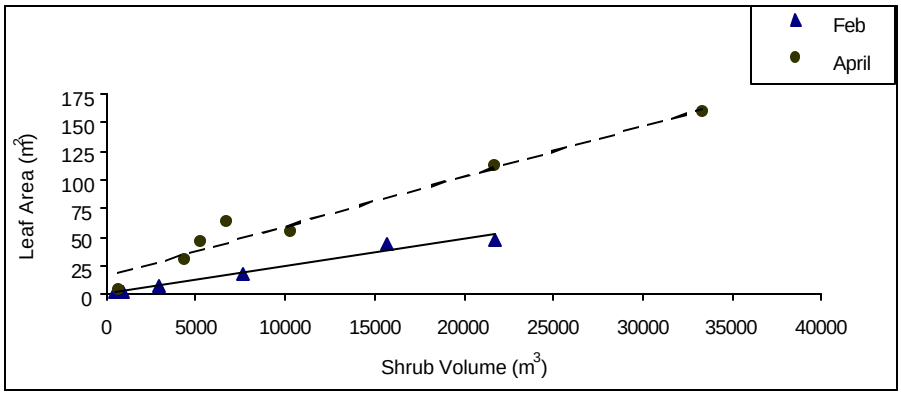


**Figure F.6**. Regression Relationship of Leaf Area to Volume for Shrubs Measured in February and April 1998

for both measurement time periods. Leaf area is not predicted as well by calculated shrub volumes. However, biomass data for entire shrubs or over large spatial areas are seldom available. Using a leaf area relationship developed on morphometric measurements allows us to estimate the spatial variability in

shrub leaf area through nondestructive measures of shrub size and canopy extent. The difference between the February and April relationships can be explained by the increase in shrub and grass leaf area during the spring growth period.

### F.3.4 Plant Water Status

Predawn and midday water potentials were measured for mature sagebrush during the 7-month period from October 1998 to May 1999. Leaf water potential of plants varies on a diurnal schedule: as the plant goes through a daily cycle of photosynthesis and transpiration, leaf water potentials become increasingly negative because the plant loses water faster than the root system and vascular system can absorb and transport water to the leaf. At night when photosynthesis and transpiration are not occurring in C-3 plants, leaf water potentials become less negative as water is taken up from the soil and plant water potentials equilibrate with soil water potentials (Kramer 1983). Measurements of predawn leaf water potential should closely represent the soil water potential integrated over the plant's rooting zone. Differences between predawn and midday water potential indicate water use or water loss through plant transpiration. The leaf water potential differences in Figure F.7 show clearly that sagebrush were active during the winter months of the 1998-1999 season.

Leaf water potential data for different size classes of shrubs (juvenile less than 50 cm, and mature greater than 75 cm) indicate significant differences in patterns of water use at different points in time. Although predawn leaf water potential measurements (Figure F.8a) initially indicated that juvenile plants might be more stressed, the data are highly variable (November measurement), and no significant difference is found for the measurement period. A pattern occurs where the midday leaf water potential of juvenile plants appears to be more negative during November, December, and February; whereas, the same plants appear less stressed (less negative leaf water potential) during April and May (Figure F.8b). Figure 8c more clearly shows this pattern as the difference between mean predawn and mean midday values for the two size classes of shrubs.

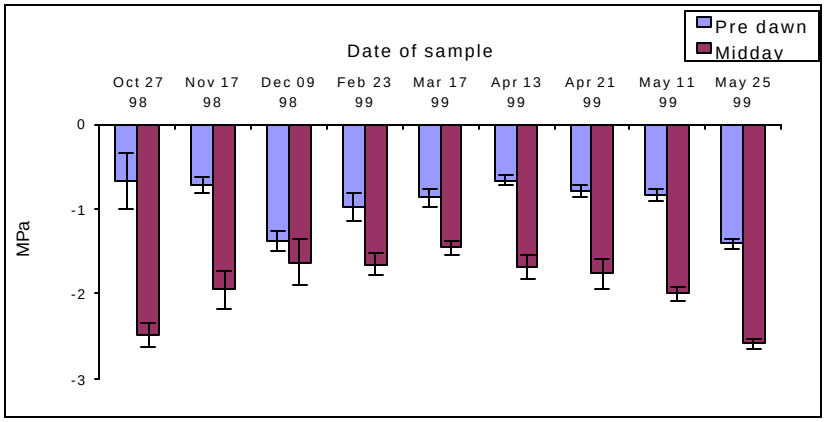


**Figure F.7**. Measured Leaf Water Potential for Mature Big Sagebrush: Predawn and Midday Measurements (error bars are ± one standard error)

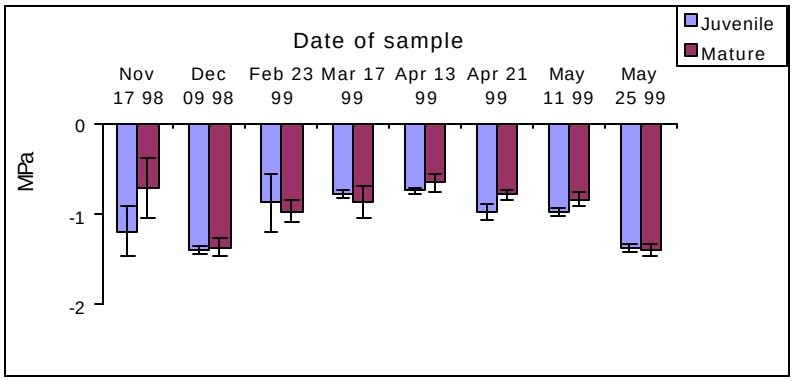


(a)

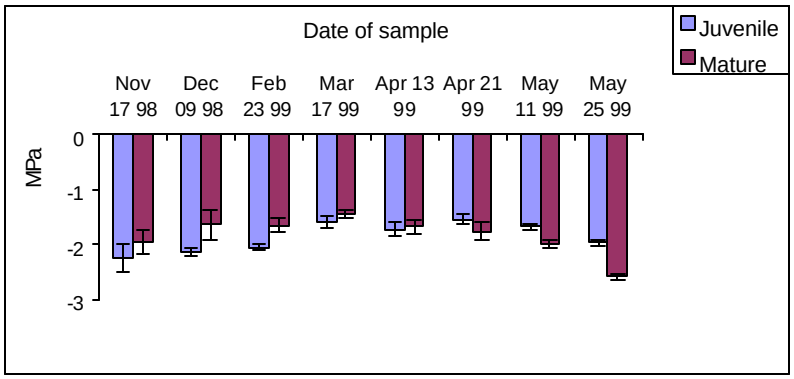


(b)

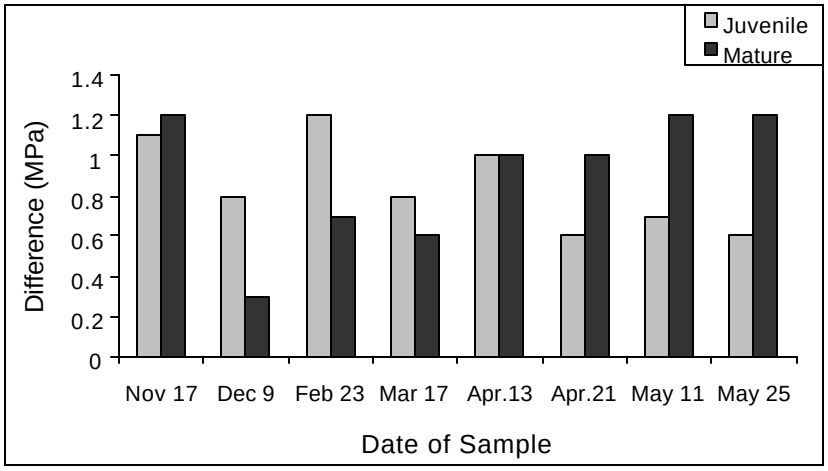


(c)

**Figure 8**. Measured Leaf Water Potential for Juvenile and Mature Big Sagebrush: a) Predawn, b) Midday, and c) Predawn Minus Midday (error bars are ± one standard error)

Mean values for predawn and midday leaf water potentials for cheatgrass over the past 8 months indicate that the understory plant is less active during the winter months in terms of water use than big sagebrush. Very small differences occurred in predawn and midday leaf water potentials during the months of November, December, January, and February (Figure F.9). In contrast, the differences between predawn and midday values during March, April, and May are large, indicating significant water loss to transpiration during the spring growing season.

Although plant cover data indicate significant plant activity during the winter season for Sandberg's bluegrass, we were unable to obtain leaf water potential measurements due to the small size of leaves and equipment used. Leaf water potential information obtained for the spring season indicates that predawn values were consistently low (approximately -0.7 MPa) for the three measurement periods and midday values were significantly lower (-2.0 to -3.0 MPa) indicating significant transpirational water loss during the daylight hours (Figure F.10). In contrast to the low predawn leaf water potentials for Sandberg's bluegrass, at early April measurement periods, cheatgrass was able to obtain predawn xylem potentials of about -0.3 MPa. This may reflect that the greater rooting depth of cheatgrass allows this species to equilibrate predawn potentials with soil water potentials in deeper, wetter portions of the soil profile. The root zone of Sandberg's bluegrass generally is limited to the top 30 to 45 cm of the soil profile, whereas cheatgrass may develop roots below 75 cm (Link et al. 1990).

Leaf-level conductance data obtained during the spring months for big sagebrush were highly variable and apparently lower than values reported previously in the literature (Figure F.11) (Evans et al. 1991). Sagebrush conductance values measured previously by the author during the spring months under different soil conditions were approximately 2 to 3 times greater than values measured at the ILAW site. Although the porometer was factory calibrated before any measurements were taken, we consider these

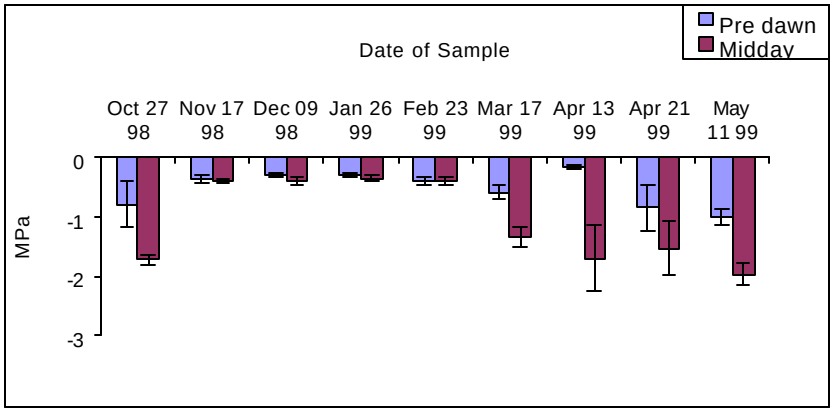


**Figure F.9**. Measured Leaf Water Potential for Cheatgrass at Predawn and Midday (error bars are ± one standard error)

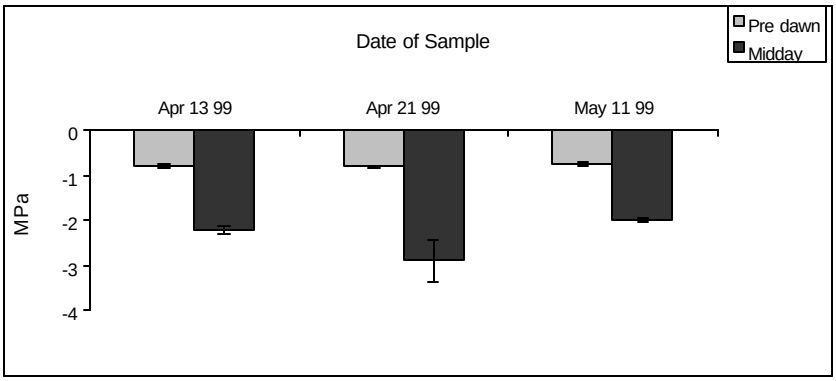


**Figure F.10**. Predawn and Midday Leaf Water Potentials for Sandberg's Bluegrass (error bars are ± one standard error)

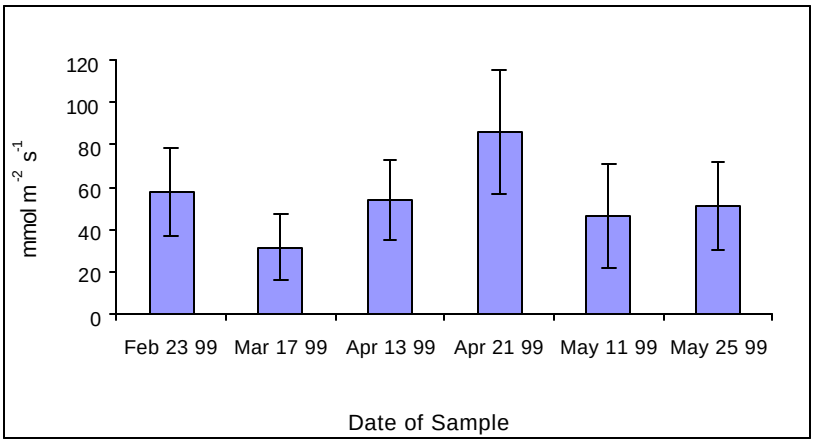


**Figure F.11**. Leaf-Level Conductance Data for Sagebrush (error bars are ± one standard error)

data suspect and will test the porometer system against a small-chamber gas-exchange system during the summer months. Conductance values measured for cheatgrass (Figure F.12) are also suspiciously lower than those reported previously (Link et al. 1990; Downs and Link 1993). Another possible explanation is that low conductance values could be a result of the combination of relatively low soil water availability along with cool springtime temperature.

### F.3.5 Soil Water and Root Characteristics

Soil water contents of the profile measured at each measurement period (Figures 13a-e) illustrate storage of water in the soil profile throughout the winter and early spring. Initial measurements in October, November, and December show the increase in water content at depths to 20 cm. The wetting

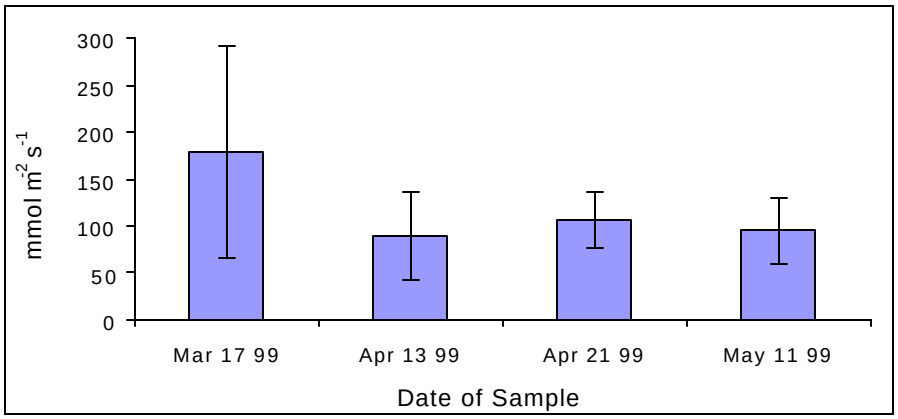


**Figure F.12**. Leaf-Level Conductance Data for Cheatgrass
(error bars are ± one standard error)

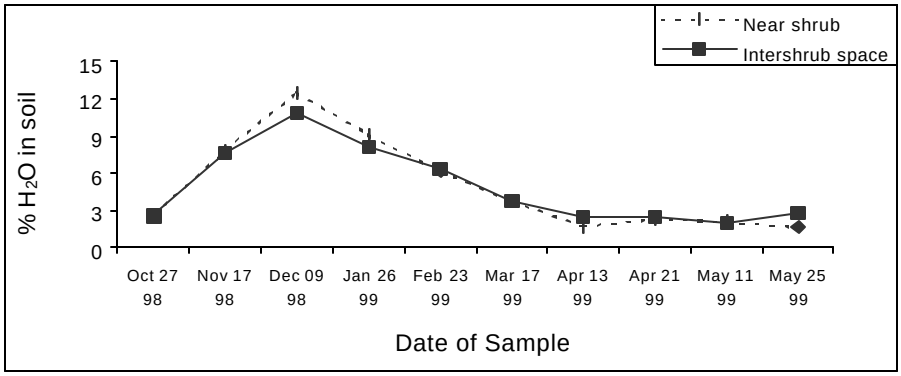


**Figure F.13 (a)**. Soil water content (%) at 0 to10-cm depth

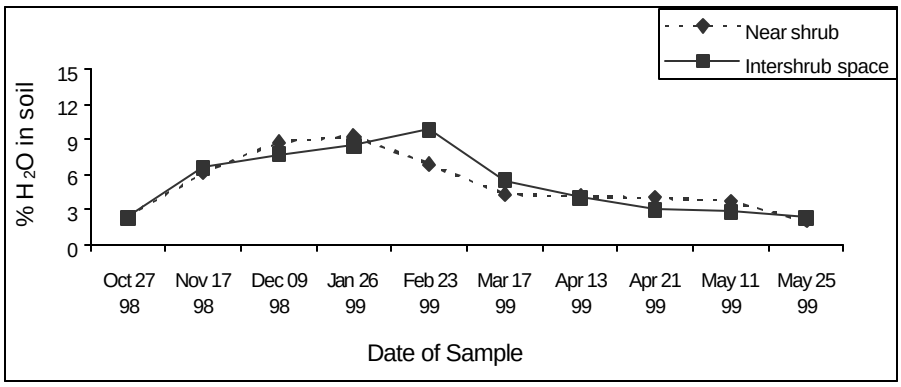


**Figure F.13 (b)**. Soil water content (%) at 10 to 20-cm depth

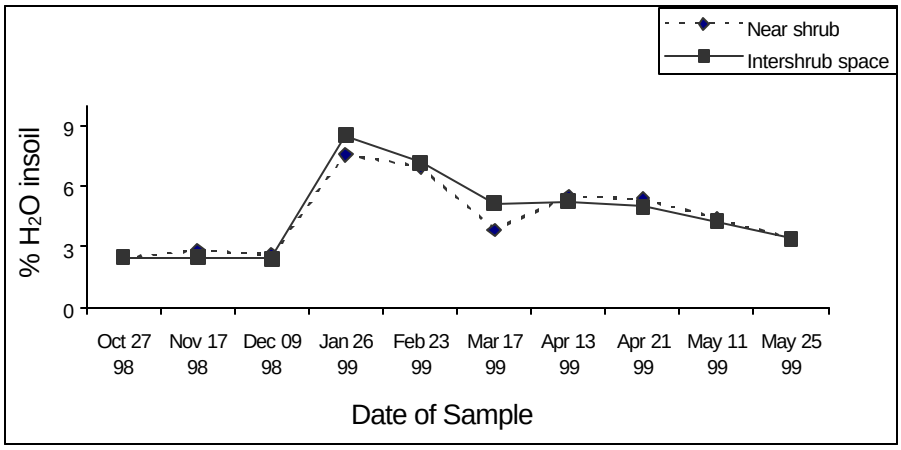


**Figure F.13 (c)**. Soil water content (%) at 40 to 50-cm depth

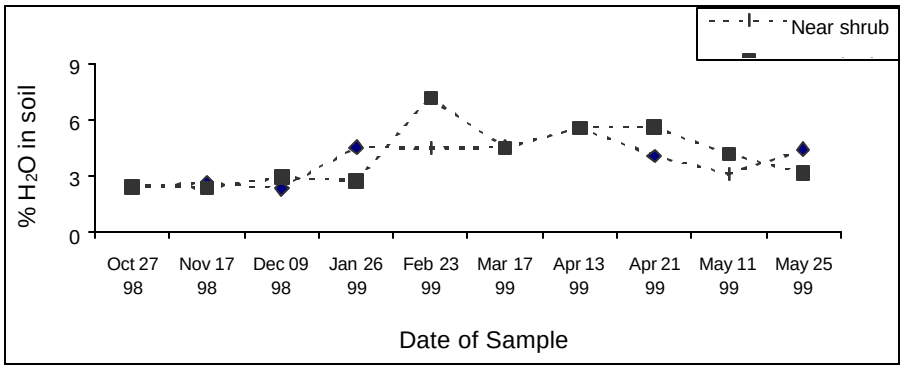


**Figure F.13 (d)**. Soil water content (%) at 90 to 100-cm depth

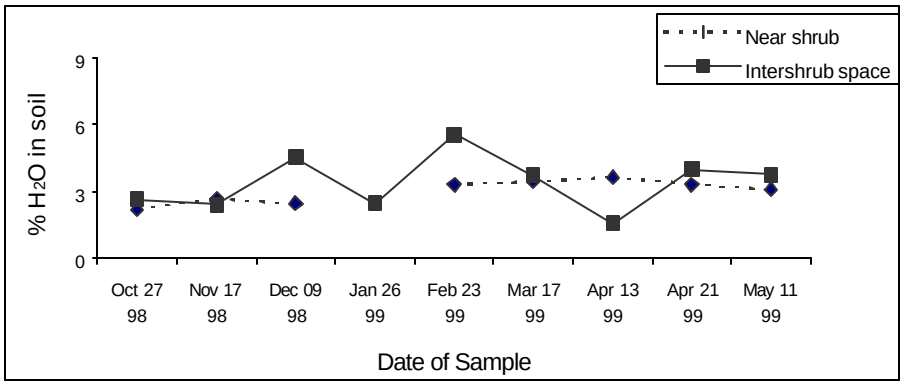


**Figure F.13 (e)**. Soil water content (%) at 90 to 100-cm depth

front resulting from fall and winter precipitation does not reach the 50-cm and 100-cm depths until January. Soil water contents of the top 50-cm of the profile begin to decline in February with the onset of significant plant activity and growth.

Small differences in water storage may occur between areas occupied by shrubs and areas between shrubs. Soils at the 100-cm and 150-cm depths below inter-shrub spaces appear to be more variable with regard to soil water content. Although the data are based on few samples, the soil water content appears to be slightly lower at both the 100-cm and 150-cm depth near shrubs in April and May. This spatial difference in soil water content may be related to water use by the deeper-rooted shrubs. These sampling efforts were not intended to fully describe the soil water conditions on a seasonal basis, but to provide supplemental information for interpretation of plant parameters. Further investigation of soil water dynamics is needed to adequately quantify soil water availability for transpiration or drainage at the proposed site.

Data collected to describe rooting density through the top meter of the profile show considerable variability in root distribution (Figure 14). Root density ($g/cm^3$) is highest near the surface in the top 30-cm regardless of where the sample was collected. However, at a distance of greater than 60 cm from the main trunk of the shrub, rooting density at the surface is less than that found closer to the shrubs, and also appears to be less variable. Because we could not separate live from non-functional roots, rooting densities reported here may likely overestimate the amount of functional root system in each category. Root separation and determination of functionality is very difficult for plants growing in arid systems and little to no information is available for turnover rates of roots in shrub-steppe systems.

Figure F.14 also depicts an apparent increase in root density between 60 and 90 cm below the surface regardless of distance from shrubs. This increase may be related to a change in soil texture noted at approximately that depth. Drill logs for two of the boreholes located in the proposed ILAW site describe a change in texture between 60 cm and deeper depths.

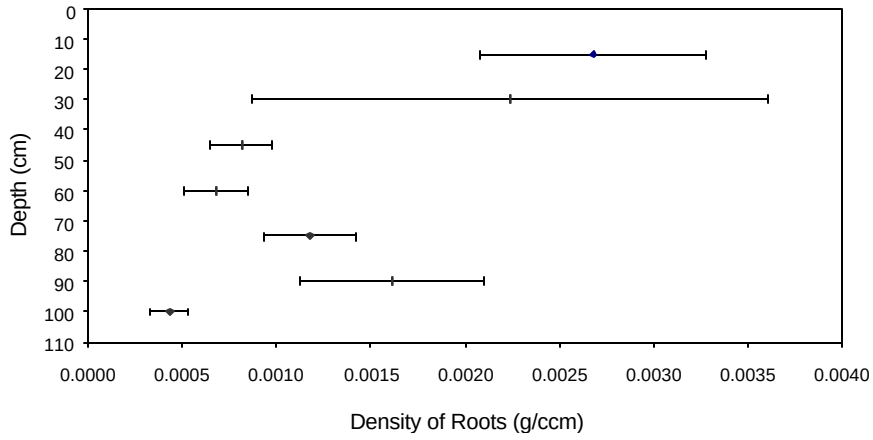


**Figure F.14 (a)**. Plot of Mean Root Density of all Samples Within 15 cm of all Shrubs

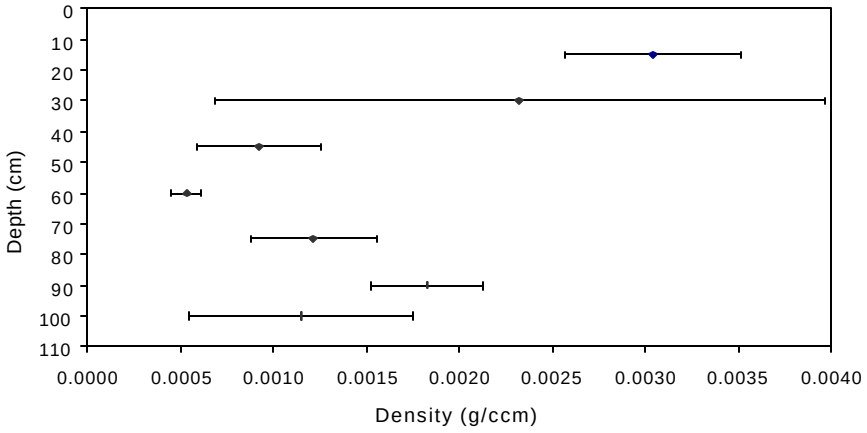


**Figure F.14 (b)**. Plot of Mean Root Density of all Samples 15 to 30 cm from Shrubs

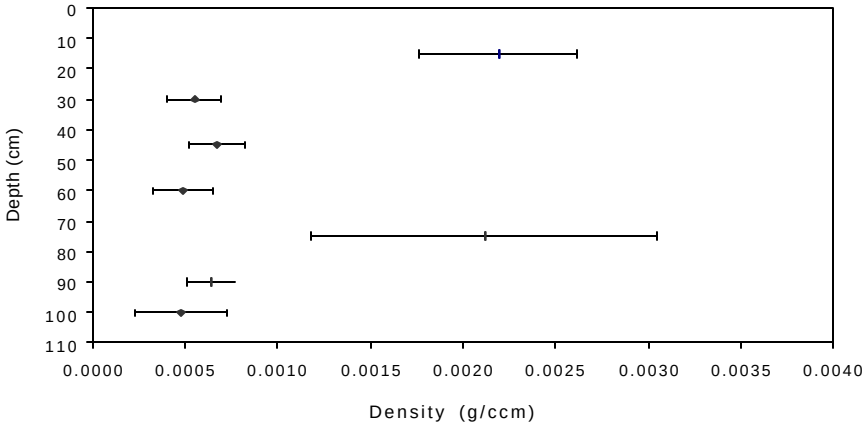


**Figure F.14 (c)**. Plot of Mean Root Density of all Samples 30 to 45 cm from Shrubs

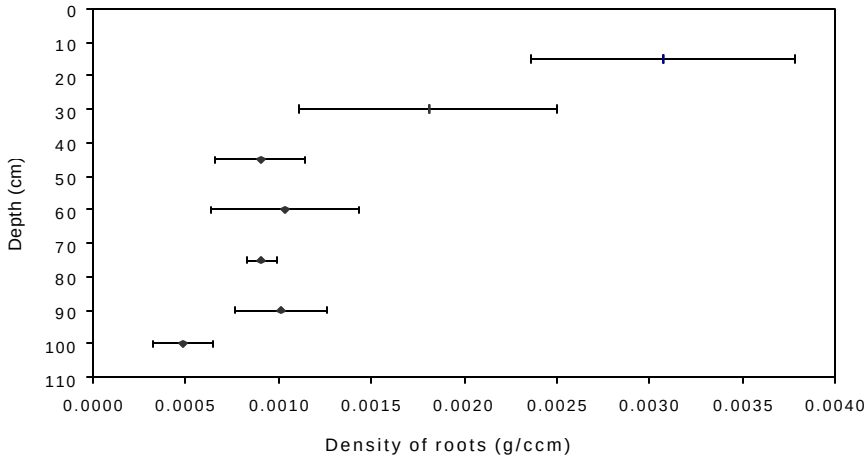


**Figure F.14 (d)**. Plot of Mean Root Density of all Samples 45 to 60 cm from Shrubs

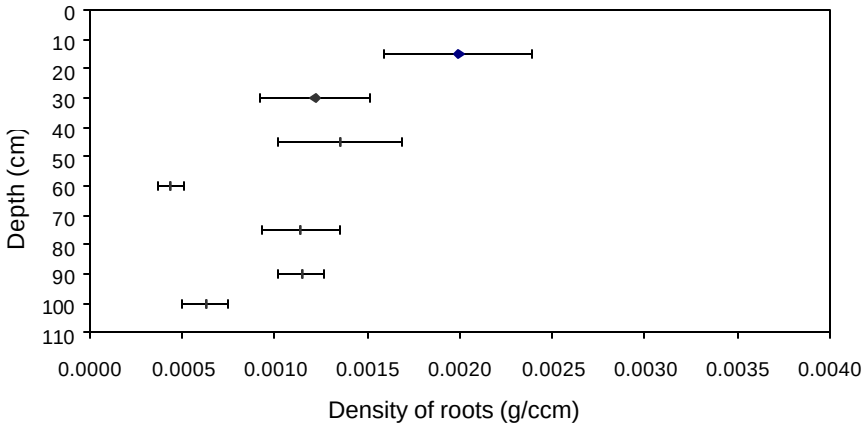


**Figure F.14 (e)**. Plot of Mean Root Density of all Samples >60 cm from Shrubs

### F.3.6 Implications for Recharge Estimation

Data collected to this point indicate that several of the assumptions generally used for plant parameters in recharge estimation may need to be revised. Current modeling simulations estimate the evapotranspiration component of recharge based only on a single species. Improvements to the model to include multiple species or multiple plant functional types (shrub, grass, and forb) would greatly improve the evapotranspiration component. The differences in timing and phenology of the multiple species likely to be present on the disposal site need to be represented in the recharge modeling efforts. Both leaf water potential and growth data indicate that all three of the dominant species, big sagebrush, cheatgrass, and Sandberg's bluegrass carry out photosynthesis and transpiration during the winter months. The current evapotranspiration component of the model also assumes that the lateral distribution of roots is uniform. Data collected under this task indicate that root distributions are highly variable, and may well be influenced by community structure.

More sophisticated modeling efforts could incorporate critical temperatures for plant growth, LAI, stomatal conductance under non-limiting soil water availability, leaf water potentials, and even values for root resistance to water uptake and transport. Determining the relationship between soil/air temperatures and plant activity and growth would allow us to better quantify seasonal evapotranspiration and provide a realistic driving force for simulations of plant water use.

## F.4 References

Allen EB. 1991. "Temporal and Spatial Organization of Desert Plant Communities." In *Semiarid Lands and Deserts: Soil Resource and Reclamation*, J Skujins, ed., Marcel Dekker, Inc., New York.

Daubenmire R. 1959. "A canopy-coverage method of vegetational analysis." *Northwest Science* 33:43-64.

Downs JL and SO Link. 1993. "Effects of Enhanced Nitrogen and Water Conditions on the Resistance of *Bromus tectorum* to Water Uptake." *In Pacific Northwest Laboratory Annual Report for 1992 to the DOE Office of Energy Research, Part 2*: Environmental Sciences, PNL-8500, Pt. 2, Pacific Northwest Laboratory, Richland, Washington.

Evans RD, RA Black, and SO Link. 1991. "Reproductive growth during drought in *Artemisia tridentata*." Nutt. Funct. Ecol. 5:676-683.

Franklin JF and CT Dyrness. 1988. *Natural vegetation of Oregon and Washington*. Oregon State University Press, Corvallis.

Gee GW, MJ Fayer, ML Rockhold, and MD Campbell. 1992. "Variations in recharge at the Hanford Site." *Northwest Science*, Vol. 66, No. 4, 1992.

Gee GW, PJ Wierenga, BJ Andraski, MH Young, MJ Fayer, and ML Rockhold. 1994. "Variations in water balance and recharge potential at three western desert sites." *Soil Science Society of American Journal*, 58:63-72.

Kramer PJ. 1983. "Water Movement in soil-plant-atmosphere continuum." *In Water Relations of Plants*. Academic Press, Inc., New York.

Koide RT, RH Robichaux, SR Morse, and CM Smith. 1989. "Plant water status, hydraulic resistance and capacitance." In *Plant Physiological Ecology, Field Methods and Instrumentation*. RW Pearcy, J Ehlringer, HA Mooney, and PW Rundel, eds., Chapman and Hall, New York.

Link SO, GW Gee, and JL Downs. 1990. "The effect of water stress on phenological and ecophysiological characteristics of cheatgrass and Sandbergs's bluegrass." *Journal of Range Management* 43:506-513.

Link SO, WJ Waugh, JL Downs, ME Thiede, JC Chatters, and GW Gee. 1994. "Effects of coppice dune topography and vegetation on soil water dynamics in a cold-desert ecosystem." *J. Arid Environments* 27:265-278.

Lockheed Martin Hanford Company (LMHC). 1999. *Statement of Work for FY 2000 to 2005 for the Hanford Low-Level Tank Waste Performance Assessment Activity*. HNF-SD-WM-PAP-062, Rev. 4, Lockheed Martin Hanford Company, Richland, Washington.

Murphy EM, TR Ginn, and JL Phillips. 1996. "Geochemical estimates of paleorecharge in the Pasco Basin: Evaluation of the chloride mass balance technique." *Water Resources Research* 32:2853-2868.

Pearcy RW, ED Schulze, and R Zimmerman. 1989. "Measurement of transpiration and leaf conductance." In *Plant Physiological Ecology, Field Methods and Instrumentation*. RW Pearcy, J Ehlringer, HA Mooney, and PW Rundel, eds., Chapman and Hall, New York.

Rockhold ML, MJ Fayer, GW Gee, and CT Kincaid. 1995. *Estimation of natural ground water recharge for the performance assessment of a low-level waste disposal facility at the Hanford Site*. PNL-10508. Pacific Northwest Laboratory, Richland, Washington.

Westinghouse Hanford Company (WHC). 1995. *Statements of Work for FY 1995 to 2000, Hanford Tank Low-Level Waste Performance Assessment Group, Westinghouse Hanford Company*. WHC-SD-WM-PAP-062. Westinghouse Hanford Company, Richland, Washington.

# Appendix G

# Quality Assurance and Safety

# Appendix G

# Quality Assurance and Safety

All laboratory and field experiments are conducted under PNNL quality assurance (QA) requirements as described in the guidance provided in PNNL's Standards Based Management System (SBMS) and as specified in the Project QA Plan. Significant modifications to the QA plan are made in accordance with the guidance in the SBMS.

Project staff members are qualified and receive any training needed to carry out their assigned responsibilities.

Staff use equipment of known accuracy for data collection. For measurements necessary to substantiate test results, staff ensure that standards used for calibration are traceable to nationally recognized standards. Measuring and Test Equipment (M&TE) lists are generated by each task and maintained in the project files applicable to the specific task. M&TE used is identified in the laboratory record books or other data recording location to provide traceability to instrument calibrations.

Test procedures and methods are documented and deviations noted. New methods developed during the course of this work are documented and reviewed. All test procedures, data processing software, and supporting documentation undergo independent technical review by qualified PNNL staff.

Staff maintain records necessary to substantiate results and processes of research activities. After activities are completed, records are filed and maintained per the project Records Inventory and Disposition Schedule (RIDS).

All precautionary measures are taken in accordance with standard PNNL safety procedures to ensure that field work is conducted in a safe manner. No hazardous wastes have been generated during the conduct of work described in this report.

# Distribution

**No. of Copies**

**OFFSITE**

B. Scanlon
Bureau of Economic Geology
University of Texas at Austin
University Station
Box X
Austin, TX 78713

J. Nimmo
U.S. Geological Survey, MS 421
345 Middlefield Road
Menlo Park, CA 94025-3591

**ONSITE**

5 **Bechtel Hanford Inc.**

| | |
|---|---|
| BH Ford | H0-21 |
| MJ Graham | H0-09 |
| GA Jewel (2) | H1-21 |
| GB Mitchem | H0-21 |

5 **U.S. Department of Energy/RL**

| | |
|---|---|
| CA Babel | H6-60 |
| BL Foley | H0-12 |
| PE LaMont | H6-60 |
| KM Thompson | H0-12 |
| RM Yasek | H6-60 |

4 **Fluor Daniel Northwest, Inc.**

| | |
|---|---|
| EJ Freeman | B4-43 |
| R Khaleel | B4-43 |
| FM Mann | H0-22 |
| RJ Puigh | B4-43 |

**No. of Copies**

5 **Lockheed Martin Hanford Company**

| | |
|---|---|
| DA Burbank | S4-45 |
| KC Burgard | S4-45 |
| CC Haass | H6-64 |
| AJ Knepp | H0-22 |
| RW Root | R2-53 |

**IT**

| | |
|---|---|
| DA Myers | H0-22 |

**Jacob's Engineering**

| | |
|---|---|
| JC Henderson | H0-22 |

**LATA**

| | |
|---|---|
| MM McCarthy | H0-22 |

41 **Pacific Northwest National Laboratory**

| | |
|---|---|
| DH Bacon | K9-33 |
| MP Bergeron | K9-33 |
| BN Bjornstad | K6-81 |
| RW Bryce | K6-75 |
| CR Cole | K9-36 |
| JL Downs | K6-85 |
| MJ Fayer (10) | K9-33 |
| MD Freshley | K9-33 |
| GW Gee | K9-33 |
| MJ Hartman | K6-96 |
| FO Khan | K6-85 |
| CT Kincaid | K9-33 |
| RR Kirkham | K9-33 |
| SJ Kowall | K8-12 |
| GV Last | K6-81 |
| CW Lindenmeier | K6-81 |

| No. of Copies | | No. of Copies | |
|---|---|---|---|
| BP McGrail | K6-81 | RJ Serne | K6-81 |
| PD Meyer | BPO | JK Tarantino | K9-41 |
| EM Murphy | K3-61 | AL Ward | K9-33 |
| WE Nichols | K9-33 | SK Wurstner | K9-33 |
| SP Reidel | K6-81 | Information Release (7) | |